SSD 102.3

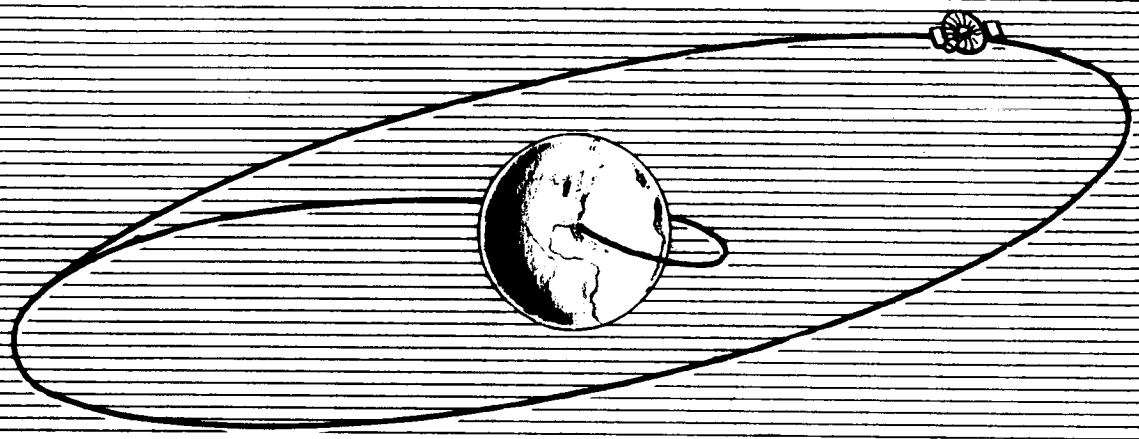

FACILITY FORM 602

N67-24610
(ACCESSION NUMBER)

(THRU)

383
(PAGES)

1
(CODE)

CR-81768
(NASA CR OR TMX OR AD NUMBER)

31
(CATEGORY)

VOLUME 7 OF 8

Final Report

ATS-4

PREPARED BY

FAIRCHILD HILLER
SPACE SYSTEMS DIVISION

FOR

NASA
Goddard Space Flight Center

DECEMBER 1966

SSD 102.3

ATS-4 STUDY PROGRAM

FINAL REPORT

(Contract NASW-1411)

VOLUME SEVEN OF EIGHT

prepared by

FAIRCHILD HILLER SPACE SYSTEMS DIVISION

Sherman Fairchild Technology Center

Germantown, Maryland

for

GODDARD SPACE FLIGHT CENTER

NATIONAL AERONAUTICS AND SPACE ADMINISTRATION

December 1966

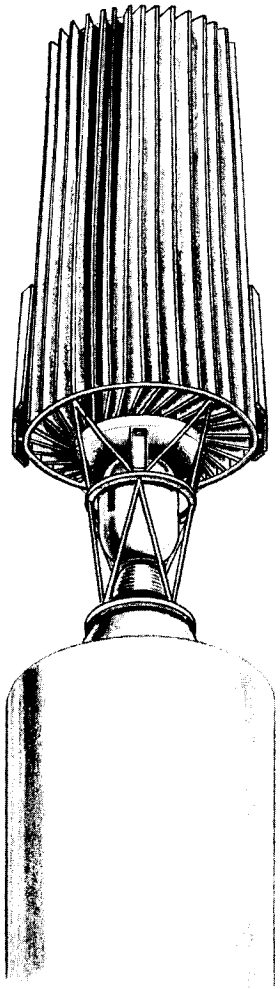

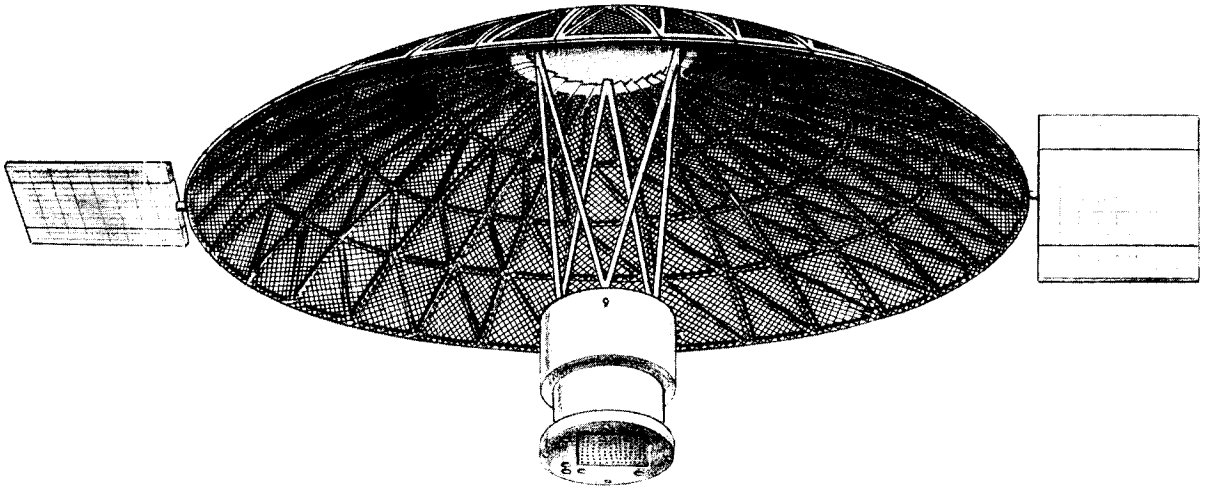

TABLE OF CONTENTS

VOLUME ONE

Section	Title	Page
1.0	Summary	1-1
1.1	Objectives and Justification	1-1
	1.1.1 Utilization	1-2
	1.1.2 Implementation	1-4
1.2	Program Feasibility	1-6
	1.2.1 Parabolic Antenna	1-6
	1.2.2 Stabilization and Control System	1-8
	1.2.3 Phased Array	1-11
	1.2.4 Interferometer	1-12
1.3	Subsystem Summaries	1-13
	1.3.1 Configuration Description	1-13
	1.3.2 Parabolic Reflector	1-19
	1.3.3 Parabolic Antenna Feed	1-22
	1.3.4 Attitude Stabilization and Control System	1-24
	1.3.5 Launch Vehicle - Ascent and Orbit Injection	1-27
	1.3.6 Interferometer System	1-32
	1.3.7 Phased Array	1-33
	1.3.8 In-Orbit Maneuvers and Auxiliary Propulsion System	1-35
	1.3.9 Additional Experiment Capability	1-37

TABLE OF CONTENTS

VOLUME TWO

Section	Title	Page
2.0	Systems Analysis	2-1
2.1	Mission Profile and Operations Plan	2-1
	2.1.1 Mission Profile	2-1
	2.1.2 Operations Plan	2-20
2.2	Experiment Plan	2-20
	2.2.1 Parabolic Antenna Experiment	2-20
	2.2.2 Monopulse System Operation	2-30
	2.2.3 Phased Array Experiment	2-32
	2.2.4 Orientation and Control Experiment	2-45
	2.2.5 Interferometer Experiment	2-49
	2.2.6 Additional Communication Experiments	2-54
2.3	Power Profiles	2-58
	2.3.1 Preorbital Power	2-58
	2.3.2 Experiment Evaluation	2-61
	2.3.3 Experiment Demonstration	2-61
	2.3.4 Power System Margin	2-61
	2.3.5 Experiment Loads	2-64
2.4	Antenna Accuracy Considerations	2-68
	2.4.1 Reflecting Surface Errors	2-68
	2.4.2 Feed Location Errors	2-73
	2.4.3 Frequency Limitations on Gain	2-74
	2.4.4 Summary of Antenna Error Effects	2-76
2.5	Antenna Efficiencies	2-79
	2.5.1 Parabolic Antenna	2-79
	2.5.2 Phased Array Figures of Merit	2-82
2.6	Faisure Modes	2-91
	2.6.1 System Considerations	2-91
	2.6.2 Parabolic Antenna	2-91
	2.6.3 Stabilization and Control System	2-93
	2.6.4 Phased Array	2-98
	2.6.5 Antenna Experiment Electronics	2-100
	2.6.6 Phased Array Monopulse Operation	2-103
2.7	Weight Summaries	2-105

TABLE OF CONTENTS

VOLUME THREE

Section	Title	Page
3.0	Vehicle Engineering	3-1
3.1	Concept Evolution	3-1
	3.1.1 Trade-off Parameters	3-1
	3.1.2 F/D Trade-offs	3-6
	3.1.3 Spacecraft Concepts	3-8
3.2	Concept Evaluation and Reference Concept	3-21
	3.2.1 Launch Vehicle Choice	3-21
	3.2.2 Split Module Concept	3-21
	3.2.3 Reference Concept	3-25
	3.2.4 Concept Comparison	3-29
	3.2.5 Titan IIIC Adaptability	3-29
3.3	Reflector Design	3-33
	3.3.1 Design Evolution and Alternate Approaches	3-33
	3.3.2 Petal Hinging Concepts	3-38
	3.3.3 Petal Structural Design	3-40
	3.3.4 Deployment System	3-47
	3.3.5 Tolerance Considerations	3-47
	3.3.6 Reflecting Surface	3-50
	3.3.7 Petal Locking System	3-53
3.4	Reflector Fabrication	3-57
	3.4.1 Fabrication Considerations	3-57
	3.4.2 Aluminum Substructure	3-57
	3.4.3 Wire Mesh Forming	3-59
	3.4.4 Sub-Assemblies	3-60
	3.4.5 Tooling	3-60
	3.4.6 Assembly Procedure	3-64
	3.4.7 Measurement of Surface Deviations	3-65
3.5	Structural and Dynamic Analyses	3-71
	3.5.1 Analytical Methods and Approach	3-71
	3.5.2 Preliminary Analysis	3-77
	3.5.3 Integrated Spacecraft-Launch Configuration	3-104
	3.5.4 Integrated Spacecraft-Orbit Configuration	3-115
	3.5.5 Orbit Maneuvering	3-121

TABLE OF CONTENTS

VOLUME THREE (Continued)

Section	Title	Page
3.6	Thermo/Structural Analysis	3-129
	3.6.1 Thermal Requirements and Approach	3-129
	3.6.2 Design Orbit	3-133
	3.6.3 Petal Thermal Analysis	3-135
	3.6.4 Thermoelastic Analysis of Reflector	3-154
	3.6.5 Feed Mast Thermal Analysis	3-166
	3.6.6 Thermal Deformation of Feed Mast	3-172
	3.6.7 Spacecraft Thermal Control	3-175
3.7	Dimensional Stability	3-178
	3.7.1 Introduction	3-178
	3.7.2 Precision Elastic Limit	3-179
	3.7.3 Residual Stress	3-179
	3.7.4 Design Application	3-180
	3.7.5 References for Dimensional Stability Discussion	3-182
3.8	In-Orbit Measurement of Antenna Surface Accuracy	3-183
	3.8.1 Basic Techniques	3-183
	3.8.2 Operational Considerations	3-183
	3.8.3 Antenna Surface Errors	3-185
	3.8.4 Equipment Location	3-185
	3.8.5 Conceptual Design	3-186
	3.8.6 Error Resolution Requirements	3-189
	3.8.7 Sampling Surface Measurements	3-191
	3.8.8 The Axial Four Camera System	3-192
	3.8.9 Illumination of the Antenna	3-208
	3.8.10 System Operation	3-209
	3.8.11 General Comments	3-209
Appendix		
3A	Expandable Truss Antennas	3-211
3B	Inflatable Antennas	3-225
3C	Rigid Panel Antennas	3-230
3D	Petal Axis of Rotation Determination	3-248

TABLE OF CONTENTS

VOLUME FOUR

Section	Title	Page
4.0	Power Systems	4-1
4.1	Solar Panel Configuration Study	4-2
4.2	Solar Cell Radiation Degradation	4-6
	4.2.1 Radiation Environment	4-6
	4.2.2 Background Flux	4-7
	4.2.3 Power Margin	4-10
4.3	Battery Characteristics	4-10
	4.3.1 Nickel-Cadmium Battery	4-13
	4.3.2 Silver-Cadmium Battery	4-13
	4.3.3 Silver-Zinc Battery	4-15
	4.3.4 Battery Comparison	4-15
4.4	Battery Charging and Control	4-23
	4.4.1 Constant Current Charging	4-23
	4.4.2 Constant Voltage Charging	4-24
	4.4.3 Modified Constant Voltage Charging	4-26
	4.4.4 Tapered Charging	4-26
	4.4.5 Recommendation	4-26
4.5	Concept Power Subsystem	4-28
	4.5.1 Design Approach	4-28
	4.5.2 Battery Complement	4-32
	4.5.3 Solar Array	4-35
	4.5.4 Power Conditioning and Control	4-36
5.0	Orbital Analysis	5-1
5.1	General	5-1
5.2	Apogee Injection Stages	5-2
5.3	Ascent Trajectories	5-4
	5.3.1 Requirements and General Considerations	5-4
	5.3.2 Synchronous Injection - Single Apogee Impulse	5-7
	5.3.3 Subsynchronous Injection - High Altitude Parking Orbit	5-10
	5.3.4 Recommended Centaur Ascent Trajectory	5-18
5.4	Orbit Payloads	5-23
	5.4.1 General	5-23
	5.4.2 SLV3A/Agena and SLV3C/Centaur	5-23

TABLE OF CONTENTS

VOLUME FOUR (Continued)

Section	Title	Page
	5.4.3 Titan IIIC	5-30
	5.4.4 Payload Data Summary	5-30
5.5	Orbit Injection Errors	5-32
	5.5.1 Error Values	5-32
	5.5.2 Associated Latitude-Longitude Deviation	5-33
	5.5.3 Associated Corrective Velocity Impulse Requirements	5-36
5.6	Orbit Perturbations	5-39
	5.6.1 General	5-39
	5.6.2 Earth Oblateness and Extraterrestrial Perturbations	5-39
	5.6.3 Terrestrial Perturbations - Equatorial Ellipticity	5-41
	5.6.4 Associated Corrective Velocity Impulse Requirements	5-45
5.7	Auxiliary Propulsion System	5-48
	5.7.1 Velocity Impulse and Thrust Requirements	5-48
	5.7.2 Initial APS Comparison Study	5-48
5.8	Orbit Guidance	5-57
	5.8.1 General Requirements	5-57
	5.8.2 Orbit Injection Error Correction	5-58
	5.8.3 Station Keeping and Repositioning	5-63
5.9	References and Symbols for Orbital Analysis	5-65
	5.9.1 References	5-65
	5.9.2 List of Symbols	5-67

TABLE OF CONTENTS

VOLUME FIVE

Section	Title	Page
6.0	ATTITUDE STABILIZATION AND CONTROL SYSTEM	6-1
	6.1 Attitude Stabilization and Control Requirements	6-1
	6.1.1 Mission Requirements	6-1
	6.1.2 Pointing Accuracy	6-1
	6.1.3 Control Modes	6-1
	6.2 Attitude Reference Subsystem	6-2
	6.2.1 Alternate Approaches	6-2
	6.2.2 Candidate Reference Sensors	6-11
	6.2.3 Selected Configuration	6-22
	6.2.4 Sensor Performance	6-23
	6.3 Disturbance Torque Model	6-25
	6.3.1 Meteoroid Import	6-25
	6.3.2 Gravity Gradient	6-34
	6.3.3 Magnetic Disturbance	6-35
	6.3.4 Internal Rotating Equipment	6-35
	6.3.5 Solar Pressure	6-35
	6.4 Torquer Subsystem	6-52
	6.4.1 Control Impulse Requirements	6-52
	6.4.2 Candidate Reaction Jet Types	6-59
	6.4.3 Inertia Wheel Subsystem	6-63
	6.4.4 Selected Torquer Configuration	6-69
	6.5 Computation and Data Handling	6-71
	6.5.1 On-Board Computation	6-71
	6.5.2 Up-Data Commands	6-71
	6.5.3 Down-Data Monitor	6-71
	6.6 System Operational Description	6-75
	6.6.1 Control Mode Operation	6-75
	6.6.2 System Block Diagram	6-85
	6.6.3 Sensor Update	6-89
	6.7 System Performance	6-90
	6.7.1 Pointing Accuracy	6-90
	6.7.2 Acquisition	6-93
	6.7.3 Control System Dynamics	6-93
	6.7.4 Reliability	6-117
	6.8 System Physical Description	6-124

Appendix

6A	Preliminary Control Torque and Impulse Requirements
6B	Preliminary Reaction Jet Considerations
6C	Preliminary Inertia Wheel Considerations For Candidate Vehicle Configurations
6D	Preliminary Combined Wheel/Jet System Considerations
6E	Preliminary Transfer Orbit Control Mode Analysis

TABLE OF CONTENTS

VOLUME SIX

Section	Title	Page
7.0	Communications Experiments	7-1
7.1	Parabolic Antenna	7-1
	7.1.1 Beam Scanning	7-1
	7.1.2 Parabolic Antenna Feeds	7-14
	7.1.3 Aperture Blockage	7-32
	7.1.4 Paraboloid Performance	7-42
7.2	Phased Array	7-58
	7.2.1 Transdirective Array	7-59
	7.2.2 The Butler Matrix Array	7-63
	7.2.3 Space Fed (Lens) Array	7-65
	7.2.4 Corporate-Fed Array	7-71
	7.2.5 Corporate-Fed Phased Array Design Considerations	7-79
	7.2.6 Antenna Definition	7-92
	7.2.7 Digital Beam Steering Unit	7-102
	7.2.8 Packaging Configuration	7-108
7.3	Communications Equipment	7-111
	7.3.1 Transmission Parameters	7-111
	7.3.2 Systems Description	7-113
	7.3.3 Weight, Volume and Power Summary	7-134
	7.3.4 System Performance Summary	7-137

Appendix

7A	Four Paraboloid Off-Set Feed Configuration	7-139
7B	Ionospheric Effects on Wave Polarization	7-147
7C	Separate 100 MHz Antennas	7-159
7D	Communication Components	7-165

TABLE OF CONTENTS

VOLUME SEVEN

Section	Title	Page
8.0	Radio Interferometer Experiment	8-1
	8.1 Introduction	8-1
	8.2 Study Approach	8-3
	8.3 Candidate Interferometer Concepts	8-5
	8.4 Candidate Interferometer Systems	8-11
	8.4.1 Selection Criteria	8-11
	8.4.2 System Block Diagrams	8-11
	8.5 Selection of Preferred Concept	8-25
	8.5.1 Candidate Evaluation and Selection of Preferred System	8-25
	8.5.2 Phased Array as an Interferometer	8-44
	8.6 Design of Preferred Interferometer System	8-48
	8.6.1 General Circuit Description	8-48
	8.6.2 Mechanical and Thermal Design	8-59
	8.6.3 Interferometer Attitude Sensor Interface	8-68
	8.6.4 Physical Characteristics	8-85
	8.7 Error Analysis of Preferred Concept	8-86
	8.8 Conclusions and Recommendations	8-116
	8.9 Bibliography and Glossary	8-117
Appendix		
8A	Interference Reduction by Correlation	8-136
8B	RF Link Calculation	8-138
8C	Interferometer Angular Error Due to Mutual Coupling	8-141
8D	System Polarization	8-146
8E	Derivation of the Received Voltage Phases on an Elliptically Polarized Interferometer Antenna Pair with an Incident Elliptically Polarized Wave	8-165
8F	Alternative Antenna Switching Systems - Direct Phase Reading Interferometer	8-172
8G	Derivation of Counter Equation	8-180
8H	Gating Time Error Analysis	8-182
8I	Conversion of θ_s into Attitude	8-187
8J	Limitation of Range and Range Rate Capability	8-201
Volume 8	Program Budgetary Costs and Schedules	10-1

TABLE OF CONTENTS

VOLUME SEVEN (Continued)

Section	Title	Page
9.0	Summary	9-1
9.1	Data Flow	9-2
	9.1.1 Definition	9-2
	9.1.2 Requirements	9-2
	9.1.3 Model of the Data Flow	9-3
9.2	Telemetry System	9-8
	9.2.1 Data Handling Requirements	9-8
	9.2.2 Data Handling System Design	9-9
	9.2.3 Data Handling System Configuration	9-17
	9.2.4 Data Transmission System Design	9-23
	9.2.5 Data Transmission Link Calculation	9-28
	9.2.6 System Size, Weight and Power Estimates	9-44
	9.2.7 Equipment Implementation	9-44
9.3	Command System	9-47
	9.3.1 Definition	9-47
	9.3.2 Requirements	9-47
	9.3.3 Word Format	9-50
	9.3.4 Description and Operation of the Onboard System	9-53
	9.3.5 Estimates of Physical Characteristics	9-60
	9.3.6 Transmission Link Power Requirements	9-62
	9.3.7 Equipment Implementation	9-64
	9.3.8 Ground Equipment Requirements	9-65
9.4	Range and Rage Rate Transponder	9-69
	9.4.1 Accuracy Requirements	9-69
	9.4.2 Transponder Operating Frequency Selection	9-69
	9.4.3 UHF Transponder Characteristics	9-70
	9.4.4 Equipment Implementation	9-71
9.5	Ground Station Requirements	9-72
	9.5.1 Ground Equipment Description	9-72
9.6	References	9-84
	Appendices	
	9A Commutator Channel Assignment	9-85
	9B Modulation Index Calculations (Mode 1)	9-101
	9C Solving for Receiver Noise Power and Channel Bandwidth Ratios (Mode 1)	9-103
	9D Solving for Receiver Noise Power and Channel Bandwidth Ratios (Mode II)	9-105
	9E Command Signal Catalog	9-106
	9F Telemetry Signal Catalog	9-116
	9G Data Questionnaire	9-131

LIST OF ILLUSTRATIONS

VOLUME ONE

Figure	Title	Page
1.3-1	Fairchild Hiller ATS-4 Concept	1-14
1.3-2	Reference Concept	1-15
1.3-3	Spacecraft Module Detail	1-18
1.3-4	Multiband Prime Focus Feed	1-23
1.3-5	SCS Block Diagram	1-29
1.3-6	ATS-4 Ascent Trajectory	1-31

LIST OF ILLUSTRATIONS

VOLUME TWO

Figure	Title	Page
2.1-1	Satellite Ground Track	2-2
2.1-2	Spacecraft/Sun Orientation in Transfer Orbit	2-4
2.1-3	Satellite Ground Track and Ground Station	2-12
2.1-4	Gross Data Flow Concept	2-17
2.2-1	Major Plane Location and Arts for Antenna Measurement	2-22
2.2-2	Ground Terminal Layout for Monopulse Calibration	2-33
2.2-3	Major Planes and Beam Positions for Station Pattern Tests	2-35
2.2-4	Multiple Pattern Arts Using Two Ground Stations	2-41
2.2-5	Crosstalk Measurement	2-41
2.2-6	Major Plane Arts - Interferometer	2-53
2.2-7	Pointing of the Z-Axis for Interferometer Measurement	2-53
2.3-1	Typical Experiment Evaluation Profile	2-62
2.3-2	Power Profile with Additional Experiments	2-62
2.3-3	Experiment Demonstration Maximum Profile	2-63
2.4-1	Classification of Parabolic Antenna Errors	2-69
2.4-2	Reflector Errors	2-71
2.4-3	Feed Location Errors	2-75
2.4-4	Feed Location Errors (F/D = 0.3)	2-78
2.4-5	Frequency Limitation on Gain	2-78
2.5-1	X-Band Radiation Pattern	2-81
2.6-1	Failed Reaction Wheel Backup Subsystem	2-94

LIST OF ILLUSTRATIONS

VOLUME THREE

Figure	Title	Page
3.1-1	Antenna Feed Location	3-3
3.1-2	C.G. Location Study	3-5
3.1-3	Concept SK513-10	3-13
3.1-4	Concept SK513-12	3-15
3.1-5	Concept SK513-11	3-16
3.1-6	Concept SK513-13	3-17
3.1-7	Concept SK513-14	3-18
3.1-8	Concept SK513-16	3-19
3.2-1	Concept SK513-18	3-23
3.2.2	Concept SK513-17 (Reference Concept)	3-24
3.2-3	Spacecraft Module Detail	3-27
3.2-4	Concept Comparison Chart	3-31
3.2-5	Reference Concept on Titan IIIC	3-32
3.3-1	Conic Scissors Parabolic Antenna	3-34
3.3-2	Inflatable Parabolic Antenna	3-36
3.3-3	Retentive Memory Petal Concept	3-39
3.3-4	Non-Radial Petals, Sheet One	3-41
3.3-5	Non-Radial Petals, Sheet Two	3-42
3.3-6	Petal Concept Parabolic Antenna	3-43
3.3-7	Skewed Hinge Design	3-45
3.3-8	Petal Structural Assembly and Hinge Details	3-46
3.3-9	Deployment Synchronizer	3-49
3.3-10	Mesh Segment Installation	3-51
3.3-11	Mesh Reflector Characteristics	3-52
3.3-12	Inter-Petal Locks	3-55
3.3-13	Inter-Petal Lock - Preferred Concept	3-56
3.4-1	Shaping of Mesh Reflecting Surface	3-58
3.4-2	Master Tool	3-58
3.4-3	Assembly Bonding Fixture	3-62
3.4-4	Hinge and Latch Alignment Fixture	3-63
3.4-5	Measurement of Surface Deviations	3-67
3.5-1	Truss Feed Mast Weights	3-78
3.5-2	Truss Feed Mast Frequencies	3-79
3.5-3	Single Tube Feed Mast Analysis	3-81
3.5-4	Four Tube Feed Mast Weights	3-82
3.5-5	Four Tube Feed Mast Frequencies	3-83
3.5-6	Analysis of Quadruped Feed Mast Structure	3-84

LIST OF ILLUSTRATIONS

VOLUME THREE (Continued)

Figure	Title	Page
3.5-7	Quadruped Feed Mast Frequencies	3-85
3.5-8	Analysis of Tripod Feed Mast Structure	3-86
3.5-9	Tripod Feed Mast Frequencies	3-87
3.5-10	Reflector Petal Loading	3-94
3.5-11	Spacecraft, Injection, Motor and Adapter Structural Properties	3-94
3.5-12	Launch Integrated S/C - Analytical Model	3-96
3.5-13	Orbit Configuration - Mass Model	3-102
3.5-14	Preferred Configuration and Analytical Model	3-105
3.5-15	Petal Restraint and Stiffness	3-106
3.5-16	Mass Point Locations and Weights	3-107
3.5-17	YY Direction Mode Shapes	3-109
3.5-18	XX Direction Mode Shapes	3-110
3.5-19	Analytical Model - Orbit Configuration	3-116
3.5-20	Frequency and Mode Shapes - Orbit Configuration, Sheet One	3-118
3.5-21	Frequency and Mode Shapes - Orbit Configuration, Sheet Two	3-119
3.5-22	Frequency and Mode Shapes - Orbit Configuration, Sheet Three	3-120
3.5-23	Response to Single Finite Duration Pulse (Roll Correction Maneuver)	3-124
3.5-24	Response to Single Finite Duration Pulse (Yaw Correction Maneuver)	3-125
3.6-1	Yearly Change in Orbit Position Relative to Sun Vector	3-134
3.6-2	Petal Thermal Analysis	3-136
3.6-3	Relation of Thermal Analysis Nodes to Orbit Position	3-136
3.6-4	Feed Module Shadowing	3-137
3.6-5	Reflection Mesh Sunlight Blockage	3-139
3.6-6	Mesh and Antenna Hub Shadowing	3-141
3.6-7	Coordinate System for Thermal Analysis	3-142
3.6-8	Antenna Feed Shadowing	3-144
3.6-9	Beam Temperatures	3-147
3.6-10	Petal Beam Cross-Section	3-151
3.6-11	Mesh Standoff Fittings	3-151

LIST OF ILLUSTRATIONS

VOLUME THREE (Continued)

Figure	Title	Page
3.6-12	Beam Geometry	3-153
3.6-13	Petal Thermal Model	3-159
3.6-14	Radial Displacement Geometry	3-159
3.6-15	Deformation of Radial Member	3-159
3.6-16	Reflector Surface Mesh Geometry	3-165
3.6-17	Surface Mesh Chord Position	3-165
3.6-18	Feed Mast Geometry	3-167
3.6-19	Electrical Simulation, Uninsulated Mast	3-168
3.6-20	Electrical Simulation, Insulated Mast	3-168a
3.6-21	Temperature of Node 4, Uninsulated Mast	3-170
3.6-22	Temperature of Node 4, Insulated Mast	3-170a
3.6-23	Feed Mast Shadowing on Support "A"	3-171
3.6-24	Feed Mast Thermal Model	3-171a
3.6-25	Feed Mast Distortions	3-174
3.6-26	Passive Control Areas Average Temperature versus Dissipation	3-176
3.8-1	Volume Available for Measurement Equipment	3-187
3.8-2	Mirror Position above Camera	3-187
3.8-3	Converse Mirror below Camera	3-187
3.8-4	Concave Mirror below Camera	3-188
3.8-5	Sighting Angles	3-188
3.8-6	Effective Mesh Spacing	3-188
3.8-7	Composite Converse Mirror	3-192
3.8-8	Basic Four Camera Axial System	3-192
3.8-9	Full View Camera System	3-194
3.8-10	Normal Deflection Geometry	3-194
3.8-11	Ring Viewing Angles	3-194
3.8-12	Vidicon Image Dimensions	3-196
3.8-13	Central Circle in Vidicon Image	3-196
3.8-14	Radial and Circular Scan Patterns	3-198
3.8-15	Rim Marker Pattern	3-198
3.8-16	Modified Marker Coding	3-198
3.8-17	Reversed Marker Pattern	3-201
3.8-18	Marker Pattern without 1/2 Inch Plates	3-201
3.8-19	Pattern for Third Ring	3-202
3.8-20	Pattern for Second Ring	3-202

LIST OF ILLUSTRATIONS

VOLUME THREE (Continued)

Figure	Title	Page
3.8-21	Pattern for Central Ring	3-202
3.8-22	Pattern of Perfect Match of Image and Standard Negative	3-203
3.8-23	Pattern of Mismatch of Image and Standard Negative	3-203
3.8-24	Marking Pattern from Deformed Mesh Wires	3-207
3.8-25	Deformed Wires Positioned along a Parabola	3-207
3.8-26	Illumination by Columnar Light Sources	3-208
3.8-27	Illumination by Toroidal Light Sources	3-208

LIST OF ILLUSTRATIONS

VOLUME FOUR

Figure	Title	Page
4.1-1	Flat Plate Array, Two Degrees Of Freedom	4-3
4.1-2	Flat Plate Array, One Degree Of Freedom	4-3
4.1-3	Flat Plate Array, Fixed	4-3
4.1-4	Two Flat Plates Array, Fixed	4-4
4.1-5	Three Flat Plates Array, Fixed	4-4
4.1-6	Cylindrical Array, Fixed	4-4
4.1-7	Double Faced Flat Plate Array	4-5
4.1-8	Double Faced Two Flat Plates Array	4-5
4.1-9	Double Faced Three Flat Plates Array	4-5
4.2-1	Solar Cell Radiation Degradation	4-8
4.2-2	Power Loss Due To Radiation Effects	4-11
4.3-1	Nickel-Cadmium Battery Life	4-14
4.3-2	Energy Per Unit Weight For Various Batteries	4-17
4.3-3	Energy Per Unit Volume For Various Batteries	4-18
4.3-4	Capacity vs. Temperature For Various Cells	4-18
4.3-5	Silver-Zinc Battery Cycle Life	4-19
4.3-6	Silver-Cadmium Battery Cycle Life	4-19
4.3-7	Nickel-Cadmium Battery Cycle Life	4-20
4.3-8	Umbra and Penumbra Patterns For A Synchronous Equatorial Satellite	4-22
4.4-1	Recommended % Overcharge is Temperature	4-25
4.4-2	Overcharge Pressure Vs Current	4-25
4.4-3	Maximum Limiting Voltage Vs. Temperature	4-27
4.4-4	Tapered Charge Characteristic	4-27
4.5-1	Typical Experiment Evaluation Power Profile	4-29
4.5-2	Power Profile With Additional Experiments	4-29
4.5-3	Experiment Demonstration Maximum Demand Profile	4-29
4.5-4	Power System Weight Vs. Load Duration	4-29
4.5-5	Power System Block Diagram	4-37

LIST OF ILLUSTRATIONS

VOLUME FOUR (Continued)

Figure	Title	Page
5.3-1	Ascent Trajectories	5-6
5.3-2	Earth Track of Ascent Trajectory	5-11
5.3-3	Injection Station Longitude Variation	5-11
5.3-4	Effect of Launch Azimuth on Required Increase in Characteristic Velocity	5-14
5.3-5	High Altitude, Ellipstic Parking Orbit Characteristics	5-16
5.3-6	Earth Track of High Altitude Parking Orbit Ascent Trajectory	5-17
5.3-7	Ground Track of Ascent Trajectories	5-19
5.3-8	Spacecraft/Sun Orientation in Transfer Orbit	5-21
5.4-1	Payload and AIS Propellant Weight vs i_c (Burner II)	5-28
5.4-2	Payload and AIS Propellant Weight vs i_c (TE364-3)	5-28
5.6-1	Satellite Semimajor Axis Perturbation	5-42
5.6-2	Satellite Inclination Perturbation	5-42
5.6-3	Long Period Oscillation	5-44
5.6-4	Required Velocity Impulse per Year	5-46

LIST OF ILLUSTRATIONS

VOLUME FIVE

Figure	Title	Page
6-1	Reference Coordinate Frame (Nominal)	6-3
6-2a	Cell Orientation	6-13
6-2b	Cell Outputs	6-13
6-2c	Sun Sensor Signals	6-13
6-3	Meteoroid Extrapolations	6-29
6-4	Percent Open Area in Each Mesh Segment as a Function of Solar Incident Angle	6-41
6-5	Antenna Projected Surface Map	6-43
6-6	Projected Antenna Shaded Area Profile	6-44
6-7	Pitch Axis Solar Pressure Disturbance Torque	6-47
6-8	Roll Axis Solar Pressure Disturbance Torque Due to Antenna and Feed System	6-48
6-9	Roll Axis Solar Pressure Disturbance Torque Due to Fixed Solar Panels Only	6-49
6-10	Roll Axis Solar Pressure Disturbance Torque	6-50
6-11	Yaw Axis Solar Pressure Disturbance Torque	6-51
6-12	Hydrazine Thruster Output Efficiency	6-62
6-13	Liquid Hydrazine System Schematic	6-64
6-14	Block Diagram - Ascent Control	6-86
6-15	SCS Block Diagram	6-87
6-16	Phase Plane Plot Sun Acquisition - Pitch Axis	6-94
6-17	Phase Plane Plot Sun Acquisition - Yaw Axis	6-95
6-18	Phase Plane Plot Earth Acquisition Roll Axis	6-96
6-19	Phase Plane Plot Star Acquisition Yaw Axis	6-97
6-20	Open Loop Bode Plot - Roll Axis	6-99
6-21	Open Loop Bode Plot - Pitch Axis	6-100
6-22	Open Loop Bode Plot - Yaw Axis	6-101
6-23	SCS and Vehicle Dynamics Block Diagram	6-102
6-24	Roll Axis - Rigid Body Amplitude Response	6-104
6-25	Roll Axis - Rigid Body Phase Response	6-105
6-26	Pitch Axis - Rigid Body Amplitude Response	6-106
6-27	Pitch Axis - Rigid Body Phase Response	6-107
6-28	Amplitude Response Roll Axis - Flexible (.01)	6-108
6-29	Phase Response Roll Axis - Flexible (.01)	6-109
6-30	Phase Response Pitch Axis - Flexible (.01)	6-110
6-31	Phase Response Pitch Axis - Flexible (.01)	6-111
6-32	Amplitude Response Roll Axis - Flexible (.005)	6-112
6-33	Phase Response Roll Axis - Flexible (.005)	6-113
6-34	Amplitude Response Pitch Axis - Flexible (.005)	6-114

LIST OF ILLUSTRATIONS

VOLUME FIVE (Continued)

Figure	Title	Page
6-35	Phase Response Pitch Axis - Flexible (.005)	6-115
6-36	Phase Plane Plot Attitude Control During Station Keeping	6-118
6-37	Reliability Diagram	6-119
6A-1	Limit Cycle Impulse Requirements	6A-7
6A-2	Disturbance Torque Impulse Requirements	6A-8
6A-3	Maneuver Impulse Requirements	6A-9
6B-1	Micro-Rocket Applicability Thrust and Total Impulse	6B-4
6B-2	Micro-Rocket Applicability Thrust and Duty Cycle	6B-5
6B-3	Estimated System Weight as a Function of On Board Total Impulse	6B-7
6B-4	Reliability Comparison of Bipropellant or Monopropellant System	6B-8
6B-5	Hydrazine Plenum System Schematic	6B-10
6B-6	Liquid Hydrazine System Schematic	6B-11

LIST OF ILLUSTRATIONS

VOLUME SIX

Figure	Title	Page
7.1-1	Prime Focus Paraboloid Scanning Performance	7-3
7.1-2	Paraboloid Gain Loss as a Function of Beamwidths Scanned	7-4
7.1-3	Beam Scanning Capability of a Multi-Element Paraboloid Switching-Feed System	7-7
7.1-4	Beam Cross-Over Level as a Function of the Beam Scanning Increment	7-8
7.1-5	Cassegrain Antenna Gain Loss with Subdish Rotation	7-11
7.1-6	Radiation Characteristics of a Tapered Circular Aperture	7-16
7.1-7	Paraboloid Subtended Angle and Feed Size as a Function of the F/D Radio	7-18
7.1-8	S-Band Feed-Edge Taper	7-23
7.1-9	800 MHz Prime Focus Feed	7-24
7.1.10	100 MHz Prime Focus Feed	7-27
7.1-11	Spiral Antenna Monopulse Operation	7-29
7.1-12	Parabolic Antenna Gain Loss as a Function of the Blockage Ratio	7-34
7.1-13	X-Band Radiation Pattern	7-35
7.1-14	Antenna Test Range	7-38
7.1-15	Source Tower	7-39
7.1-16	Feed Support Mast	7-44
7.1-17	Paraboloid Assembly	7-45
7.1-18	Back View of Feed Support	7-46
7.1-19	Left Side View of Feed and Feed Support	7-47
7.1-20	Right Side View of Feed and Feed Support	7-48
2.1-21	Right Side View of Feed	7-49
7.1-22	Feeds, End View	7-50
7.1-23	Feeds, Side View	7-51
7.1-24	E-Plane Radiation Patterns, Frequency 4.6 GHz	7-52
7.1-25	E-Plane Radiation Patterns, Frequency 10.5 GHz	7-53
7.1-26	E-Plane Radiation Patterns, Frequency 12.0 GHz	7-54
7.1-27	E-Plane Radiation Pattern, Frequency 18.0 GHz	7-55
7.1-28	E-Plane Radiation Pattern, Frequency 29.6 GHz	7-56

LIST OF ILLUSTRATIONS

VOLUME SIX (Continued)

Figure	Title	Page
7.2-1	Transdirective Array	7-60
7.2-2	Butler Matrix Array - Block Diagram	7-64
7.2-3	Space Fed (Lens) Array - Block Diagram	7-67
7.2-4	Stripline Diplexer	7-69
7.2-5	Stripline Latching Phase Shifter	7-70
7.2-6	Corporate-Fed Array	7-72
7.2-7	Artist Conception of Corporate-Fed Array	7-75
7.2-8	Schematic of Microwave Subsystem	7-80
7.2-9	Detail of Feed Horn Assembly	7-83
7.2-10	Possible Configuration of 4 Channel Diplexer - Circulator Strip Line Module	7-86
7.2-11	Waveguide Latching Phase Shifter	7-89
7.2-12	Array Element Layout	7-94
7.2-13	Phased Array Patterns	7-95
7.2-14	Phased Array Beam Spacing	7-101
7.2-15	Block Diagram for Digital Beam Steering Unit	7-103
7.2-16	Schematic Diagram for Bit Driver	7-105
7.2-17	Plan View of Radiating Elements	7-107
7.2-18	Side View of Corporate-Fed Array	7-108
7.2-19	End View of Corporate-Fed Array	7-109
7.3-1	RF Power vs Ground Antenna Gain	7-116
7.3-2	ATS-4 Communications System	7-119
7.3-3	Frequency Generator	7-120
7.3-4	Monopulse and Phased Array X-Band Transfer Characteristics-Series 100	7-126
7.3-5	100 MHz Relay Transfer Characteristics-Series 200	7-127
7.3-6	X-Band Transponder Output-Reflector and Phased Array Transfer Characteristics-Series 300	7-128
7.3-7	800 MHz Relay Transfer Characteristics-Series 400	7-129
7.3-8	Filter Response	7-130
7.3-9	S-Band Data Link Transfer Characteristics-Series 500	7-131
7.3-10	X-Band Frequency Generator-Representative Transfer Characteristics-Series 600	7-132
7.3-11	Multipliers in Frequency Generator, Representative Transfer Characteristics-Series 700	7-135

LIST OF ILLUSTRATIONS

VOLUME SIX (Continued)

Figure	Title	Page
7A-1	Four Paraboloid Offset Feed Configuration	7-140
7A-2	Radiation Pattern of a 15-Foot Paraboloid 10 db Tapered Distribution	7-141
7A-3	Radiation Pattern Four Paraboloid Array	7-142
7A-4	Monopulse Radiation Pattern of the Four Paraboloid Array	7-144
7A-5	Four Paraboloid Array Scanning Performance	7-145
7B-1	Faraday Rotation as a Function of Frequency	7-152
7B-2	Attenuation between Arbitrarily Polarized Antenna Caused by Faraday Rotation AF - Axial Ratio	7-156
7B-3	Attenuation between Arbitrarily Polarized Antennas Caused by Faraday Rotation AR - Axial Ratio	7-158
7C-1	Helical Antenna Gain as a Function of Antenna Length	7-161
7C-2	Array Element Spacing as a Function of Array Element Gain	7-163

LIST OF ILLUSTRATIONS

VOLUME SEVEN

Figure	Title	Page
8.4-1	LF Phase Reading Interferometer	8-13
8.4-2	RMS Phase Difference Reading Interferometer Technique	8-16
8.4-3	RF Cross Correlation Interferometer Technique	8-19
8.4-4	Spread Spectrum Interferometer Technique	8-22
8.5-1	Resultant Nonambiguous Pattern after Correlation	8-26
8.5-2	Partial System Schematic of Cross Correlator Interferometer	8-30
8.5-3	Monopulse Space Angle RMS Error	8-31
8.5-4	RMS Space Angle Error Direct Phase Reading Interferometer	8-33
8.5-5	Direct Phase Reading Interferometer Relationship, Space Angle Element Separation, Unambiguous Interval vs D/λ	8-36
8.5-6	Interferometer Phase Error Due to Temperature Differential in Transmission Lines	8-37
8.5-7	Layout of Phased Array	8-45
8.6-1	Direct Phase Reading Interferometer	8-48
8.6-2	Interferometer	8-53
8.6-3	Horn Design	8-63
8.6-4	Interferometer Thermal Flow Diagrams	8-66
8.6-5	Interface between the SCS and Interferometer	8-69
8.6-6	Mode Selection and Phase Measurement	8-72
8.6-7	Timing Diagram for Phase Measurement	8-74
8.6-8	Arithmetic Unit for $\epsilon'_z + \epsilon''_z$ and $\epsilon'_y + \epsilon''_y$	8-78
8.6-9	Arithmetic Unit for $\epsilon'_x + \epsilon''_x$	8-79
8.6-10	Timing Diagram for Computational Instruction	8-81
8.6-11	Time Distribution of the Arithmetic Units	8-82
8.7-1	System Model	8-87
8.7-2	Simplified Block Diagram of Direct Phase Reading Electronics	8-88
8.7-3	Basic Interferometer Relationship	8-90
8.7-4	Geometrical Relationship of Spacecraft Position and Ground Station	8-92
8.7-5	Error in Count vs θ_s	8-96
8.7-6	Refraction Effects	8-97
8.7-7	Atmospheric Effect on Elevation Angle	8-98
8.7-8	Atmospheric Effect on the Slant Range Difference	8-99

LIST OF ILLUSTRATIONS

VOLUME SEVEN (Continued)

Figure	Title	Page
8.7-9	Spacecraft Coordinate System	8-105
8.7-10	Pitch Axis 3 σ Error vs Pitch Angle, θ	8-107
8.7-11	Yaw Axis 3 σ Error vs Pitch Angle, θ	8-108
8.7-12	Vector Diagram of Satellite - Ground Station Geometry	8-109
8.7-13	Orientation of R_s	8-113
8B-1	ERP vs SNR	8-140
8C-1	Space Angular Error ($\Delta \theta_m$) vs Antenna Separation (D/λ) for Different Mutual Couplings (C)	8-142
8C-2	Space Angle Error Due to Mutual Coupling - Coarse Antenna Pair	8-143
8C-3	Comparison of Antenna Elements - Mutual Coupling	8-145
8D-1	Elliptically Polarized Interferometer Antenna Pair with Elliptically Polarized Incoming Wave	8-149
8D-2	Phase Angle Error vs Axial Ratio Inequality	8-152
8D-3	Phase Angle Error vs Ellipse Tilt Angle Inequality	8-155
8D-4	Phase Angle Error vs Roll Angle (δ)	8-160
8D-5	Phase Angle Error vs Pitch Angle (θ)	8-161
8E-1	Elliptically Polarized Plane Wave	8-166
8E-2	Elliptically Polarized Plane Wave Incident at Angles θ, δ	8-167
8E-3	Receive Antenna with Inclined Polarization Ellipse	8-168
8F-1	Switched Signal Lines	8-174
8F-2	Switched Oscillator Lines	8-175
8F-3	Switched IF Lines	8-176
8F-4	Switched Multipliers	8-177
8H-1	Phase Error Distribution at Start of Count	8-186
8H-2	Phase Error Distribution at End of Count	8-186
8H-3	Phase Error Density Function	8-186
8I-1	Interferometer Illumination	8-188
8I-2	Satellite Orientation	8-193
8J-1	Geometry for Range and Range Rate Analysis	8-201

LIST OF ILLUSTRATIONS

VOLUME SEVEN (Continued)

Figure	Title	Page
9.1-1	Onboard System Data Flow, Interfaces to Ground Equipment	9-4
9.1-2	Ground Station Data Flow; Interfaces to Spacecraft and Other Ground Stations	9-5
9.2-2	Basic Commutation Configuration	9-15
9.2-2	Data Handling System Configuration	9-18
9.2-3	Telemetry Data Transmission System	9-25
9.2-4	Telemetry Data Handling and Transmission Configuration	9-33
9.2-5	Block Diagram of Basic Telemetry Receiver	9-38
9.3-1	Command Word Structure	9-51
9.3-2	Command System	9-54
9.3-3	Command Decoder	9-55

PREFACE

This report covers the efforts of Fairchild Hiller Corporation and its team of subcontractors on NASA Contract (NAS-W-1411). The team organization and responsibilities during the study effort are shown on the accompanying chart. The report is divided into eight volumes, as follows:

Volume 1	Summary
Volume 2	Systems Analysis
Volume 3	Vehicle Engineering
Volume 4	Power System
	Orbital Analyses, Propulsion and Guidance
Volume 5	Stabilization and Control
Volume 6	Communication Experiments
Volume 7	Radio Interferometer Experiment
	Telemetry and Command Systems
Volume 8	Program Budgetary Costs and Schedules

ATS-4 TEAM ORGANIZATION

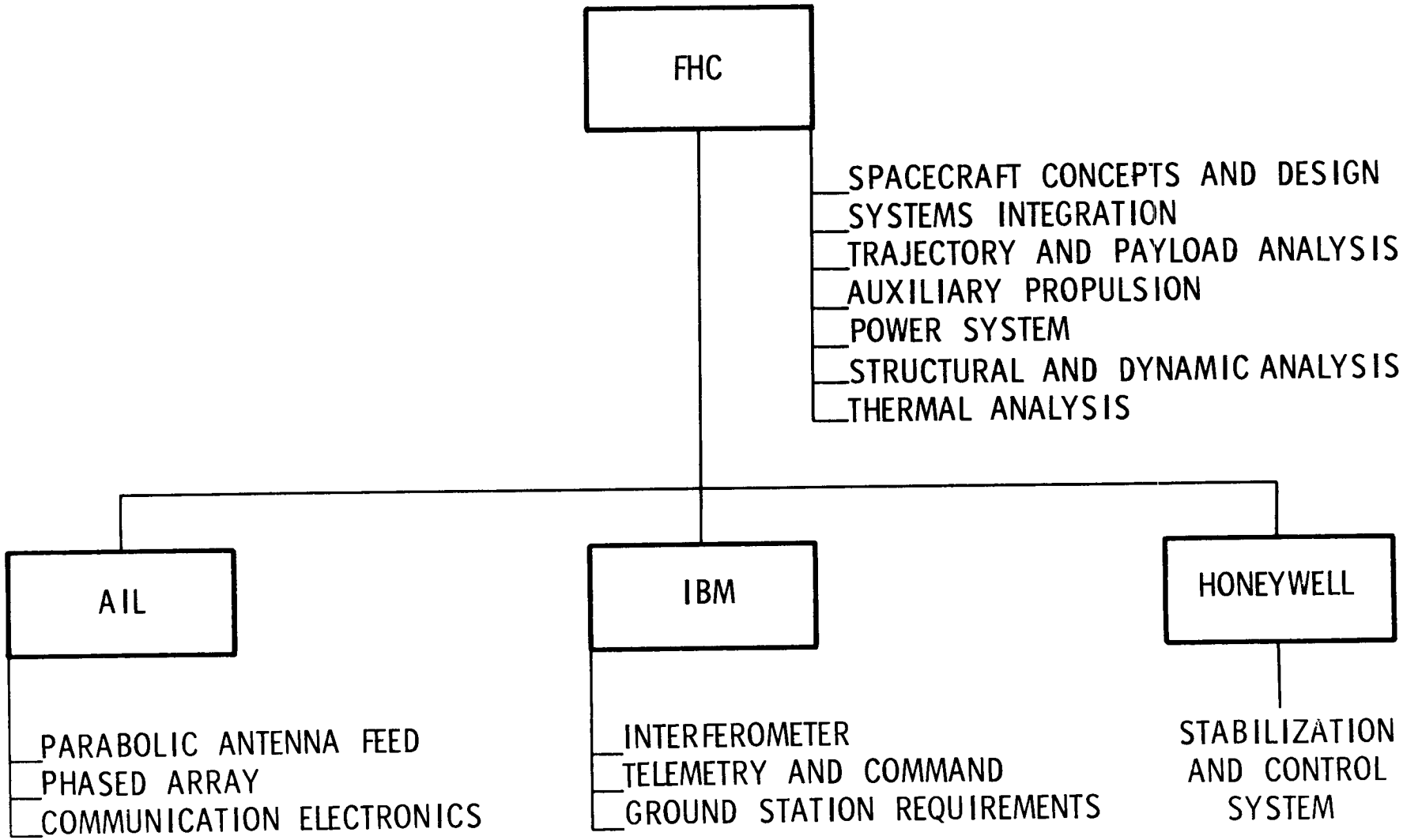

A-1

8.0 RADIO INTERFEROMETER EXPERIMENT

8.1 INTRODUCTION

Results of this study indicate that a state-of-the-art direct phase reading X-band radio interferometer is capable of determining spacecraft attitude (pitch and roll) to an accuracy of better than $\pm$ 0.05 degree, which exceeds the requirements for ATS-4. This accuracy can be improved further by incorporating filters which are used in conjunction with the associated processor. High accuracy is obtained by employing signal-to-noise ratios of 30 dB or greater and by using a superinsulated aluminum box beam for the interferometer arms (which minimizes phase errors that can result from bending or expansion). The interferometer arm assembly is the most critical subassembly in the interferometer. However, preliminary analysis indicates that by applying well-known mechanical and thermal design techniques, residual inaccuracies can be made acceptably small. Instrumentation errors, such as electrical phase errors due to variation in cable length, are reduced by performing amplification and conversion near the antenna location.

Demonstration of a precision radio interferometer as a sensor for spacecraft attitude and/or antenna pointing reference is feasible for the 1969-1970 time period. The ATS-4 interferometer is the next logical step in evolution of this technology to provide precision, long life space hardware.

Flying a radio interferometer experiment is particularly attractive in conjunction with precision stabilization and control equipment which can

exploit the high resolution and accuracy of the interferometer. Integrated with large aperture antennas for communications relay, the interferometer can be used as an attitude and pointing reference. In addition, the presence of a monopulse system with its precision pointing capability permits very accurate evaluation of the interferometer.

8.2 STUDY APPROACH

The purpose of this study is to define a realizable RF interferometer whose performance characteristics will satisfy the ATS-4 mission objectives based on the following constraints and requirements.

Constraints and Requirements

- Spacecraft Pointing Mode Accuracy $\pm 0.1^{\circ}$
- Spacecraft Slewing Mode Accuracy $\pm 0.5^{\circ}$

  (The above requirements are those imposed on the stabilization and control system.)
- Field of view: $\pm 17.5^{\circ}$
- Interferometer Design Goal

  Accuracy in determining satellite attitude - in roll and pitch axis. $\pm 0.05^{\circ}$
- The interferometer antenna system will operate in a frequency range consistent with the attainment of the maximum resolution and accuracy performance characteristics required for the spacecraft attitude control system.
- The selection of a preferred approach will consider interfaces with other spacecraft experiments, power, telemetry and structural subsystems in addition to ground support elements.

Study Tasks

A broad review of angle measuring concepts was made with particular emphasis placed upon interferometer techniques applicable to the ATS-4 satellite and its mission. Study of the techniques found in the

literature and practice produced a large number of feasible interferometer system designs potentially capable of meeting or exceeding the performance requirements of the ATS-4 mission. However in view of the total mission requirements and constraints a selection was made eliminating all but four of the total number of systems. Parametric studies of these systems were carried to the point of obvious incompatibility with the spacecraft or performance limitation. One particular system, the "Direct Phase Reading Interferometer", emerged as the leading candidate or "preferred system". Finally, a detailed design of this system was made.

The study tasks can be grouped into the following major categories.

- Identification of candidate interferometer concepts
- Selection of most realizable interferometer systems from the candidate concepts
- Evaluation of the selected systems and identification of the preferred concept
- Design of the preferred interferometer system
- Error analysis of the preferred system
- Conclusions and recommendations

8.3 CANDIDATE INTERFEROMETER CONCEPTS

Concept generation began with a literature search which included a large number of relevant technological areas (see Section 8.9), such as

1. Navigation
   a. Own position determination from signals received from distant stations (both cooperative and non-cooperative types)
   b. Surveillance type position determination of traffic from ground, or air based station, or surveillance satellite.
2. Target Detection and Location
   a. Pencil beam radars (electrical and mechanical scan), including monopulse radar, other sequential and simultaneous lobing systems)
   b. System using Doppler plus angle measuring
   c. Spread spectrum systems
   d. Triangulation systems
3. Astronomy (Section C of the Bibliography)
   a. Mills Cross, Christiansen and other similar "unfilled aperture" interferometers.
   b. Brown, Hanbury and Twiss type interferometers.
4. Special radio interferometers (Section D of the Bibliography)
   a. Direct phase reading
   b. Cross correlation
   c. Optical type signal processes.

Areas 2a, 2c, 4a, 4b, and to some extent 4c offered potentially feasible system designs capable of meeting the ATS-4 requirements. Concepts from these areas were detailed. Block diagrams and functional descriptions are given in paragraph 8.4, "Candidate Interferometer Systems".

In addition to the systems which were surveyed in literature study, data on components, especially critical components, error sources, and special data processing systems were covered. Items requiring development, new designs, or no difficulty in procurement were identified for each system. This information was used in selection of the preferred system.

The literature search was directed toward clarifying and categorizing basic principles of high resolution angle determination. The objective was to identify the most effective basic principle of measurement and to compare and optimize various techniques of implementation.

Interferometry is a classical field of optical technology and derives by definition from the use of radiation interference to obtain measurements of distances, frequencies, wavelengths, angles, alignments of surfaces, collimation of optical devices, and other metric applications. The essential principle involves the vectorial addition of two or more signals (light waves, radio waves) arriving from different immediate sources (e.g. two slits, two radio antenna, two prisms, two mirrors, etc.) in such a way that one or both of the source positions is related to the angle or distance measured and in such a way that the sum of the signals can be sensitively detected.

The term interferometry has often been broadened in the literature to include any techniques of distance or angle measurement wherein the

measurements are obtained by detecting the differential arrival times of distant signals detected by two reasonably closely located receivers. A configuration of two such receivers (such as in the Brown-Twiss interferometer arm" bears a physical resemblance to the classical two-slit diffraction interferometer sometimes used in optical interferometry. For this reason, and others, the term is broadly applied, not only to two receiver systems but to many "unfilled aperture" systems.

Direct "Interference" of the received signals need not be the essential signal detection process. The "Direct Phase Reading" interferometer does not add the incoming signals to produce interference but first converts them to lower frequencies and then measures the difference in phase by detecting time difference between "cross-over" points. Thus in a general sense, the direct phase reading interferometer and direct interference interferometers (signal adding types) are identical in that they measure the "coincidence" of two signals. Thus, perhaps it does no violence to the term "interferometry" and its definition if all such variations of usage are included, the exception being full "imaging" of the source by "filled" aperture systems.

More than a dozen potential candidate techniques for the interferometer were selected from those reviewed. These were tabulated (see the first column of Table 8.3-1) and analyzed as to their essential features such as Antenna Type, Signal Handling Process, and Signal Handling Techniques. Table 8.3-1 indicates two basic groups of Interferometer Systems based upon use of either a single antenna element pair or upon multiple pairs of elements. Signal Handling processes are principally Circuit Processing and Direct Processing of Received Radiation.

TABLE 8.3-1 CANDIDATE INTERFEROMETER TECHNIQUES

Interferometer System	Antenna Array Type	Signal Handling Process											
		Circuit Processing of Received Signals								Direct Processing of Received Radiation			
		RF Phase Reading		IF and LF Phase Reading		Signal Adding		Spread Spectrum (PRN, Swept Freq., Etc.)		Signal Adding (Cross-Correlation of Multiple Element, Single Freq. Sys.)		Spread Spectrum (PRN, Swept freq., etc.)	
		Closed Phase Loop	Open Phase Loop	Closed Phase Loop	Open Phase Loop	Closed Loop Beam Search	Open Loop Autom. Alarm	Closed Loop Spectrum Search	Open Loop Spectrum Band Guard	Open Phase Loop - Intensity Pattern Search			
										Elec.	Mech.	Elec.	Mech.
A Systems	Single Element Pair Interferometers												
1. Closed Loop, RF Phase Reading		X											
2. Open Loop, Phase Reading			X										
3. Closed Loop, IF, LF Phase Reading				X									
* 4. Open Loop, IF, LF Phase Reading					X			X	X				
B Systems	Multiple Element Interferometers												
1. Closed Loop RF, RMS Phase Difference Reading		X											
* 2. Open Loop, RF, RMS Phase Difference Reading			X										
3. Open Loop, IF, LF, RMS Phase Difference Reading				X									
4. Closed Loop, IF, LF, RMS Phase Difference Reading					X								
* 5. Beam Search, Cross Correlation						X	X						
6. Sequential and Simultaneous Lobing						X	X						
* 7. Spread Spectrum, Signal Search								X					
8. Spread Spec., Spectrum Band Guard									X				
9. RF Imag. Single Freq. Source (A)										X			
10. RF Imag. Single Freq. Source (B)											X		
11. Matched RF Rad. Filter (A)													X
12. Matched RF Radiation Filter (B)													

*Selected Interferometer Concepts (See Section 8.4)

The former divides into Direct Phase Difference reading circuits, Signal Adding circuits (cross correlation, monopulse, simultaneous lobing, sequential lobing), and Spread Spectrum Circuits (FM altimeter techniques, other modulation techniques, dual frequency systems, etc).

Tabulation of concepts as in Table 8.3-1 is a logical step toward finding new approaches to interferometer design. For example, "signal adding" is conventional (e.g. grating interferometers in optics) but is less common with radio frequencies. However, the existence of signal adding processes with circuits and with optics suggests that the analogue of this process can be obtained at radio frequencies. As is commonly known this analogue has been realized in a number of zoned, or grating like antennas or antenna arrays, wherein the radiation intercepted by each antenna element is guided to a common adding point (focus, first order diffraction zone, or other equivalent term).

A second example of such system origination is the potentially feasible technique of using a radio, grating interferometer to separate the spectrum of a spread spectrum (e.g., wide deviation fm) signal into spatially separate line images of the ground transmitter. Position of the line images in the plane of principal focus would be space angle dependent and thus sensitive to direction of arrival of the signal.

Table 8.3-1 denotes the signal handling processes of each tabulated system by an "X". However, by the reasoning shown by examples above, many other alternate concepts were considered. Most were eliminated as impractical for the ATS-4 or not realizable because of necessary hardware developments.

The literature search concluded with:

1. A fairly comprehensive bibliography of interferometry for special reference.
2. A number of potentially feasible systems for the ATS-4.
3. A number of alternate system concepts and a logical approach to their synthesis. Confidence was gained that some of the most important design concepts were exposed and the likelihood of overlooking a significant technique was considerably reduced.

8.4 CANDIDATE INTERFEROMETER SYSTEMS

The interferometer concepts produced through literature search were critically reviewed according to certain selection criteria and certain outstanding ones were block diagrammed and detailed in subsystem function for further parametric study and evaluation.

8.4.1 Selection Criteria

A number of selection criteria were produced to aid evaluation of the many interferometer concepts. The principal criteria are given in Column 1 of Table 8.4-1, and parameter values for four selected systems are given in the right hand columns. Some of the important criteria, such as Spacecraft Considerations involve many complex factors. In these cases, the systems were ranked in relative value as objectively as possible. Table 8.4-1 shows only the concepts (systems) retained for further study.

8.4.2 System Block Diagrams

Figures 8.4-1 through 8.4-4 are block diagrams of the selected systems. The system descriptions are given in Tables 8.4-2 through 8.4-5. Each table is comprised of two parts

Part A, summarizing the system characteristics

Part B, a detailed description of the signal flow and operation of the system.

TABLE 8.4-1 SELECTION CRITERIA FOR INTERFEROMETER CONCEPTS

SYSTEM SELECTION CRITERION	DIRECT PHASE READING INTERFEROMETER	RMS PHASE READING INTERFEROMETER	RF CROSS CORRELATION INTERFEROMETER	SPREAD SPECTRUM INTERFEROMETER
Performance Feature	Rank 3	Rank 2	Rank 1	Rank 4
1 S/N Requirement at Antenna	10 log kTB + 40 dB margin	10 log kTB + 34 dB margin estimated on basis of error averaging technique	10 log kTB + 6 dB margin	10 log kTB + 12 dB margin (can use very narrow band-locked loop circuits)
2 Ambiguity Signal Rejection	Has multiple space angle ambiguities, requires auxiliary antenna elements or frequencies for resolution of ambiguities	Type discussed has no space angle ambiguities	18 db (using array phasing techniques and peak clipping)	Resolves ambiguities by auxiliary antenna element and circuitry
3. RFI Rejection (Earth Transmitting)	None except high operating S/I at input	Partially rejects RFI due to 1) high operating S/I; 2) data averaging technique	18 dB	May reject off-frequency RFI by virtue of narrow band techniques
4 External Noise Rejection	None except high operating S/I at input		18 dB	May reduce out-of-band noise by virtue of narrow band techniques
5 Space Angle Resolution	0.1°	Better than 0.1°	0.1°	Better than 0.1°
6 Field-of-View (and FOV search requirements)	Determined by single element beam width (~20°)	Determined by single element beam width (~20°)	Determined by single element beam width (~20°); requires serial or parallel space angle search by beam sweeping; or may use multiple parallel automatic alarm circuits	Determined by single element beam width (~20°) - does not require search
7 Single Angle Measurement Time	Milliseconds for open loop type 10's of ms for closed loop types	10-100 milliseconds	Milliseconds	Milliseconds (depends only on response time of frequency measuring circuit)
Design Simplicity	Rank 2	Rank 4	Rank 3	Rank 1
1 Antenna Type (required number of antenna elements)	Two arms of minimum length, $D = (\lambda/2\pi)(\Delta\phi/\Delta O)$, carrying one antenna element at each end	Multiple elements on crossed interferometer arms	Multiple elements on crossed interferometer arms - No. up to D/λ	Either two crossed pairs with ambiguity resolving elements, or may use multi-elements
2 Signal Handling Type	Direct phase reading	Direct phase reading plus cross-correlation of phase differences	Signal adding and cross correlation of array element signals	Direct phase reading
3 Computer Requirements (for phase measurement)	None	Four single computers and one logic net in "phase Gradient Computer" required	None	None
4 Equipment Requirements Summary (Major)	2-3 RF frequency converters 2-3 IF amplifiers 2-3 HF counters 1 high precision clock	4 computers 1 frequency measuring circuit as in preceding column	Phase controllers for each element Single RF frequency converter Single IF Auxiliary signal search circuitry.	2 RF to IF mixer-amplifier chains - phase stabilities in L. O.'s not essential 2 audio frequency meters (counter type)
State-of-the-Art	Rank 1	Rank 3	Rank 2	Rank 4
Operational Considerations	Rank 2	Rank 3	Rank 1	Rank 4
Spacecraft Considerations	Rank 2	Rank 4	Rank 3	Rank 1

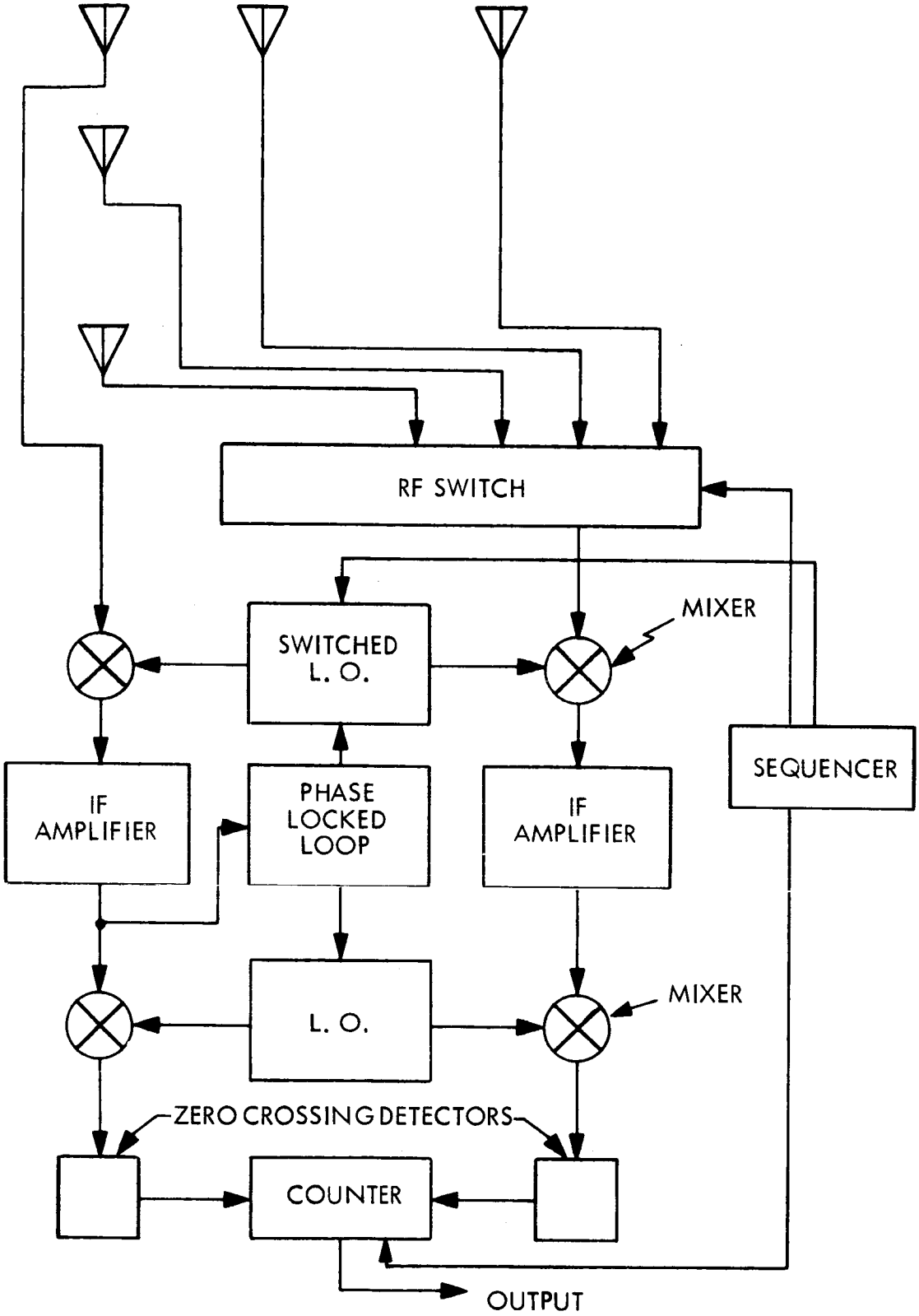

Figure 8.4-1 LF PHASE READING INTEROMETER

Table 8.4-1

(A)

IF, LF Direct Phase Reading Interferometer

Operating Principles

- Receives signal power at a known point in wave front relative to other elements.
- Produces I-F signal in each antenna element channel. Preserves phase.
- Measures phase difference by counting cycles of internal 36MHz clock and provides count proportional to phase.

Implementation - System configuration consists of following subsystem components, given in the order of signal flow from received RF signal to final computed space angle.

- Multi element antenna array
- Multiple channel RF to LF converters
- Electronic Counter
  - Zero crossing detector
  - Clock
  - On-off gate

Signal Flow and System Function

- Receives signal power at separate antenna elements.
- Produces an I-F signal in each antenna element signal channel.
- Sends I-F signal to electronic counter
  - Detects zero crossing of I-F signals
  - Turns on then off 36 MHz clock signal by means of zero crossing detector outputs
  - Counts clock cycle between zero crossing
- Count output proportional to phase.

TABLE 8.4-2(B) SYSTEM A4 - OPEN LOOP IF, LF PHASE READING

Device	Device Characteristics	Device Function	Subsystem Function	Subsystem Characteristic
1 Ground Stations	requisite power output and frequency stability	produce plane wave front at frequencies f_1 and f_2		
2 Antenna Element	15-20° beamwidth Narrow bandwidth. Fixed Phase Center for variable incidence angle and polarization	to receive signal power at a known point in wave front relative to other elements		produces signals indicative of spatial orientation (angle of arrival) of wave front
3 RF Mixer	non-linear impedance at RF	to produce IF signal		produces IF signal at difference frequency
4 Multiplier Chain(s)	stable output amplitude at frequency f_1 LO (or f_2 LO), low spurious output	multiples 30 MHz signal to f_1 LO (or f_2 LO)		
5 RF Switch 4-Throw	single pole, 4 throw, low insertion loss, high isolation	connects mixer (3) sequentially to antenna elements		enables measurements with vernier and coarse antenna ambiguities
6 RF Switch 2-Throw	single pole, 2 throw, low insertion loss, high isolation	connects mixers (3) sequentially to multiplier chains (f_1 LO, f_2 LO)		enables measurement of two different ground stations for 2-axis angle reading
7 Phase Locked Loop	requisite gain and phase margin to yield desired acquisition time and bandwidth at the chosen switching rate	locks voltage controlled oscillator (VCO) to IF signal		enables LO switching while preserving constant IF frequency; gives narrow IF bandwidth to reduce noise while maintaining phase stability
8 IF Amplifier	amplifies IF signals to requisite level with narrow pass band	amplifies IF signals to requisite level with narrow pass band		
9 IF Mixer	non-linear impedance at IF phase stable	to produce IF (100 kHz) signal		produces IF signal at difference frequency between IF (30 MHz) and IF LO (29.9 MHz)
10 Offset Oscillator	generates stable IF signal	provides 100 kHz signal to generate IF LO		
11 IF LO Mixer	non-linear impedance at IF phase stable	generates local oscillator signal for IF mixer (9)		produces IF LO signal at difference frequency between IF (30 MHz) and Xtal. osc. (100 kHz)
12 Xtal. Filter 29.9 MHz	narrow bandwidth; high center frequency stability; low spurious outputs	selects proper IF LO mixer (11) sideband		
13 Filter	narrow bandwidth; high center frequency stability; high phase stability	narrows mixer output bandwidth		reduces system noise by reducing post detection bandwidth
14 Electronic Counter	counts cycles between zero crossings	measures time interval between IF signals	measures phase difference between reference antenna signal and coarse (or vernier) signal	measures phase difference by counting cycles of internal 36 MHz clock

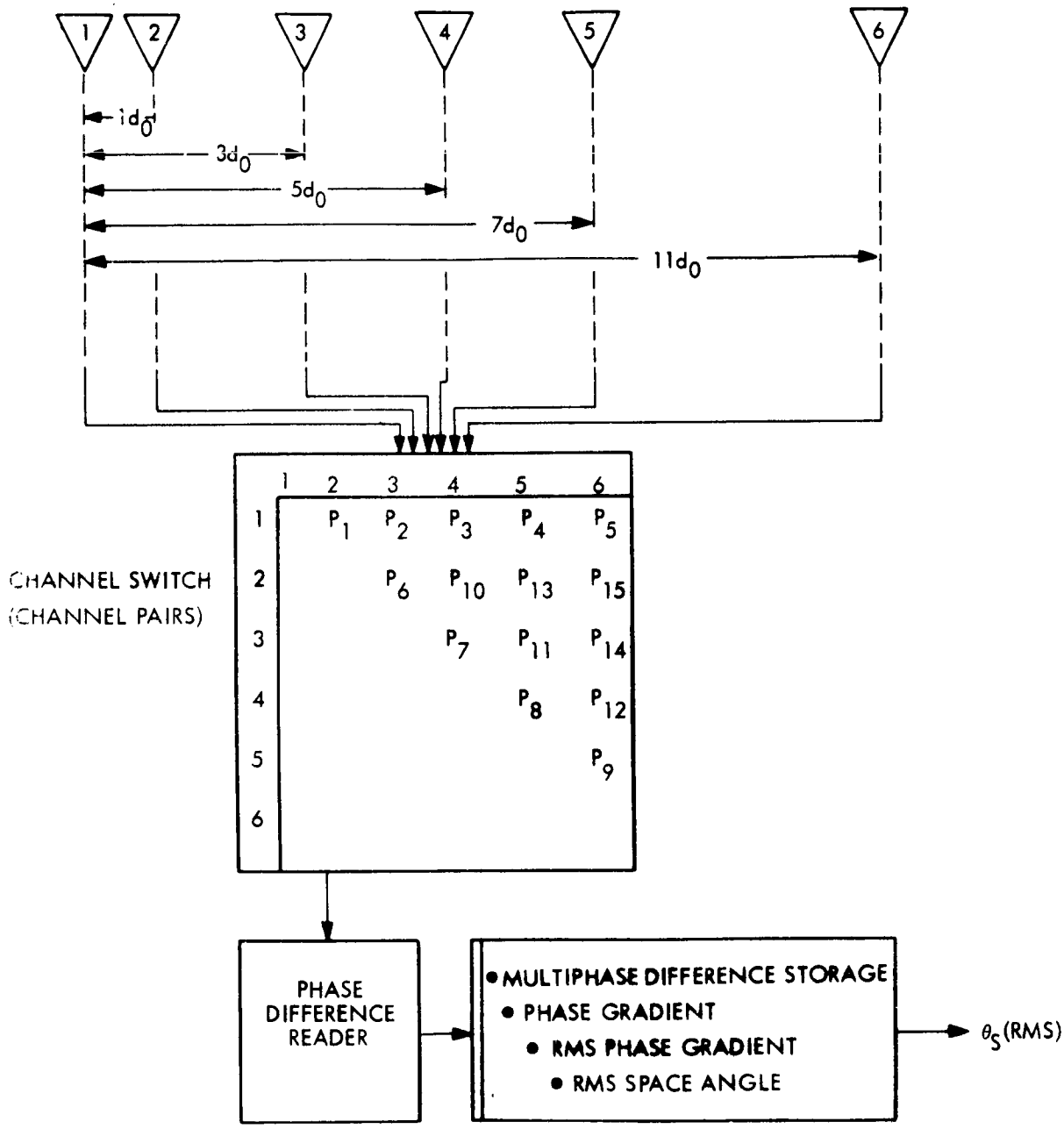

FIGURE 8.4-2 RMS PHASE DIFFERENCE READING INTERFEROMETER TECHNIQUE

Table 8.4-2

(A)

RF, RMS Phase Reading Interferometer

Operating Principle

- o Samples the radiation of wave front at prime number distances along a known line (interferometer arm) of mechanical reference.
- o Measure phase differences and transmit them to Multi-phase Difference Computer.
- o To obtain an unambiguous electrical phase gradient function dependent (or directly related to) upon wave front angle of arrival by least squares or other correlation technique.

Implementation - System configuration consists of following subsystem components, given in the order of signal flow from received RF signal to final computed space angle.

- o Linear multi element array.
- o RF Phase Difference Reader (device can be LF or IF Phase Difference Reader).
- o Multi Phase Difference Computer
- o Phase Gradient Computer
- o RMS Gradient Computer
- o Space Angle Computer

Signal Flow and System Function

- o Elements receive signal power at known points in wave front, relative to other elements.
- o Antenna Element Switch switches all non-redundant pairs, P , of antenna element outputs to the RF Phase Difference Reader as indicated in Switching Matrix, Figure 2.
- o RF Phase Difference Reader measures differences and transmits them to multi phase difference to multi-phase difference computer.
- o Computes and stores a matrix of all element pair phase differences.
- o To obtain a unique linear fit of $k_n = \emptyset / d$ for all $\emptyset_n$. Determines phase gradient having least probable error. Computes space angle.

TABLE 8.4-3(B)
SYSTEM B2 - OPEN LOOP RF, RMS PHASE DIFFERENCE READING

Device	Device Characteristics	Device Function	Subsystem Function	Subsystem Characteristic
1 Antenna Element(s)	15-20° beam width - narrow band - fixed phase center for variable incidence angle and polarization	To receive signal power at known point in wave front, relative to other elements	To sample radiation of wave front at prime number distances along a known line of mechanical reference	Produces signals indicative of spatial orientation (angle-of-arrival) of wave front
2 Antenna Element Switch (switch may be alternately in the RF or IF circuitry)	Two pole (channel), multi-throw switch	To switch all non redundant pairs of antenna element outputs to the RF Phase Difference Reader as indicated in Switching Matrix	To sequence all antenna elements for all relative phase difference measurements	
3 RF Phase Difference Reader (device can be LF or IF Phase Difference Reader)	Measures (by clock cycle counting) phase difference between signal pairs	To measure phase differences and transmit them to Multi-phase Difference Computer		
4 Multi-Phase Difference Computer	Computes pairs of phase differences, ϕ, for all combinations of elements. Stores all computations for each computation sequence.	To compute and store a matrix of all element pair phase differences		
5 Phase Gradient Computer	1) Computes a value "k" for all phase differences ϕ, by $\phi_n = k_n \ell$ where ℓ = 1d, 3d . . . 11d and d is unit spacing of antenna elements 2) Multiplies ϕ_n by integer values to obtain equal values of k_n (except for measurement error differences)	To obtain a unique linear fit of $k_n = \phi/\ell$ for all ϕ to $k = (\phi/\ell)^n$ except for measurement error difference in ϕ. Prime number element spacing makes unique fit possible for useful field-of-view, space angle.	To obtain an unambiguous electrical phase gradient function dependent (or directly related to) upon wave front angle of arrival	
6 RMS Gradient Computer	RMS computer; or "least squares fit" computer, or other function to be determined for computation economy and for error reduction	Determine phase gradient having least probable error	To obtain accurate phase gradient for space angle computation	
7 Space Angle Computer	Solves space angle equation	Computes space angle		Derives unambiguous space angle from ground station signal

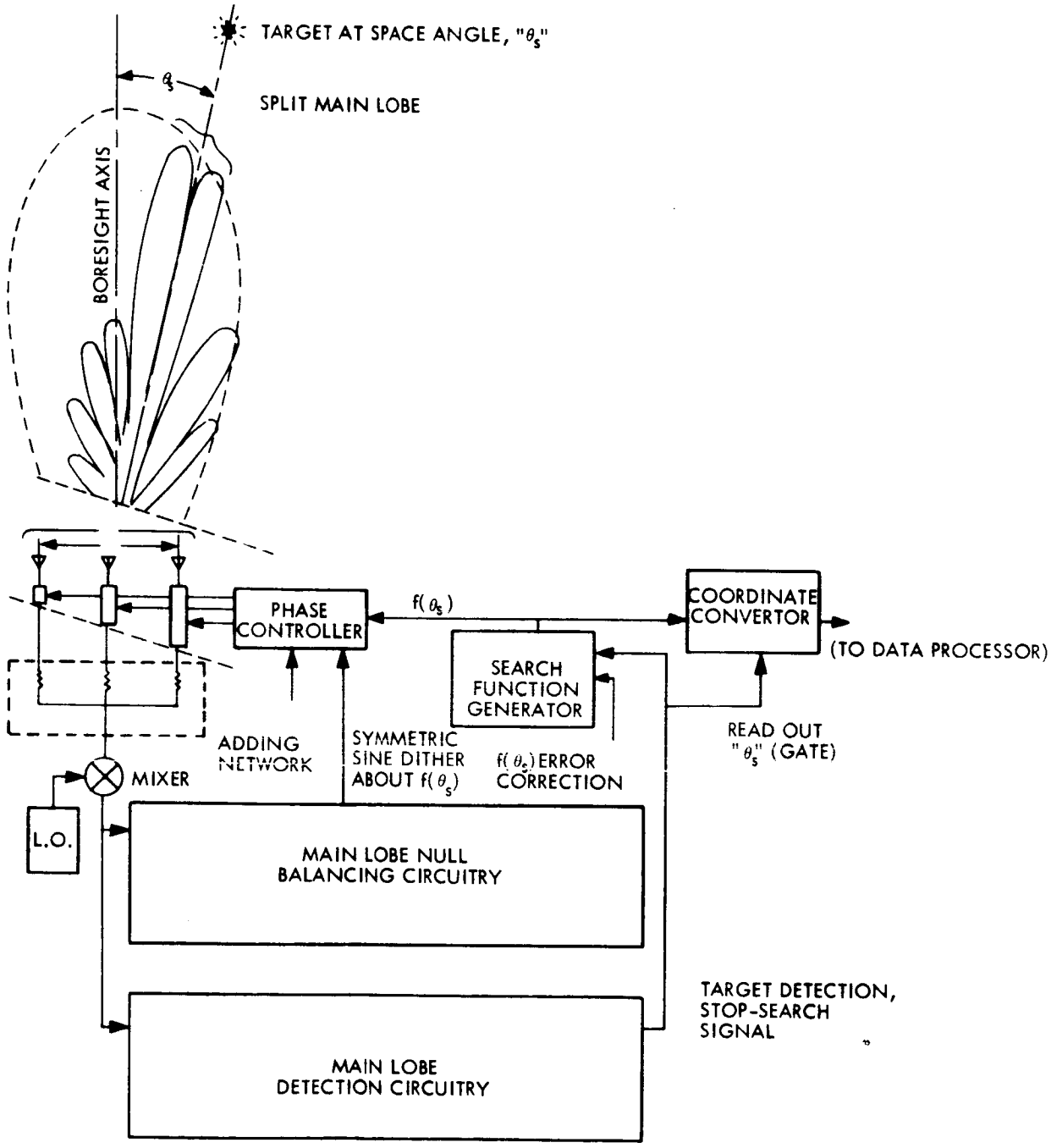

FIGURE 8.4-3 RF CROSS CORRELATION INTERFEROMETER TECHNIQUE

Table 8.4-3

(A)

Beam Search, Cross Correlation Interferometer Technique

Operating Principle

- Receives signals at multiple points in wavefront by means of antenna array.
- Generates an internal signal whose space angle sensitivity is the pattern f(Ø) of the array.
- Searches for target by controlling direction of maximum array sensitivity; and value of maximum sensitivity; f(Ø) max.
- Locates target in terms of f(Ø) max by searching.

Implementation - System configuration consists of following subsystem components, given in the order of signal flow from received RF signal to final computed space angle.

- Multiple Elements in an antenna array.
- Correlator
  - RF summing network; Mixer, Filter or Synch detector
- Ground Station Search Subsystem (onboard)
  - Search Generator; Phase control of antenna element signals; Target Detection Subsystem.

Signal Flow and System Function

- Receives and adds separate antenna signals.
- Generates sensitivity pattern f(Ø) by forming the product and integrating separate antenna signals.
- Controls phase function f(Ø) to control space angle of maximum sensitivity by proportional control of phase delay elements in each antenna circuit.
- Varies f(Ø) through field of view to locate target.
  - Stops search when ground station search subsystem gives signal above threshold.

TABLE 8.4-4(B)
SYSTEM B4 - BEAM SEARCH, CROSS CORRELATION INTERFEROMETER TECHNIQUE

Device	Device Characteristics	Device Function	Subsystem Function	Subsystem Characteristic
1 Single Antenna Element	Single low gain - low directivity pattern	Receives signal at single point in wave front		
2 Multiple Elements In an Antenna Array	Multiple low gain - low directivity	Receives signals at multiple points in wave front		
3 RF Summing Network	Linear coherent addition of RF fields	Adds separate antenna signals	Performs correlation of signals in time	
4 Mixer	Square law, or higher order response	Obtains product of signals		Provides many higher order signal products
5 Filter or Synch Det.	Band pass at IF; or, low pass at video	Selects squared or higher order terms and integrates signal over period of 2T		Selects a signal whose space angle sensitivity is the pattern of the array
6 Phase Control of Antenna Element Signals	Produces currents necessary to control phase delay elements in accordance with $f(\theta_s)$, $f\left(\frac{d\phi}{dD}\right)$	Controls phase function for space angle of maximum sensitivity. Controls phase function $f\left(\frac{d\phi}{dD}\right)$ to obtain maximum directivity.	Performs cross correlation of $f\left(\frac{d\phi}{dD}\right)$ with arriving phase front in space	Provides means to control direction of maximum array sensitivity; and value of maximum sensitivity
7 Search Generator	Ramp voltage generator	Varies $f(\theta_s)$ through field of view to locate target. Stops search when signal detection indicated.		Locates target in terms of f( ) when 7 gives indication
8 Threshold Detector	Voltage sensitivity gate thresholds the received signals	Selects signal return above arbitrary threshold level; level set between side lobe and maximum gain levels	Detects peak of cross correlation signal	Limits reception of signals to maximum lobe only; rejects side lobe RFI, noise, ambiguous response
9 Coordinate Convertor	Solves equation $\theta = f(v)$, where "v" is phase control voltage	Transforms phase control voltage to space angle	Interfaces between system measurement coordinates and attitude control coordinates	Provides space angle
10 Balancing Circuit for Main Lobe Nulls	1) Dithers 6 2) Detects unequal amplitudes of main lobe nulls 3) Sends nulling control signal to 7	To center 7 and 6 with respect to target signal. Main lobe peak lies midway to nulls.	To center main lobe peak on target	To enable search function generator to read out precise phase control voltage for target relative direction
11 Balancing Circuit for Nulling Split Main Lobe on Target	1) Dithers 6 2) Detects biased signal, off center of main lobe null 3) Sends nulling control signal to 7	Same as Above	Same as Above	Same as Above

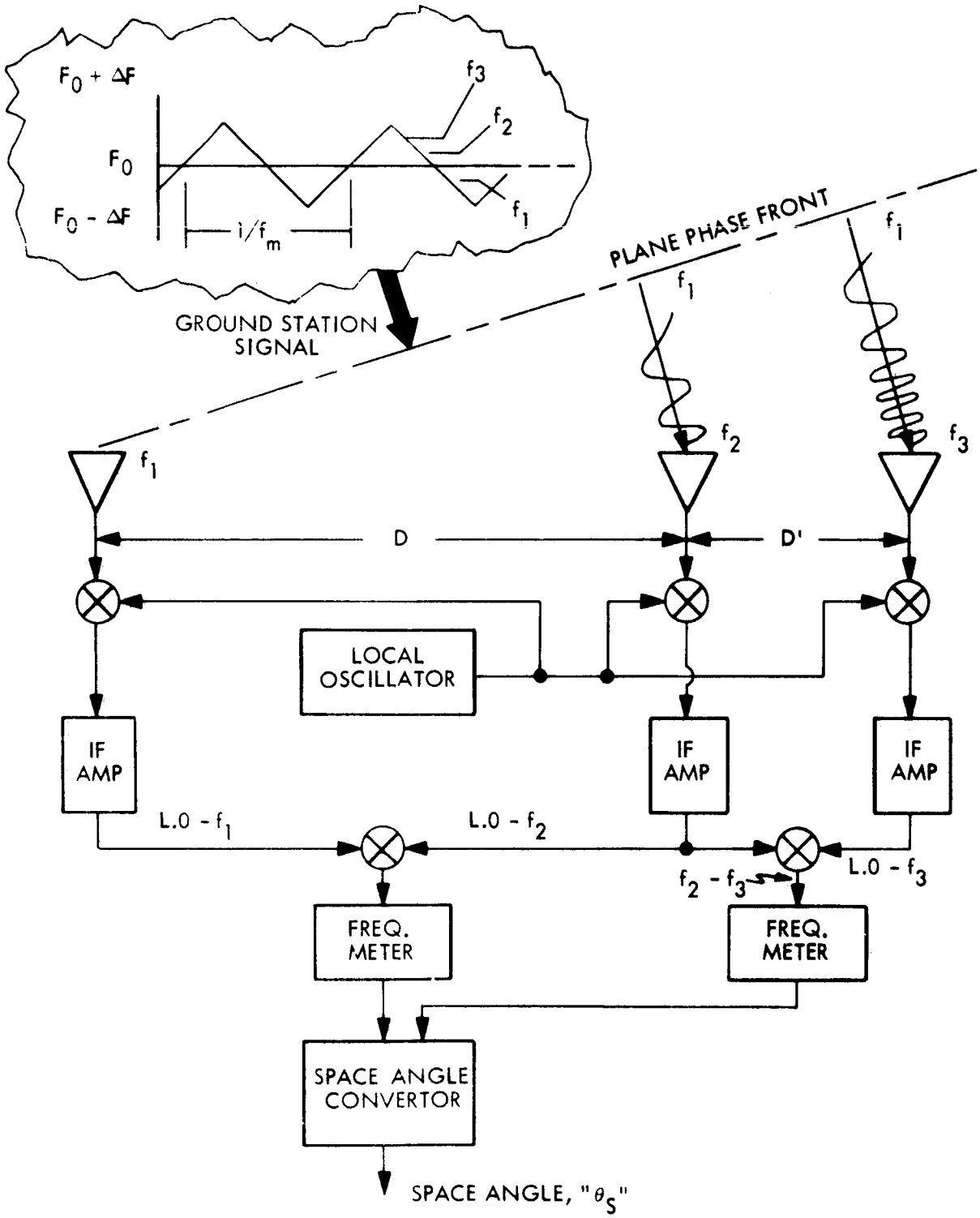

FIGURE 8.4-4 SPREAD SPECTRUM INTERFEROMETER TECHNIQUE

(A)

Spread Spectrum (FM) Signal Search

Operating Principle

- o Ground station produces frequency gradient across interferometer antenna elements by transmitting linear sawtooth FM signal.
- o Obtains beat frequency between antenna element signals.
- o Converts beat frequency to equivalent space angle.

Implementation - System configuration consists of following subsystem components, given in the order of signal flow from received RF signal to final computed space angle.

- o Multiple element antenna array
- o RF and I-F circuitry
- o Frequency meter
- o Space angle converter

Signal Flow and System Function

- o Receives signal power at known point in wavefront
- o Generates cross channel I-F signals
- o Measures frequency difference between channels
- o Converts frequency to a space angle

TABLE 8.4-5(B) SYSTEM B7 - SPREAD SPECTRUM SIGNAL SEARCH

Dev	Device Characteristics	Device Function	Subsystem Function	Subsystem Characteristic
0 Ground Station	To produce Sawtooth FM Signal		To produce frequency gradient across interferometer antenna elements.	
1 Antenna Element	15-20° beamwidth narrow-band - fixed phase center for variable incidence angle and polarization	To receive signal power at known point in wave front, relative to other elements.		Produces signals indicative of spatial orientation (angle-of-arrival) of wavefront.
2 RF Mixer(s)	Non-linear impedances at RF	To generate IF signals		
3 IF Mixer	Non-linear impedance at HF	To generate cross IF signals.	To obtain beat frequency between main antenna element signals.	Obtains a beat signal which is frequency dependent upon space angle.
4 IF Mixer	Non-linear impedance at HF	To generate cross IF signals.	To produce beat frequency between auxiliary antenna element signals.	Resolves polarity ambiguity of space angle frequency dependance.
5 Frequency Meters	Cycle Counter 1.75 Hz to 3500 Hz, ± 1.75 Hz	To measure frequency difference.	To measure beat frequency.	Provides a frequency dependent upon space angle from beat signal.
6 Space Angle Convertor	Computes $\theta_s = f(f_{12})$	Converts a frequency to a space angle.		Determines space angle.

8.5 SELECTION OF PREFERRED CONCEPT

The Direct Phase Reading Interferometer System was selected as the preferred system from the four systems described in Section 8.4. The selection was based upon the performance parameters and other selection criteria discussed in Paragraph 8.4-1 and upon an analysis of the error sources and errors within each system.

This section discusses the error sources identified for the Direct Phase Reading Interferometer and gives an evaluation of the candidates and the logic in selecting the preferred system.

8.5.1 Candidate Evaluation and Selection of Preferred System

A semi-quantitative comparison was made of the candidate interferometer techniques using those criteria listed in Table 8.5-1. Using these criteria and examining the functional block diagrams, the candidate systems were ranked as shown on Table 8.5-2. The two most promising candidates are the Cross-Correlation and Direct Phase Reading Interferometers. The cross-correlation technique was ranked higher for the performance criteria since it can be designed so that potentially it can provide a greater accuracy by judicious beam design and by increasing the signal-to-noise ratio due to the signal correlation process. The latter is accomplished by multiplying the output of two additive arrays. For example, each array produces a multi-lobed pattern as shown in Figure 8.5-1. The position of these lobes is determined entirely by element separation. If the respective element spacings in the two arrays are made different, then one can arrange matters in such a way that one major lobe of one array coincides with one major lobe of the second, but that other major lobes do not coincide. When the two patterns are multiplied, the results are shown in Figure 8.5-1.

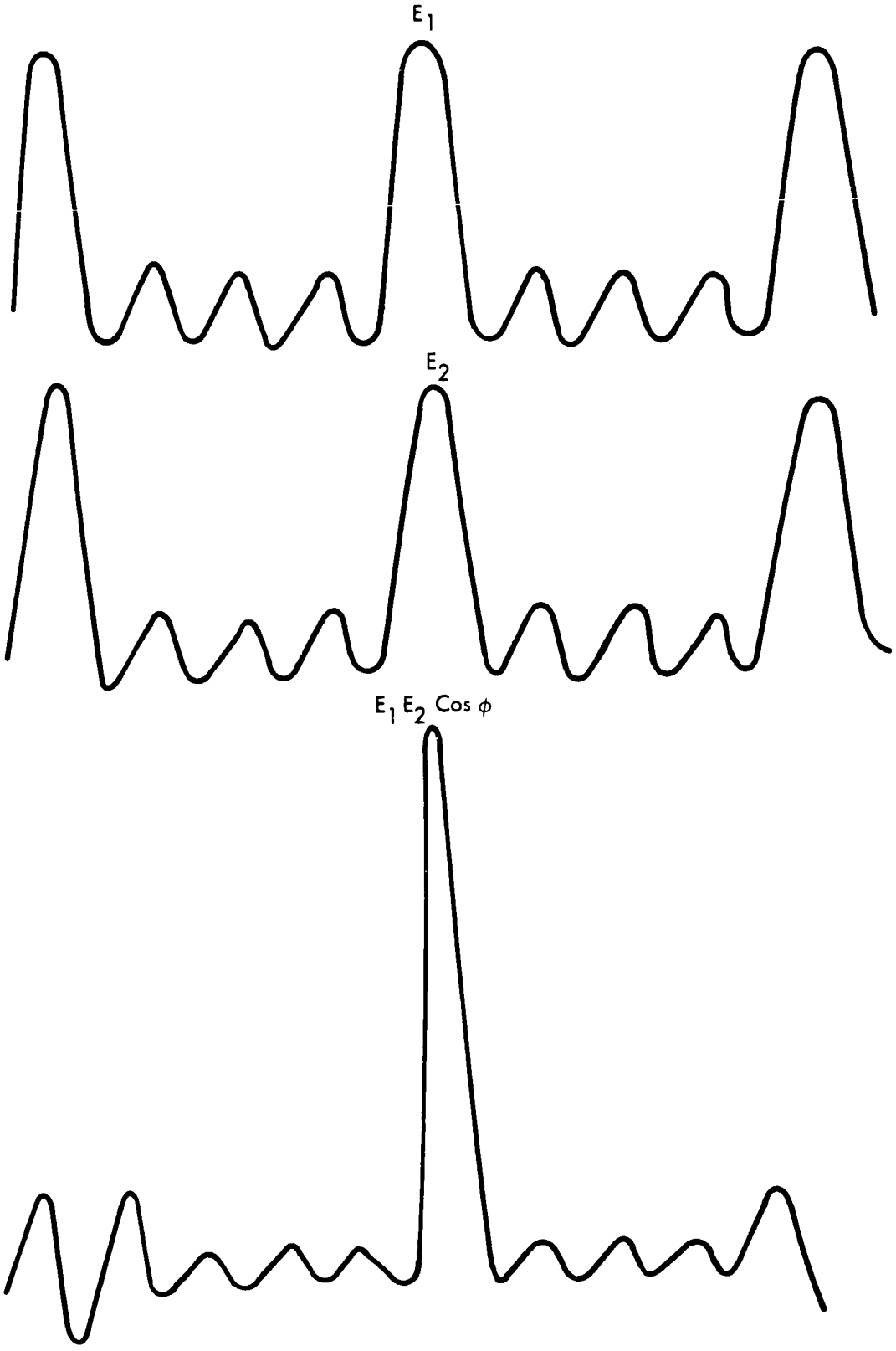

FIGURE 8.5-1 RESULTANT NON-AMBIGOUS PATTERN AFTER CORRELATION

Table 8.5-1

IDENTIFICATION OF ERROR SOURCES

The principal errors and their sources which govern the design of the interferometer are the following:

1. Antenna and receiver noise	1. Basic performance parameters (space angle resolution, ambiguity resolution, etc.).
2. Component error sources.	2. See Table 8.5-2 (1-4)
3. System error sources	3.
a) Ephemeris errors	a) 100 feet
b) Ground coordinate errors important to interferometer evaluations).	b) 50 feet
c) Interference from other on-board systems (e.g., phased array).	c) Coupling errors (estimated 20-30db)
d) Ambiguity resolution errors	d) (0.01° to $.1^{\circ}$.)
e) Polarity errors	e) $\pm$ ambiguity errors and $\pm$ space angle. (See Appendix 8.10A)
f) Data sampling errors	f) $\pm 0.1^{\circ}$ IF electrical phase angle meas. (estimated).
g) Propagation errors	g). 005° to $.01^{\circ}$ error in ground location
h) Antenna coupling and purity and alignments of polarizations	h) Negligible - See Appendices 8.C, 8.D, and 8.E

Table 8.5-2

CANDIDATE INTERFEROMETER COMPARISON

Criteria \ Rank	1	2	3	4
Performance	Cross Correlation	RMS Phase Reading	Direct Phase Reading	Spread Spectrum
Design Simplicity	Spread Spectrum	Direct Phase Reading	Cross Correlation	RMS Phase Reading
State-of-the-Art	Direct Phase Reading	Cross Correlation	Spread Spectrum	RMS Phase Reading
Operational Considerations	Cross Correlation	Direct Phase Reading	RMS Phase Reading	Spread Spectrum
Spacecraft Considerations	Spread Spectrum	Direct Phase Reading	Cross Correlation	RMS Phase Reading

I-9

The peaks of the pattern come at locations where a main lobe of one array is multiplying a side lobe of the other. A schematic of such an array is shown on Figure 8.5-2. If each array consists of point sources with uniform element spacings and a uniform in-phase amplitude distribution, we have for a normalized product pattern (Ref. "Interferometer Development", Pickard and Burns, Inc. Needham, Mass.)

$$F(x_1, x_2, D) = \frac{\sin q_1 X_1 \sin q_2 X_2}{N_1 \sin X_1 N_2 \sin X_2} \cos\left(\frac{2\pi D}{2} \sin \Theta_s\right)$$

where

$$X_{1,2} = \left(\frac{\pi d_{1,2}}{2} \sin \Theta_s\right)$$

and where

$q_{1,2}$ = number of elements in the arrays

D = phase center spacing

$d_{1,2}$ = respective element spacing

Θ_s = propagation angle of incident plane wave measured from array normal.

Using these techniques, it appears feasible for the interferometer to operate closer to the thermal noise threshold. Although a complete analysis is not available at this time, it is estimated that the signal-to-noise ratio above thermal noise will be 6dB - 12 dB. The manner in which this technique reduces interference by correlation is discussed in Appendix 8.A An indication of the space angle accuracy achievable with array antennas can be seen by examining the monopulse equation and curve shown in Figure 8.5-3. No attempt to derive a similar expression for the cross-correlation interferometer was made due to the following reasons. If the assumption regarding an ERP of 64 dBW is valid, then a system with this inherent sensitivity is not warranted for the present ATS-4 mission objectives.

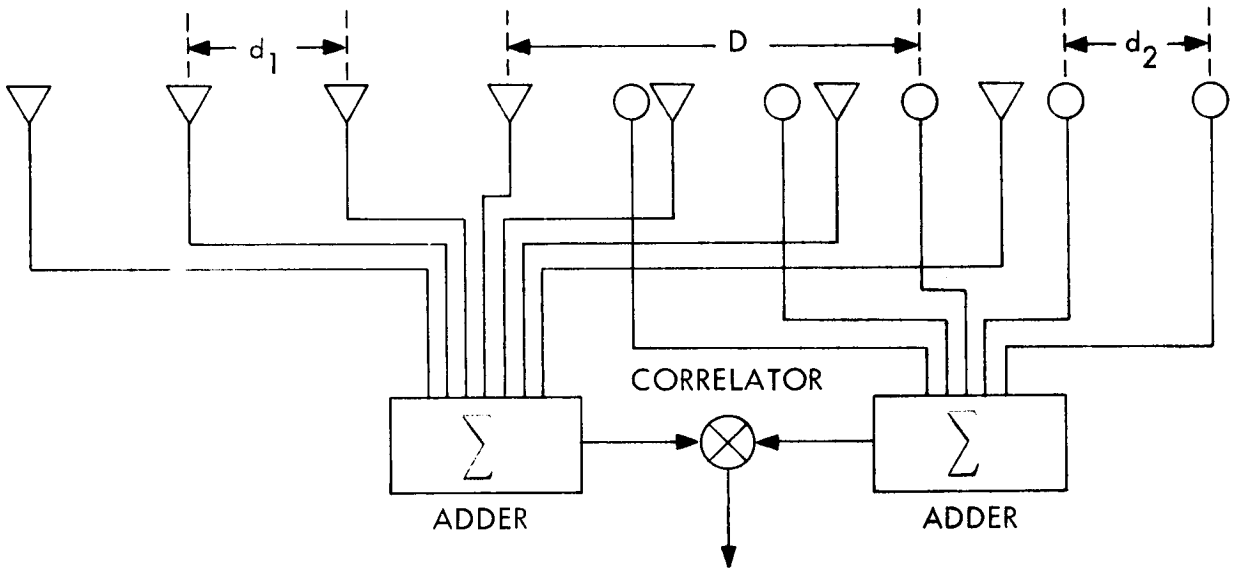

Figure 8.5-2 PARTIAL SYSTEM SCHEMATIC OF CROSS CORRELATOR INTERFEROMETER

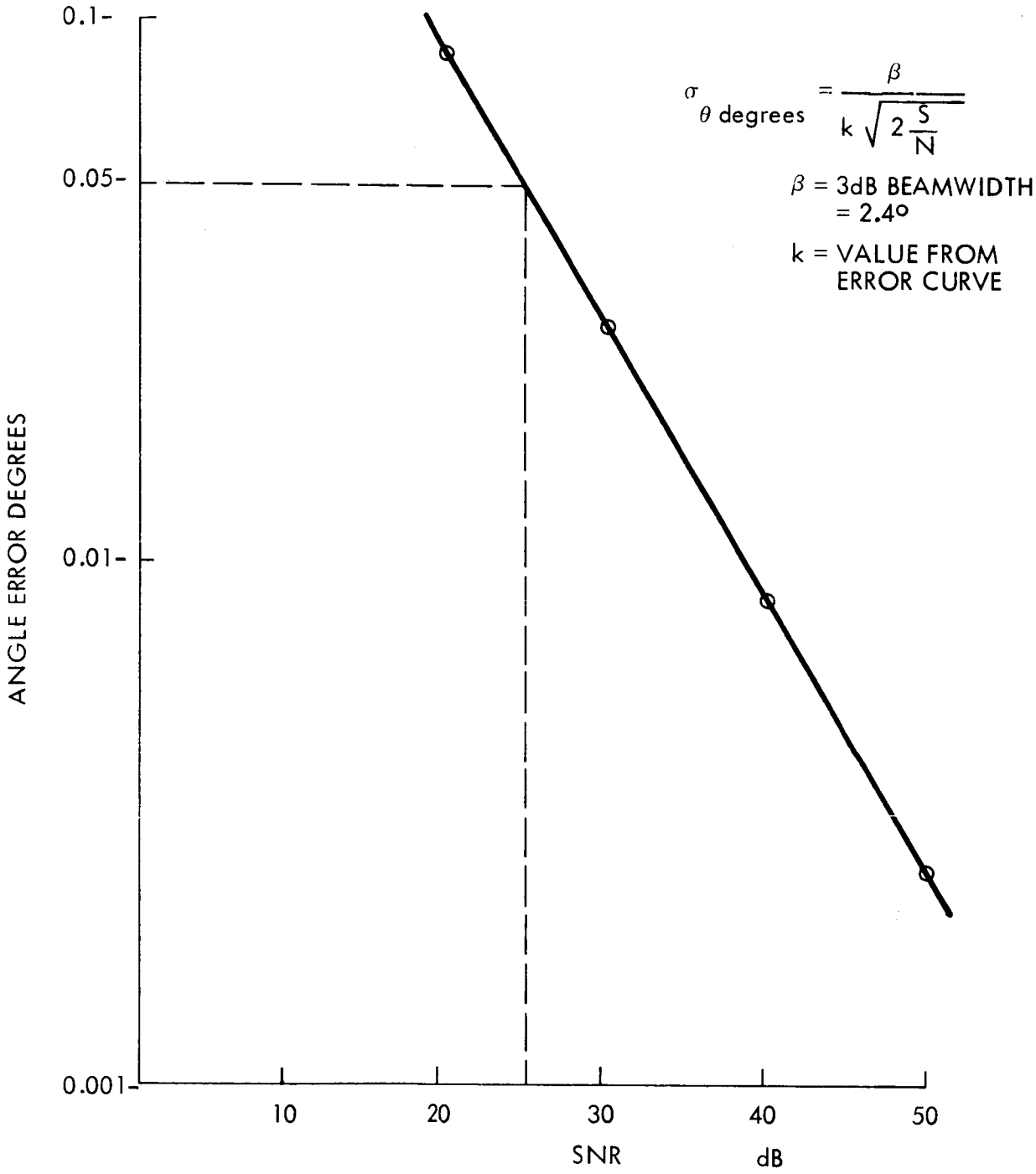

Figure 8.5-3 MONOPULSE SPACE ANGLE RMS ERROR

On the other hand, it may find application in a system wherein a station has a low ERP illuminator.

The Direct Phase Reading Interferometer meets the design goal accuracy requirements. The results of a total system error analysis, described in detail in Section 8.7, are shown on Figures 8, 7, -10 and 8, 7, 11. Theoretically the error is less than one degree for a signal-to-noise ratio of 20 dB. However, when the implementation of the cross-over detector is considered, it is ascertained that without undue complexity; the best that can be done is to measure to an accuracy of one degree at a signal-to-noise ratio of 30 dB. Therefore, a SNR equal to 30 db is given in Figure 8.5-4.

The Direct Phase Reading Interferometer was ranked above the Cross-Correlation Interferometer in the design simplicty and state-of-the-art category. While it is recognized that the interferometer arm assembly is a critical subassembly in the interferometer, by applying well-known mechanical and thermal design techniques, the errors in this subassembly can be made negligible. All of the components, techniques and circuits required for this design can be considered state-of-the-art. The design of the cross-correlation interferometer requires the manipulation of the antennas and arrays proper, such as phasing, judicious positioning (including element spacing) and controlled amplitude distribution over the aperture. Two methods of phase shifting were investigated. A mechanical phase shifter besides requiring motion, could not be driven at a rate greater than 100 cycles per second.

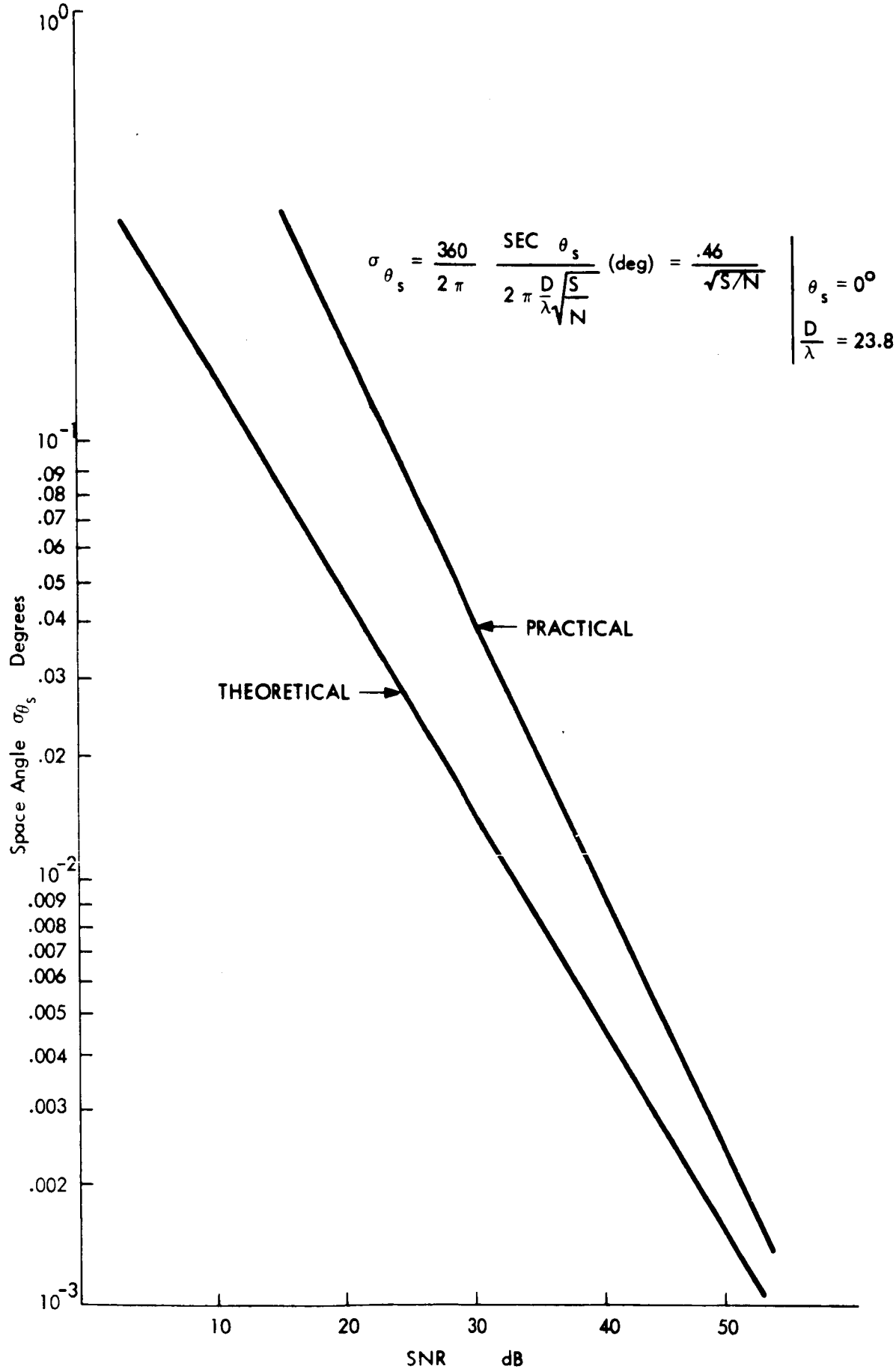

FIGURE 8.5-4 RMS SPACE ANGLE ERROR DIRECT PHASE READING INTERFEROMETER

Ferrite phase shifters present a problem due to errors in phase as a function of temperature. The phase shifter is a critical component and requires an R & D effort to achieve phase accuracies of one degree or less. According to L. R. Whicker and R. R ones (*), the following are representative of the state-of-the-art.

	Low Cost	Med. Cost	High Cost
$\Delta \varphi$ ambient temp	$\pm$ 50%	$\pm$ 5%	$\pm$ 3%
	0° -60%	0° - 60%	-40° to $+60^{\circ}$C
Bandwith $\Delta \varphi$ vs. freq.	$\pm$ 5%	$\pm$ 3%	$\pm$ 3%
Cooling	Circ.	air or liq.	liq.
Material	Ferrite	temperature compensated garnet	fine grained doped temp. comp. garnet

For the two methods considered, there is no appreciable difference with regard to spacecraft considerations. Based on the results of the analysis performed, the Direct Phase Reading Interferometer is the preferred system.

(*) "Design Guide to Latching Phase Shifters," Microwaves - Vol. 5, pp. 31-39, November 1966.

Antenna and Receiver Noise Errors

Figure 8.5-5 shows the relationships between the space angle resolution, the interval of unambiguous measurement, and the frequency as a function of the antenna element separation to wavelength ratio. At the chosen design point, the required electrical phase reading accuracy must equal or exceed 1°. The error source limiting this accuracy is primarily the antenna and receiver noise. It has been shown that this error is given by the following formula:

$$\sigma_{\theta_s}(\text{degree}) = \frac{360}{2\pi} \cdot \frac{\text{Sec}\,\theta s}{2\pi \frac{D}{\lambda}} \frac{1}{\sqrt{\frac{S}{N}}}$$

This error is plotted as a function of the signal-to-noise ratio in Figure 8.5-4 From this curve it is seen that a signal-to-noise ratio of 30-40 dB at the crossover detector is sufficient to give the required space angle accuracy of $.05^{\circ}$ degrees. It has been shown in Appendix 8.B that a 40ft. dish supplied by 10W of power at the ground station will be sufficient to give this signal-to-noise ratio with allowance made for the noise figure introduced by the antenna and receiver and by other system propagation losses.

Component Errors

The results of the error analysis made on the components indicated that the two major components which contributed significantly to the phase error budget were the transmission lines and crossover detector.

A plot of the phase error due to various type lines versus temperature differential is shown in Figure 8.5-6 By good thermal and electronic design it is shown in the Section 8.6, that the error can be reduced to a negligible amount.

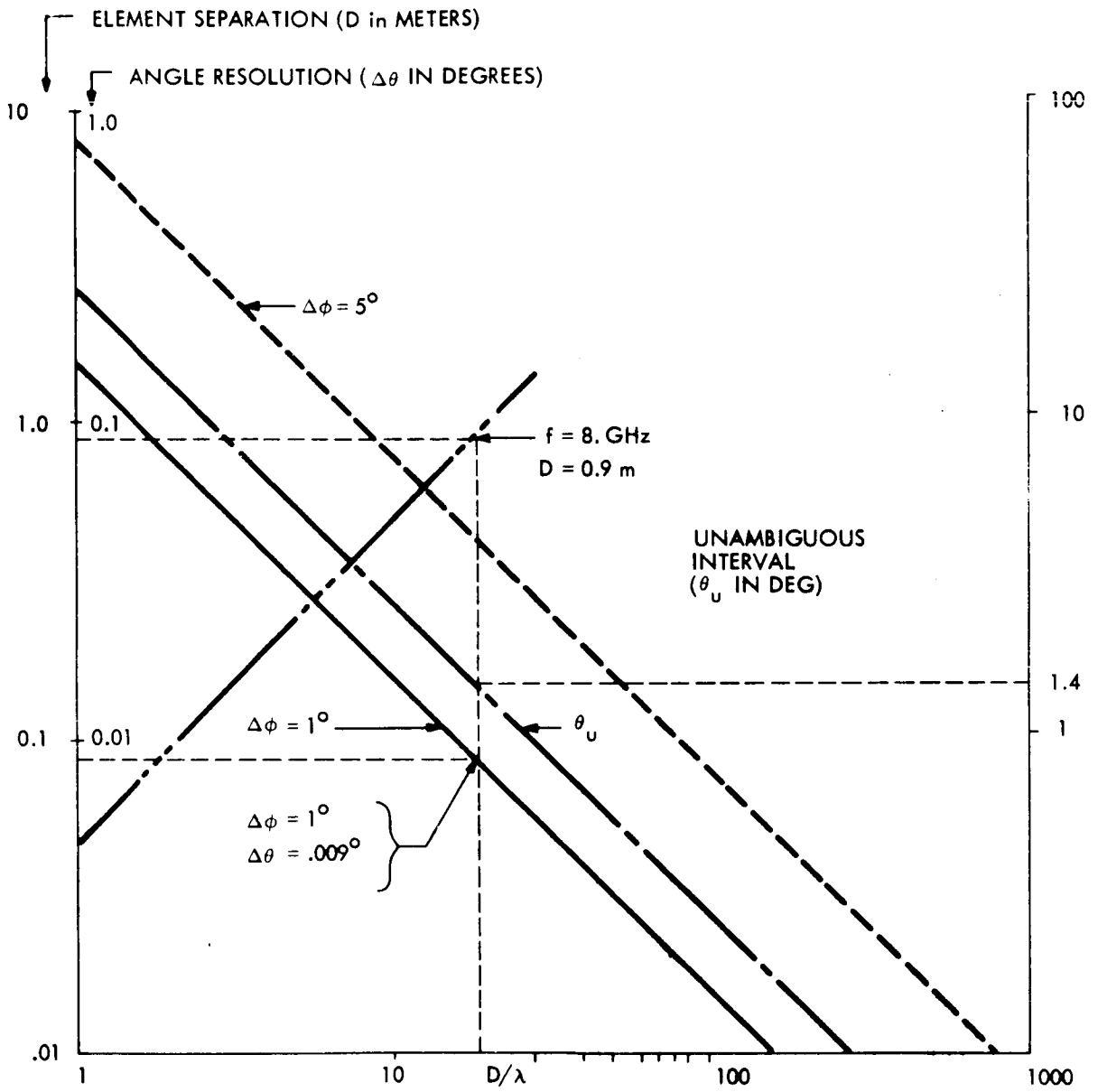

FIGURE 8.5-5 DIRECT PHASE READING INTERFEROMETER RELATIONSHIPS, SPACE ANGLE ELEMENT SEPARATION± UNAMBIGUOUS INTERVAL VS D/λ

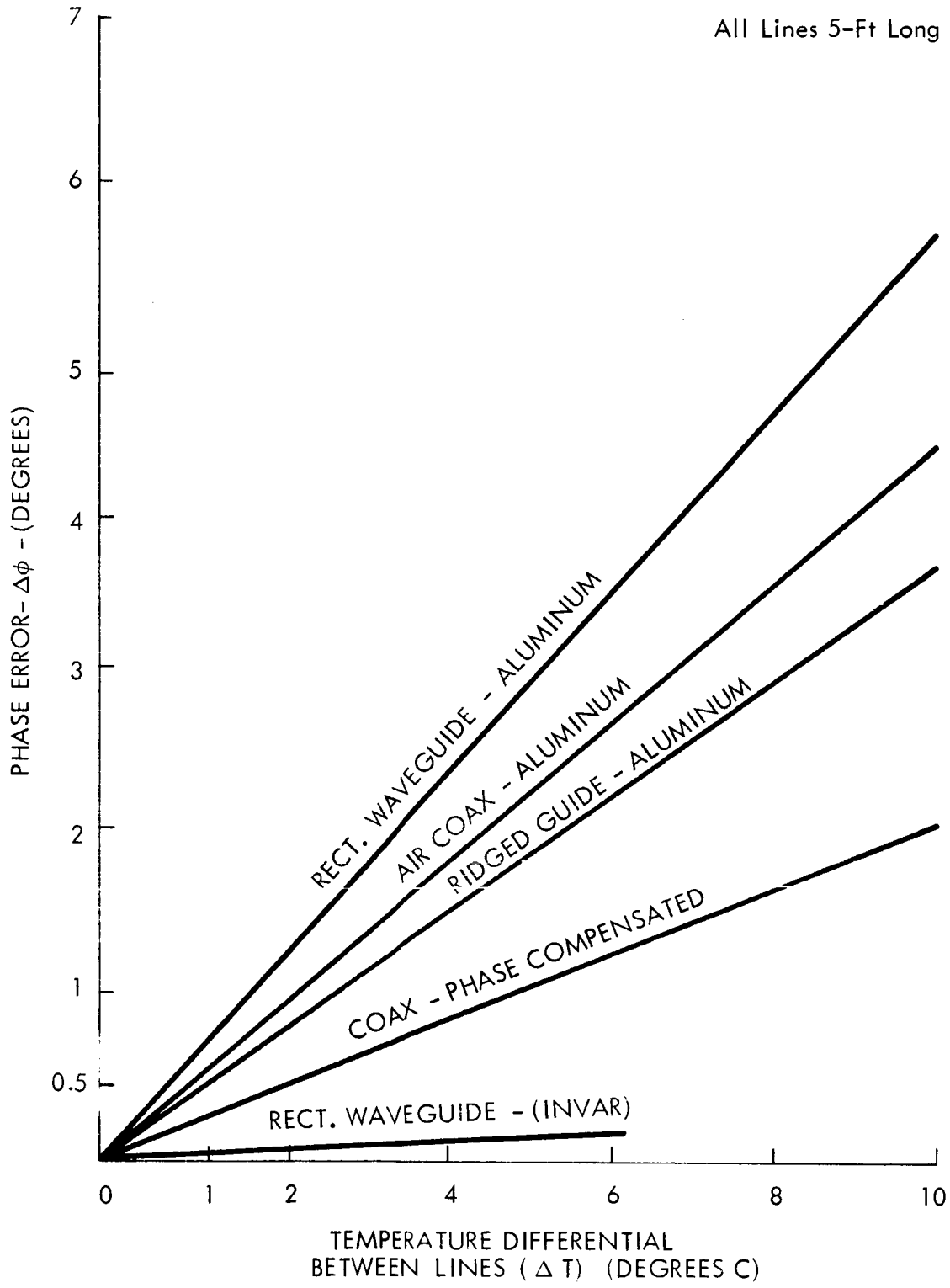

Figure 8.5-6 INTERFEROMETER PHASE ERROR DUE TO TEMPERATURE DIFFERENTIAL IN TRANSMISSION LINES

In the case of the crossover detector, for SNR greater than 30 db, the phase error is such that the space angle error is $.05^{\circ}$ which is the design requirement.

Other component errors are shown in Table 8.5-3 through 8.5-6.

TABLE 8.5-3

System #A4 - Component Errors - Direct Phase Reading System

No.	Device Name	Error Source	Est. Order of Magnitude
2	Antenna Element	Phase center variation with space angle (due to radiation coupling and/or polarization)	0.1 mm
		Individual antenna element identicality	± 0.5 db ± 1°
		Mechanical Alignment: a) Canister base warpage (thermal) b) Element placement (assembly tolerance, launch upset) c)Boresight alignment	 0.1 mm displacement 0.1 mm displacement ± 0.01°
3	RF Mixer	Conversion Loss Stability Phase Shift Stability Phase Shift Tracking RF Line Lengths	± 0.5 db ± 0.5° ± 0.5° ± 1°
4	Multiplier	Amplitude Stability Spurious Outputs	± 0.5 db -40 db
5, 6	RF Switches	Insertion Loss Stability Isolation Stability	± 0.05 db ± 0.5 db
7	Phase Locked Loop	Filter Phase Stability Phase Detector Stability	± 0.5° ± 1°
8	IF Amplifier	Gain Stability Gain Tracking Phase Stability Phase Tracking	± 0.5 db ± 0.5 db ± 1° ± 1°
9, 11	IF Mixer	Conversion Loss Stability Phase Shift Stability Phase Shift Tracking	± 0.3 db ± 0.3° ± 0.3°
10	Xtal. Oscillator	Freq. Stability Amplitude Stability	$1:10^8$ ± 0.2 db
12	Xtal. Filter	Phase Stability	± 1°
13	Filter	Phase Stability Phase Tracking	± 0.5° ± 0.5°
14	Electronic Counter	Clock Stability Relay Skew Zero Crossing Detector Error	$1:10^8$ ± 0.1° ± 0.5°

TABLE 8.5-4

Component Errors

(Spread Spectrum)

Device No	Device Name	Error Source	Estimated Order of Magnitude
1	Antenna Elements	Same as for System A 4	
2, 3	RF Mixer, IF Mixer	Same as for System A 4	
	Local Oscillator	Frequency Stability Amplitude Stability Spurious Outputs	$1:10^7$ $\pm$ 0.3 db $>$ -40 db
	IF Amplifier	Same as for System A 4	
5	Frequency Meter	Clock Stability Zero Crossing Detector	$1:10^8$ $\pm 0.5^\circ$

TABLE 8.

Component Errors

(Cross Correlation)

Device No	Device Name	Error Source	Estimated Order of Magnitude
2	Antenna Elements	Same as System A4	
3	RF Summing Network	Amplitude for balance RF line length differential stability	$\pm$ 0.1 db $\pm$ 1°
4	RF Mixer	Conversion Loss Stability Phase Shift Stability	$\pm$ 0.5 db $\pm$ 0.5^{o}
5	Filter or Synchronous Detector	Phase Stability	$\pm$ 0.5^{o}
6	Phase Control of Antenna Element Signals	Phase Stability Phase Accuracy	$\pm$ 0.1^{o} $\pm$ 0.2^{o}
7	Search Function Generator	Voltage drift, nonlinear Amplifications, etc.	Output Voltage 1: 5×10^{4}
8	Threshold Detector	Threshold level, spurious voltages	.01 db
9	Coordinate Connector	Voltage Stability	Space angle error $.001^{o}$
10	Balancing Circuit for Main Labe Nulls	Phase stability with amplitude variation change of operating level, aging of components - balance between channels	Output Voltage Tolerance = $1{:}10^{4}$
11	Balancing Circuit for split main lobe	Same as for 10	Same as for 10

TABLE 8.5-6

Component Errors

RMS Phase Reading

Device No	Device Name	Error	Estimated Order of Magnitude
1	Antenna Element	Phase center variation with space angle (due to radiation coupling and for polarization)	0.1 mm
		Individual element identicality	±.5db gain; ± 0.1° relative phase err
		Mechanical Alignment	
		a) Canister Base warpage (thermal)	0.1 mm
		b) Element Placement (assembly tolerance, launch upset	0.1 mm
		c) Boresight alignment	± .01°
2	Antenna Element Switch	Insertion Loss Stability	0.1° elect. phase variation
		Isolation Stability	20 db ± 3db
3	RF Phase Difference Reader	Sources similar to those for System A 4, Table VIII A	± 1.0° elect. phase accuracy

System Error Sources

One of the major system error sources is the number of effects due to cross-coupling of the antenna elements of the interferometer, coupling with the nearby phased array antenna elements, and various kinds of polarization errors. Section 8.5.2 provides the results of an analysis of the effects of coupling between these various antenna elements. It was concluded that the interferometer should be so designed that the elements should have linear polarization sensitivity and should be illuminated by circular polarization from the ground antenna. The reference antenna polarization should be linear and parallel with one of the antenna arms. The coarse measurement antenna elements located nearby in the two interferometer arms should be polarized orthogonally to the reference antenna in order to minimize cross-coupling with it. Appendix 8.C shows the degree of coupling for several combinations of horn types and waveguide structures.

In the final design all considerations lead to a horn constructed with an exponential flare necking down from a square mouth (polarization parallel with one of its diagonals) smoothly to a circular cross-section and then smoothly making a transition into a rectangular throat. The shape of this horn is illustrated in Section 8.6. The rectangular throat of the horn acts as a polarization filter. The square mouth excited along a diagonal insures that the antenna gain pattern is as nearly circular as possible.

Another system error source is the system polarization. The choice of the polarization of the interferometer antenna elements and the polarization of the ground station antenna will influence the accuracy of the interferometer system. Appendis 8.D and 8.E shows that the best system is one in which the ground station polarization is circular and the interferometer elements are linearly polarized.

8.5.2 Phased Array as an Interferometer

Introduction

It has been suggested that some of the antenna elements of the x-band phased array be used as antenna elements for the interferometer. The practicality of this suggestion will be examined.

Necessary Characteristics of Interferometer Antenna Elements

Beamwidth and gain - approximately 1 dB down at $\pm 17^{\circ}$ off antenna axis.

Polarization - Preferably linear, so that cross-polarization can be used to isolate coarse antennas. If circular, very good axial ratio.

Input Impedance match - Good; preferably less than 1.2.

Mutual coupling - as low as possible.

Phased Array Configuration

A section of the phased array is shown in Figure 8.5-7. It can be seen that each antenna element consists of a triangular array of helix antennas.

Beamwidth - A 7-1/2 turn helix has a 3 dB beamwidth of about 42° (1 dB $\cong 23^{\circ}$). The triangular arraying will not affect this beamwidth significantly; this beamwidth is satisfactory.

Polarization - The polarization of the phased array element is circular with a very good axial ratio. As mentioned above, linear polarization would be more desirable.

* The phased array evaluated in this section is the preliminary design presented to GSFC in October, 1966.

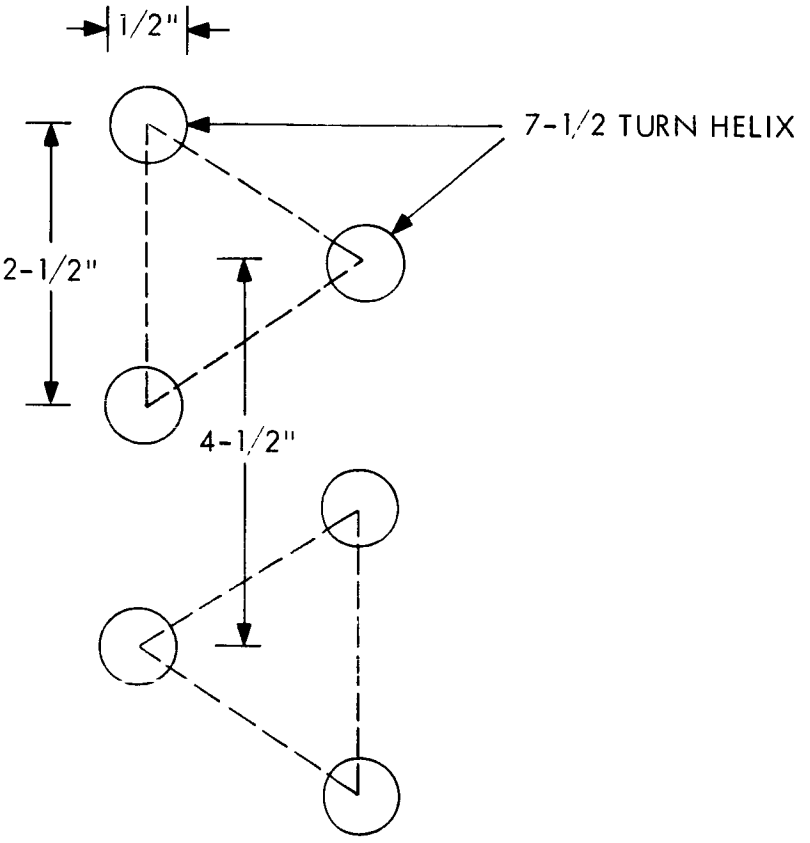

Figure 8.5-7 LAYOUT OF PHASED ARRAY

However, since the mutual coupling between antenna elements is low and the axial ratio is so good, circular polarization could be satisfactory.

Input Impedance Match - While impedance matching seems to be fairly easy for low frequency helix antennas, no data could be found for x-band helix antennas. It would seem that impedance matching might be a rather sensitive function of helix dimensions.

Mutual Coupling - The mutual coupling between two helices spaced 3.25 inches = 2.2 wavelengths apart is about -49 dB. This is rather good since the phased array elements that would be used are the edge elements in the array, there would be some mutual coupling with all the other array elements. It is difficult to evaluate the magnitude of this effect without detailed calculations.

General Comments

SPDT switches would have to be inserted in the line between each helix triad and its feed line that is to be shared with the interferometer. This switch would be a factor in the interferometer system reliability.

It seems likely that the uniformity between the array helix elements would probably not be as controllable as the uniformity between the horn elements proposed for the interferometer.

The spacing between the proposed interferometer horn is larger than that between the edge elements of the array. This will give increased angular accuracy.

It would be difficult to mount the array elements on a temperature-controlled beam because of the intricate corporate feed structure behind them.

Conclusions

While there is no single item that obviously precludes the use of some of the phased array elements as interferometer elements, the many small difficulties mentioned above seem to indicate that separate antenna systems for the interferometer and the phased array would be preferable.

8.6 DESIGN OF PREFERRED INTERFEROMETER SYSTEM

Study of system errors and spacecraft constraints indicates that the direct phase reading interferometer satisfies the ATS-4 mission requirements and is an economical choice in terms of design, development and experiment operation.

Principal preliminary design efforts on the interferometer system were concentrated on the most difficult design problems. Final result of these efforts is an interferometer system consisting of two physically separate units as follows.

1. Interferometer Arms and RF sub-units
2. Electronics Package

Principal problems of design of these units are summarized in Table 8.6-1. Their subsystems are given in column 1 with their respective design problems and solutions in the second and third columns.

The following paragraphs describe the overall design of the interferometer system and discuss the solutions to the design problems. A general circuit description is given below.

8.6.1 General Circuit Description

The selected direct phase reading system is shown in functional form in Figure 8.6-1 and is laid out for easy following of signal flow from the RF antennas down to the phase difference counter. Antenna Element 5 is the reference element and its mixer output, No. 5, at the IF frequency, enters IF Switch No 2 and follows down the right hand receiver channel in Figure 8.6-1. The antenna element signal to be compared with the reference element signal follows down the left hand receiver channel. Provision is made to switch the reference channel to the other mixer outputs if, for any reason, the RF portion of the reference channel should fail and it would be desirable to use other antenna outputs for the reference.

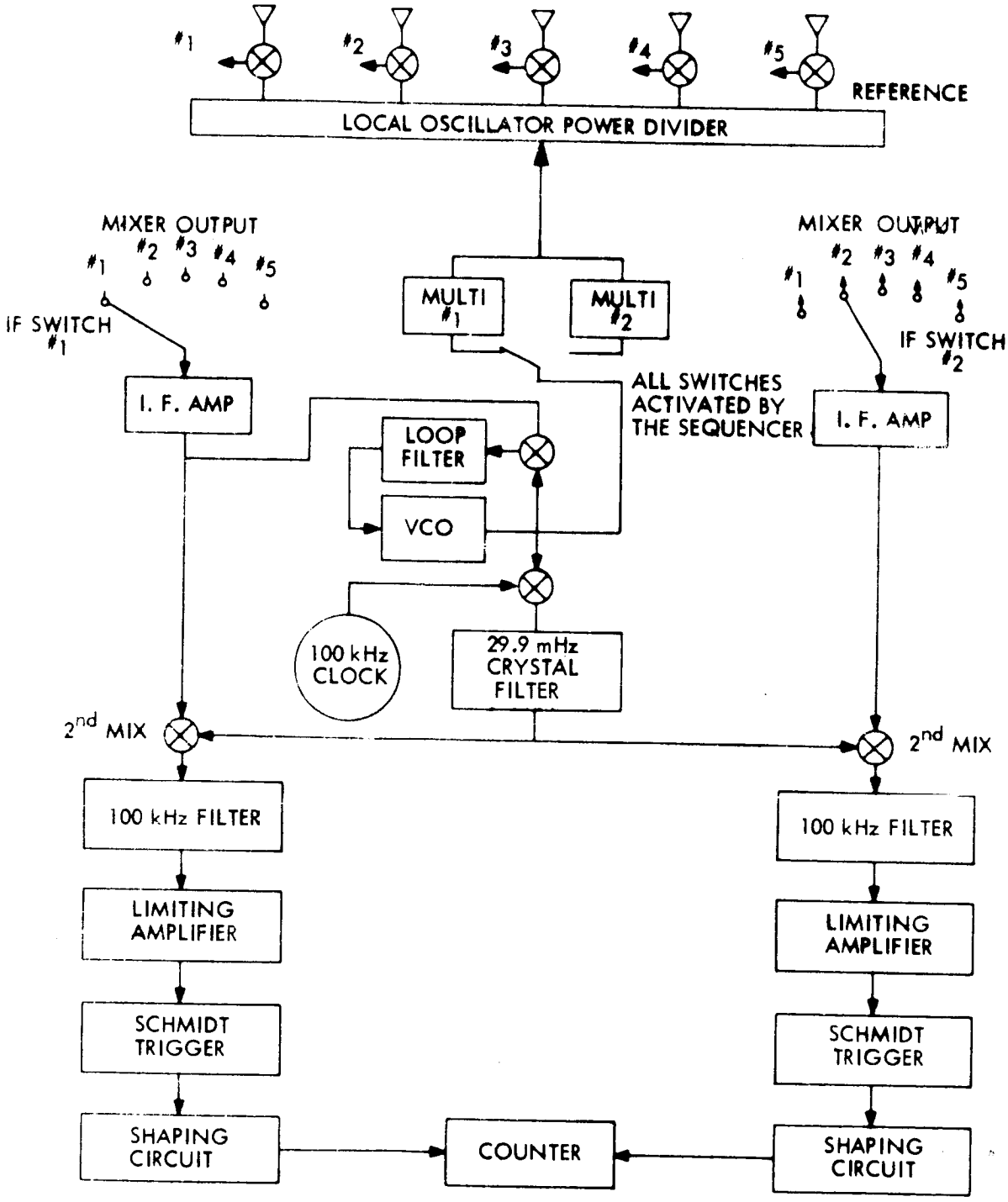

FIGURE 8.6-1 DIRECT PHASE READING INTERFEROMETER

All horn mixer outputs, likewise, go to IF Switch No. 1, in the left hand channel in Figure 8.6-1. In normal operation IF Switch No. 1 will switch through positions 1, 2, 3 and 4, A measurement of the phase difference between that respective antenna element and the reference will be made during the dwell time of the switch at each position.

The local oscillator switch under control of the onboard sequencer-processor will excite either multiplier No. 1 or multiplier No. 2, thus providing two different LO frequencies to the mixers in order that one of a pair of ground stations may be selectively received. The multiplier frequencies are controlled by a phase-lock loop which decreases the noise bandwidth of the system to approximately 20 cycles and thereby provides a stable reference frequency.

The 100 kHz clock, its associated mixer and crystal filter, provide a 29.9 MHz signal locked to the received carrier and injects this signal to a mixer fed by the IF output signal in the right hand channel. The output of this mixer is then a 100 kHz signal which is phase-locked to the RF signal received by the antenna element selected by IF Switch No. 1.

This reference IF signal is processed to obtain a sharply differentiated signal corresponding with each zero crossover. Figure 8.6-1 illustrates a simplified technique to provide this processing by means of a limiting amplifier, a Schmidt trigger and a differentiation and clipping circuit.

Simultaneously to processing of the reference signal, the signal of the selected antenna element is given similar processing in the left hand channel. The result is two signal pulses separated in time proportional to the phase difference between the reference and selected antenna element signals. The selected signal pulse starts the counter which is subsequently stopped by the reference signal pulse. The count of the counter is

thus proportional to the phase difference between the signals arriving at the antenna elements.

The counter output is transmitted to the on-board sequencer-processor. Its operations are described in paragraph 8.6.3.

The following paragraphs describe some of the particulars of the subsystems discussed in the above general operation of the system.

RF Circuit Design

Three principal types of RF lines were considered in the design of the interferometer, namely:

1. Wave guides; rectangular, circular and elliptical:
2. Filled dielectric coaxial lines.
3. Rigid un-filled coaxial lines .

The primary criteria used in consideration for these lines are as follows:

1. Independence of electrical characteristics upon temperature, mechanical deformation and electrical impedance properties, alterations in standing wave ratio, electrical loss or system noise.
2. Thermal properties, such as heat conductivity and specific heat.
3. Weight and size.
4. Manufacturing tolerances.

A summary of the analysis of each type of line for the interferometer is is follows. The circular waveguide offers weight saving when embedded in a supporting material due to the volume it displaces (for example, the line could be formed by drilling and internally electroplating a solid low weight plastic bar). Extruded tubes on the other hand are simple in mechanical structure and have high strength. However, this line was

quickly removed from further consideration because of the well-known problems of cross-moding and of matching to other components. An elliptical guide, easier to operate with a single polarization, is somewhat more subject to bending and other mechanical deformation affects than circular guides and offers no other advantages. Further, circular and elliptical guides, as well as rectangular waveguides, are sharply phase-dependent upon lateral mechanical dimensions when near cutoff frequency. Rectangular waveguides, of conventional materials, have significant thermal expansion with increase in temperature which affects both the cutoff frequency and overall length of the guide.

Coaxial lines of the types having solid dielectrics, such as teflon, ceramic disks, posts and spiral wound ribbons, have excellent electrical properties in regard to temperature. However, in the interest of the most stable structure possible, it is desirable that the line have as few discontinuities in structure as possible due to the possibility that variations or thermal stress may introduce errors through their properties. Particular care must be taken in regard to the internal supporting structure at transition elements such as couplers and terminations.

Rigid coaxial line has the following desirable properties.

1. Electrical length is nearly independent of cross-sectional dimensional changes.
2. Inner conductor position changes introduce impedance variations but little effect on electrical length.
3. The line is simple in structure; has no inherent discontinuities.

For these characteristics the rigid unfilled coaxial line was chosen for the interferometer RF circuitry.

The geometry of the RF lines with regard to length and explicit path to the mixers, was given careful consideration. In many respects, it would have been desirable to have all RF lines to the mixers have equal length. If this could be accomplished so that all lines were subjected to the same thermal gradients and absolute temperatures, the thermally induced phase errors would cancel each other. However, it was clear that such a configuration was not possible without adding extra length of line to one or more of the horns. Thus, this approach was abandoned because it is better to minimize line length as far as possible.

Several alternate approaches to the problem of placement and geometry of the local oscillators and the mixers were considered. Most of these are illustrated and discussed in Appendix 8. F.

The final solution to the RF line geometry is illustrated in Figure 8.6-2. The antenna horns are connected by RF lines, of as short a length as possible, running inward along the interferometer arm toward the reference horn located at the juncture of the arms. They were brought out symmetrically with respect to the reference horn to the mixer base plate. Thermal design is such that the RF lines within the interferometer arms are insulated and should not introduce errors due to either mechanical or thermal stress. The design of the arm will be described in Section 8.6.2.

Because of the heat produced by the frequency multipliers, they were mounted external to the interferometer arms. The RF lines emerging from the insulated interferometer arm and connecting to the mixers, are of special construction. They are of the rigid unfilled coaxial line type, identical in dimensions to the other RF lines but are constructed of a ceramic of low thermal conductivity and are internally

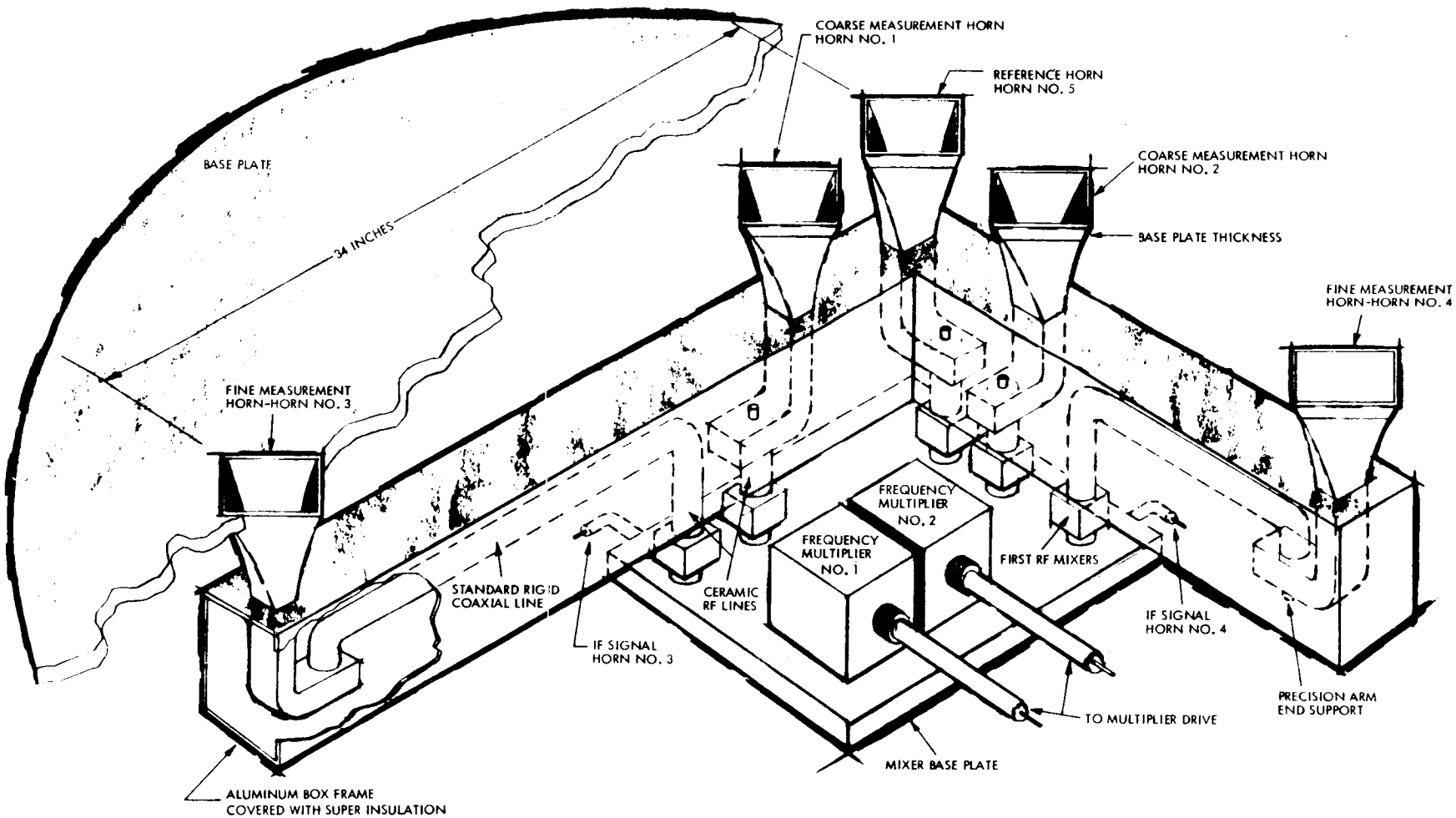

FIGURE 8.6-2 INTERFEROMETER

silver-plated in order to provide the proper RF properties. A proper choice of such materials should provide a thermal barrier to heat-produced by the multiplier-mixer unit.

The mixers are mounted on the common base plate so that they are equal in distance to a common LO feed point and thus are equi-phased. The base plate encloses a power-dividing network and frequency multipliers which inject a local oscillator signal of equal power to each mixer. Because of the high thermal conductivity of the mixer base plate and because of the equal line lengths to each mixer, each mixer will receive a LO signal of the same electrical phase within a tolerance of less than one electrical degree. Thus, in the overall structure, thermal errors in the RF signal lines and Local Oscillator lines should be minimized.

Local Oscillator Power Divider Design

There are two principal types of power dividers: reactive power dividers and resistive power dividers. The phase performance of the selected type is a paramount consideration. It would be highly desirable to minimize the local oscillator power requirements in regard to the output demanded from the multipliers since they are inherently very inefficient.

However, it is considered that the design of a resistive power divider, for the precision phase requirements of the interferometer, is more practicable. The disadvantageous effects of low efficiency and heat production will be allowed and it is expected that the thermal design of the multiplier-mixer base plate described in Section 8.6.2 will alleviate the deleterious effects of the resistive heat sources due to the power divider.

RF Mixers

The RF mixers utilize barrier (Schottky) diodes to obtain a low noise figure for the receiver system. It is expected that the present emphasis on development of these components in the band of selected operating frequency will provide a reliable and suitable diode in the 1968-1970 time frame. Alternative to the Schottky diode is the ordinary germanium point contact diode which, however, has a 2 to 3 dB higher noise figure.

Electronic Component Design

The IF amplifiers are of conventional design. However, a special requirement is that the IF amplifiers in the reference channel and the switch channel is that their total phase shift be equal. Besides identical construction and bench mating for similar pairs of IF channels, the IF strips will be mounted in a common thermal environment and fed from a common power supply.

The second mixers will be simple video germanium crystal diode mixers since they will not appreciably affect the noise figure of the receiver.

The 100 kHz IF filter serves to improve the signal-to-noise ratio. The bandwidth must be sufficient to permit sampling of the antenna outputs by the IF switch at the required rate. Similar to the requirment for the

IF amplifiers, these filters shall have identical phase shifts in the reference and switch channels. The limiting amplifiers shall have the same phase tolerance as the other IF equipment. The Schmidt trigger and the differentiation and clip circuit, as well as the gating circuits leading to the main counter input, shall have a total delay variance for each channel of less than one electrical degree. The main counter must operate at 36 MHz or above.

Local Oscillator Multiplier

The L. O. multipliers consist of diode multipliers with amplification only at the lowest frequencies (to be determined).

Tuning to several ground stations can be normally done by inserting an offset or interpolation frequency increment with an auxiliary oscillator plus a mixer, and by picking off the difference or sum frequency. In the system at hand this increment would result in a second IF that is entirely outside the pass band of the second IF filters of the phase lock loop. Thus a shift in operating frequency must be accomplished by either pulling the VCO frequency until the loop locks on the second station or supplying a second multiplier. Since the VCO range is limited, and operating it far from its natural frequency is not advisable, a second method of operation is used in this system.

Study shows that if each multiplier stage multiplies by a factor of factor of five (five being considered the maximum permissable multiplication in any one stage), then for a nominal 30 MHz VCO, and X band RF, the choice of multipliers narrows to 250 ($5^3 \times 2$); 256 (2^8); 270 ($2 \times 3^3 \times 5$). Using 250 and 256 will result in RF frequencies of 7.5 gHz and 7.65 gHz when working with 30MHz or 8.00 gHz and 8.192 gHz with an IF of 32 MHz.

A third alternative is to use two VCO's each with a slightly different natural frequency, or to switch the frequency determining components in the VCO. Either of these alternatives may be chosen in final design analysis.

Onboard Interferometer Calibration

It is evident that reasonable effort should be expended to assure uniformity and predictability of sensor characteristics. However, the ultimate accuracy depends more on instrument calibration and component stability than on a priori design characteristics. The primary reason being the difficulty in defining installed array geometry and phase response to the requisite precision.

An onboard means for implementing a calibrating loop completely around r-f and phase measuring portions of the system would be desirable. However, two basic factors make it certain that an operational method must be used instead: first, indeterminacy of a physical array's phase response versus signal angle of arrival; second, inability to couple a colocated source into the array aperture in such a way as to simulate an incident plane wave. An operational calibration method is described in Section 2.2.5.

Though self-contained overall system calibration means is not feasible, calibration of the electronics portion is feasible and highly desirable. Since injection of a calibrating signal at one of the operating x-band frequencies would require phase control of the calibrator lines somewhat better than the interferometer signal lines themselves, the test will be performed by introducing a signal into the first IF's. Thus, performance of all

electronics can be measured except for the mixers. The IF test generator will also prove useful in providing a reference test condition for obtaining measurements prior to launch which can be directly correlated with performance during the mission.

The following conclusions were made after careful study of the above approaches to system calibration and several variations in the approaches taken to find means of overcoming their disadvantages.

1. Calibration systems which calibrate around the most serious system errors (RF) are themselves subject to the same error sources, and sometimes to a greater degree than interferometer system itself and thus are not effective as calibration means.

2 Although not shown as part of the present equipment implementation, a test circuit providing an IF signal should be integrated into both channels to exercise the active electronic circuitry whose output will provide a reference throughout ground test and the experiment.

8.6.2 Mechanical and Thermal Design

The central problem of design of the interferometer arm is to prevent significant changes in electrical length (RF phase) of the RF circuitry, or shifts in phases of the RF signals due to temperature and mechanical effects. Therefore, the design of the interferometer arms consists of three principal aspects (refer to Figure 8.6-2):

1. RF Design (lines or waveguides, transition elements, couplers, and the antenna elements themselves).
2. Mechanical Design (Structure to maintain alignment of antenna elements and orientation of interferometer base lines with respect to canister carry-through structure).
3. Thermal Design (Insulation or surface treatments to effect practical operating temperature range for all components).

These aspects must be considered together, for example, the RF lines not only transmit the proper RF signal to each RF mixer, but unavoidably provide a thermal leakage path. In addition to providing mechanical self-support which may be helpful in mechanical design, the lines may incur deleterious variations in length (electrical length is of the final importance) due to temperature variations.

The simple preliminary design approach taken is to separate these problems as far as possible and thus to solve each by itself.

1. RF Line Problem

   RF lines were chosen having a minimum of: electrical dependence upon physical dimensions; electrical and mechanical dependence upon temperature and temperature gradients; and, in case of coupling to thermal sources, RF chokes constituting thermal barriers were used.

2. Mechanical Support Problem

   A rigid aluminum box section enclosing the RF lines was chosen. This structure is intended to maintain mechanical connection and alignment with respect to the canister by means of a central cantilever support and a single sliding support at each arm so as to permit longitudinal play.

3. Thermal Problem

   To insure a practical operating temperature: 1) superinsulation is wrapped around or affixed to the surface of the box channel support; 2) the antenna elements are painted with a reflective paint so as to limit their maximum temperature excursion when in sunlight and to minimize conductive heat transfer into the RF lines; 3) thermal barriers are interposed between the antenna elements and RF lines and between the mixers and RF lines internal to the interferometer arm.

The interferometer system, and, in particular, the interferometer arms must be able to survive the acceleration and vibration of launch. They must be supported by the load carrying structure of the canister so that no boresight error of the interferometer is produced.

The thermal considerations are most important during the operational phase. The thermal environment during this phase includes principally the effects of direct sunlight incident upon the interferometer antenna elements, the radiant and conductive heat transferred to the interferometer arm from the on-board electronics systems, the heat generated by the necessary RF elements of the interferometer, the radiation of the interferometer to free space and secondarily the effect of the earth's black body radiation, and the lunar and stellar radiation.

Horn Design

Figure 8.6-3 shows a cross section of one of the horn antennas. There are three principal features affecting its mechanical design and placement in the arm, namely:

1. Orientation and position
2. Shape and size
3. Material

A reference horn is placed at the corner of the L and two other horns, the "fine measurement" horns, at each end of the arm. The spacing is approximately 34 inches. The coarse measurement horns are placed approximately 4 1/2 inches from the reference horn on the center line to the fine measurement horns. The horns are boresighted at infinity by electrical ground test and are oriented accurately in their respective planes of polarization. The reference horn is polarized parallel to one arm of the interferometer and the adjacent coarse horns are respectively oriented with polarizations orthogonal to the reference horn. The fine measurement horns are oriented with polarizations parallel to their respective coarse measurement horns. The diagonals of the horns lie approximately along their respective planes of polarization.

The shape and configuration of the horn is a rectangular wave guide at the base merging smoothly into a circular cross section approximately 3 inches from the base and then smoothly into a rectangular mouth. The result is a high sensitivity to linear polarization in the polarization plane of the waveguide, and a horn gain pattern which is very nearly symmetrical about the horn boresight axes. The inside of the horn is painted with a coating such as $MgCO_3$ having high reflectivity to the sun spectrum, low heat

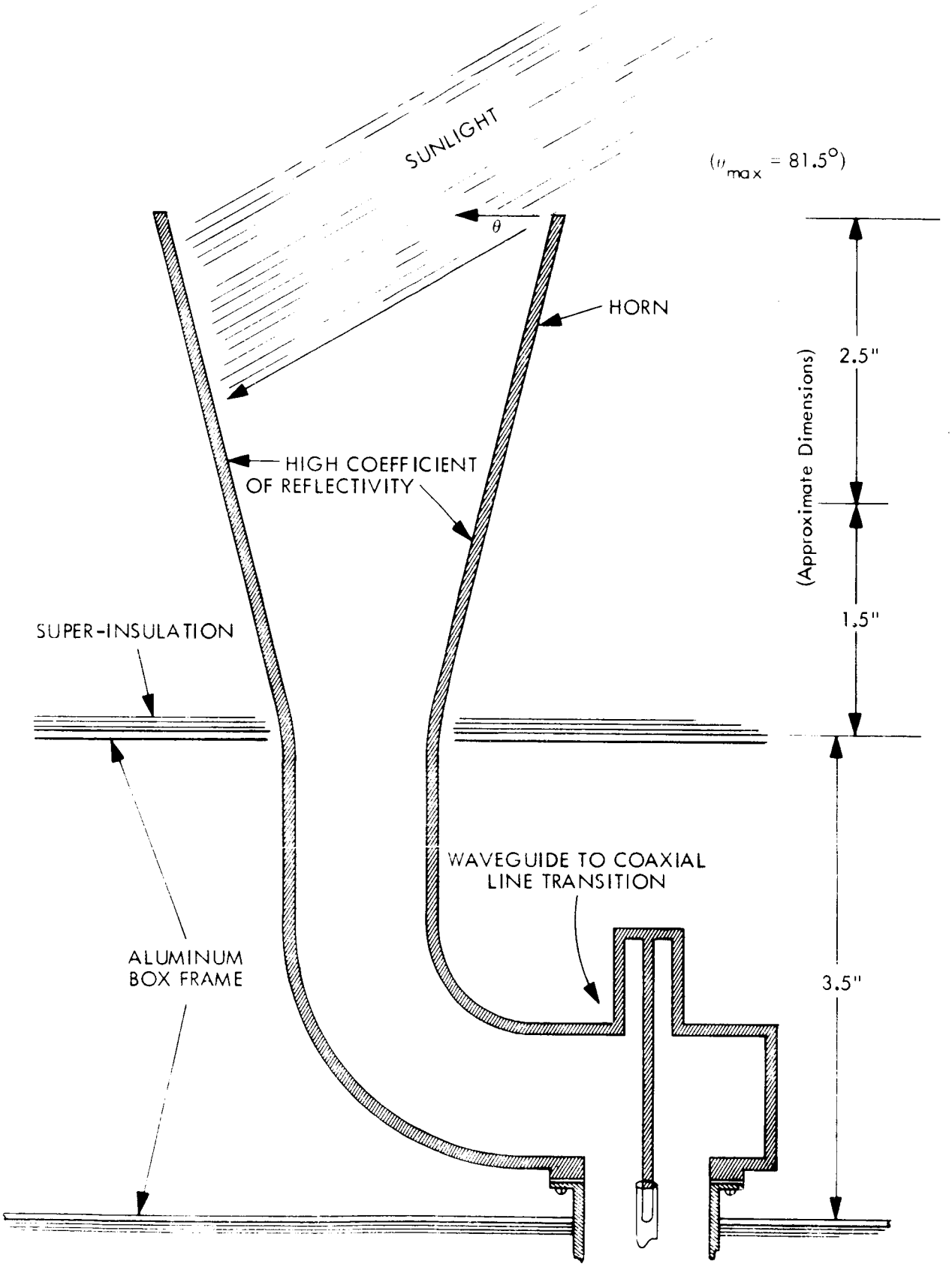

FIGURE 8.6-3 HORN DESIGN

conductivity, and relatively little effect upon the RF properties of the horn due to a reasonably low loss tangent and to the thinness of the coating required. The horn itself may be constructed of several materials. The thermal analysis shows that the temperature will vary between room temperature and the ambient temperature of the box channel support structure which is roughly at the average temperature inside the canister. Although no great extremes will be encountered, the horn should have low expansion with temperature changes.

It is important that the mechanical tolerances of the horn be maintained during the temperature excursions because the phase center of the horn must be fixed to less than a millimeter variation.

The throat of the horn ends in a 90-degree bend. The heat reflective paint is carried around the bend. The bend itself may be constructed of a separate silicate material of low heat conductivity or may be terminated by a separate short section of such material. The net purpose of either approach is to prevent conducted or radiant heat from entering the wave guide to coaxial line transition, since this element may be most critical in fixing the effective phase center of the antenna horn.

Thermal Design of the Interferometer

The thermal design of the interferometer is affected by the following constraints:

1. Average temperature between metallic RF lines, less than 10 degrees Fahrenheit variation
2. Temperate gradients RF lines, 10° F.
3. Mixers tolerance plus or minus 20° F.
4. Multipliers plus or minus 20° F.

The heat budget of the interferometer must be such that these temperature excursions are not exceeded. The principal thermal paths connecting the interferometer arm to its environment are: (1) its mechanical supports, (2) its surface radiation to the inner of the canister, (3) irradiation of the horn by the external satellite environment, (4) electrical inputs to the interferometer components.

Figure 8.6-4 shows the passive RF components, consisting principally of the RF lines and horns, inside of an insulator and the active components embedded separately in a base plate of high conductivity. This figure shows the heat sources acting to change the temperature of the passive RF components and consists principally of the electronic packages within the canister, the external radiation environment of the satellite and the heat flow from the active component embedment into the passive RF lines. All these paths are made as highly resistant to the heat flow as possible. As described above, the horns are designed to provide a path of low conductivity to the insulated RF lines. The mounts which must support the interferometer arm are constructed of ceramic posts of low heat conductivity. Finally, the RF lines which are necessary to conduct the signals to the external mixers are made of silver-plated ceramic tubing of low heat conductivity. Calculations show that the temperature of the external sections of the horn will be a maximum of 254 degrees Kelvin. It is concluded that the passive interferometer elements can be closely controlled in temperature and temperature gradient.

The active components are anchored thermally to the canister.

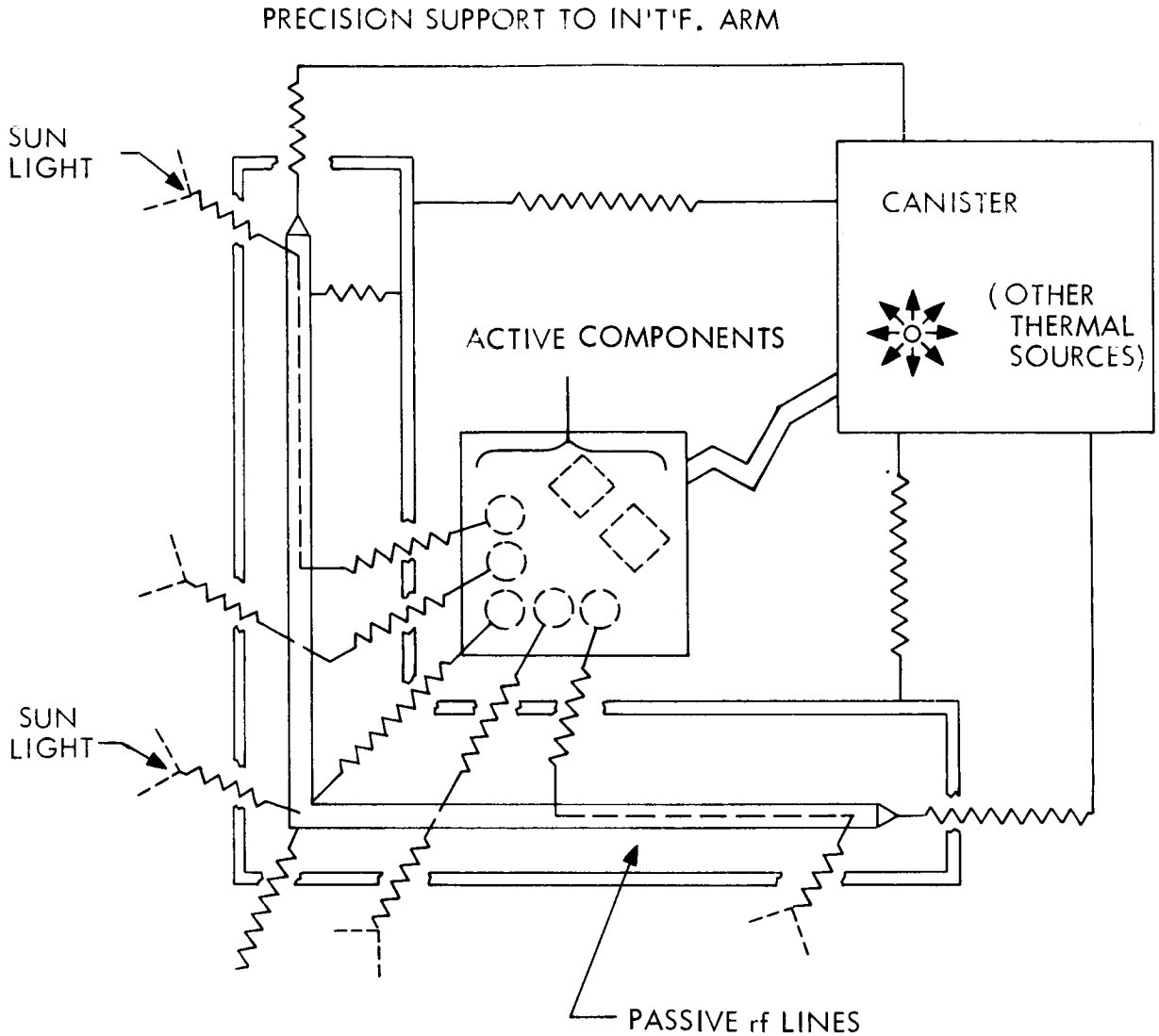

Separate Embeddment of Passive (in insulating jacket) and Active (in high conductivity matrix) RF Components.

Figure 8.6-4 INTERFEROMETER THERMAL FLOW DIAGRAMS

TABLE [illegible]-1 SUBSYSTEM DESIGN PROBLEMS

SUBSYSTEM	DESIGN PROBLEMS	DESIGN SOLUTION
1. Interferometer Arms and RF Sub-units		For Subsystem 1
(a) Mechanical supporting structure	Thermal leakage, thermal stability, vibration, weight	Aluminum, rectangular channel, enclosing RF lines and supporting antenna:
(b) Thermal control components	Conflicting requirements of 1(a), isolation or shielding of RF lines from heat inputs (sun, mixer-multiplier)	channel to be super-insulated: All mixers and multipliers mounted on nearby, thermally isolated base plates, antenna elements painted internally to reject sun's radiation; elements are plane polarized, have circular gain pattern (12 dB), and are cross-polarized in orientation to reduce coupling; supports for arms at three points by material of low thermal conductivity.
(c) Antenna elements	Phase center stability, coupling, polarization purity, heat shielding (from sun)	
(d) RF lines	Thermal stability, weight, simplicity	
(e) RF multipliers and mixers	Phase accuracy and stability (line lengths (absolute and increments)	
2. Electronics Package		
(a) IF amplifiers	No major problem	
(b) Phase lock loop	No major problem	
(c) Crossover detection components (low frequency IF, clock generator, crossover, discriminator, etc.)	No major problem	
(d) Counter	Moderate development required.	Solid-state unit available as required.
(e) Sequencer processor	No major problem	

8.6.3 Interferometer Attitude Sensor SCS Interface

The objective of this all-digital special-purpose subsystem is to compute the spacecraft attitude and to provide a control signal that will maintain desired attitude to within $\pm 0.10^{\circ}$. The attitude angle computations together with the error corrections are performed in real-time. Therefore, the system is designed with the following objectives in mind (ref Fig 8.6-5).

1. To compute the attitude angles in a three coordinate system (x, y, z) using phase angle difference measurements from different antenna pairs.

2. Mode selection: If position 5 is treated as a reference, each of the remaining four positions, together with the reference position, will constitute a pair of signals whose phase difference is to be measured. These four readings comprise one mode of operation.

3. Phase Difference Measurements: The phase difference measurements between the reference signal and that from any of the four antenna positions is measured. This measurement is made at two different frequencies which results in eight different readings. The eight readings will, therefore, be repeated periodically and hence will constitute one frame. The eight readings

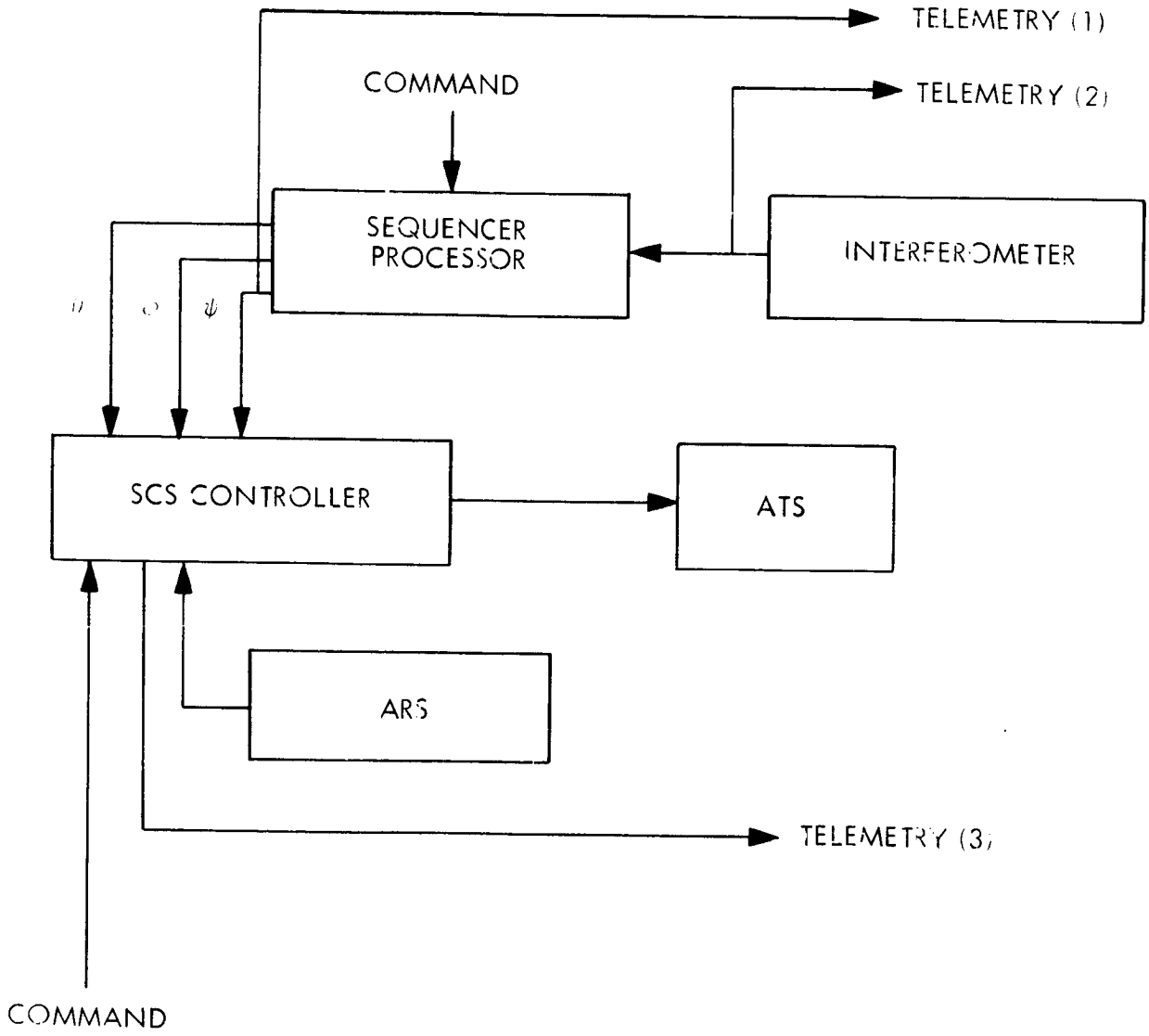

Figure 8.6-5 INTERFACE BETWEEN THE SCS AND INTERFEROMETER

within each frame corresponds to four vernier readings and four coarse readings. In order to accomplish the above objectives, the following subsystems are required.

A. Mode Selector: capable of selecting any of the above-mentioned four modes.

B. Phase Difference Detector: measures the phase difference between any antenna position signal and the reference signal and hence provides the correct readings for both vernier and coarse counters.

C. Arithmetic Unit: Having determined the phase difference measurements, the arithmetic unit utilizes these measurements to compute the three components of spacecraft attitude error.

$$\varepsilon_x, \ \varepsilon_y \text{ and } \varepsilon_z$$

where $\varepsilon_x = \varepsilon'_x + \varepsilon''_x$

$$\varepsilon_y = \varepsilon'_y + \varepsilon''_y$$

$$\varepsilon_z = \varepsilon'_z + \varepsilon''_z .$$

These equations which will be used by the stabilization and control system are derived and described in Section 8.7.

D. Timing and Control Subsystem : The purpose of this subsystem is to generate all timing signals which will perform various instructions, sub-command operations and other computational requirements within

the system. These control signals will coordinate the flow of data from one subsystem to the other and regulate the traffic within each subsystem. Thus, any operation, regardless of how minute or important it is, takes place under the control of this subsystem.

In order to accomplish the foregoing objectives by means of the above subsystems, it is desirable to describe each of the subsystems separately and show how they interact between each other to form the special purpose processor shown in Figure 8.6-6, that will interface with the SCS. A bank of filters can receive the three signals from the arithmetic unit and may be considered as an option rather than an essential part of the system. Their purpose is simply to smooth these signals and thus improve the accuracy of the computed attitude error. Therefore, despite the fact that the system is designed to provide very high accuracy of the attitude measurement, such accuracy can be further enhanced if desired by introducing these filters without adding too much complexity to the overall system.

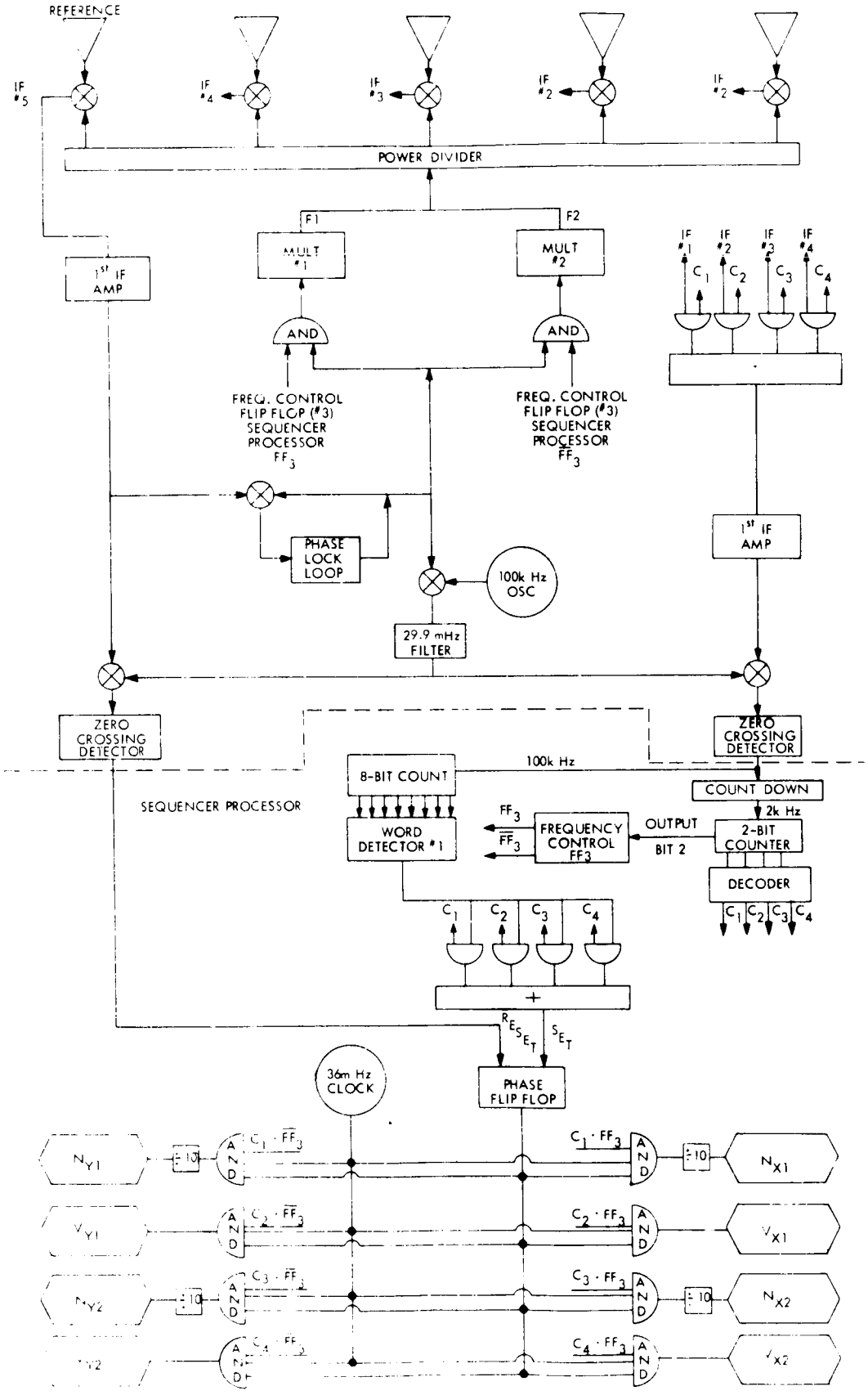

FIGURE 8.6-6 MODE SELECTION AND PHASE MEASUREMENT

System Requirements

Mode Selection and Phase Measurements:

Figure 8.6-7 is a logic diagram for the mode selection and phase measurement. This is the operation mode when the reference antenna element is position 5 and the remaining positions are Nos. 1-4, inclusive. In this diagram, elements 1-4 are sampled sequentially with respect to element 5 by the sequencing control signals C1, C2, C3 and C4. The duration of each of these control signals is determined by the geometry basic to the interferometer. That is, the control signals shall be of a duration which is determined by the maximum phase difference to be measured which is at least 4×10^{-5} seconds. For this value, the maximum clock rate is 25 kHz. Any lower rate is permissible. A 2 kHz clock was selected providing a 500 microsecond sampling duration. This value insures that there is no correlation between count errors, and in addition is consistent with other subsystem requirements.

An insight into the operation can better be comprehended and thus appreciated if the signal from the antenna position elements is traced all the way through to the point of establishing the phase measurement. The 30 Mc signals from antenna positions 1-4 are brought to the sequencing gates together with the sampling control signals, C1 through C4. The outputs of these four AND gates are OR gated together to drive the IF amplifier which in turn drives the crossover detector via the 100 kHz second IF and filter. The purpose of this analog loop is to convert the 30 Hz frequency to 100 kHz and also digitize and shape the output signal. Thus, the output of the detector and shaper is a digital pulse at 100 kHz frequency.

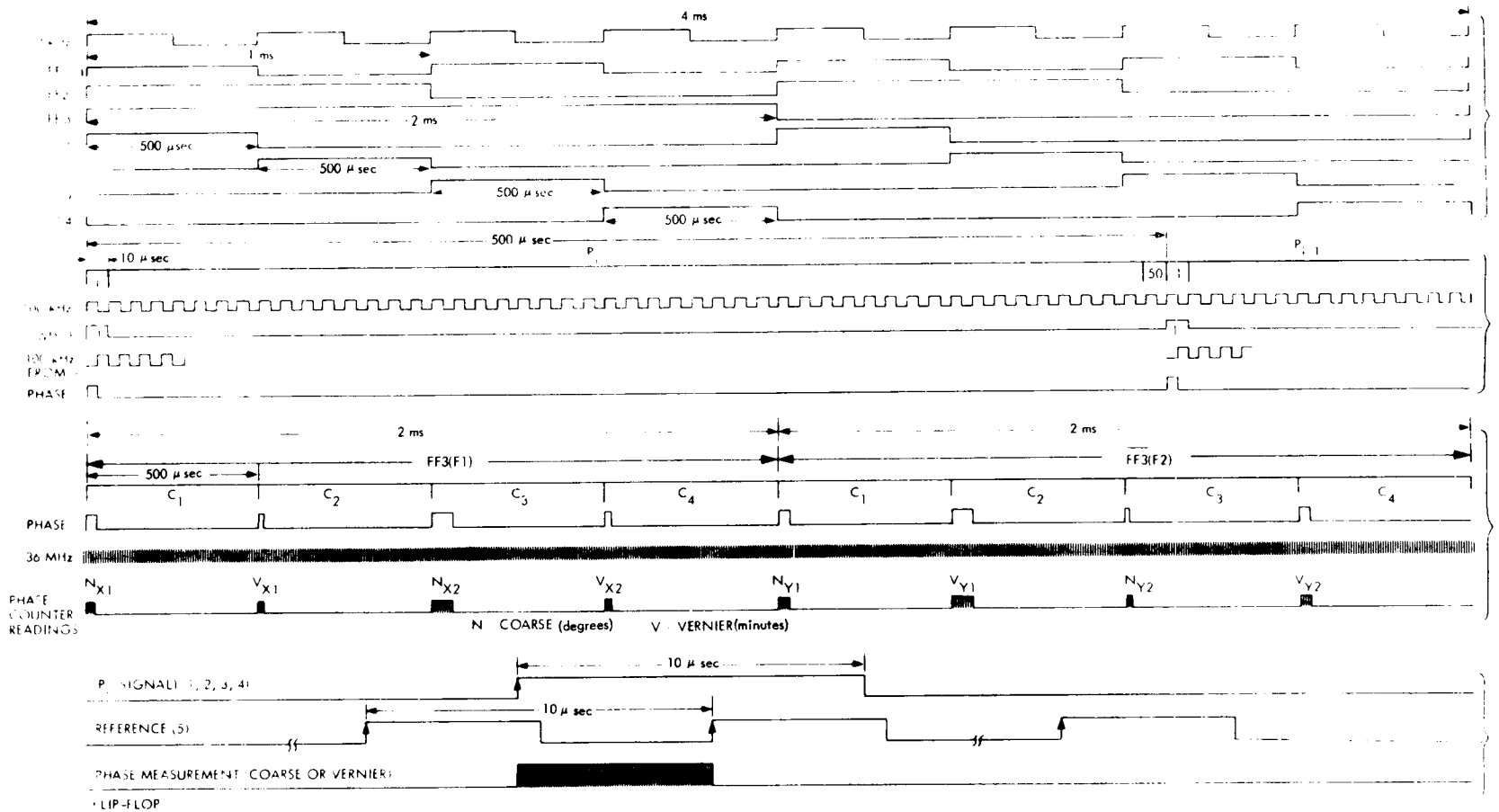

FIGURE 8.6-7 TIMING DIAGRAM SHOWING HOW PHASE MEASUREMENT IS PERFORMED

The output of the shaper is extended to drive an 8-bit binary counter that counts 1-50, and a word detector that produces a pulse corresponding to count of one. This circuitry is required since we are sampling the signal from the antenna positions at the rate of 2 kHz. This means each sample at 2 kHz rate will embrace fifty cycles at 100 kHz and that only one of the fifty cycles is required to perform phase measurement with respect to the reference element. The output of this word detector together with the sampling control signals, C1-C 4, enables an array of four AND gates whose outputs are OR gated to set the phase detector flip-flop. This flip-flop is reset by the reference signal. The output of the phase detector, therefore, has a duration that is a measure of the phase difference. This duration will vary from zero to the duration of the word slot depending upon the angle of arrival of the wavefront (signal from the illuminator). If the phase difference is $\emptyset$ then $\emptyset = \omega t_d$ where t_d represents the duration of the signal coming out of the phase detector flip-flop.

The output signal of the phase detector controls an array of eight counters whose readings represent the actual measure of the phase difference. A 36 MHz clock is AND gated with the phase detector output together with the sequencing control signals. A single gate is enabled at each time and thus the pertinent counter is operating during the interval that this gate is enabled. This is evident since the sampling of the antenna position is carried out in a sequential manner. The eight counters correspond to the eight readings within the frame of eight samples.

Vy1 and Vy2, and the remaining four give the coarse readings designated by Nx1, Nx2, Ny1 and Ny2 over two illuminating frequencies F_1 and F_2. The counters which are preceded by a divide circuit are the coarse reading counters which read up to a maximum of 360 clock pulses which corresponds to 36°, whereas the vernier counters read up to a maximum of 360 clock pulses which corresponds to 60 minutes. These counters are also shift registers whose contents provide inputs to the arithmetic unit for the computation of the equations required by the stabilization and control subsystem.

The remaining logic circuitry in this diagram is strictly to provide control signals for switching from one frequency to the other. Also, it provides means to distribute the power evenly among the five antenna positions. The details of the above operations can be clearly seen from the timing diagram of Figure 8.6-7. In this diagram, the basic 2 kHz clock rate is shown at the top of the figure and is derived from the 100 kHz clock that comes out of the crossover detector circuitry. Flip-flop 3 driven by the 2-bit control signal counter is required to control the up conversion operation of the multiplying chain corresponding to illuminating frequency F_1 or F_2. The control signals C1, C2, C3 and C4 are derived from the 2-bit control signal counter which is driven by the two kHz pulse train. The scale of the next four waveforms is different from that of the preceding set. For reasons of clarity, P_i is the antenna element position. The word detector No. 1 pulses are derived from the one word detector. The phase difference between the reference and other channel is shown in the next two waveforms. The next set of the waveforms, again expanded in scale, show the relationship between the control signals (C_i), the duration of the phase differential, and the 36 MHz clock of the phase counter

readings The latter are the N's for the coarse count and the V's for the vernier count. The last set of waveforms are details of the reference and antenna element signal with the resulting phase measurement.

Arithmetic Unit and Timing and Control:

The equations to be used in determining attitude angle errors are derived in Sect. 8.10. They are stated here and a method for their implementation is given. The three equations are:

$$S(\varepsilon_z' + \varepsilon_z'') = \rho^D_{z1}(V_{x2} + N_{x2}) - \rho^D_{z2}(V_{x1} + N_{x1})$$

$$S(\varepsilon_y' + \varepsilon_y'') = \rho^D_{y1}(V_{x2} + N_{x2}) - \rho^D_{x2}(V_{x1} + N_{x1})$$

$$S\rho_{z1}(\varepsilon_x' + \varepsilon_x'') = \rho_{x1}\rho^D_{z1}(V_{x2} + N_{x2})$$
$$(-)\ \rho^D_{x1}\rho^D_{z2}(V_{x1} + N_{x1})$$
$$(-)\ S(V_{y1} + N_{y1})$$

The logic implementation for solving the first two equations is given in Figure 8.6-8. The implementation for solving equation 3 is similar to that of the first two except for the additional binary multipliers. This is shown in Figure 8.6-9. The values for the vernier counts, Vx1, Vx2,

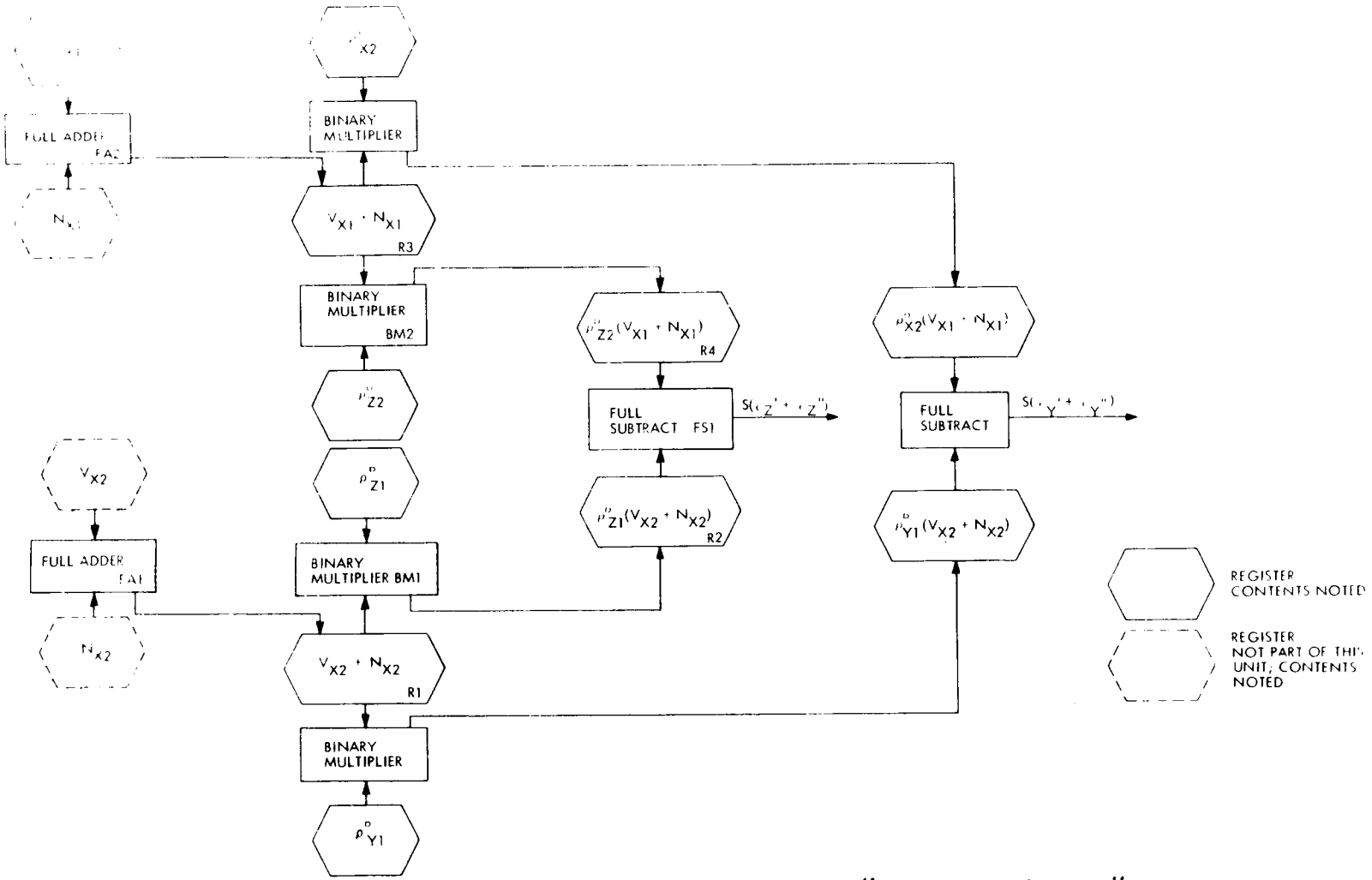

FIGURE 8.6-8 ARITHMETIC UNIT FOR $\epsilon'_Z + \epsilon''_Z$ AND $\epsilon'_Y + \epsilon''_Y$

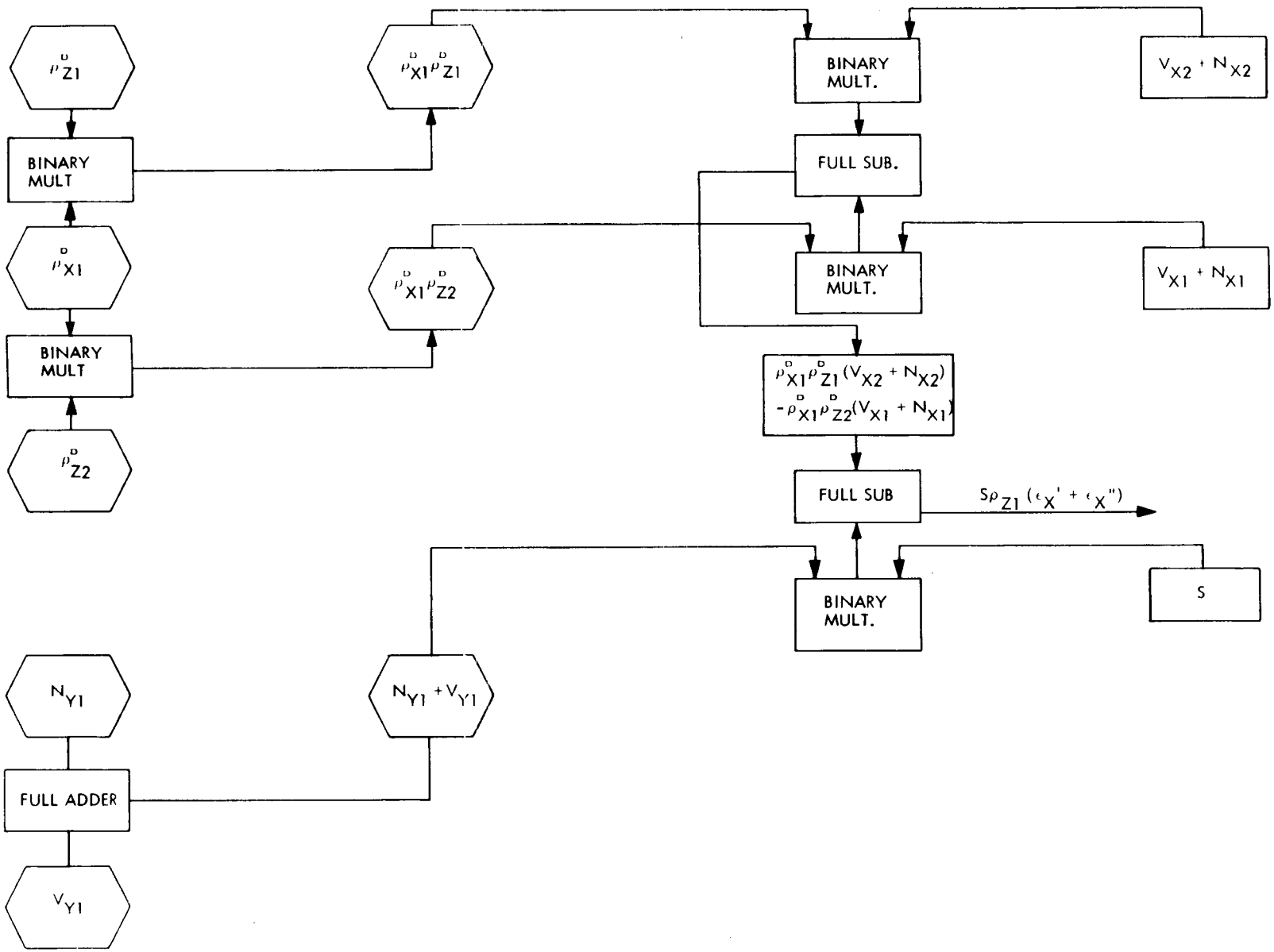

FIGURE 8.6-9 ARITHMETIC UNIT FOR $\epsilon_X' + \epsilon_X''$

Vy1 and Vy2 and the coarse counts Nx1, Nx2, Ny1 and Ny2 are derived from the interferometer shift counter logic. The other constants are determined at the ground computer complex and are transmitted to the spacecraft via the command link.

The implementation to mechanize the above equations is clearly seen from Figures 8.6-8 and 9. Therefore, no further description in this regard is felt to be necessary.

The most important point that should be noted in these two diagrams that constitute the arithmetic unit is the question of how to coordinate and control these computations by means of hardware. This has been accomplished by means of various control signals that are specifically generated by the time distribution circuitry of Figure 8.6-10. A total of sixteen time pulses are generated by the circuit to execute the computation of instructions required by the arithmetic unit. It should be noted that all the computations have to start after the eighth sample is completed. This is important since the complete set of phase measurements are available from the vernier and coarse counters only at the end of the eighth sample. Since the eighth sample is completed effectively by the end of the signal that corresponds to ω1 (the first pulse out of fifty within the eighth sample), the computational instructions should start at the end of this signal. Hence the computational time pulses TP1 through TP16 are generated beyond this point but still within the eighth sample. The method of generating these control signals is done by the time pulse distributor matrix which is driven by x and y counters as shown in Figure 8.6-11. The x and y counter bits are designated by A, B, C, D. For example,

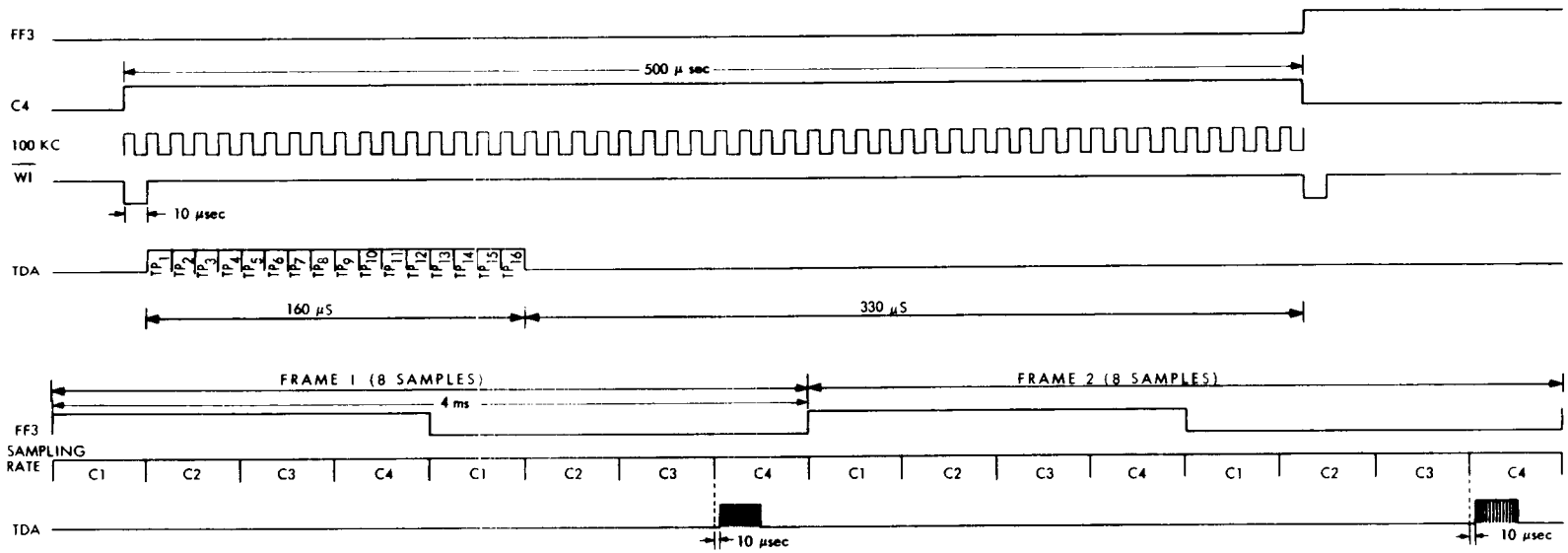

FIGURE 8.6-10 TIMING DIAGRAM FOR THE COMPUTATIONAL INSTRUCTIONS WITH RESPECT TO THE OVER-ALL SYSTEM TIMING

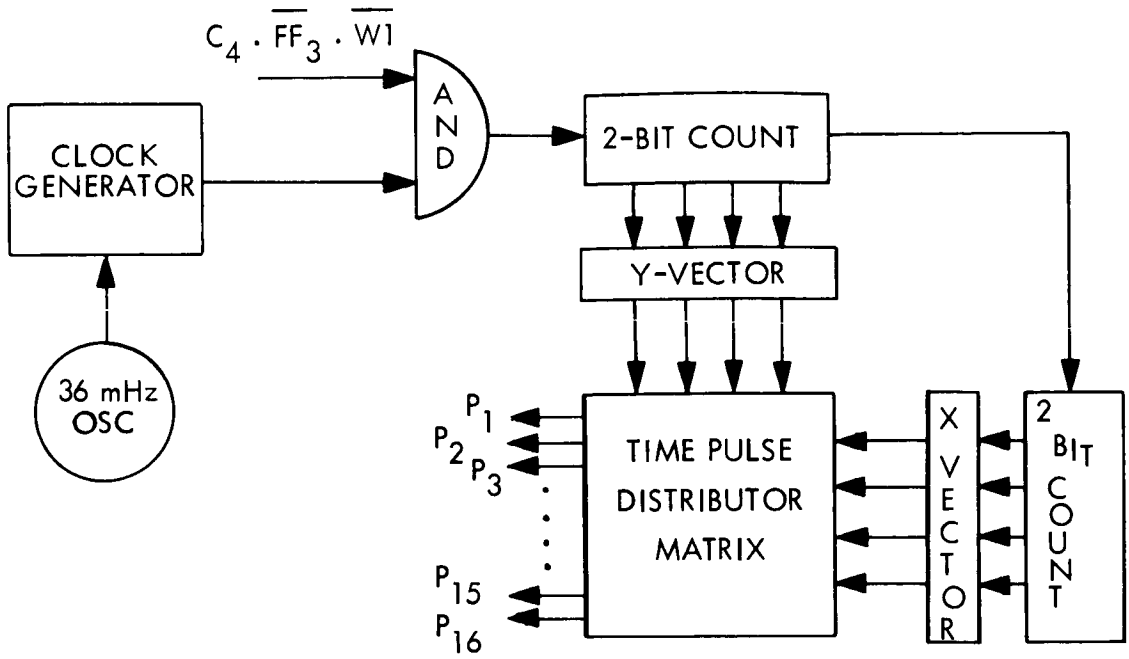

$$
\begin{bmatrix} P_1 \\ P_2 \\ P_3 \\ P_4 \\ P_5 \\ P_6 \\ P_7 \\ P_8 \\ P_9 \\ P_{10} \\ P_{11} \\ P_{12} \\ P_{13} \\ P_{14} \\ P_{15} \\ P_{16} \end{bmatrix}
=
\begin{array}{c}
\begin{array}{cccccccccccccccc} 1 & 2 & 3 & 4 & 5 & 6 & 7 & 8 & 9 & 10 & 11 & 12 & 13 & 14 & 15 & 16 \end{array} \\
\begin{bmatrix}
1 & 0 & 0 & 0 & 0 & \cdot & \cdot & & & & & & & & & \\
0 & 1 & 0 & 0 & \cdot & \cdot & \cdot & & & & & & & & & \\
0 & 0 & 1 & 0 & \cdot & \cdot & \cdot & & & & & & & & & \\
0 & 0 & 0 & 1 & & & & & & & & & & & & \\
0 & \cdot & \cdot & \cdot & 1 & & & & & & & & & & & \\
\cdot & \cdot & \cdot & \cdot & & 1 & & & & & & & & & & \\
\cdot & \cdot & \cdot & & & & 1 & & & & & & & & & \\
\cdot & & & & & & & 1 & & & & & & & & \\
 & & & & & & & & 1 & & & & & & & \\
 & & & & & & & & & 1 & & & & \cdot & \cdot & \cdot \\
 & & & & & & & & & & 1 & \cdot & \cdot & \cdot & \cdot & \cdot \\
 & & & & & & & & & & & 1 & \cdot & \cdot & \cdot & \cdot \\
 & & & & & & & & & & & & 1 & 0 & 0 & 0 \\
 & & & & & & & & & & & \cdot & \cdot & 1 & 0 & 0 \\
 & & & & & & & & & & \cdot & \cdot & \cdot & 0 & 1 & 0 \\
 & & & & & & & & & & \cdot & \cdot & \cdot & 0 & 0 & 1
\end{bmatrix}
\end{array}
\begin{bmatrix}
\overline{D} & \overline{C} & \overline{B} & \overline{A} \\
\overline{D} & \overline{C} & \overline{B} & \overline{A} \\
\overline{D} & \overline{C} & \overline{B} & \overline{A} \\
 & & \cdot & \\
 & & \cdot & \\
 & & \cdot & \\
 & & & \\
 & & & \\
 & & & \\
 & & & \\
 & & & \\
 & & & \\
 & & \cdot & \\
 & & \cdot & \\
 & & \cdot & \\
D & C & B & A
\end{bmatrix}
$$

Figure 8.6-11 TIME DISTRIBUTION OF THE ARITHMETIC UNITS (TDA)

TP1 corresponds to $\overline{D}\overline{C}\overline{B}\overline{A}$ and TP2 corresponds to $\overline{D}\overline{C}\overline{B}A$, etc. The matrix notation in this diagram gives the representation of the time pulses in terms of the binary variables A, B, C and D.

In order to have a better insight as to how these signals are used to compute the above three equations, let us consider as an example the case of executing the first equation and thus reference to Figure 8.6-8, is recommended.

TP1 Clear "FAI' adder and "R1" register.

TP2 Add Nx2 and Vx2 and transfer to R1 register.

TP3 Clear "BMI" multiplier and "R_2" register.

TP4 Add ρ^D_{z1} and the contents of R_1 and transfer to R_2 register.

TP5 Shift the contents of R_2 to the right. (Note that this register contains now the product $\rho^D_{z1}(V_{x2} + N_{x2})$.

TP6 Clear "FA2" adder and "R_3" register.

TP7 Add N_{x1} and V_{x1} and transfer to R_3 register.

TP8 Clear "BM2" multiplier and "R4" register.

TP9 Add $\rho^D_{z_2}$ and the contents of R_3 and transfer to R_4.

TP10 Shift the contents of R_4 to the right. (Note that this register contains now the product $\rho^D_{z_2}(V_{x1} + N_{x1})$.

TP11 Clear "FS1" subtractor.

TP12 Subtract the contents of "R_4" register from the contents of "R_2" register. (Note this output is now $S(\mathcal{E}'_z + \mathcal{E}''_z)$.

TP13 through TP16 are not used.

It follows from the above that in order to compute any of the three equations, at least twelve such instructions are needed. Therefore, all these computations, as mentioned earlier, have to be performed within the eighth sample. Since only ten microseconds out of 500 microseconds are used for the phase detection during the eighth sample, the remaining 490 microseconds will be allotted for housekeeping operations, such as executing the above arithmetic operations. The timing diagram of Figure 8.6-10 shows how these command operations are generated and utilized within the eight sample, i.e., during $C4.\overline{FF3}.\overline{W1}$. For practical purposes, sixteen of these time pulses corresponding to sixteen independent instructions are generated. It should be noted that a given time pulse may be used to perform more than a single operation provided such operations do not interfere with each other. It should be further noted that the total time required to compute all the three equations do not exceed 160 microseconds. Thus, the remaining 330 microseconds will be used as needed.

8.6.4 Physical Characteristics

Weight (Est.)	lbs.
Antenna Array and Mixer Assembly	15
Processor (Including Sequencer)	7
I.F. Amp. Strip	1
Counter	2
Clock	1
Phase Lock Loop	1.5
Local Oscillator (100KC)	0.5
Multiplier	1.5
Miscellaneous Circuitry	1.5
Total	30.5

Power (Est.)

	Preorbital	Normal
R.F. Amp	1 Watt	1 Watt
I.F. Amp	5 Watt	5 Watt
Processor (Including Sequencer)	0	8 Watt
Counter and Clock	0	10 Watt
	0	5 Watt
L.O. and Mult.	0	
		34 Watts

95 A

8.7 ERROR ANALYSIS OF PREFERRED CONCEPT

Preferred Concept, Simplified

The description of the operation of the direct phase reading interferometer system pertinent to the analyses follows.

Based on this model (Figure 8.7-1) the major results of these analyses are given. Error curves for the composite or total system summarize the analysis.

The system operation may be conveniently divided into three parts; the interferometer electronics which converts an RF signal into something proportional to electrical phase; a scale factor which converts this result into a signal which gives the direction, Θ_S, of the RF wavefront relative to the baseline; and lastly a geometrical transformation which converts Θ_S into spatial attitude, ϵ (e.g. pitch, roll and yaw).

The first block is discussed in an earlier section. However, for purposes of analysis Figure 8.7-2 provides a reasonable basis. As seen from this figure, the output is the count, N which is proportional to electrical phase. In Appendix 8.F this relationship is developed and is given by equation 1.

$$N = \omega_c \left(t_{on} - t_{off}\right)$$

$$N = \underbrace{\frac{\pi(n-m)}{\omega_g}}_{\text{Ambiguity}} \omega_c + \underbrace{\frac{u+1}{2}\left[\frac{R_A^* - R_B^*}{C}\right]}_{\text{Signal}} \omega_c + \underbrace{\frac{c}{2\omega_g}\left(\phi_{IFA} - \phi_{IFB}\right)}_{\text{Calibration}} \qquad (1)$$

The term $(\pi/\omega_G)(n-m)\,\omega_c$ represents the ambiguity which is removed via the long-short baseline concept. The last term $\omega_c/2\omega_G\,(\phi_{IFA} - \phi_{IFB})$ represents the bias count produced by an uncalibrated system. A calibration

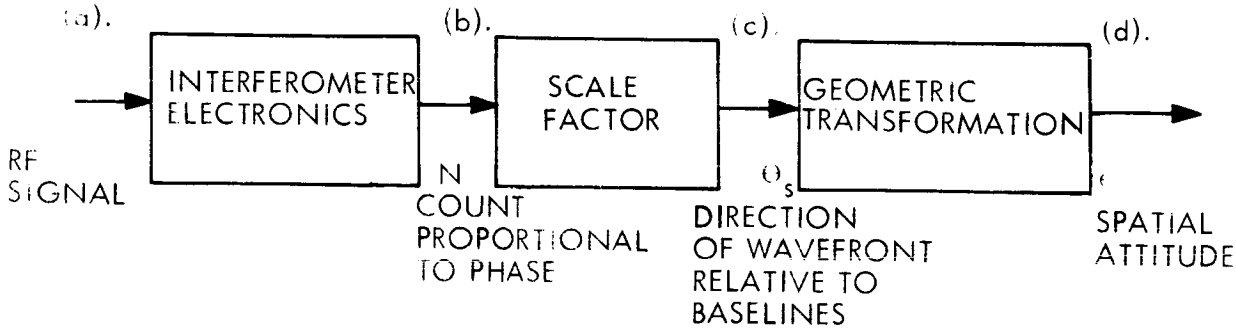

Figure 8.7-1 SYSTEM MODEL

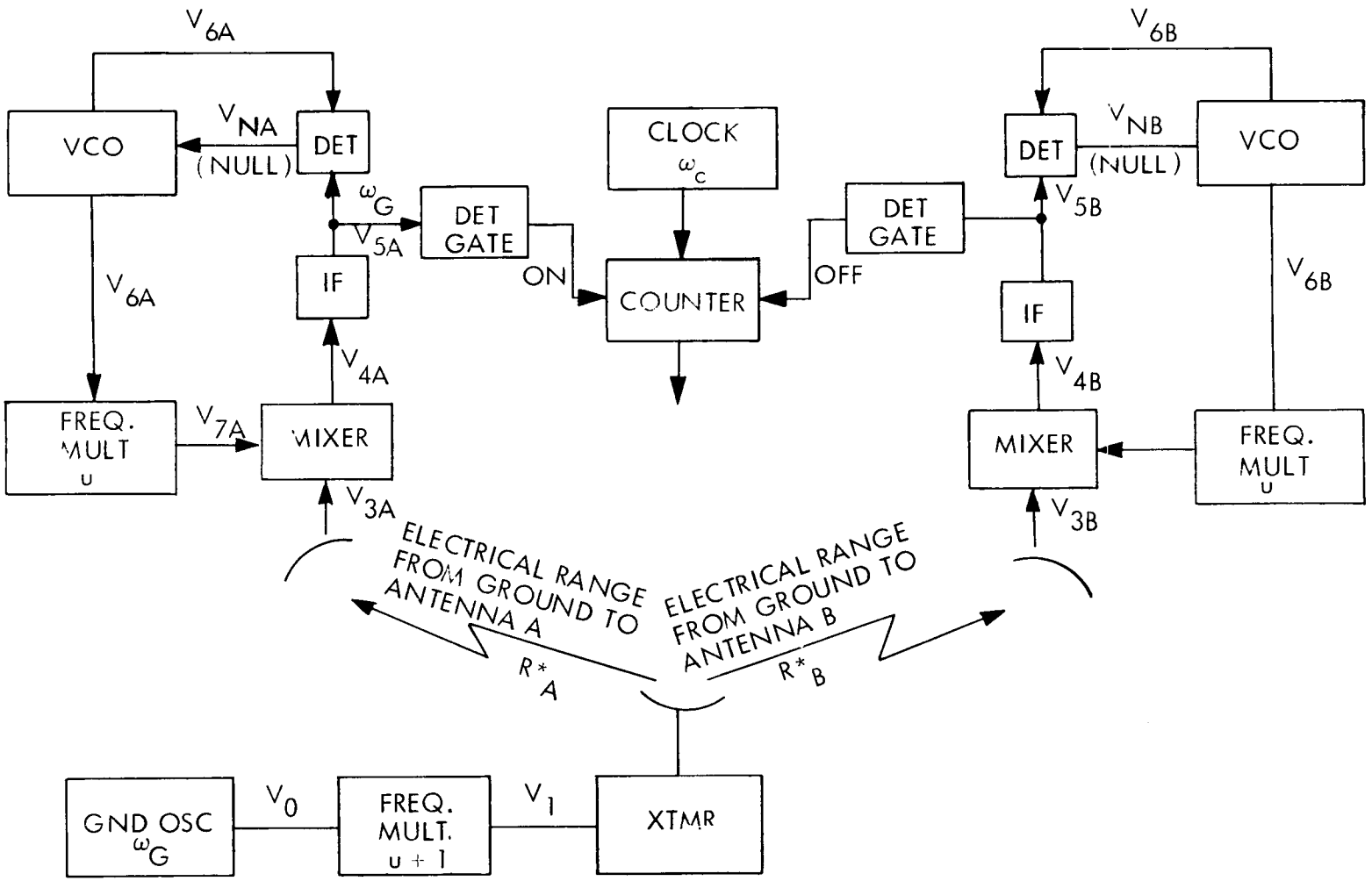

Figure 8.7-2 SIMPLIFIED BLOCK DIAGRAM OF DIRECT PHASE READING ELECTRONICS

procedure removes this bias to an acceptable level. The center term is the desired signal. For purposes of analysis the expression $\omega_c(t_{on}-t_{off})$ will be used except where the effects of atmospheric refraction are concerned. It will be assumed therefore that ambiguity and bias errors have been removed from the count N.

The conversion of counts to Θ_S is given by equation 4. The development of this equation follows directly from Figure 8.7-3. Clearly

$$\cos \Theta_S = \frac{CT}{D} = \frac{\lambda_{RF}}{2\pi D} \phi_{RF} \qquad (2)$$

The effect of the phase locked loop is to preserve phase such that

$\phi_{RF} = \phi_{IF}$ or phase at the output of the IF.

But $\quad (t_{on}-t_{off}) = N/\omega_c$ (in radians) $\qquad (3)$

$$\text{therefore} \quad \cos \Theta_S = \frac{\lambda_{RF}}{2\pi D} \frac{\omega_{IF}}{\omega_c} N \qquad (4)$$

As will be shown directly it is not necessary to calculate the arc cosine. Hence the scale factor is $\frac{\lambda_{RF}\,\omega_{IF}}{2\pi D\ \omega_c} = \frac{A\lambda_{RF}}{2\pi D_i} = F_i$

The geometrical transformation which converts Θ_S into spatial attitude ϵ is somewhat more complex. The details of the development may be found in Appendix 8I. There are two results; one for large attitude error angles and the other for small attitude error angles. Attitude error angles are defined here as the difference between the commanded and actual attitude angles. The large attitude error angle equation uses four (4) phase readings to determine three (3) spatial angles (a redundancy of one). The small attitude error signal equations uses three (3) phase readings to

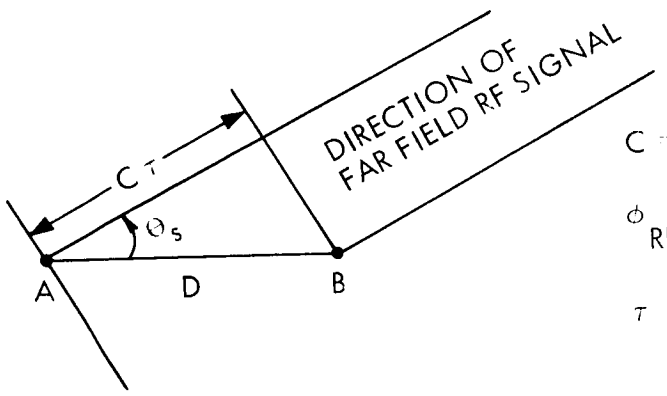

$$C = \lambda f = \frac{\omega_{RF}}{2\pi} \lambda_{RF}$$

$$\phi_{RF} = \omega_{RF} \tau$$

$$\tau = \frac{R_A^* - R_B^*}{C}$$

Figure 8.7-3 BASIC INTERFEROMETER RELATIONSHIP

to determine three (3) spatial angles. The advantage of the small error signal equations is simplicity. Though the large error signal equations will provide slightly more accuracy due to the redundancy, the small attitude error signal equations will be used here as they provide considerably more physical insight into the problem.

The small attitude error signal equations are given by equations 5, 6 and 7.

$$\epsilon_z = \left(\frac{\rho^D_{z1}}{S}\right)\rho_{x2} - \left(\frac{\rho^D_{z2}}{S}\right)\rho_{x1} \tag{5}$$

$$\epsilon_y = \left(\frac{-\rho^D_{x2}}{S}\right)\rho_{x1} + \left(\frac{\rho^D_{y1}}{S}\right)\rho_{x2} \tag{6}$$

$$\epsilon_x = \left(\frac{\rho^D_{x1}}{S}\right)\rho_{x2} - \left(\frac{\rho^D_{x1}}{\rho^D_{z1}}\right)\left(\frac{\rho^D_{x2}}{S}\right)\rho_{x1} - \left(\frac{1}{\rho^D_{z1}}\right)\rho_{y1} \tag{7}$$

where $S = \left(\rho^D_{y1}\ \rho^D_{z2} - \rho^D_{y2}\ \rho^D_{z1}\right)$

$$\rho_{x1} = F_1 N_{11};\quad \rho_{x2} = F_1 N_{21};\quad \rho_{y1} = F_2 N_{12}$$

N_{ij} is the count produced across baseline leg i from ground station j. Notice the ρ_{y2} is not used in equations 5, 6 or 7. ρ_{y2} would be used in the large attitude error signal equations.

Figure 8.7-4 provides a graphic picture of equations 5, 6 and 7.

Error Analysis Results of Interferometer Electronics

There are several identifiable sources of error exclusive of ambiguity and calibration. They are:

1) error in N, ΔN

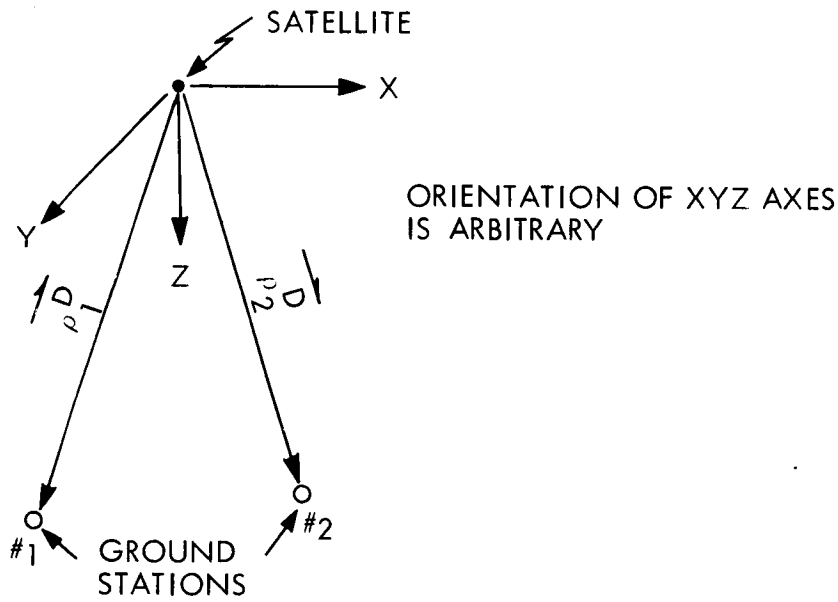

$$\vec{\rho}_1^D = \vec{i}\,\rho_{X1}^D + \vec{j}\,\rho_{Y1}^D + \vec{k}\,\rho_{Z1}^D$$

$$\rho_2^D = \vec{i}\,\rho_{X2}^D + \vec{j}\,\rho_{Y2}^D + \vec{k}\,\rho_{Z2}^D$$

$$|\vec{\rho}_1^D| = |\vec{\rho}_2^D| = 1$$

Figure 8.7-4 GEOMETRICAL RELATIONSHIP OF SATELLITE POSITION AND GROUND STATION

2) refraction error $\Delta\left(\frac{R_A - R_B}{c}\right)$

These errors in turn may be shown to be composed of other error sources. Taking each error in turn;

N is composed of errors in turning the counter ON, turning it OFF and the quantization error in the count. The error in turning the counter on or off is caused by noise superimposed on the IF signal which causes the gate to trigger at a false time. The noise is caused primarily by thermal noise which enters through the antenna, and internally generated noise.

Appendix 8H shows that the variance of this triggering error is given by

$$\sigma_t^2 = \frac{4-\pi}{4\,\omega_{IF}^2}\,\frac{1}{S/N} \approx \frac{.463}{\omega_{IF}^2}\,S/N \tag{8}$$

where S/N is the signal to noise ratio at the input to the gate and ω_{if} is the IF frequency.

The error in the count due to errors in triggering the counter on and off is given by

$$\Delta N = \omega_c\left(\Delta t_{on} - \Delta t_{off}\right) \tag{9}$$

The variance of ΔN is given by

$$\begin{aligned}\sigma_N^2 &= \omega_c^2\left[\sigma_{ton}^2 + \sigma_{t\,off}^2 - 2\,\sigma_{t\,on\,t\,off}^2\right] \\ &= \left(2\,\omega_c\,\sigma_t\right)^2\left[1 - k_{on\,off}(T)\right]\end{aligned} \tag{10}$$

where k on off (T) is the cross correlation coefficient between the on and off gating errors.

The cross correlation coefficient is given by

$$k_{on\ off}(T) = \frac{\sin \pi BT}{\pi BT} \cos \omega_o T \qquad (11)$$

where T is the time between ON and OFF pulses, B is the bandwidth of the IF section and ω_o is the center frequency of the IF.

The ON and OFF gating errors are correlated because the white noise entering via the antenna travels down the A and B circuits and becomes highly correlated (colored) by the narrow band IF section. Thus the noise that causes an error in turning the counter ON tends to be the same noise that causes an error in turning if OFF. The net effect as shown by equation 10 is to provide a smaller count variance than would ordinarily be expected.

The quantization error is caused by the fact that the counter "counts" only at the clock oscillator positive going zero crossing. Thus it is possible to "gain" time at the start of the count and "lose" time at the end of the count. This effect is analyzed in Appendix 8H and is given here as

$$\sigma \phi_T = \sqrt{\frac{2}{3}} \frac{\pi}{\omega_c} \qquad (12)$$

The quantization error and the gating errors are satistically independent. Thus the variance of the combined errors is the sum of the respective variances.

$$\sigma^2_{NT} = \sigma^2_N + \frac{2}{3} \pi^2 \qquad (13)$$

Equation 13 is plotted in Figure 8.7-5 versus θ_S (which establishes the nominal T for equation 11) and for several values of signal to noise ratio.

Error Produced by Refraction

There are two effects here as shown by Figure 8.7-6 and described below.

E_G	is the elevation angle in the absence of an atmosphere
E^*	is the apparent elevation angle in the presence of an atmosphere
R_A, R_B	are the ranges in the absence of an atmosphere
R_A^*, R_B^*	are the ranges in the presence of an atmosphere.

$E^* - E_G$ versus elevation angle is sketched in Figure 8.7-7 for an RF signal of about 10,000 GHZ.

Figure 8.7-8 shows the difference in slant range due to atmospheric refraction versus the effective baseline length.

The cross hatched areas show the region in which the system is normally expected to operate. As will be shown, both effects are negligible compared to the error in the count or the desired system accuracy.

Errors in the Scale Factor

The scale factor which converts N into $\cos \theta_S$ is given by

$$F_i = \lambda_{RF} \; A/_{2 \pi D_i} \qquad (14)$$

Therefore any error in scale factor caused by the system not having the proper RF wavelength and/or baseline length produces an error in $\cos \theta_S$ in addition to that produced by the count.

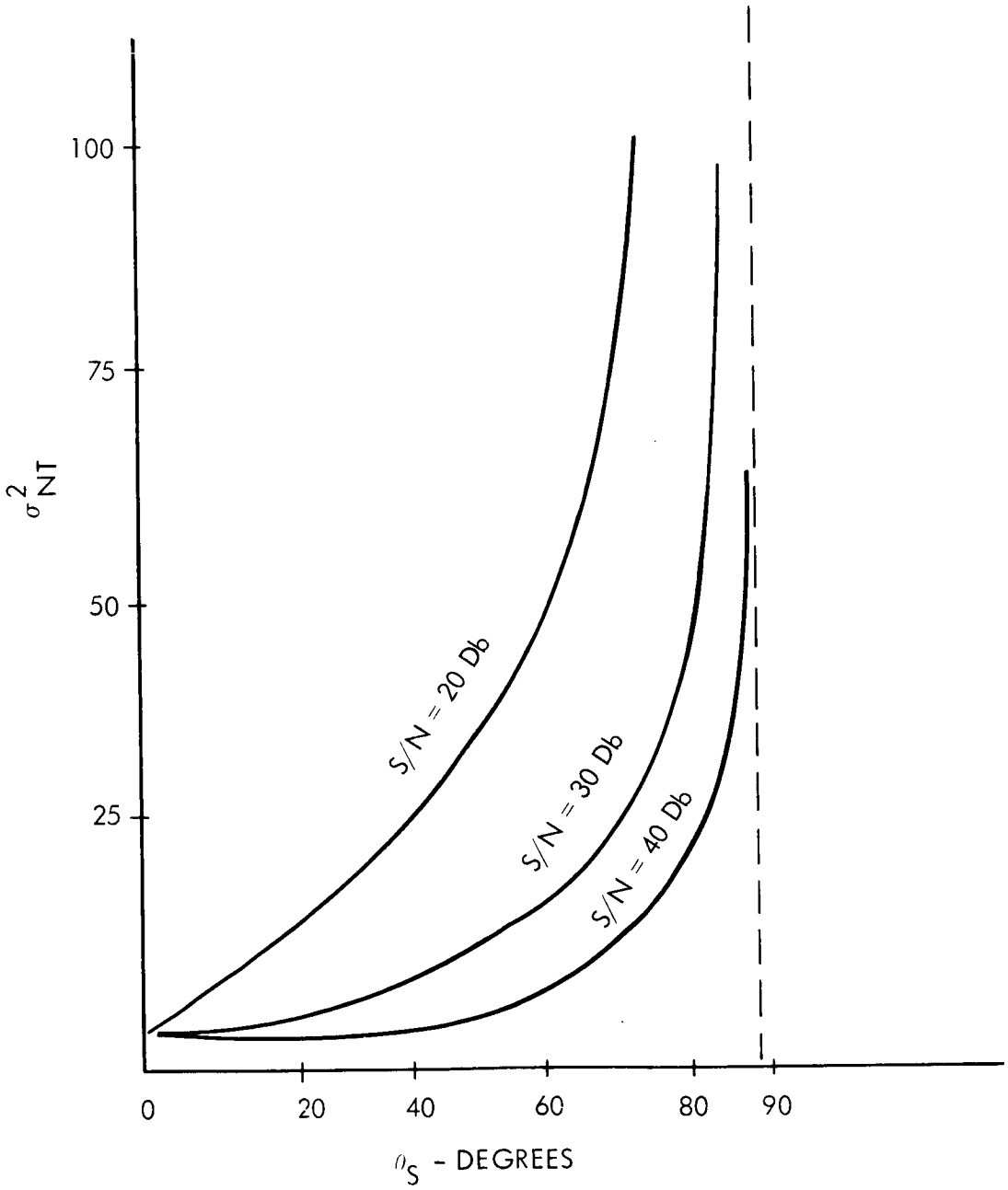

Figure 8.7-5 ERROR IN COUNT VERSUS θ_S

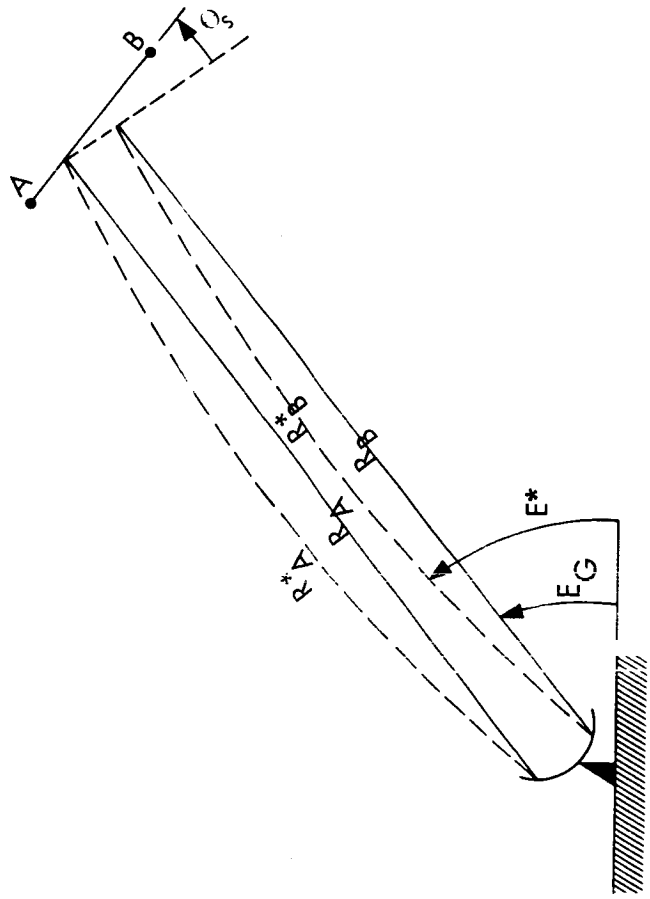

Figure 8.7-6 REFRACTION EFFECTS

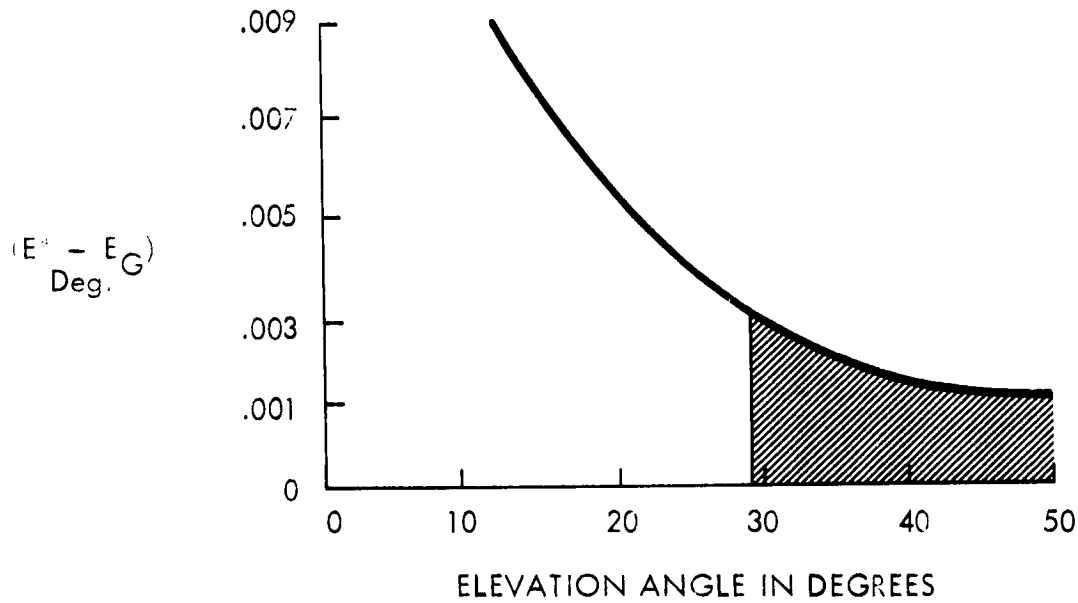

Figure 8.7-7 ATMOSPHERIC EFFECT ON ELEVATION ANGLE

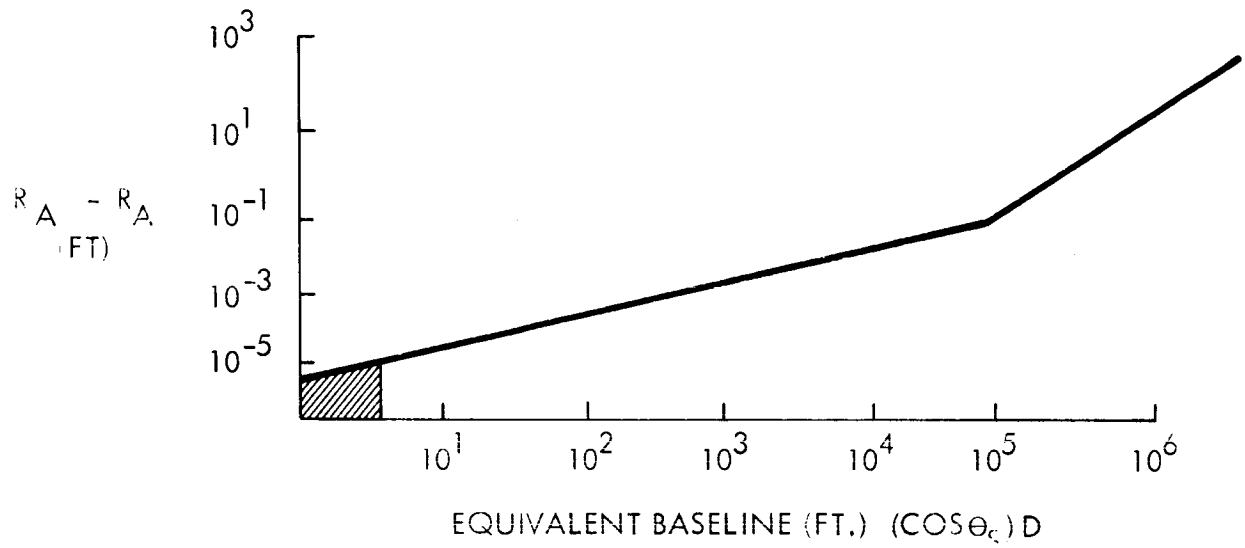

Figure 8.7-8 ATMOSPHERIC EFFECT ON THE SLANT RANGE DIFFERENCE

$$\Delta \cos \theta_S = \left(\frac{AN\lambda_{RF}}{2\pi D_i}\right)\left(\frac{\Delta\lambda_{RF}}{\lambda_{RF}}\right) - \left(\frac{AN\lambda_{RF}}{2\pi D_i}\right)\left(\frac{\Delta D_i}{D_i}\right) + \left(\frac{AN\lambda_{RF}}{2\pi D_i}\right)\frac{\Delta N}{N} \tag{15}$$

$$\frac{\Delta \cos \theta_S}{\cos \theta_S} = \frac{\Delta\lambda_{RF}}{\lambda_{RF}} - \frac{\Delta D_i}{D_i} + \frac{\Delta N}{N}$$

It is apparent that the F_i error depends on the nominal θ_S. It is zero when the wavefront is parallel to the baseline. At $\theta_S = 60^o$ (wavefront is 30° with respect to the baseline), the nominal N is $12\pi X10^3$ radians (6000 counts). The 3σ probable ΔN at that attitude (from Figure 8.7-5) is 15 radians ($^S/N$ = 40 Db). Hence

$$\Delta N/N = \frac{15}{12\pi X10^3} \approx .4 \times 10^{-3}$$

From equation 15 for the baseline error to be negligible requires that

$$\Delta D < .4X10^{-4}\ D = 1.59 \times 10^{-4}\ \text{ft} \approx .002 \text{ inches}$$

Similarly

$$\Delta\lambda_{RF} < .4X10^{-4}\ \lambda_{RF} = .4X10^{-5}\ \text{ft.}$$

or $\Delta\lambda f_{RF} < 4000$ cps.

These are highly conservative requirements and may be relaxed by 3:1 without appreciable loss of performance.

An error of 3 parts per million in the speed of light produces an error in λ_{RF} equal to

$$\Delta\lambda_{RF} = -\lambda\frac{\Delta c}{c} = -.1\,(3X10^{-6}) = -3X10^{-7}\ \text{ft}$$

which is negligible.

The significant sources of error have been shown to be combined and the overall system performance determined.

Spatial Attitude Errors Resulting from Interferometer Errors

Equations 5, 6 and 7 are the key equations. It is assumed that those variables with superscript D are errorless. This assumes a perfect navigation system and an error less survey between the two ground stations. In any event the errors in ϵ x, y, z as caused by the interferometer are independent of the navigation and survey errors and may therefore be treated separately.

A linear relationship is seen to exist between the count, N, and the attitude error signal ϵ. Therefore the error equations which relate errors in N to errors in ϵ may be derived directly from equations 5, 6 and 7. The error equations are given by equation 16 and have been arranged in matrix notation.

$$\begin{bmatrix} \Delta\mathcal{E}_x \\ \Delta\mathcal{E}_y \\ \Delta\mathcal{E}_z \end{bmatrix} = \begin{bmatrix} -\left(\frac{\rho^D_{z2}}{\rho^D_{z1}}\right)\left(\frac{\rho^D_{x1}}{S}\right) & \left(\frac{\rho^D_{x1}}{S}\right) & \left(\frac{-1}{\rho^D_{z1}}\right) \\ -\left(\frac{\rho^D_{x1}}{S}\right) & \left(\frac{\rho^D_{y1}}{S}\right) & 0 \\ -\left(\frac{\rho^D_{z2}}{S}\right) & \left(\frac{\rho^D_{z1}}{S}\right) & 0 \end{bmatrix} \begin{bmatrix} \Delta\rho_{x1} \\ \Delta\rho_{x2} \\ \Delta\rho_{y1} \end{bmatrix} \tag{16}$$

where

$$S = \rho^D_{y1}\rho^D_{z2} - \rho^D_{y2}\rho^D_{z1}$$

Two singularities exist: one, where ρ^D_{z1}, is zero and the other where S is zero. Referring to Figure 8.7-4 it is seen that ρ^D_{z1} is unlikely to be zero since this would point the main antenna axis out into space.

However, the possibility of S being small is quite high.

Noting that

$$\vec{\rho}_1^{\,D} \times \vec{\rho}_2^{\,D} = \vec{i} \sin \gamma = \vec{i} \left(\rho_{y1}^{D} \rho_{z2}^{D} - \rho_{z1}^{D} \rho_{y2}^{D} \right) = \vec{i}\, S \qquad (17)$$

where γ is the angle subtended between the lines of sight to the two ground stations and that $\sin \gamma \approx L/H \approx 2000/20,000 = .1$, it is clear that a magnification factor of approximately 10 is present in the conversion of $\Delta \vec{\rho}$ errors to $\Delta \epsilon$ errors.

But Figure 8.7-4 shows that ρ_{x1}^{D} and ρ_{x2}^{D} will ordinarily be very small. The net effect is that only the ϵ_z axis errors are amplified by this factor of 10. The ϵ_x and ϵ_y axes amplification factor is about unity.

A typical satellite-ground station configuration would produce the following matrix.

$$\begin{bmatrix} \Delta \epsilon_x \\ \Delta \epsilon_y \\ \Delta \epsilon_z \end{bmatrix} = \begin{bmatrix} 0 & 0 & -1 \\ 1 & 0 & 0 \\ 9.5 & -9.6 & 0 \end{bmatrix} \begin{bmatrix} \Delta \rho_{x1} \\ \Delta \rho_{x2} \\ \Delta \rho_{y1} \end{bmatrix} \qquad (18)$$

This configuration assumes a ground station separation of 2000 n. mi and ρ_{z1}^{D} is pointed at one of the ground stations. The pitch axis is assumed normal to the plane formed by the satellite and tow ground stations. (see Glossary entry at "y", "y", "z")

Total System Performance (Interferometer Only)

In this section the results of the separate analyses will be combined and the overall system performance determined.

The significant sources of error have been shown to be:

1) error in the count due to external thermal noise

2) error in the count due to quantization.

The errors caused by refraction, ground oscillator stability, speed of light, baseline stability can be shown to be negligible.

It has also been shown that the error in N due to external thermal noise depends to a large extent on the bandwidth of the IF section and the orientation of the baseline relative to the RF wavefront.

The accuracy of conversion of counts into spatial attitude depends heavily on the geometry between the satellite and the ground station. For a normal mode of operation only one axis, the axis pointed toward the ground (i.e. the yaw axis) is susceptible to inaccuracies an order of magnitude larger than the other two (i.e. pitch and roll axes).

The system error equation which relates error in the count to errors in spatial attitude is given by

$$\begin{bmatrix} \Delta\varepsilon_1 \\ \Delta\varepsilon_2 \\ \Delta\varepsilon_3 \end{bmatrix} = \frac{F}{S} \begin{bmatrix} \left(-\frac{\rho^p_{z_2}}{\rho^p_2}\frac{\rho^p_{x_1}}{D_1}\right) & \left(\frac{\rho^p_{x_1}}{D_2}\right) & \left(-\frac{S}{\rho^p_{21}D_1}\right) \\ \left(\frac{\rho^p_{x_2}}{S_1}\right) & \left(\frac{\rho^p_{z_1}}{D_2}\right) & (0) \\ \left(-\frac{\rho^p_{z_1}}{D_1}\right) & \left(\frac{\rho^p_{z_1}}{\rho^p_2}\right) & (0) \end{bmatrix} \begin{bmatrix} \Delta N_{11} \\ \Delta N_{21} \\ \Delta N_{12} \end{bmatrix} \tag{19}$$

$$= \frac{F}{S} M_\varphi \Delta N$$

The covariance matrix of attitude errors is given by

$$S_\varepsilon = \langle \varepsilon\varepsilon^T \rangle = (F/S)^2 M_\varphi S_N M_\varphi^T \tag{20}$$

where $S_N = \begin{bmatrix} \sigma^2_{N_{11}} & 0 & 0 \\ 0 & \sigma^2_{N_{21}} & 0 \\ 0 & 0 & \sigma^2_{N_{12}} \end{bmatrix}$

and < > denotes mathematical expectation.

The count errors are uncorrelated by virtue of the time lapse between counting N_{11} and N_{21}, N_{22} and N_{12}, and N_{11} and N_{12}. The time lapse is dictated by the switching time which is on the order of 10^{-3} seconds which is at least an order of magnitude greater than the time between ON and OFF pulses. The quantization error portion of N is also assumed independent among the three counts.

Thus equation 20 may be written as follows

$$S_{\varepsilon} = \left(\frac{F}{S}\ \sigma_{NT}\right)^2 M_{\emptyset}\ M_{\emptyset}^{T} \tag{21}$$

The attitude variances are given by equations 22, 23 and 24 respectively.

$$\sigma_{\varepsilon x}^2 = \left(\frac{F}{S}\sigma_N\right)^2 \left\{\left(\frac{\rho_{z2}^{D}}{\rho_{z1}^{D}}\ \frac{\rho_{x1}^{D}}{D_1}\right)^2 + \left(\frac{\rho_{x1}^{D}}{D_1}\right)^2 + \left(\frac{S}{\rho_{z1}^{D} D_2}\right)^2\right\} \tag{22}$$

$$\sigma_{\varepsilon y}^2 = \left(\frac{F}{S}\sigma_N\right)^2 \left\{\left(\frac{\rho_{x2}^{D}}{D_1}\right)^2 + \left(\frac{\rho_{y1}^{D}}{D_2}\right)^2\right\} \tag{23}$$

$$\sigma_{\varepsilon z}^2 = \left(\frac{F}{S}\sigma_N\right)^2 \left\{\left(\frac{\rho_{z2}^{D}}{D_1}\right)^2 + \left(\frac{\rho_{y1}^{D}}{D_2}\right)^2\right\} \tag{24}$$

In order to present the results of equations 22, 23 and 24 numerically the following has been done. First only motion about the pitch axis will be investigated. The results for the yaw axis motion should be very similar. Second, the pitch axis is assumed normal to the plane formed by the satellite and the two ground stations. Figure 8.7-9 illustrates the situation.

The angle θ will be varied from zero to 30 degrees, γ being held constant at 4.74°. The standard deviations of $\Delta\varepsilon_z$ and

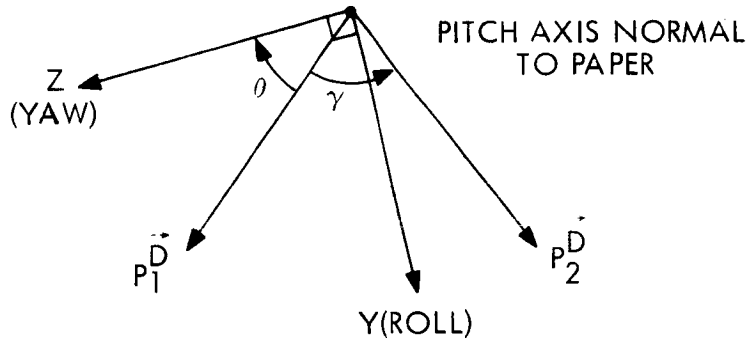

Figure 8.7-9 SPACECRAFT COORDINATE SYSTEM

$\Delta \epsilon_x$ is plotted versus θ for S/N = 20, 30 and 40 Db in Figures 8.7-10 and 8.7-11.

The Problem of Computing Desired Attitude from Navigation and Survey Data

Before beginning the error analyses of the navigation systems, the equations which transform navigation and survey data into desired attitude will be developed.

Consider Figure 8.7-12

clearly $$\vec{R}_1^D = \vec{R}_S - \vec{R}_{1G} \tag{27}$$

and $$\vec{R}_2^D = \vec{R}_S - \vec{R}_{2G} \tag{28}$$

The navigation filter yields $\vec{\rho}_S$ in an xyz ECI system which is probably aligned with the z axis along the earth's spin axis and the xy plane in the equator. $\vec{\rho}_{1G}$ and $\vec{\rho}_{2G}$ are also expressed in this frame. Thus the x axis is therefore probably directed along the Greenwich meridian at some arbitrary reference time. The vector substractions are then performed as indicated by equations 27 and 28.

The results of equations 27 and 28 are next transformed into the desired set of axes. This may be done easily by rotations about two axes. Equation 29 represents this rotation in matrix rotation.

$$R^D = M_A M_B R_{EF} \tag{29}$$

where M_A and M_B are 3 X 3 orthonornal rotation matrices whose elements are functions only of the desired rotation. This last set of rotations is errorless.

The error in ρ_1^D or ρ_2^D is therefore expressable without

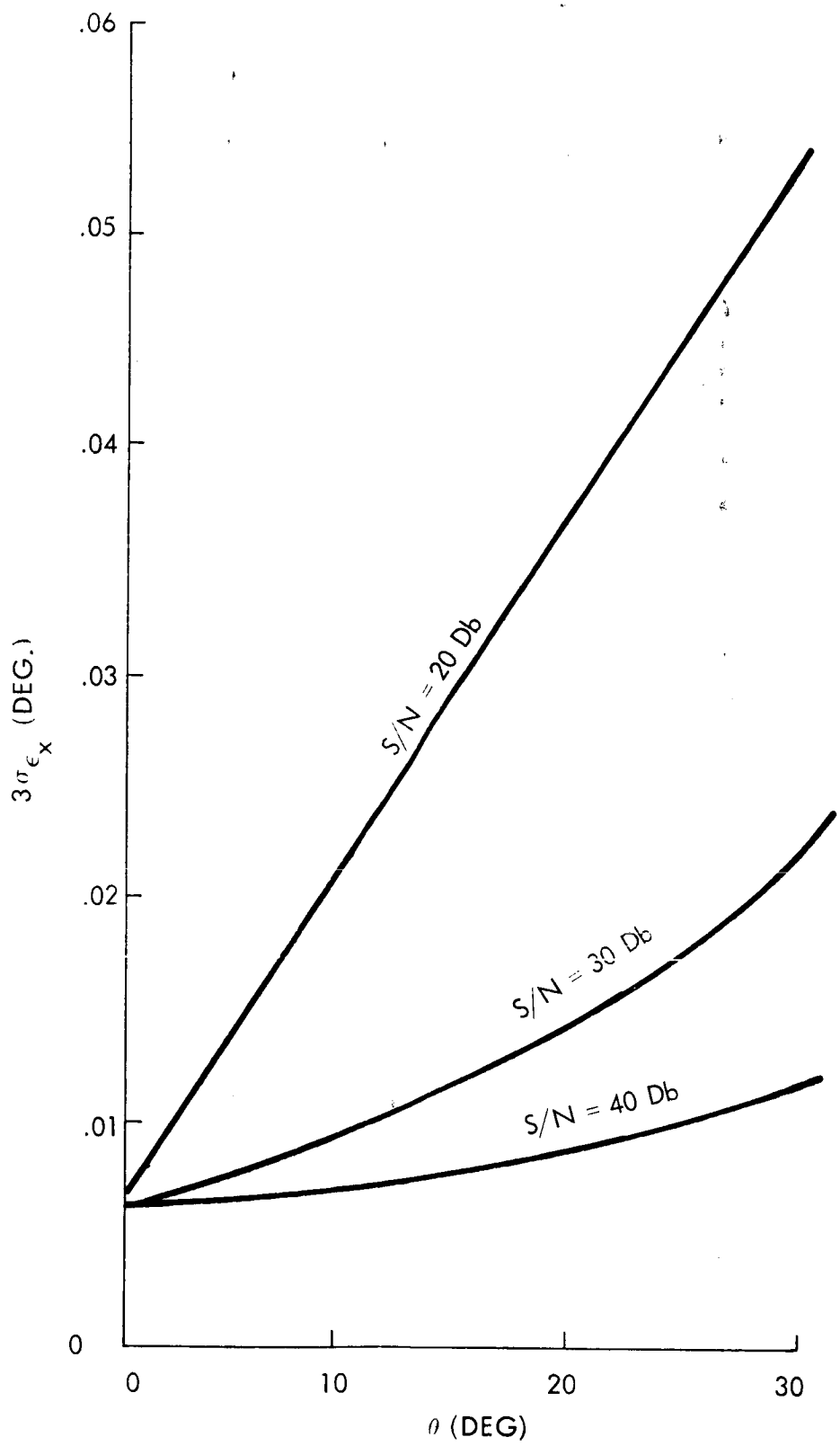

Figure 8.7-10 PITCH AXIS 3σ ERROR VERSUS PITCH ANGLE θ

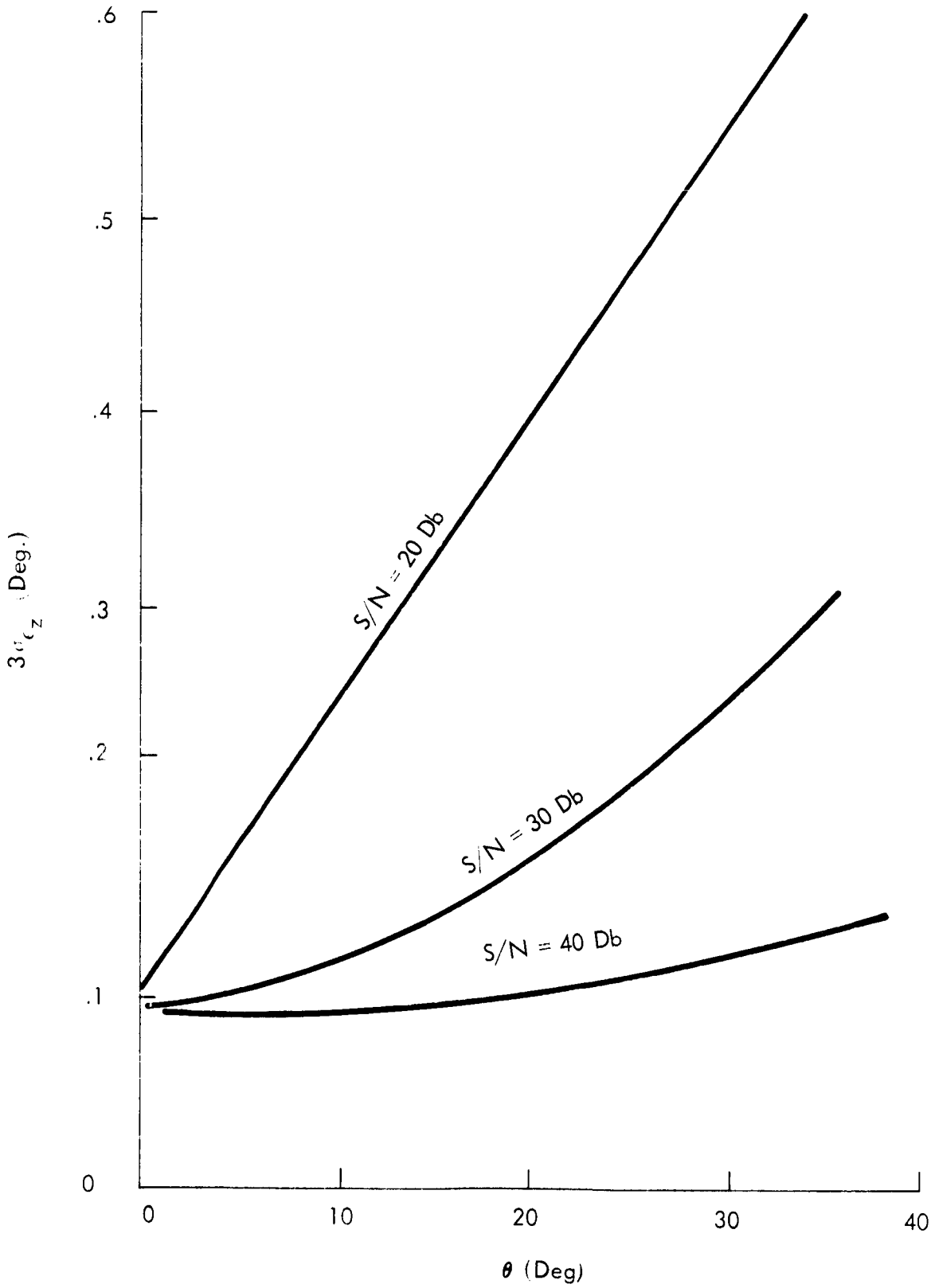

Figure 8.7-11 YAW AXIS 3σ ERROR VERSUS PITCH ANGLE θ

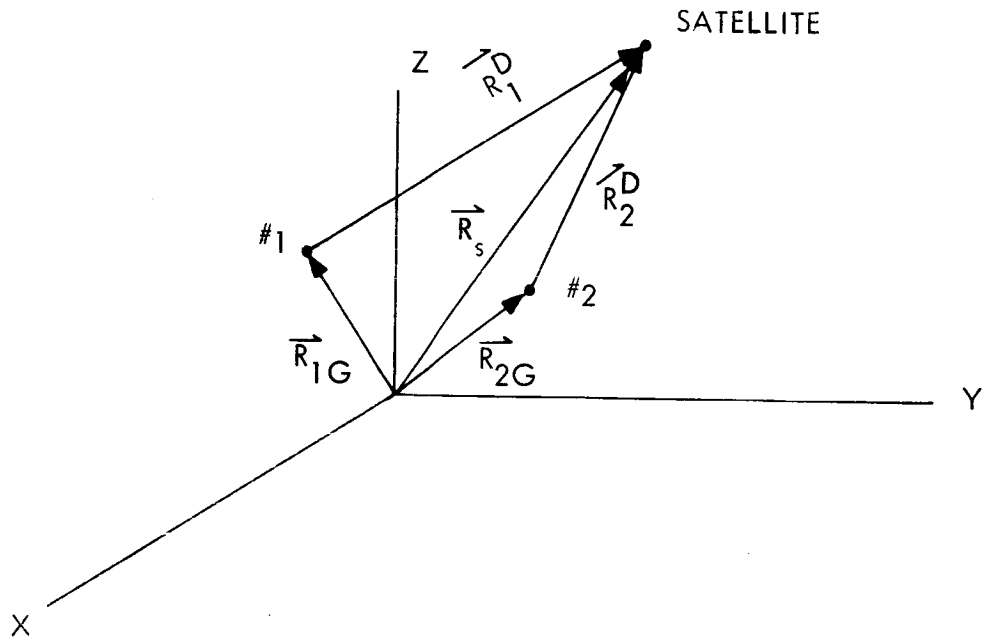

Figure 8.7-12 VECTOR DIAGRAM OF SATELLITE-GROUND STATION GEOMETRY

loss of generality or accuracy directly from equations 27 and 28. Converting to normalized vectors first yields

$$\vec{\rho}_1^{\,0} = \frac{\vec{R}_1^{\,0}}{|R^0|} = \frac{\vec{R}_1}{|R_1|} - \frac{\vec{R}_{1S}}{|R_{1S}|} \tag{30}$$

$$\vec{\rho}_2^{\,0} = \frac{\vec{R}_2^{\,0}}{|R_2^0|} = \frac{\vec{R}_2}{|R_2|} - \frac{\vec{R}_{2S}}{|R_{2S}|} \tag{31}$$

The error in ρ_1^0 or ρ_2^0 is given by

$$\Delta\vec{\rho}_1 = \frac{\Delta\vec{R}_1}{R_1} - \frac{\vec{R}_1}{R_1}\,\frac{\Delta R_1}{R_1} - \frac{\Delta\vec{R}_{1S}}{R_{1S}} + \frac{\vec{R}_{1S}}{R_{1S}}\,\frac{\Delta R_{1S}}{R_{1S}} \tag{32}$$

$$\Delta\vec{\rho}_2 = \frac{\Delta\vec{R}_2}{R_2} - \frac{\vec{R}_2}{R_2}\,\frac{\Delta R_2}{R_2} - \frac{\Delta\vec{R}_{2S}}{R_{2S}} + \frac{\vec{R}_{2S}}{R_{2S}}\,\frac{\Delta R_{2S}}{R_{2S}} \tag{33}$$

The first two terms on the RH side of equations 32 and 33 represent the navigation errors while the last two terms represent the survey errors.

Survey Errors

The error in S due to survey errors may be expressed as

$$\Delta S : \frac{\Delta \mathcal{E}_1 + \Delta \mathcal{E}_2}{H} \tag{34}$$

where H is the attitude of the satellite and $\Delta \mathcal{E}_j$ is the survey error of the j th station measured in the plane formed by the satellite and the two ground stations.

Within the Zone of the Interior $\Delta \mathcal{E}_j < \pm .1$ n. mi (3σ value). The survey errors for stations 2000 n. mi apart are reasonably expected to be uncorrelated. Therefore the variance of S is given by

$$\sigma_S^2 = \frac{2\left(\frac{\Delta \xi}{3}\right)^2}{(20,000)^2} \qquad (35)$$

Then $\sigma\ s/S = 0.25 \times 10^{-4}$

The propagation of ΔS into $\Delta \epsilon$ is given by

$$\sigma_\epsilon \doteq \left(\frac{\lambda}{2} \frac{RF^K}{\pi\ SD} M_\emptyset N\right) \sigma\ s/S \qquad (36)$$

.005 degrees
which is negligible

The survey error also propagates into ρ_x^D or ρ_y^D by virtue of an error in establishing a true bearing between the ground stations. The error is approximately

$$\Delta B = \frac{\Delta \xi_1 + \Delta \xi_2}{L} \qquad (37)$$

where L is the distance between ground stations. It follows from equations 34 and 35 that

$$\sigma_B = \frac{\sqrt{2}\left(\Delta \xi/3\right)}{2000} = .0015 \text{ deg.} \qquad (38)$$

which is also negligible.

Note that the error in B is approximately the error in ρ_x for the orientation which has the ρ_x axis normal to the plane.

It is clear that survey errors do not seriously affect the absolute accuracy of the interferometer system.

Navigation Errors

Referring to Figure 8.7-13 and equations 27 through 31 it is seen that the major error effect of navigation on attitude is to orient

$\vec{R}_s$ incorrectly.

The orientation of $\vec{R}_s$ is shown by Figure 8.7-13. Therefore, errors in α_s or β_s result in errors in the commanded attitude. Several navigation systems have been considered. They are:

1) Range and Range Rate from one ground station
2) Range and Range Rate from two ground stations
3) Range, Range Rate and Angular Data from one ground station.
4) Range, Range Rate and Angular Data from two ground stations.

Two and four were discarded since only one station currently has RR capability. This capability would not be requested unless all four systems proved inadequate.

The range and range rate system can obviously not determine the position and velocity of the satellite with a single set of readings. At least 3 sets of RR readings spaced in time must be made. These sets of data must then be filtered to the equations of motion of the satellite to estimate the satellite's position and velocity. The filter is commonly referred to as the navigation filter. A brief study was made regarding the accuracy of an RR system using an optimal filtering technique.

The optimal filter consisted of an 8 state Kalman type recursive filter. The 8 states were six for the satellite's position and velocity parameters and two for the systematic errors in range and range rate (e.g. the calibration errors). The results of this analysis are shown in Table 8.7-1.

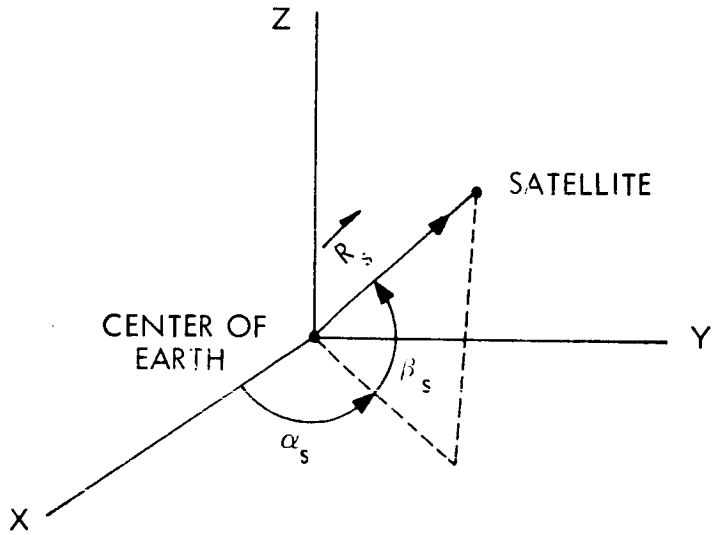

Figure 8.7-13 ORIENTATION OF $\vec{R}_s$

TABLE 8.7-1 RR SYSTEM ACCURACY

No. of RR readings taken 1 hr apart	Error in β_s (deg) σ_{β_s} (deg)	Error in α_s σ_{α_s} (deg)
0	.6	.60
1	.6	.60
2	.57	.58
3	.53	.58
4	.02	.58
5	.012	.58
6	.009	.58

The RR accuracy is 15 meters and .1 meter/sec respecitvely. Systematic errors of 30 meters in range and .2 meters/sec in range rate were assumed. The non improvement of σ_{α_s} is apparent. The value given is simply the assumed apriori standard deviation as derived from the injection guidance accuracy and has no absolute significance. These results show the inability of the RR system to improve on the error in α_s. There is a reason for this which is explained in Appendix 8C.

The possibility of using angular measurements was also investiagted. NASA document "General Specifications for the ATS Program", gives the angular accuracy of the monopulse system as $\pm$ .05 degrees or $\pm$ 1 mr. Though this document did not make it absolutely clear whether this angular capability would be available for ATS-4, the possibility seemed to exist and therefore an analysis was made of a navigation system based on R, R and angular (A, E) measurements.

The navigation filter for this system was also optimal but incorporated a 10 state filter, the additional two states for the angular biases. The results of the analysis are given in Table 8.7-2.

TABLE 8.7-2

No. of RAER readings taken 1 hr apart.	Error in β_s σ_{β_s} (deg)	Error in α_s (deg) σ_{α_s}
0	.6	.6
1	.024	.024
2	.025	.024
3	.013	.024
4	.010	.024
5	.0084	.024

As seen from this table, the accuracy of α_s is improved considerably. However, the accuracy does not improve with redundancy. An investigation into this effect shows that α_s depends on the aximuth bias. Unfortunately the filter is unable to improve the apriori estimate of the azimuth bias. Thus the error in α_s depends strongly upon the error in the apriori azimuth bias.

The conclusion is that RAER system can meet overall system specifications where as the RR system cannot.

8.8 Conclusion and Recommendation

The use of a precision radio frequency interferometer as an attitude sensor is shown to be feasible. The preferred concept, namely, a Direct Phase Reading Interferometer, is shown to meet the accuracy requirements in determining spacecraft attitude and, in addition, all components of this system are within the state-of-the-art. No major problems exist in using this system with the ATS ground stations. The accuracy of the Direct Phase Reading Interferometer deisgn shown here can be improved incorporating filters which are used in conjunction with the associated processor; consequently this system has growth potential.

Recommendation

For the ATS-4 mission, the Direct Phase Reading Interferometer design outlined above is recommended since the mission objectives are satisfied and feasibility has been shown.

8.9 BIBLIOGRAPHY AND GLOSSARY

BIBLIOGRAPHY (A)

Minitrack

1. J. T. Mengel, "Tracking the Earth Satellite, and Data Transmission by Radio"
   Proc. IRE, V. 44, June 1956, p. 755-760

2. J. T. Mengel, "Minitrack System Design Criteria"
   Electrical Engineering, Aug. 1957, p. 667

3. R. F. Filipowsky and E. I. Muehldorf, "Space Communications Systems"
   Prentice-Hall, 1965, p. 425

4. W. E. Smitherman, "Army Participation in Project Vanguard",
   IRE Trans Mil Electr. V. MIL-4, Apr-July '60 p. 323-327

5. "New Minitrack Station in Great Britain, " Jour Brit IRE
   Feb '61, p. 150-152

6. "Rockets and Satellites, Radio Tracking System," IGY
   Bulletin No. 2, July '57, p. 7-11

7. C. A. Schroeder et-al., "Tracking Orbits of Man-Made Moons,"
   Electronics, V, 32, Jan 2, 1959, pp. 33-37

8. R. L. Easton, "Radio Tracking of the Earth Satellite,"
   Q.S.T., Vol. 11, July 1956, pp. 38-41

Micro Lock

1. L. L. Richter et. al, "Micro Lock, A Minimum Weight Radio Instrumentation System for a Satellite",
   Vistas in Astronautics, Pergamen Press, 1958

Navy Space Surveillance System (SPASUR)

1. R. L. Easton and T. T. Fleming "The Navy's Space Surveillance System",
   Proc. IRE V. 48, April '60, pp. 663-69

2. M. G. Kaufman "A Phase-Channel Combiner for the NRL Space Surveillance System" IRE Intl Conv. Rec. V. 10, Pt. 9, 1962
   p. 129-150

3. W. B. Gordon and J. W. Wood "A Theoretical Error Analysis of U.S. Naval Space Surveillance System,"
   NRL Dept. 5864, Jan '63 (AD 225 606) N64-15127

Rocket Interferometer Tracking System (RIT)

1. J. C. Seddon "Preliminary Report on the Single Station Doppler-Interferometer Rocket Tracking Technique,"
NASA Technical Note TND-1344

2. M. Spafford et. al. "The Rocket Interferometer (RIT) System"
NASA Technical Note TND-2682 (N65-17967)

Related Systems

Phase Comparison Monopulse

1. D. R. Rhodes, Introduction to Monopulse,
McGraw-Hill 1959

2. M. Cohen and C. M. Steinmetz "Amplitude and Phase-sensing Monopulse System Parameters, Pts. 1 and II,
Microwave Journal V.2, Oct. 1959, pp. 27-33 and
Nov. 1959, pp. 33-38

3. D. K. Barton, "Accuracy of a Monopulse Radar", Proc.
3rd MIL-E-CON 1959 p. 179-186

4. R. M. Page, "Monopulse Radar" IRE Nat. Conv. Rec.
V.3 pt. 8, p. 132-134, 1955

5. W. Hanz, "Angular Location"
Microwave Journal, V , Feb. 1964, p.

6. Anderson and Wells, "A Note on the Spatical Information Available From Monopulse Radar"
Proc. IRE MIL-E-CON 1961 p. 268

7. R. Manasse, "Maximum Angular Accuracy + Tracking a Radio Star by Lobe Comparison"
IRE Transactions on Antennas and Propagation,
Vol. AP-8, (1959) p. 50

8. Eichter "Limit . + Angular Radar Resolution"
Proc. IRE MIL-E-CON, 1960, p. 249

9. W. R. Nester, "A Study of Tracking Accuracy in Monopulse Phases Arrays"
IRE Transactions, Antennas and Propagation,
Vol. Phap-10, May 1962, p. 237-246

10. L. E. Brennan, "Angular Accuracy of Phased Array Radar",
IRE Trans on Ant. and Prop., Vol. AP-y,
May 1961 p. 268-275

Direction Finder Systems

1. F. E. Terman, "Radio Engineers Handbook", McGraw-Hill, 1943, Section 12

2. R. Keen, Wireless Direction Finding Iliffe and Sons, Ltd. 1949

3. H. J. Reich, Editor, Very High-Frequency Techniques, McGraw-Hill, 1947, Chapter 9

4. A. D. Bailey and W. C. McClurg, "A Sum and Difference Interferometer System for HF Radio Direction Finding", IEEE Transactions on Aerospace and Navigational Electronics, Vol. PG-Ane-March 1963 p. 65-72

5. R. C. Benoit and F. Coughlin, "Designing RDF Antennas" Electronic Industries, April 1959, pp. 77-83

6. A. G. Richardson, Direction Finding Antennas Ch. 28 in H. Tusik "Antenna Engineering Handbook" McGraw-Hill, 1961

Microwave Phase Shifters - Electronic - Diode Type

1. M. E. Hines, "Fundamental Limitations in RF Switching and Phase Shifting using Simiconductor Diodes" Proc. IEEE, Vol. 52, June 1964, pp. 697-

2. K. E. Mortenson, "Microwave Semiconductor Control Devices" Microwave Journal, Vol. 7, May 1964, pp. 49-

3. H. N. Dawirs and W. G. Swarner, "A Very Fast Voltage Controlled Microwave Phase Shifter" Microwave Journal, Vol. 5, June 1962, pp. 99-107

4. J. F. White, "High Power, P-I-N Diode Controlled Microwave Transmission Phase Shifters" IEEE Transaction on Microwave Theory and Technique Vol. MTT-13, March 1965, pp. 233-242

5. G. L. Hanley "Diode Digital Phase Shifters" Sperry Engineering Review, Winter 1965, pp. 11-17

Low Frequency Phase Shifters

1. F. E. Terman and J. M. Pettit "Electronic Measurements" McGraw-Hill, 1952 pp. 277-278

Low Frequency Phase Shifters (continued)

2. Blackburn. Components Handbook, Vol. 17
Rad. Lab Series, McGraw-Hill, 1947

Radio Telescope Interferometers

1. R. C. Hansen "Microwave Scanning Antennas, Vol. 1"
Academic Press, 1964 Ch. 4

2. J. D. Kraus, Radio Telescope Antennas, Ch. 29 in
H. Jasik, "Antenna Engineering Handbook"
McGraw-Hill 1961

3. "Radio Astronomy Issue",
Proc. IRE, Vol. 46, January 1958

4. "Radio Astronomy Issue",
Antennas and Propagation, January 1961

5. "Special Issue on Radio Astronomy", IEEE
Transactions on Antennas and Propagation
December 1964

6. J. L. Powseg and R. N. Bracewell, "Radio Astronomy"
Oxford 1955

RF Phase Measurements

1. R. A. Sparks, "A Comparative Review of Phase Measurement Methods at Microwave Frequencies"
Proc. 5th MIL-E-CON June 1961 pp. 65-73
(extensive bibliography)

2. R. A. Sparks "Microwave Phase Measurements"
Microwaves, January 1963 pp. 12-25

3. P. Lacy "Analyses and Measurement of Phase Characteristics in Microwave Systems"
IRR Wescon Record, August 1961

Transmission Lines

A. Coaxial Cables

1. G. L. Ragan, "Microwave Transmission Circuits",
Vol. 9, Rad. Lab. Series, Boston Tech. Dubl.
1964, p. 243

Transmission Lines (continued)

2. "Coaxial Cables, 1966", Electro-Technology
January, 1966 p. 71-76

3. "Variation of the Electrical Length of Coaxial Transmission Lines with Temperature"
Tech. Bull. No. 6, Phelps Dodge Electronic
Prod. N. Haven, Conn.

B. Waveguide

1. G. L. Ragan, op cit

2. R. Henry and C. Walsh, Electronic Components Handbook
Vol. 2, McGraw-Hill, 1958, Chap. 8

3. L. Young, "Incremental Phase Shift Due to Changes in Crossection of Rectangular Waveguides"
Microwave Journal, Vol. 9 May 1966 p. 45-46

Mixers

1. H. C. Torreg and C. A. Whitmer, "Crystal Rectifiers"
Vol. 15 Rad Lab Series, Boston Tech. Pub., 1964

2. Pound, "Microwave Mixers", Vol. 16
Rad. Lab Series, Boston Tech Pub., 1964

3. C. G. Messeager and C. T. McCoy "Theory and Operation of Crystal Diodes as Mixers"
Proc. IRE V. , Sept. 1957, p. 1269-1283

4. P. D. Strum, "Some Aspects of Mixer Crystal Performance"
Proc. IRE V. , July 1958, p. 875-889.

5. T. Kawahaski and T. Uchida, "Delay Distortion in Crystal Mixers"
IRE Transactions, Prof. Group on Micro. Theory and' Techniques Vol. MTT-7, April 1959, p. 247-256

Microwave Phase Shifters - Mechanical

1. A. G. Fox, "An Adjustable Waveguide Phase Changer"
Proc. IRE, Vol. 35, December 1947, pp. 1489-1498

Microwave Phase Shifters - Mechanical (continued)

2. M. Magid, "Precision Microwave Phase Shift Measurement, IRE Transactions on Instrumentation Vol. 1-7, December 1948, p. 321

Microwave Phase Shifters - Electronic - Ferrite Type

1. B. Lax and K. Button, Microwave Ferrites and Ferrimagnetics McGraw-Hill, 1962, Section 12-7

2. D. R. Taft et. al, "Ferrite Digital Phase Shifters" Digest, Symposium IEEE Group on Microwave Theory and Techniques, 1965, p. 115

3. J. Brown et. al. "Ferrite Digital Phase Shifters" Sperry Engineering Review, Winter, 1965, pp. 24-30

4. H. S. Jones and F. Reggia, "Design of Three Miniature Ferrite Phase Shifters", Microwaves, Vol. 3, July 1964

Gemini Rendezvous Radar

1. M. W. Quigley "Gemini Rendezvous Radar" Microwave Journal, Vol. 8, June 1965, pp. 39-45

2. J. R. Carl and S A. Guccione, "Gemini Rendezvous Radar Error" Microwave Journal, Vol. 9, June 1966, pp. 75-78

BIBLIOGRAPHY (B)

1. Super-Limiting in an Array Antenna System - Kovaly, J. J. Sylvania Electronic Systems - East - Sylvania Electronic Systems - Ninth Annual Radar Symposium Record 4, 5, 6 June 1963, Contract DA-36-039-SC-78801.

2. An Approach to Superdirectivity through Multiple Beam Processing, Kashihara, Thomas K. Philco Scientific Laboratory-NARSR '63.

3. Self-Aligning Phased Arrays, Stinson, D. F., Sylvania Electronic Systems, NARSR '63.

4. Angle-of-Arrival Measurements with a Ku-band Phase Interferometer - Kosowsky, L. H., Chanzit, L., United Aircraft Corporation - ARSR '63.

5. RASTAR - An AICBM Tracking Phased Array of Milliradian Resolution, Goldman, R.B. and Woodward, C.P., Philco Corporation, 5th ARSR, 27, 28, 29 Jan. '59.

6. Post-Detection in the Navy Space Surveillance System, Kaufman, Maxime G., IEEE Trans. Aerospace Internat. Conf. Aerospace Electrot., Phoenix.

7. Accuracy of an Angle-Measuring System, Kendall, W.B., J. P. L. Space Progr. Summ.

8. A New Radio Interferometer Tracking System, Grace, Chas. H., Smith Electronics, Inc.

9. Turbulence Measurements at High Altitudes by Second-Difference Interferometry, Dwight W. Batteau, Thomas E. Beling, and Richard H. Spencer, United Research, Inc., Cambridge, Mass.

10. 108 MC/S Interferometer for Satellite Tracking, Fance, D. F., Royal Aircraft Establishment (Gt. Brit.)

11. Scattering Error in a Radio Interferometer, Harrison, Jr., Charles W., IEEE Trans. Ant. Propag.

12. A Compound Interferometer with a 1.5 Minute of Arc Fan Beam, N. R. Labrum, E. Harting, T. Krishman and W. J. Payten, Proc. Instn. Radio Engrs. Australia, Sp. Issue on Radio Astronomy.

13. Unambiguous Accuracy of an Interferometer Angle-Measuring System, Kendall, William B., IEEE Trans. Space Elec. Telemetry.

14. Radio-Interferometer Analog Phase-Channel Combiner (Mod II) for Unambiguous Space Angle Measurements in the Navy Space Surveillance System, M. G. Kaufman and C. H. Weaver, Naval Research Lab., Wash., D. C. NRL [illegible].

15. Comparison of the Interferometry and Doppler Methods of Satellite Tracking, Plottin. G. G., Onde Electr.

16. Electronic Interferometer Tracking, Schroeder, Clarence A., IRE Trans. 5th Natl. Symp. Space Elecs. & Telem.

17. Radio Interferometry Applied to Geodesy, Kahn, Werner D., Army Map Service, Wash., D. C.

18. Interferometer Techniques Applied to Radar, Gehrels, E. and Parsons, A., IRE Trans. Mil. Elec.

BIBLIOGRAPHY (C)

1. Blythe, J. H. (1957). "A New Type of Pencil Beam Aerial for Radio Astronomy,"
   Monthly Notices Roy. Astron. Soc., 117, 644.

2. Booker, H. G., and Clemmow, P. C. (1950). "The Concept of an Angular Spectrum of Plane Waves, and its Relation to that Polar Diagram and Aperture Distribution",
   Proc. Inst. Elec. Engrs. (London)
   Pt. iii, 97, 11.

3. Born, M. and Wolf, E. (1959). "Principles of Optics",
   Pergamon Press, New York.

4. Bowen, E. G. (1962). "A New Radioheliograph for Australia,"
   Nature 195, 649.

5. Braccesi, A., and Ceccarelli, M. (1962). "The Italian Cross Radio Telescope,"
   Nuovo Cimento (10) 23, 208, 254.

6. Bracewell, R. N., and Swarup, G. (1961). "The Stanford Microwave Spectroheliograph, a Microsteradian Pencil Beam Interferometer,"
   IRE Trans. Antennas and Propagation 9, 22.

7. Bracewell, R. N. (1962). Radio Astronomy Techniques in "Encyclopedia of Physics (S. Flugge, ed.), Vol. 54,
   Springer, Berlin.

8. Bracewell, R. N., Swarup, G., and Seeger, C. L. (1962). "Future Large Radio Telescopes,"
   Nature 193, 412.

9. Covington, A. E.. and Broten, N. W. (1957). "An Interferometer for Radio Astronomy with a Single-Lobed Radiation Pattern,"
   IRE Trans. Antennas Propagation 5, page 247.

10. Hanbury Brown, R., and Twiss, R. Q. (1954). "A New Type of Interferometer for use in Radio Astronomy,"
    Phil. Mag. 45, 663.

11. Hansbury Brown, R., and Twiss, R. Q. (1958). "Interferometry of the Intensity Fluctuations in Light, Iv. A Test of an Intensity Interferometer on Sirius A, "Proc. Royal Soc. 248, 222.

BIBLIOGRAPHY (D)

1. Systems

Kendall, W. B., "Unambiguous Accuracy of an Interferometer Angle Measuring System," IEEE Trans. Space Elec. Telemetry

Mullen, E. B. and Woods, C. R., "State-of-the-Art in Radio Tracking," Proc. Intern. Astron. Congr., Aug. 1960, Stockholm, Vol. 1

Douglas, S. N., "Space-Frequency Synthesis Arrays," NEREM Rec. (Northeast Electr. Res. Engng. Mtg.)

Kaufman, M. G. "Radio Interferometry" Corresp. Proc. IEEE 64 (52)

2. Techniques

"Techniques Used by the U. S. Naval Surveillance System," Proc. IEEE 64(52).

Drane, C. J. and Parrent, G. B. Jr., "On the Mapping of Extended Sources with Non-Linear Correlation Antennas," IEEE Trans. Ant. Prop.

Drane, C. J. "Phase-Modulated Antennas", AFCRC-TR-59-138, ASTIA #AD 215374

"Very High Resolution Techniques," prepared by Ksienski, A. A. of Hughes Aircraft Company for U.S. Army Electronics Command.

BIBLIOGRAPHY (E)

General

1. AD 474376 - Research on Compact and Efficient Antennas, J.F. Ramsay, W. M. Mulqueen, B. V. Popovich, W. J. McEvoy, W. Rueggeberg, Airborne Instruments Lab., Deer Park, L.I., N.Y., Oct. 31, 1964 to 30 June 1965.

2. AFCRL 63-51 - Modern Antennas for Space Communications, C. J. Sletten, AF Cambridge Research Labs. Office of Aerospace Research, USAF, L. G. Hanscom Field, Mass., Feb. 1963.

3. RM-3053-PR-Recent Soviet Advances in Aerospace Technology, F. J. Krieger, Rand Corp., Santa Monica, Calif. Feb. 1962, (N62-17332).

4. N 66-16259 - Investigation of Radio Wave Refraction in the Lower Layers of the Atmosphere at Low Angles of Elevation, A.I. Sazonov, USSR, U.S. Dept. of Commerce, Wash., D.C. 20 Jan. 1966.

5. N66-18413 - A Proposal for a Circularly Polarized Tracking Antenna and its Evaluation, E. R. Graf, Director, Antenna Research Lab. June 24, 1964.

6. DDC 438208 - Derivation of Aerospace Antenna Coupling - Factor Interference Prediction Techniques, P.J. Khan, W. R. DeHart, R. M. Kalafus, D. M. Oliver, A. I. Simanyi, R. B. Harris, W. S. Heath, AF System Command, Wright-Patterson AFB, Ohio, April 1964.

7. N66-17600 - A High Performance Log Video Amplifier, Paul E. Harris, Defense Systems Lab., Syracuse Univ. Research Corp., Oct. 1965.

8. AD 249516 - The Stanford Microwave Spectroheliograph Antenna, A Microsteradian Pencil-Beam Interferometer, R. N. Bracewell, G. Swarup, Radioscience Lab., Standord Electronics Lab., Stanford Univ. Standord, California, Nove. 25, 1960.

9. AD 254043 - The Delay-Lock Discriminator - An Optimum Tracking Device, J. J. Spilker, Jr., D. T. Magill, Lockheed Missiles and Space Division, Lockheed Aircraft Corp., Sunnyvale, Calif., March 1961.

10. NASA TND 1344 - Preliminary Report on the Single Station Doppler - Interferometer Rocket Tracking Technique, J. Carl Seddon, Goddard SFC, Greenbelt, Md. NASA Wash. D.C. Jan. 1963

11. High Power Varactor for UHF Transmission, Beorge Louis, et. al., Motorola, Inc., Phoenix, Ariz., June 30, 1965, (AD 628131).

12. AD 272955 - The Study of Electromagnetic Techniques for Space Navigation, R. G. Franklin, J. A. Palladino, D. L. Birx, The Franklin Institute, Phila., Pa., Nov. 16, 1961 to Feb. 15, 1962.

13 AD 624080 - Minimum-Scattering Antennas, Walter K. Kahn, et al, Polytechnic Institute of Brooklyn, N.Y. Microwave Research Institute. 7 April 1964.

14. AD 133280 - Propagation of Radio Waves through the Troposphere and Ionosphere. Virgil A. Counter, Lockheed Aircraft Corp. Missile Systems Div., Palo Alto, Calif., 28 Dec. 1965.

15. AD 273455 - Multiple-Beam Interferometry for Small-Step Measurement. J.W. Beck, Stanford Electronics Lab., Stanford Univ., Stanford, Calif. 15 Nov. 1961.

16. AD 152364 - A New Single Antenna Interferometer System using Proximity - Coupled Radiators, Carlyle J. Sletten, F. Sheppard Holt, Philipp Blacksmith, Jr., George R. Forbes, Jr., Loenard F. Shodin, Harold J. Henkel, Onics Research Directorate, AF Cambridge Research Center, Air Research and Development Command, USAF, March 1958.

17. N66-17255 - The Goddard Range and Range Rate Tracking System: Concept, Design and Performance, G. C. Kronmiller, Jr., and E. J. Baghdady, Goddard SFC, Greenbelt, Md., NASA Oct. 1965.

18. AD 236235 - The Use of Radar Interferometer Measurements To Study Planets, Roger Manasse, MIT Lincoln Lab., Lexington, Mass. 18 March 1959.

19. AD 477951 - Modulation, Coding and Information Theory, Gordon Raisbeck, Advanced Research Projects Div. Institute for Defense Analyses, the Pentagon Was. 25, D.C., June 15, 1960.

20. AD 627364 - Transit Orbit Improvement Program, Vol. I, Applied Physics Lab., The Johns Hopkins University, Silver Spring, Md., March 1961.

21. AD 627365 - Transit Orbit Improvement Program, Vol. II, APL, The Johns Hopkins Univ., Silver Spring, Md., March 1961.

22 L. R. Whicker, "Recent Advances in Digital Latching Ferrite Devices", Westinghouse Defense and Space Center, Baltimore, Md., pp. 49-57.

23 J. K. Parks, B. R. Savage, L. J. Lavedan, and J. Brown, Jr., "IX-4. A Miniaturized C-Band Digital Latching Phase Shifter", Sperry Microwave Electronics Co., Clearwater, Florida, pp. 235-239.

24 Max C. Mohr and Stephen Monaghan, "IX-2. Circularly Polarized Phase Shifter for Use in Phased Array Antennas", Raytheon Company, Bedford, Massachusetts, pp. 224-229.

25 William H. Nester, "A Study of Tracking Accuracy in Monopulse Phased Arrays", IRE Transactions on Antennas and Propagation, pp. 237 - 246, May 1962.

26 L. E. Brennan, "Angular Accuracy of a Phased Array Radar", IRE Transactions on Antennas and Propagation, pp. 268-274, May 1961.

27 S. Sharenson, "Angle Estimation Accuracy with a Monopulse Radar in the Search Mode", IRE Transactions on Aerospace and Navigational Electronics, pp. 175-179, September 1962.

28 Richard R. Kinsey, "Monopulse Difference Slope and Gain Standards", IRE Transactions on Antennas and Propagation, pp. 343-344, May 1962.

29 D. K. Cheng, B. J. Strait, "An Unusually Simple Method for Sidelobe Reduction", IEEE Transactions on Antennas and Propagation, pp. 375-376, May 1963.

30 Peter W. Hannan, "Maximum Gain in Monopulse Difference Mode", IRE Transactions on Antennas and Propagation, pp. 314-315, May 1961.

31 H. Unz, "An Approximation to Chebyshev Distributions", IEEE Transactions on Antennas and Propagation, pp. 707-709.

32 O. R. Price and R. F. Hyneman, "Distribution Functions for Monopulse Antenna Difference Patterns", IRE Transations on Antennas and Propagation, pp. 567-576, November 1960.

33 Jean A. Develet, Jr., "Thermal-Noise Errors in Simultaneous-Lobing and Conical-Scan Angle-Tracking Systems, IRE Transactions on Space Electronics and Telemetry, pp. 42-51, June 1961.

GLOSSARY

A	=	Constant = $\frac{\omega_{IF}}{\omega_c}$
B	=	Bandwidth, hertz
c	=	Velocity of light (2.9979×10^8 meters per second)
D	=	Distance - between antenna elements on interferometer arm
D'	=	D with perturbations
d	=	Distance, incremental, between antenna elements
f	=	Frequency, in hertz unless subscripted.
$f(\ )$	=	Function of ( )
G_t	=	Transmitting Antenna Gain
G_r	=	Receiving Antenna Gain
^oK	=	Degrees Kelvin
$k_{on\text{-}off}(\tau)$	=	Correlation factor of on and off gating time errors
k	=	Boltzmann's Constant 1.38×10^{-23}
k_n	=	Phase correlation coefficient
k_e	=	Monopulse error coefficient
L_{fs}	=	Free space loss
L_{mis}	=	Miscellaneous loss
M	=	Matrix of earth station constants ($\rho_{(\ )}^{(\ )}$)
m	=	Number of wavefronts that have passed first antenna since an arbitrary reference time
N_o	=	Noise spectral density, watts/cycle

$N_{(\ )}$ = Count or binary number representing a course phase angle subscripted (1 or 2) to designate ground station and (x or y) for axis

N = Generalized count representing phase

n = Same as small m above except second antenna

$n-m$ = Number of wavefronts between first and second antennas

P_t = Transmitted power

P_n = Noise power (in general received noise power)

q = Number of antenna elements on interferometer arm

R = Distance, transmitter to receiver subscripted to designate reference and measurement antennas in error analysis

R^* = Distance, transmitter to receiver, with atmospheric bending accounted for

S/N = Signal-to-noise ratio in dB

T_{ant} = Equivalent noise temperature degrees Kelvin, Antenna

T_{feed} = Equivalent noise temperature degrees Kelvin, Antenna Feed

T_{rec} = Equivalent noise temperature degrees Kelvin, Receiver

T_{sys} = Equivalent noise temperature degrees Kelvin, Entire Receive System

T = Period, in seconds

t = Time, in seconds

u = Frequency multiplication of local oscillator of satellite

v = Count or binary number representing a vernier phase angle, subscripted to denote ground station (1 or 2) and axis (x or y)

Glossary

X, x Y, y Z, z		Spacecraft coordinate system
α_s	=	Angular estimate in navigation system
β	=	3 dB antenna beamwidth, degrees
β_s	=	Angular estimate in navigation system
ε	=	Spacecraft attitude errors, subscripted x, y or z to indicate axis about which measured
θ	=	Pitch angle
θ_s	=	Space angle
θ'	=	Interferometer estimate of θ_s when arm is perturbated

λ	=	Wavelength (generally in meters)
ξ	=	Survey position ($\Delta\xi$ = survey error)
ρ_i	=	Unit vector along the LOS (line-of-sight) pointing from the vehicle to the i-th station.
σ	=	In general, the standard deviation of the subscripting parameter
σ_{θ_s}	=	Standard deviation of space angle
σ_t	=	Standard deviation of triggering time
σ_N	=	Standard deviation of phase angle count due to noise
σ_{tq}	=	Standard deviation of phase angle count due to quantization
σ_{Nt}	=	Standard deviation of sum of σ_N and σ_{tq}
τ	=	Delay, in seconds, of illuminating wavefront
Υ	=	Space angle ground station to perturbated interferometer arm
ψ	=	Roll angle
ϕ	=	Phase angle, in radians unless otherwise stated
ψ	=	Yaw angle
ω	=	Angular frequency, radians per second
ω_c	=	ω of clock in counter
ω_G	=	ω station oscillator
ω_{IF}	=	ω 100 kHz IF signal
ω_{RF}	=	ω ground station transmitter

ATS-4	=	Applied Technology Satellite, Series 4
ERP	=	Effective Radiated Power
dB	=	Decibel; 10 times common log of power ratio
dBW	=	Decibel; 10 times common log of power divided by one watt
$\frac{S}{N}$	=	Signal to Noise Ratio in dB
kHz	=	kilo hertz = one thousand cycles per second
gHz	=	giga hertz = one billion (10^9) cycles per second
MHz	=	mega hertz = one million cycles per second
SNR	=	Signal to noise ratio
RF	=	Radio Frequency
n. m.	=	Nautical miles
FM	=	Frequency modulation
IF	=	Intermediate Frequency
LF	=	Low Frequency
RMS	=	Root mean square
PRN	=	Pseudo random noise
RFI	=	Radio frequency interference
HF	=	High frequency
LO	=	Local Oscillator
VCO	=	Voltage Controlled Oscillator
Xtal	=	Crystal
TP	=	Timing Pulse
RR	=	Range, Range Rate Navigation System
RAER	=	Range, Angle Estimate, Range Rate Navigation System

APPENDIX 8A

INTERFERENCE REDUCTION BY CORRELATION[1]

This appendix discusses the reduction of interfering signals appearing on the secondary major lobes of either antenna of Figure 8.5-2

Let the illuminating signal

$$e = E \cos(\omega t)$$

be the desired signal appearing on the center main lobe of either array.

$$e_1 = E_1 \cos\left[\omega t + \phi_1(t)\right]$$ an

interfering signal simultaneously appearing on a secondary major lobe of one antenna array, and

$$e_2 = E_2 \cos\left[\omega t + \phi_2(t)\right]$$

be another interfering signal simultaneously appearing on a secondary major lobe of the other array. Assume the phases of ϕ_1 and ϕ_2 vary randomly with time. (e_1 and e_2 are incoherent with e). The first array will receive a signal

$$V_1 = e + e_1$$ and the second will yield

$$V_2 = e + e_2$$

Cross-correlating these outputs with zero time delay yields :

$$\Phi_{12}(0) = \lim_{T \to \infty} \frac{1}{2T} \int_{-T}^{T} V_1(t) V_2(t)\, dt = \overline{(e+e_1)(e+e_2)}$$

(1) John E. Walsh, Final Report on Interferometer Development," Pickard and Burns, Inc., Needham, Mass.

$$= \overline{\left\{E\cos\omega t + E_1\cos\left(\omega t + \varphi_1(t)\right)\right\}\left\{E\cos\omega t + E_2\cos\left(\omega t + \varphi_2 t\right)\right\}}$$

$$= \overline{E^2\cos^2(\omega t)} + \overline{E E_2 \cos\omega t \cos\left[\omega t + \varphi_2(t)\right]}$$

$$(+)\ \overline{E E_1 \cos\omega t \cos\left[\omega t + \varphi_1(t)\right]}$$

$$(+)\ \overline{E_1 E_2 \cos\left[\omega t + \varphi_1(t)\right]\cos\left[\omega t + \varphi_2 t\right]}$$

$$= \frac{1}{2}\left[E^2\,\overline{(1+\cos 2\omega t)} + E E_2\left\{\overline{\cos(2\omega t + \varphi_2(t))} + \overline{\cos(\varphi_2(t)}\right.\right.$$

$$(+)\ E E_1\left\{\overline{\cos(2\omega t + \varphi_1(t))} + \overline{\cos(\varphi_1(t))}\right\}$$

$$(+)\ E_1 E_2\left\{\overline{\cos(2\omega t + \varphi_1(t) + \varphi_2(t)} + \overline{\cos(\varphi_1(t) - \varphi_2(t))}\right\}$$

Since φ_1, and φ_2 are random, all terms containing them average to zero for a sufficiently long integration interval. Thus $\Phi_{1,2}(0) = \frac{E^2}{2}$

The result of this analysis shows that e_1, and e_2 have been suppressed by cross-correlation.

APPENDIX 8B

R. F. LINK CALCULATION

The required ground station ERP-versus the signal-to-noise ratio required at the input to the crossover detector is determined in the following manner.

Atmospheric and precipitation losses at X band can be accounted for with a simple additive factor whose magnitude, outside of tropical areas, seldom is greater than 3 to 4 dB. This is a very conservative figure if a 98 or 99% availability of the satellite is sufficient for the experiment. Other losses include tracking errors of the ground station, polarization losses and miscellaneous (e.g. mismatch) losses. For this calculation all these minor losses (atmosphere, other and miscellaneous) are lumped in one term called Miscellaneous Losses and given a value of 5 dB.

1 The range equation then becomes:

$$G_t + P_t = ERP_{dBW} = S/N + P_{mdBW} - G_r + L_{fs} + L_{mis} \qquad (1)$$

where

P_t = Transmitted Power in d_{BW}

G_t = Transmitting Antenna Gain in dB

S/N = Signal to noise ratio in dB

P_n = Received Noise Power in dBW

G_r = Received Antenna Gain in dB = 12 dB for whole earth coverage

L_{fs} = Free Space Loss in dB = $(4\pi R/\lambda)^2$ = 204.15 dB
R = distance from transmitter to receiver = 4.82×10^7 max
λ = wavelength = 3.75×10^{-2}
both in meters

L_{mis} = miscellaneous losses = 5 dB (see above)

This reduces to:

$$ERP_{dBW} = S/N + P_n + 197 \qquad (2)$$

The noise power is a function of the noise figure of the receiver (assumed to be 6.6 dB), the area illuminating the antenna (assumed to make the antenna noise temperature 300°K) and the loss in the antenna feed (assumed to be 1 dB), and the equivalent noise bandwidth of the system. The noise equivalent temperature method of calculating the system noise is used.

$$T_{sys} = T_{ant} + T_{feed} + T_{rec} = 300 + (1.26 - 1)\,300 + (4.55 - 1)\,300$$
$$= 300 + 1065 + 78 = 1443 \text{ deg. K}$$

The noise sperctral density in watts per cycle may be calculated from:

$$N_o = k\,T = 1.38 \times 10^{-23}\,T + 1.98 \times 10^{-20} = -197 \text{ db W/Hz} \qquad (3)$$

where

N_o = noise spectral density, k = Boltzman's constant

If the noise bandwidth ratio is now expressed in dB = + 40 dB) the noise power in any bandwidth may be rapidly obtained. Assuming a one kilohertz bandwidth (30 dB) the noise power is -167 dBW. Returning to equation (2)

$$ERP_{dBW} = S/N - 167 + 197 = S/N + 30 \text{ dBW} \qquad (4)$$

Figure 8.B-1 shows the relationship of ERP, S/N and bandwidth.

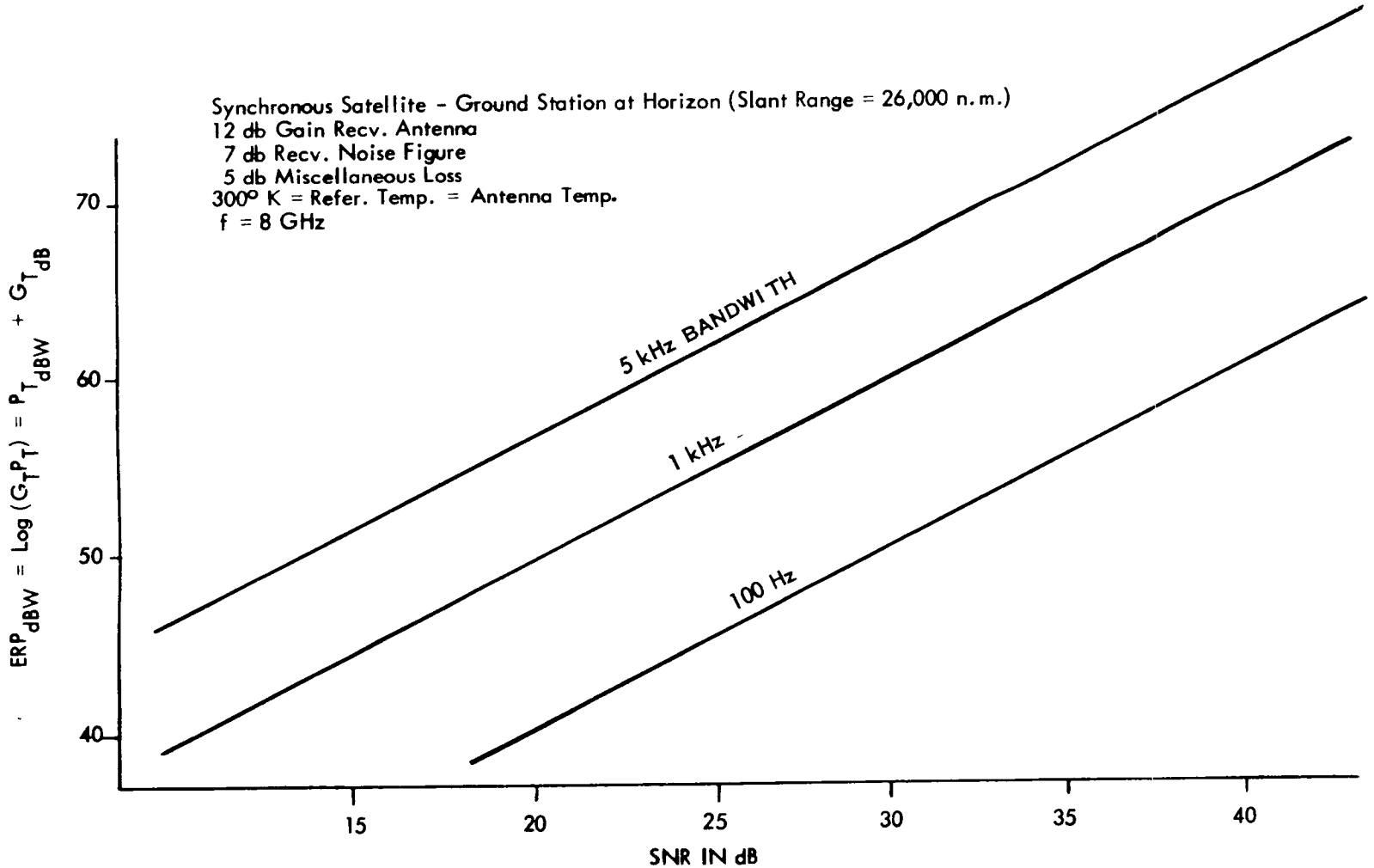

FIGURE 8.B-1 ERP VS SNR

APPENDIX 8C

INTERFEROMETER ANGULAR ERROR DUE TO MUTUAL COUPLING

Representative System: Direct Phase Reading System - 2 orthogonal arms, each having coarse antenna pair closely spaced for ambiguity resolution. Figure 8C-1 shows the maximum angle error as a function of the antenna separation and mutual coupling. The allowable angular error is different for coarse antenna pair and vernier antenna pair.

Allowable Angular Error for Coarse Antenna Pair

If the mutual coupling induced error in the coarse pair angle characteristic is too large, the ambiguity in the vernier pair phase angle will be resolved incorrectly.

Figure 8C-2 shows phase angle as a function of the space angle for coarse and vernier antenna pair respectively, and how a displaced curve due to mutual coupling can result in incorrect ambiguity resolution. Maximum allowable coarse angular error ($\Delta \Theta_{mc}$) is equal to the vernier unambiguous interval, which is equal to the spacing between the vernier phase characteristics.

The mutual coupling (C) is related to the maximum angle error by

$$\Delta \Theta_m = \frac{\sqrt{C}}{\pi \frac{D}{\lambda}} .$$

As an example for $\Delta \Theta_{mc} = 0.0875^{\circ} = 1.53 \times 10^{-3}$ radians and $\frac{D}{\lambda} = 2.73$,

$C = 1.71 \times 10^{-4}$, $10 \log C = -37.8$ db.

Allowable Angular Error for Vernier Antenna Pair

The allowable angular error for the vernier antenna pair is determined by the desired angular accuracy.

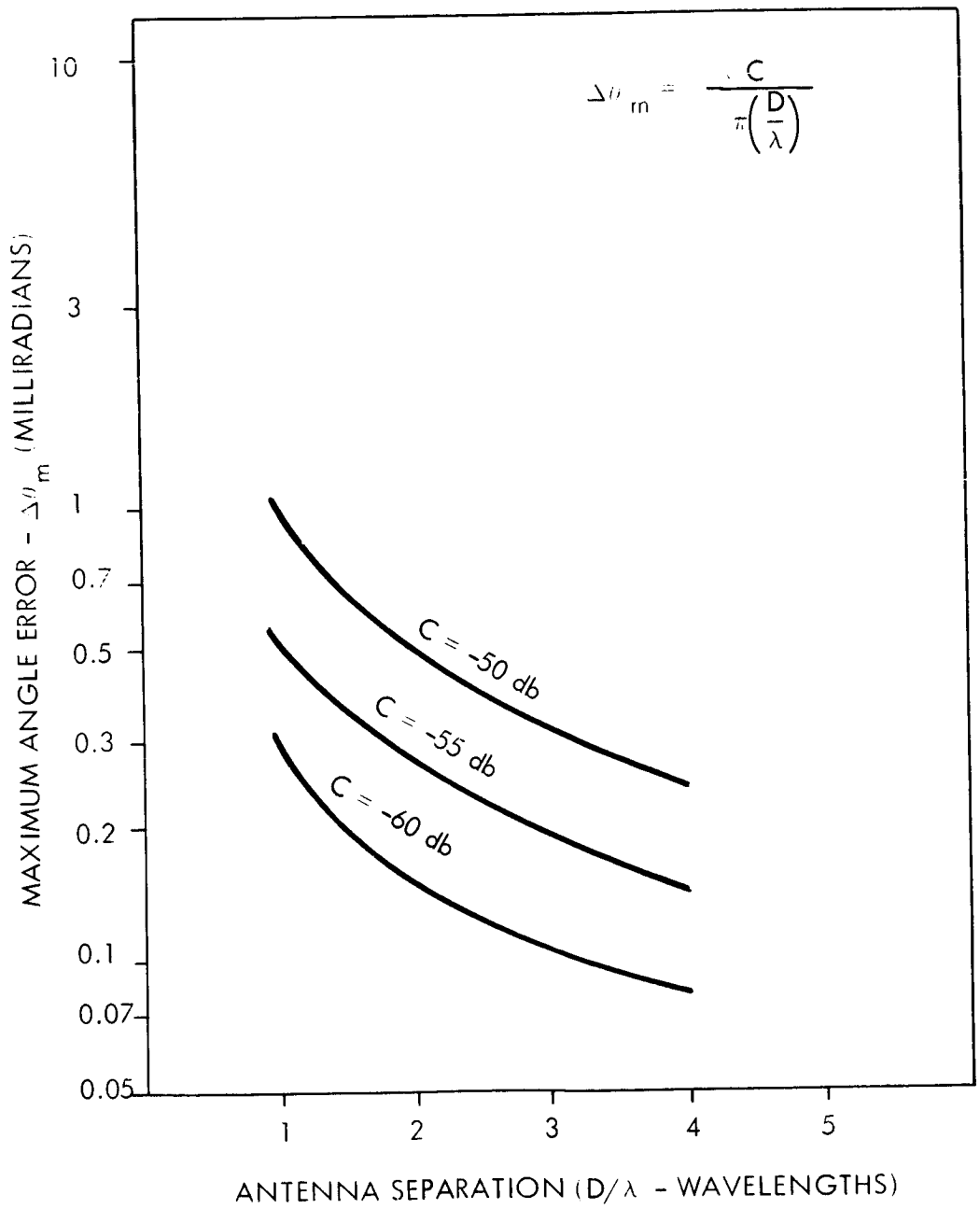

Figure 8.C-1 SPACE ANGULAR ERROR ($\Delta\theta_m$) VS ANTENNA SEPARATION (D/λ) FOR DIFFERENT MUTUAL COUPLINGS (C)

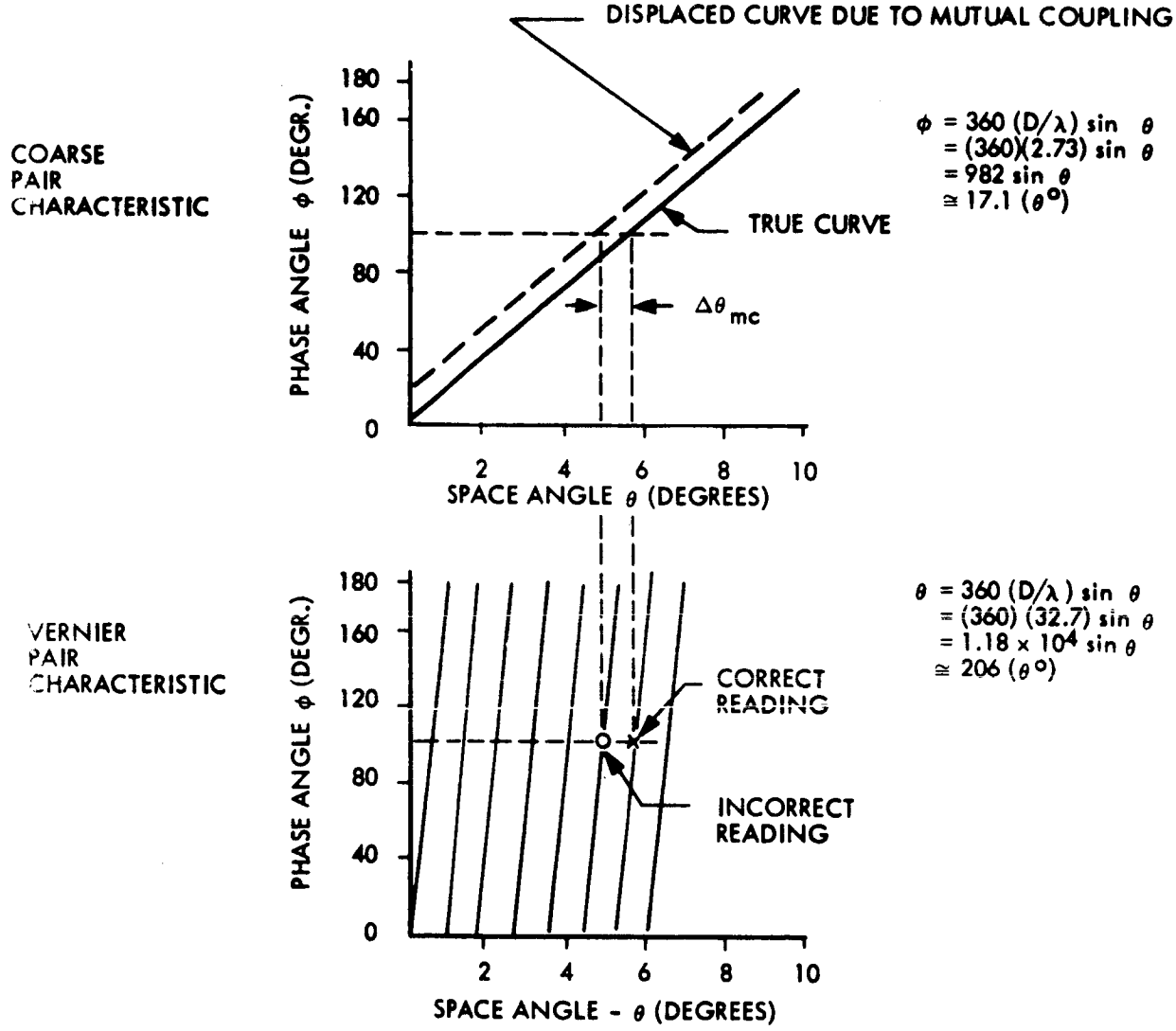

FIGURE 8.C-2 SPACE ANGLE ERROR DUE TO MUTUAL COUPLING-COARSE ANTENNA PAIR

The mutual coupling will depend on antenna type (linear or circularly polarized) antenna gain (higher gain results in lower coupling), relative antenna orientation, and antenna environment (ground plane, reflecting surfaces).

Fig. 8C-3 shows the mutual coupling antenna spacing for different antenna types (based on half-wave dipole model) and shows the maximum coupling allowable for coarse antenna pair and vernier antenna pair.

Conclusions - Comparison of Mutual Coupling between Antenna Elements

For the coarse antenna pairs the only antenna elements that have a low enough mutual coupling are collinear rectangular horns and orthogonal rectangular or diagonal horns.

For the vernier antenna pairs, any of the antenna types shown have a low enough mutual coupling.

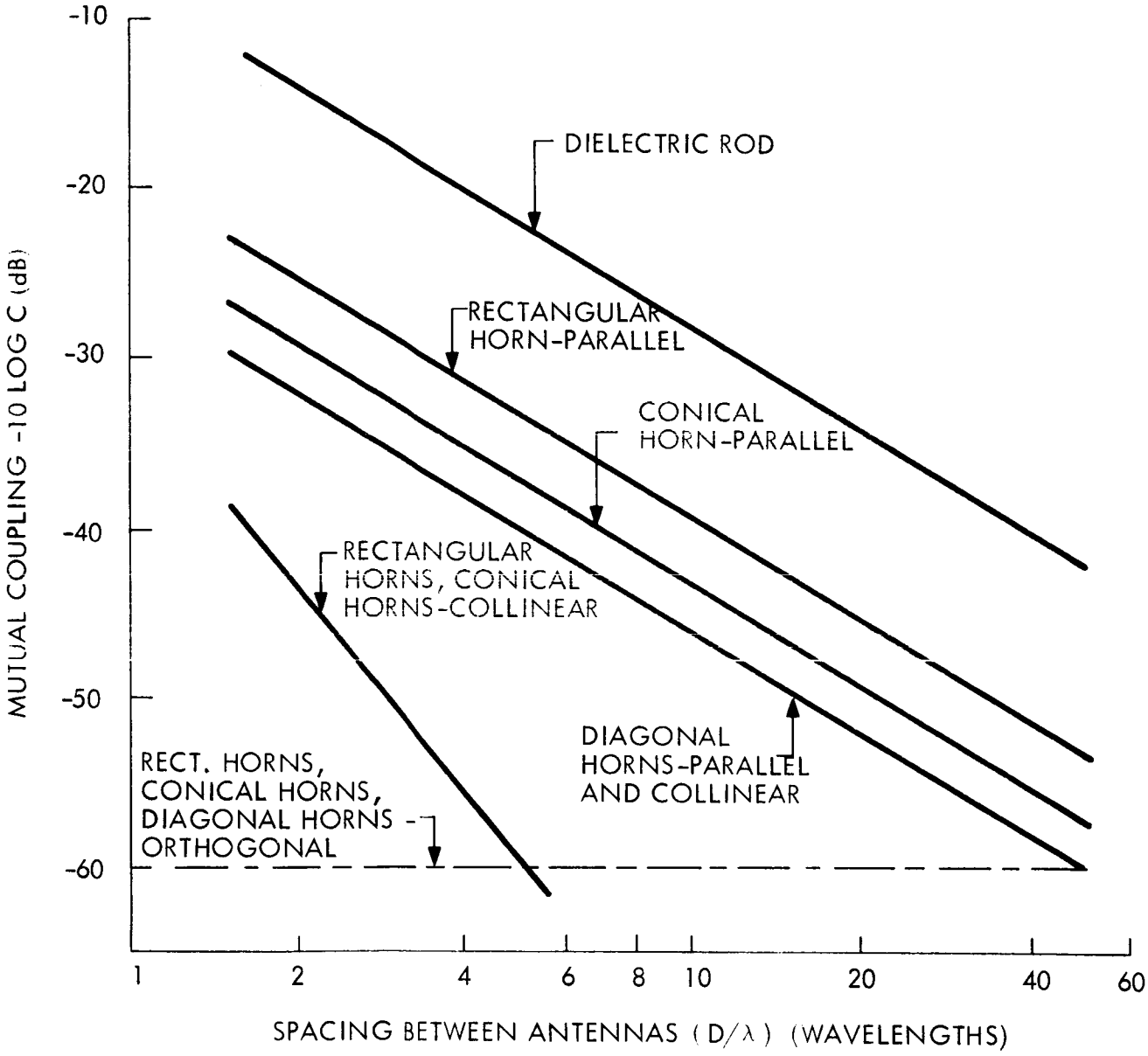

Figure 8. C-3 COMPARISON OF ANTENNA ELEMENTS-MUTUAL COUPLING

APPENDIX 8D

SYSTEM POLARIZATION

Introduction

The choice of the polarization of the interferometer antenna elements and the polarization of the ground station antenna will influence the accuracy of the interferometer system. In the following section the errors due to antenna polarization will be analyzed and a preferred polarization

Alternative Systems

The four possible alternative systems of polarization are shown in Table 8D-1.

TABLE 8D-1

System	Ground Station Polarization	Interferometer Polarization
1	Linear	Linear
2	Linear	Circular
3	Circular	Linear
4	Circular	Circular

For system 1 the relative orientation of the satellite and ground station might be such as to orient the two linear antennas orthogonally. This cross-polarization would cause complete signal dropout. Therefore system 1 is impractical and will not be considered.

Effects of System Polarization on System Performance

Phase Error

a) Phase Error as a Function of Antenna Uniformity

The polarization of an antenna can be characterized by its axial ratio R and the orientation angle B of its polarization ellipse. Since it is impossible to make the interferometer antenna elements exactly alike there will be a small phase

error introduced by the non-uniformity in axial ratio (ΔR) and the non-uniformity in ellipse angle (ΔB).

(b) Phase Error as a Function of Orientation

For slightly non-uniform antenna elements the phase error that exists when the incoming wavefront is on boresight will change as the incident angle departs from boresight. This means that a slightly different phase error will exist when working with different ground stations. There will also be an orientation dependent phase error due to changes in the axial ratio and/or ellipse tilt angle in the ground station antenna for angles off the boresight axis.

Mutual Coupling

The type of interferometer antenna element used (linear or circular) will affect the mutual coupling between the elements. For example, if linearly polarized elements are used these can be orientated orthogonally to reduce their mutual coupling.

Signal Amplitude

Since perfect circularity cannot be obtained in a practical antenna, the amplitude of the received signal will vary as a function of the ground station-satellite orientation angles. For small amplitude changes, the amplitude variations will introduce a second order phase error.

System Comparison - Phase Error

To evaluate the maximum phase errors that each system might have, a two element interferometer was analyzed. The interferometer

elements 1 and 2 were assumed to have axial ratios R_1 and R_2 and polarization ellipse tilt angles B_1 and B_2 (see Figure 8D-1). The wavefront from the ground station is incident on the interferometer at angle Θ and δ and has an axial ratio of R_T. Then the phases of the voltages received on interferometer antenna element Nos. 1 and 2 is given in Table 8D-2.

The phase error (due to polarization) is

$$\Delta\phi_b = \phi_1 - \phi_2 - \frac{2\pi D}{\lambda} \sin\Theta$$

<u>Phase Error due to Interferometer Element Axial Ratio Inequality</u>

On boresight $\Theta = \delta = 0^o$ so

$$\Delta\phi = \tan^{-1}\left[\left(\frac{R_1 + R_T}{1+R_1R_T}\right)\tan B_1\right] - \tan^{-1}\left[\left(\frac{R_2 + R_T}{1+R_2R_T}\right)\tan B_2\right]$$

Let the axial ratio of antenna 2 be slight different than that of antenna 1, i.e. $R_1 = R_2 - \Delta R$

For System 2 - Linear G/S, Circular Interferometer

Let $R_T = 0$, $R_1 \cong R_2 \cong 1$, and $B_1 = B_2$

$$\Delta\phi(\Delta R) = \tan^{-1}\left[\left(\frac{R_1}{R_1}\right)\tan B_1\right] - \tan^{-1}\left[\left(\frac{R_2}{R_2}\right)\tan B_2\right]$$

$$\Delta\phi_2\ (\Delta R) = 0$$

For System 3 - Circular G/S, Linear Interferometer

Let $R_T \cong 1$, $R_1 = 0$, $R_2 = \Delta R$

$$\Delta\phi_3\ (\Delta R) = \tan^{-1}\left[\left(\frac{1}{1}\right)\tan B_1\right] - \tan^{-1}\left[\left(\frac{1+\Delta R}{1+\Delta R}\right)\tan B_1\right]$$

$$\Delta\phi_3\ (\Delta R) = 0$$

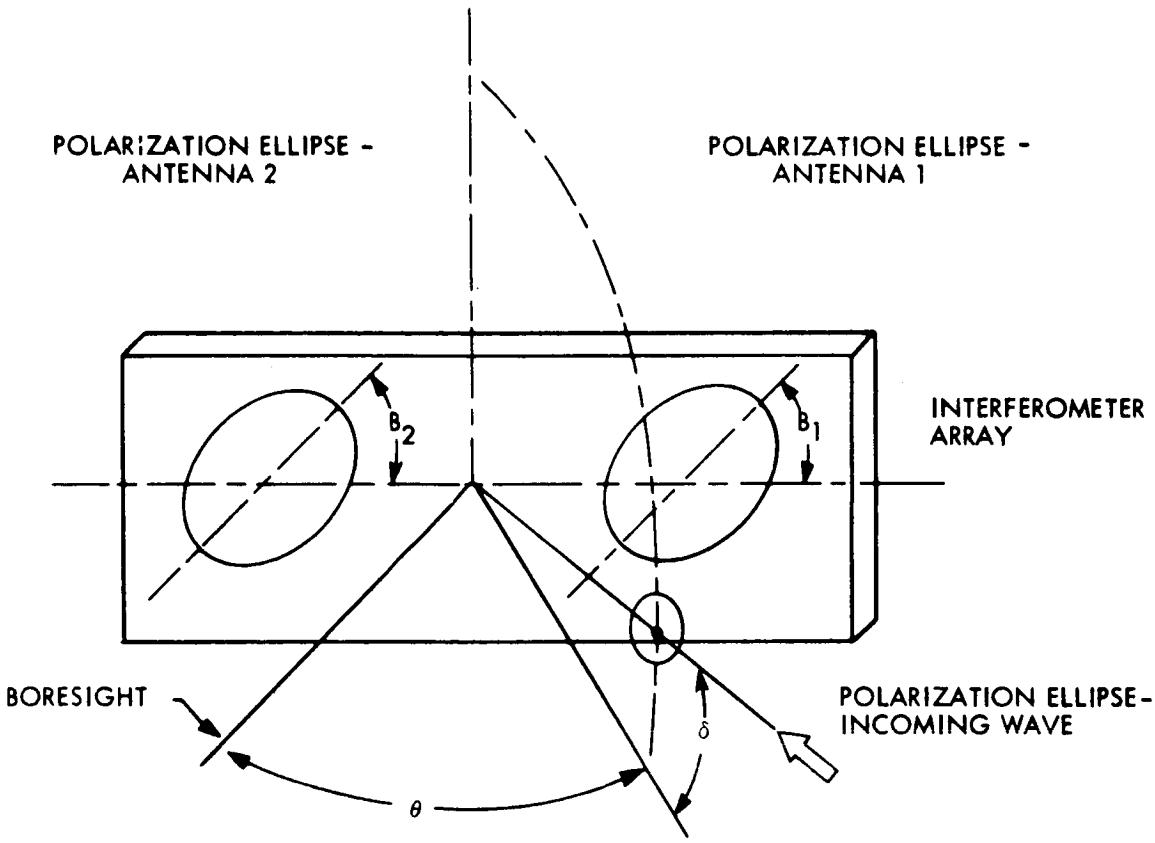

B_1, B_2	=	Tilt angles of polarization ellipses, Ant. 1 and 2
R_T	=	Axial ratio of incoming wave
θ, δ	=	Angular coordinates of incoming wave
R_1	=	Axial ratio of interferometer antenna No. 1
R_2	=	Axial ratio of interferometer antenna No. 2
$V_1 \angle\phi$	=	Received voltage phasor, antenna 1
$V_2 \angle\phi$	=	Received voltage phasor, antenna 2
$\Delta\theta_b$	=	Polarization space angle error = $\dfrac{\Delta\phi_b}{2\pi\left(\frac{D}{\lambda}\right)}$
$\Delta\phi_b$	=	Phase error
$\Delta\phi_b$	=	$\phi_2 - \phi_1$

FIGURE 8.D-1 ELLIPTICALLY POLARIZED INTERFEROMETER ANTENNA PAI WITH ELLIPTICALLY POLARIZED INCOMING WAVE

$$\phi_1 = \tan^{-1}\left[\frac{E_1 \sin B_1 \cos\Theta + E_T \sin B_1 \cos\delta - E_T \cos B_1 \sin\Theta \sin\delta}{\cos B_1 \cos\Theta + E_1 E_T \cos B_1 \cos\delta + E_1 E_T \sin B_1 \sin\Theta \sin\delta}\right]$$

$$\phi_2 = \tan^{-1}\left[\frac{E_2 \sin B_2 \cos\Theta + E_T \sin B_2 \cos\delta - E_T \cos B_2 \sin\Theta \sin\delta}{\cos B_2 \cos\Theta + E_2 E_T \cos B_2 \cos\delta + E_2 E_T \sin B_2 \sin\Theta \sin\delta} \quad \frac{2\pi D}{\lambda} \sin\Theta\right]$$

$$\Delta\phi_r = \text{phase error} = \phi_1 - \phi_2 - \frac{2\pi D}{\lambda} \sin\Theta$$

$$\Delta\Theta_r = \text{angular error} \cong \frac{\Delta\phi_r}{\frac{2\pi D}{\lambda}}$$

TABLE 8D-2

Phases of Interferometer Antenna Received Voltages

For System 4 - Circular G/S, Circular Interferometer

Let $R_T = 1-K \quad R_1 = 1, \; R_2 = 1 - \Delta R$

$$\Delta\phi_3 \; (\Delta R) = \tan^{-1}\left[\left(\frac{2-K}{2-K}\right)\tan B_1\right] - \tan^{-1}\left[\left(\frac{2-(K+\Delta R}{2-(K+\Delta R)+K\Delta R}\right)\tan B_1\right]$$

Since $\tan^{-1}(a) - \tan^{-1}(b) = \tan^{-1}\dfrac{a-b}{1+ab}$

$$\Delta\phi_3 \; (\Delta R) = \tan^{-1}\left[\frac{(K\Delta R)\;\tan B_1}{[2-(K+\Delta R)]\,[1+\tan^2 B_1]}\right]$$

For systems 2 and 3 the phase error due to axial ratio inequality is zero. For system 4, however, the phase error can become large if the inequality becomes very large (i.e. axial ratio difference of 0.5 or more).

In Figure 8D-2 the phase angle error $\Delta\phi$ is plotted versus the axial ratio inequality for system 4.

<u>Phase error due to Interferometer element polarization ellipse tilt-Angle Inequality</u>

The polarization ellipse tilt angles of the two interferometer antennas may differ either because the two elements are not identical or because one element is misaligned (has a different angle to the interferometer axis)

For the three systems on boresight

$$B_2 = B_1 + \Delta B \qquad \Theta = \gamma = 0^\circ \qquad R_1 = R_2 = R$$

$$\Delta\phi\,(\Delta B) = \tan^{-1}\left[\left(\frac{R_1 + R_T}{1+R_1R_T}\right)\tan B_1\right] - \tan^{-1}\left[\left(\frac{R_2 + R_T}{1+R_2R_T}\right)\tan B_2\right]$$

For System 2 - Linear G/S, Circular Interferometer

Let $R_T = 0 \qquad R \cong 1$

$$\Delta\phi_2 \; (\Delta B) = \tan^{-1}\left[R\tan B_1\right] - \tan^{-1}\left[R\tan(B_1+\Delta B)\right]$$

$$\tan(B_1+\Delta B) \quad \frac{\tan B_1 + \tan\Delta B}{1-\tan B_1\tan\Delta B} \cong \frac{\tan B_1 + \Delta B}{1-\Delta B\tan B_1}$$

$$\Delta\phi_2\,(\Delta B) \cong \tan^{-1}\left[(\Delta B)\,\frac{(R)\,(1+\tan^2 B_1}{1+R^2\tan^2 B_1}\right] \cong \Delta B$$

System 4 - Elliptically Polarized Ground Station Antenna, Elliptically Polarized Interferometer Antennas

Conditions

Axial Ratio, Ground Station Antenna	$R_T = 0.9$ ($K = 0.1$)
Axial Ratio, Interferometer Antennas	$R_1 = 1.0$ (Exactly Circular)
Tilt Angles	$R_2 = 1.0$ to 0.5
Antennas	$B_1 = B_2 = 45^\circ$

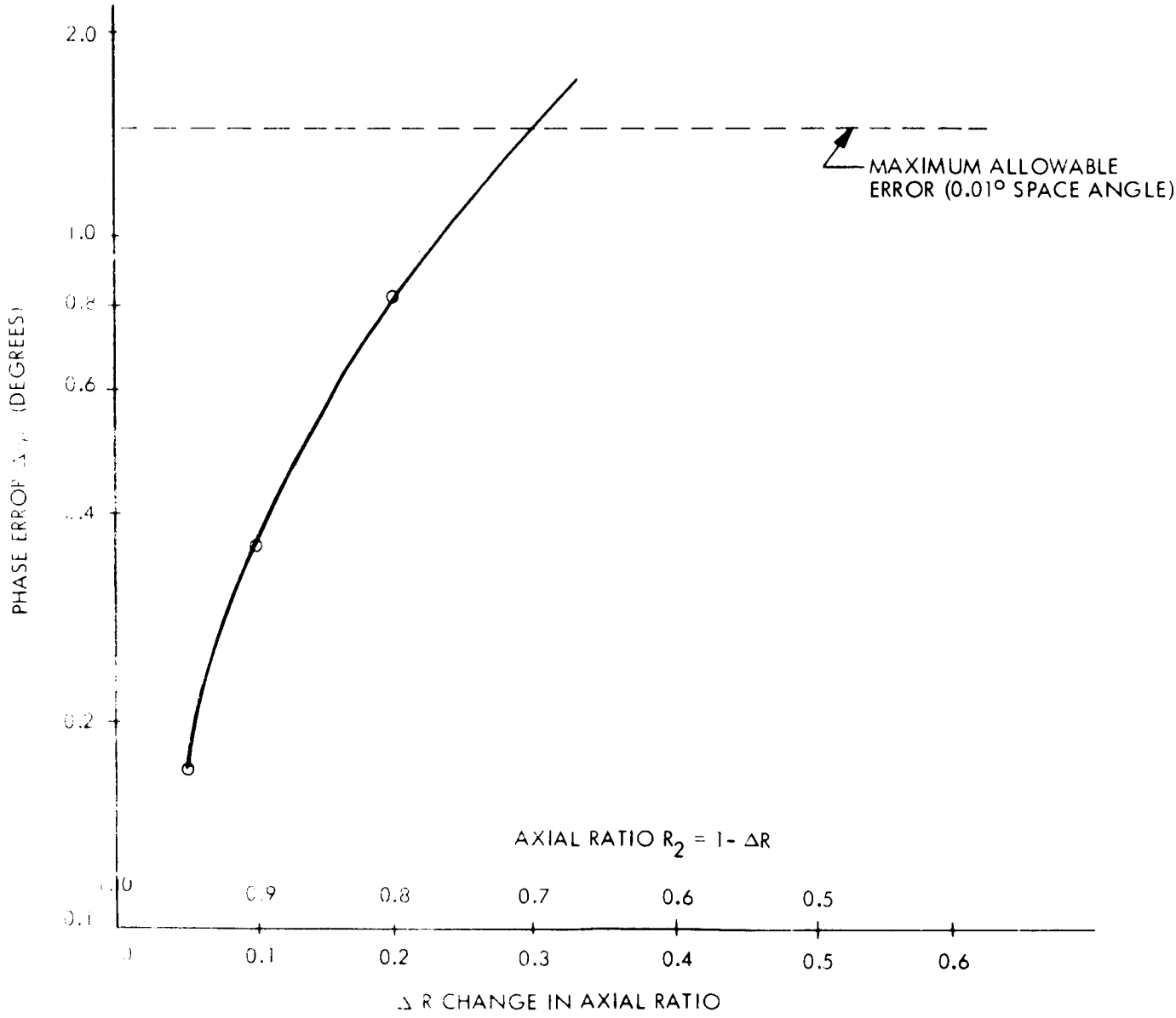

FIGURE 8.D-2 PHASE ANGLE ERROR VERSUS AXIAL RATIO INEQUALITY

For System [illegible] - Circular G/S Linear Interferometer

Let $P_{[illegible]} \cong 1$, $R = 0$

$$\Delta\phi_{3}(\Delta B) = \tan^{-1}\left[(R_{[illegible]}\tan B_1)\right] - \tan^{-1}\left[(R_{[illegible]}\tan(B_1+\Delta B)\right]$$

$$\Delta\phi_{3}(\Delta B) = \tan^{-1}\left[\frac{(\Delta B)(R_T)(1+\tan^2 B_1)}{1+R_T^2\tan^2 B_1}\right] \cong \Delta B$$

For System 4 - Circular G/S, Circular Interferometer

Let $P_{[illegible]} = 1-k$ $R = 1-\lambda$ $k, \lambda \leq 1$

$$\frac{[illegible]+P}{1+P_T} = \frac{2-(k+\lambda)}{2-(k+\lambda)+k} \cong 1$$

$$\Delta\phi_4(\Delta B) = \tan^{-1}\left[\tan B_1\right] - \tan^{-1}\left[\tan(B_1+\Delta B)\right]$$

$$\cong \tan^{-1}\left[(\Delta B)\right] \cong \Delta B$$

These equations are summarized in Table 8D-3; $_4$ is plotted in Figure 8D-3. Typical phase errors for the three different systems are also given. It can be seen that systems 2 and 3 are very slightly better than system 4.

Phase Error due to Off-Boresight Operation

When the wavefront from the ground station is not incident along the boresight axis a phase error which is slightly dependent on the inclination angles Θ, ζ exists.

a) For constant Yaw and Roll and variable Pitch ($\zeta = 0^\circ$ Θ variable)

$$\Delta\phi = \tan^{-1}\left[\left(\frac{R_1\cos\Theta + R_T}{\cos\Theta + R_1R_T}\right)\tan B_1\right] - \tan^{-1}\left[\left(\frac{R_2\cos\Theta + R_T}{\cos\Theta - R_2R_T}\right)\tan B_2\right]$$

System		General Equation	Typical Case Conditions	
			Typical Phase Error	($\theta = \psi = 0^{\circ}$ (boresight)) for All Systems
No. 2	Linear G/S Circular Interferometer	$\Delta\phi_2 = \tan^{-1} \dfrac{(\Delta B)(R)(1 + \tan^2 B_1)}{1 + R^2 \tan^2 B_1}$	$\Delta\phi = 0.98^{\circ}$	$R = 0.8$ $B_1 = B_2 = 45^{\circ}$ $\Delta B = 1^{\circ} = 17.5$ mrad.
No. 3	Circular G/S Linear Interferometer	$\Delta\phi_3 = \tan^{-1} \left[\dfrac{(\Delta B)(R_T)(1 + \tan^2 B_1)}{1 + R_T^2 \tan^2 B_1} \right]$	$\Delta\phi = 0.98^{\circ}$	$R_T = 0.8$ $B_1 = B_2 = 45^{\circ}$ $\Delta B = 1^{\circ} = 17.5$ mrad.
No. 4	Circular G/S Circular Interferometer	$\Delta\phi_4 = \tan^{-1} (\Delta B)$	$\Delta\phi = 1.0^{\circ}$	$R = 0.8$ $R_T = 0.8$ $B_1 = B_2 = 45^{\circ}$ $\Delta B = 1^{\circ}$

Table 8D-3

Comparison of Phase Error due to Ellipse Tilt Angle

Non-Uniformity for Various Polarization Systems

System 4 - Elliptically polarized ground station antenna, elliptically polarized interferometer antennas.

Conditions

Axial Ratio, ground station antenna	$R_T - \cong 1$
Axial ratio, interferometer antennas	$R_1, R_2 \cong 1$
Tilt Angles	B_1, B_2 arbitrary

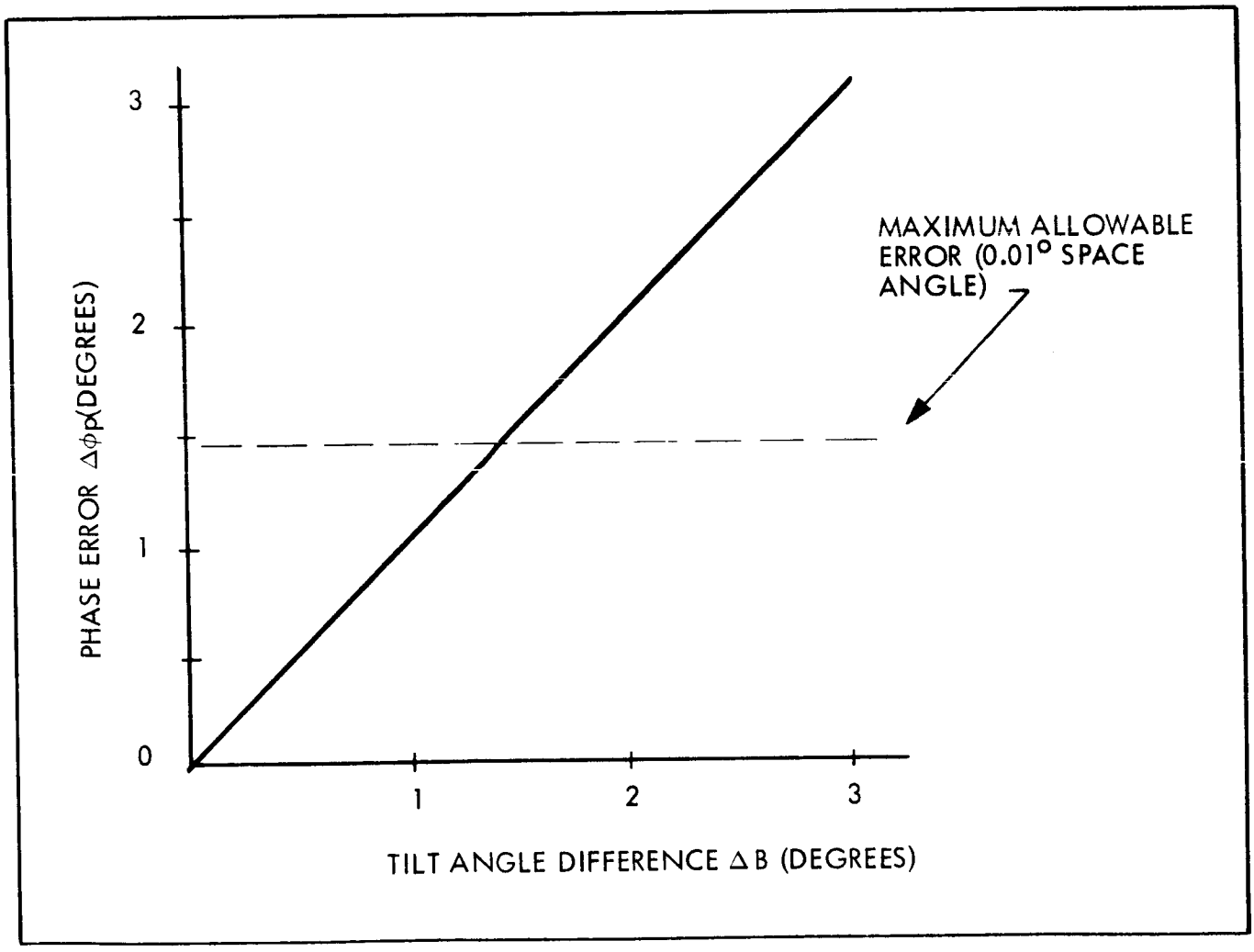

Figure 8. D-3 PHASE ANGLE ERROR VERSUS ELLIPSE TILT ANGLE INEQUALITY

b) For constant Yaw and Pitch and variable Roll ($\Theta = 0^{\circ}$, ϕ variable)

$$\Theta = \tan^{-1} \frac{R_1 + R_T \cos\phi}{1 + R_1 R_T} \tan B_1 - \tan^{-1} \frac{R_2 + R_T \cos\phi}{1 + R_2 R_T} \tan B_2$$

The particular values for this equation for systems 2, 3 and 4 are listed in Tables 8.D-4 and 8.D-5. Typical examples are also given in Tables 8.D-4 and 8.D-5. It can be seen that system 2 has no phase error variation with changing Θ or ϕ. System 3 has a very small variation, and system 4 has a small variation.

c) For constant Yaw, variable Pitch and Roll (Θ and ϕ variable)

The general equation for this case is given in Table 8.D-2 particular values are listed in Table 8D-6 From the typical example given in Table 8D-6 the phase error variation with changing Θ and ϕ is zero for system 2, is small for system 3 and is large for system 4. The phase error for system 4 versus the roll angle is given in Figure 8.D-4. The phase error versus the pitch angle is given in Figure 8.D-5.

Signal Amplitude

The power loss between a linearly polarized antenna and a circularly polarized antenna is

$$L\ (db) = 10 \log \frac{2\,(1 + R^2)}{(1 + R^2) + (1 - R^2) \sin 2B}$$

For two circularly polarized antennas with axial ratios near one (and the same polarization sense) the power loss is

$$L\ (db) = -10 \log \left[\sin^2 B + \frac{(R + R_T)^2}{(R_1 R_2 + 1)^2} \cos^2 B \right]$$

Systems		General Equations	Typical Case: Typical Phase Error	Typical Case: Conditions ($\delta = 0^\circ$ for All Systems)
No. 2	Linear G/S Circular Interferometer $R_1 \cong 1,\ R_2 \cong 1,\ R_T = 0$	$\Delta\phi_2 = \tan^{-1}\left[(R_1)\tan B_1\right] - \tan^{-1}\left[(R_2)\tan B_2\right]$	at $\theta = 0^\circ$ $\Delta\phi = 5.46^\circ$ at $\theta = 17^\circ$ $\Delta\phi = 5.46^\circ$ $\Delta(\Delta\phi) = 0^\circ$	$R_1 = 1$ $R_2 = 0.8$ $R_T = 0$ $B_1 = 45^\circ$ $B_2 = 46^\circ$
No. 3	Circular G/S Linear Interferometer $R_1 = R_2 = 0,\ R_T \cong 1$	$\Delta\phi_3 = \tan^{-1}\left[\left(\frac{R_T}{\cos\theta}\right)\tan B_1\right] - \tan^{-1}\left[\left(\frac{R_T}{\cos\theta}\right)\tan B_2\right]$	at $\theta = 0^\circ$ $\Delta\phi = 0.895^\circ$ at $\theta = 17^\circ$ $\Delta\phi = 0.896^\circ$ $\Delta(\Delta\phi) = 0.001^\circ$	$R_1 = 0$ $R_2 = 0$ $R_T = 0.8$ $B_1 = 45^\circ$ $B_2 = 46^\circ$
No. 4	Circular G/S Circular Interferometer $R_1 \cong 1,\ R_2 \cong 1,\ R_T \cong 1$	$\Delta\phi_4 = \tan^{-1}\left[\left(\frac{R_1\cos\theta + R_T}{\cos\theta + R_1R_T}\right)\tan B_1\right] - \tan^{-1}\left[\left(\frac{R_2\cos\theta + R_T}{\cos\theta + R_2R_T}\right)\tan B_2\right]$	at $\theta = 0^\circ$ $\Delta\phi = 0.258^\circ$ at $\theta = 17^\circ$ $\Delta\phi = 0.428^\circ$ $\Delta(\Delta\phi) = 0.170^\circ$	$R_1 = 1$ $R_2 = 0.8$ $R_T = 0.8$ $B_1 = 45^\circ$ $B_2 = 46^\circ$

Table 8.D-4

Comparison of Phase Error Due to Off Boresight Operation

Variable Pitch (Variable θ) for Various Polarization Systems

System	General Equation	Typical Case: Typical Phase Error	Typical Case: Conditions ($\theta = 0^\circ$ for All Systems)
No. 2 Linear G/S Circular Interferometer $R_1 \cong R_2 \cong 1,\ R_T = 0$	$\Delta\phi_2 = \tan^{-1}\left[(R_1)\tan B_1\right] - \tan^{-1}\left[(R_2)\tan B_2\right]$	at $\delta = 0^\circ$ $\Delta\phi = 5.46^\circ$ at $\delta = 17^\circ$ $\Delta\phi = 5.46^\circ$ $\Delta(\Delta\phi) = 0^\circ$	$R_1 = 1$ $R_2 = 0.8$ $R_T = 0$ $B_1 = 45^\circ$ $B_2 = 46^\circ$
No. 3 Circular G/S Linear Interferometer $R_1 = R_2 = 0,\ R_T \cong 1$	$\Delta\phi_3 = \tan^{-1}\left[(R_T \cos\delta)\tan B_1\right] - \tan^{-1}\left[(R_T \cos\delta)\tan B_2\right]$	at $\delta = 0^\circ$ $\Delta\phi = 0.895^\circ$ at $\delta = 17^\circ$ $\Delta\phi = 0.879^\circ$ $\Delta(\Delta\phi) = 0.017^\circ$	$R_1 = 0$ $R_2 = 0$ $R_T = 0.8$ $B_1 = 45^\circ$ $B_2 = 46^\circ$
No. 4 Circular G/S Circular Interferometer $R_1 \cong 1,\ R_2 \cong 1,\ R_T \cong 1$	$\Delta\phi_4 = \tan^{-1}\left[\left(\frac{R_1 + R_T \cos}{1 + R_1 R_T}\right)\tan B_1\right] - \tan^{-1}\left[\left(\frac{R_2 + R_T \cos}{1 + R_2 R_T}\right)\tan B_2\right]$	at $\delta = 0^\circ$ $\Delta\phi = 0.258^\circ$ at $\delta = 17^\circ$ $\Delta\phi = 0.146^\circ$ $\Delta(\Delta\phi) = 0.112^\circ$	$R_1 = 1$ $R_2 = 0.8$ $R_T = 0.8$ $B_1 = 45^\circ$ $B_2 = 46^\circ$

Table 8.D-5

Comparison of Phase Error Due to Off-Boresight Operation

Variable Roll (Variable δ) - For Various Polarization Systems

Systems		General Equations	Typical Case: Typical Phase Error	Typical Case: Conditions
No. 2	Linear G/S Circular Interferometer $R_1 \cong R_2 \cong 1,\ R_T = 0$	$\Delta\phi_2 = \tan^{-1}\left[R_1 \tan B_1\right]$ $- \tan^{-1}\left[R_2 \tan B_2\right]$	at $\theta = 0^\circ$, $\delta = 0^\circ$ $\Delta\phi = 5.46^\circ$ at $\theta = 17^\circ$, $\delta = 17^\circ$ $\Delta\phi = 5.46^\circ$ $\Delta(\Delta\phi) = 0^\circ$	$R_1 = 1$ $R_2 = 0.8$ $R_T = 0$ $B_1 = 45^\circ$ $B_2 = 46^\circ$
No. 3	Circular G/S Linear Interferometer $R_1 = R_2 = 0,\ R_T \cong 1$	$\Delta\phi_3 = \tan^{-1}\left[R_T \frac{\cos\delta}{\cos\theta} \tan B_1 - \tan\theta \sin\delta\right]$ $- \tan^{-1}\left[R_T \frac{\cos\delta}{\cos\theta} \tan B_2 - \tan\theta \sin\delta\right]$	at $\theta = 0^\circ$, $\delta = 0^\circ$ $\Delta\phi = 0.895^\circ$ at $\theta = 17^\circ$, $\delta = 17^\circ$ $\Delta\phi = 1.185^\circ$ $\Delta(\Delta\phi) = 0.29^\circ$	$R_1 = 0$ $R_2 = 0$ $R_T = 0.8$ $B_1 = 45^\circ$ $B_2 = 46^\circ$
No. 4	Circular G/S Circular Interferometer $R_1 \cong 1,\ R_2 \cong 1,\ R_T \cong 1$	see Table -2	at $\theta = 0^\circ$, $\delta = 0^\circ$ $\Delta\phi = 0.258^\circ$ at $\theta = 17^\circ$, $\delta = 17^\circ$ $\Delta\phi = 2.96^\circ$ $\Delta(\Delta\phi) = 2.70^\circ$	$R_1 = 1$ $R_2 = 0.8$ $R_T = 0.8$ $B_1 = 45^\circ$ $B_2 = 46^\circ$

Table 8.D-6

Comparison of Phase Error Due to Off-Boresight Operation

Combined Pitch and Roll - for Various Polarization Systems

System 4 - Elliptically polarized ground station antenna, elliptically polarized interferometer antennas.

Conditions

Axial ratio, ground station antenna	$R_T = 0.8$ (almost circular)
Axial ratio, interferometer antennas	$R_1 = 1.0$ (exactly circular)
	$R_2 = 0.8$ (almost circular)
Tilt angles, interferometer antennas	$B_1 = 45^\circ$
	$B_2 = 46^\circ$

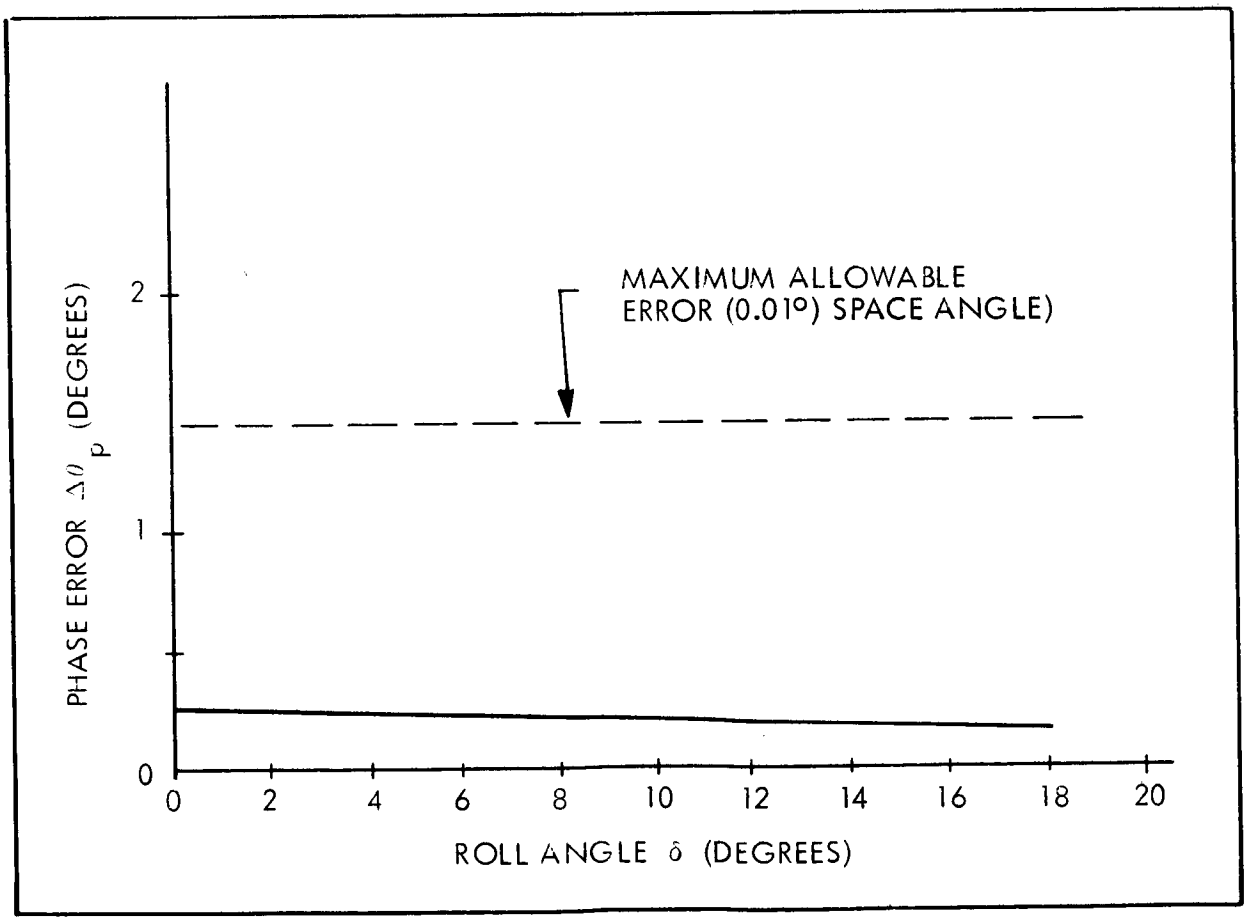

Figure 8.D-4 PHASE ANGLE ERROR VERSUS ROLL ANGLE (δ)

SYSTEM 4 - ELLIPTICALLY POLARIZED GROUND STATION ANTENNA, ELLIPTICALLY POLARIZED INTERFEROMETER ANTENNAS

CONDITIONS

AXIAL RATIO, GROUND STATION ANTENNA	R_T = 0.8 (ALMOST CIRCULAR)
AXIAL RATIO, INTERFEROMETER ANTENNAS	R_1 = 1 (EXACTLY CIRCULAR)
TILT ANGLES, INTERFEROMETER ANTENNAS	R_2 = 2 (ALMOST CIRCULAR)
	$B_1 = 45^\circ$
	$B_2 = 46^\circ$

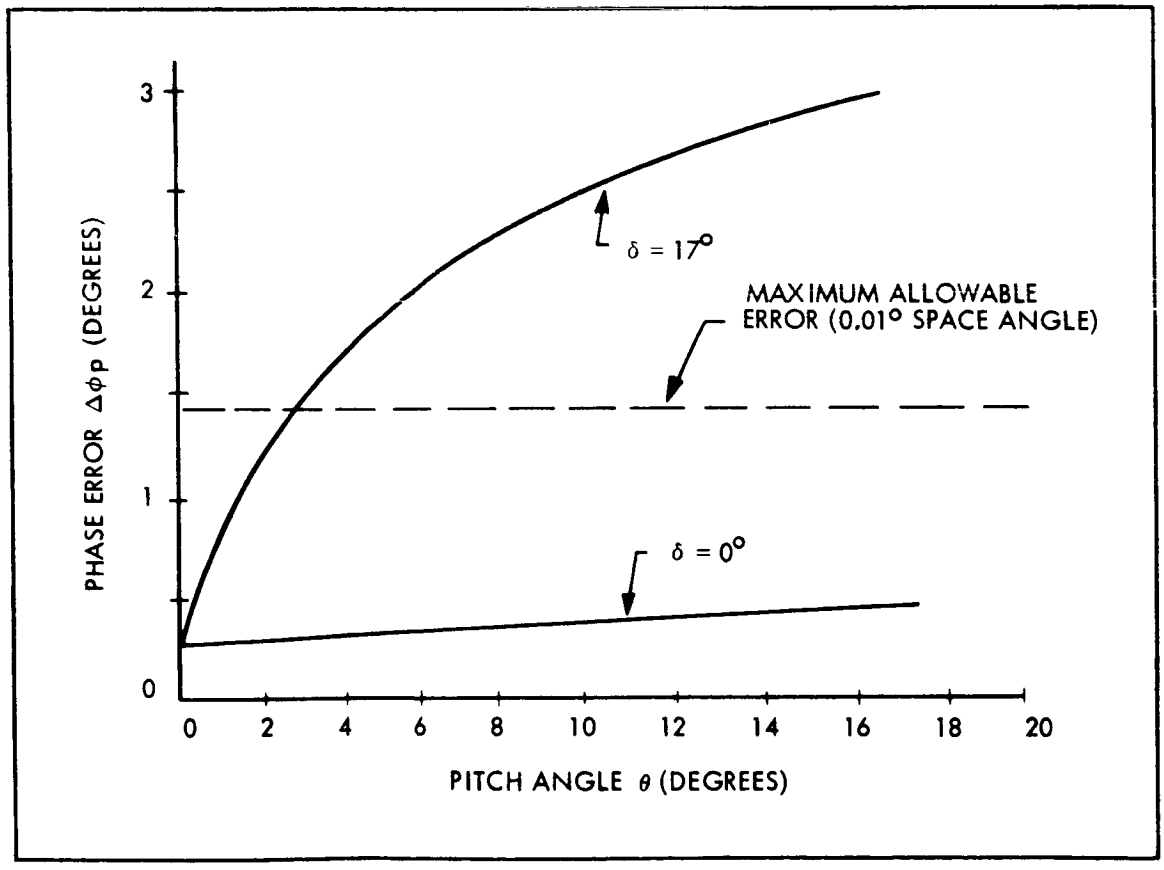

FIGURE 8.D-5 PHASE ANGLE ERROR VERSUS PITCH ANGLE (θ)

The particular equations for the three polarization systems are listed in Table 8D-7 as is an example. It can be seen that systems 2 and 3 have an average loss of -3db and the signal can fluctuate +1.1db and -0.8db from this average as the spacecraft rolls. This small amount of signal fluctuation will influence the phase measurement accuracy only a small amount. On the other hand system 4 has a minimum loss of 0 db and a maximum loss of only -0.26 db.

Selection of Polarization System

From the previous sections the following conclusions can be reached.

1) The phase errors due to differences between the axial ratios of the interferometer antenna elements are negligible for systems 2 and 3. The error is small for system 4 if the inequality is not large.

2) The phase errors due to differences in the angle of the polarization ellipse of the interferometer antenna elements are large. For all three systems one degree of ellipse angle difference results in approximately one degree of phase error. The polarization ellipse angle inequality can be caused by manufacturing differences or mechanical misalignments.

3) The phase errors due to off-boresight incidence angles are zero for system 2, are small for system 3 and are fairly large for system 4.

4) The power loss is about -3 db for both systems 2 and 3 and is only -0.3 db maximum for system 4.

System 4, (circular ground station polarization and circular interferometer polarization) has the disadvantage of having larger phase errors, and the sole advantage of having approximately 3 db less loss. Since the interferometer-ground station system is not power limited (i.e., it requires only a few watts of transmitter power) this 3 db loss is not greatly significant. System 4 will therefore be eliminated from consideration

System	General Equation	Typical Power Loss	Conditions
No. 2 Linear G/S Circular Interferometer $R_1 \cong R_2 \cong 1, \quad R_T = 0$	$L_{min} = 10 \log (1 + R^2)$ $L_{max} = 10 \log (1 + \frac{1}{R^2})$	$L_{min} = 2.2$db $L_{max} = -4.1$db. $\Delta L = 1.9$db	$R = 0.8$ $B = 90^\circ$
No. 3 Circular G/S Linear Interferometer $R_1 = R_2 = 0, \quad R_T = 1$	$L_{min} = 10 \log (1+R^2)$ $L_{max} = 10 \log (1 + \frac{1}{R^2}$	$L_{min} = -2.2$db $L_{max} = -4.1$db $\Delta L = 1.9$ db	$B = 90^\circ$ $B = 0^\circ$
No. 4 Circular G/S Circular Interferometer $R_1 \cong 1, \; R_2 \cong 1, \; R_T \cong 1$	$L_{min} = 0$ $L_{max} = 20 \log \left(\frac{1+RR_T}{R + R_T} \right)$	$L_{min} = 0$db $L_{max} = 0.26$db $\Delta L = 0.26$ db	$R = 0.8, \; R_T = 0.8$ $B = 90^\circ$ $B = 0^\circ$

Table 8.D-7

Comparison of Power Loss Due to Interferometer Rotation

The choice is now between system 2 (linear Ground Satellite circular interferometer) and system 3 (circular Ground Satellite linear interferometer). For a linearly polarized interferometer antenna element such as a rectangular horn the axial ratio of each horn can be made very close to zero. Thus, $R_1 = R_2 = 0$. (The orthogonal polarization will be below cutoff in the rectangular waveguide feeding the horn and will be very rapidly attenuated.) The inclination of the polarization eclipse of a linearly polarized horn (which is a straight line) can be readily controlled by the mechanical alignment of the horn (i.e. $B_1 = B_2$).

On the other hand, it is difficult to construct a set of circularly polarized horns that will have exactly the same axial ratio (i.e. $R_1 \neq R_2 = 1$) and that will have the same polarization ellipse orientation (i.e. $B_1 \neq B_1$). Obtaining polarization circularity requires controlling the amplitudes and the phase shifts in the horn feed exactly. For example, Dorne and Margolin quotes an axial ratio of O to 1db (R = 1 to 0.8) for their Model P9A conical horn. These considerations tend to favor system 2.

Using system 3 with linearly polarized interferometer elements also has an advantage as far as mutual coupling is concerned. For the closely space antenna elements, where it is difficult to obtain the required decoupling, the two linearly polarized horns could be placed orthogonal to each other. While this introduces a 90° phase shift in the received signal on boresight this 90° can be calibrated out. On the other hand if system 2 is used the coupling that exists between the two circularly polarized elements must be accepted.

To summarize, the use of a circularly polarized ground station antenna and linearly polarized interferometer elements is recommended because of antenna element reproducability and stability and because of lower mutual coupling.

APPENDIX 8E

DERIVATION OF THE RECEIVED VOLTAGE PHASES ON AN ELLIPTICALLY POLARIZED INTERFEROMETER ANTENNA PAIR WITH AN INCIDENT ELLIPTICALLY POLARIZED WAVE

Consider an elliptically polarized plane wave traveling in the positive Z direction [1] (see Figure 8. E-1). Assume that the coordinate system is oriented so that the minor and major axes of the polarization ellipse coincide with the X and Y axis. Then the electric field of this wave can be written as

$$\bar{E} = (\bar{a}_x E_x + \bar{a}_y j E_y) e^{j(wt-kz)}$$

Let it be assumed that the power carried by this wave is constant, so

$$E_x^2 + E_y^2 = 1$$

Now let the axial ratio R be defined as

$$R = \frac{E_y}{E_x} = \frac{\sqrt{(1 - E_x^2)}}{E_x}$$

$$E_x = \frac{1}{\sqrt{1 + R^2}}$$

$$E_y = RE_x = \frac{R}{\sqrt{1 + R^2}}$$

therefore

$$\bar{E} = \bar{a}_x \frac{1}{\sqrt{1 + R^2}} + \bar{a}_y \, j \frac{R}{\sqrt{1 + R^2}}$$

$$= \frac{1}{\sqrt{1 + R^2}} (\bar{a}_x + j R \bar{a}_y) = \bar{E}_x + \bar{E}_y$$

1. R. W. Hartop, "Power Loss between Arbitrarily Polarized Antennas", J. P. L. Tech. Report No. 32-457 (NASA N65-14806)

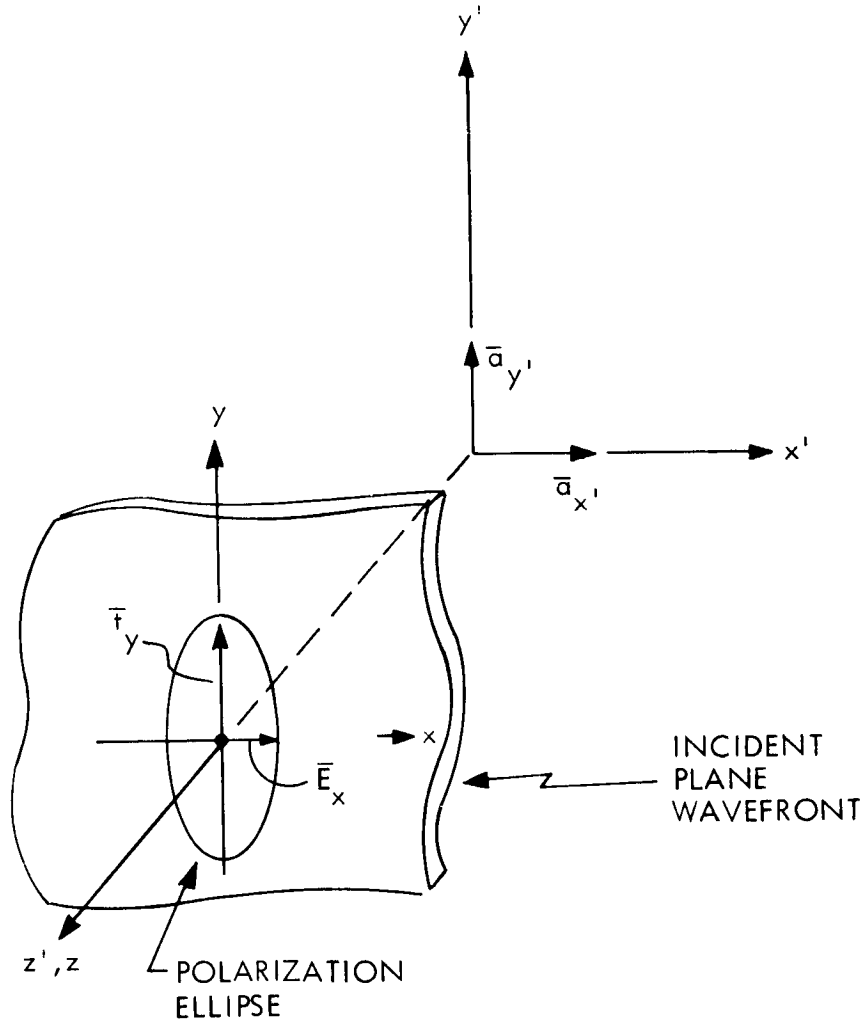

Figure 8. E-1 ELLIPTICALLY POLARIZED PLANE WAVE

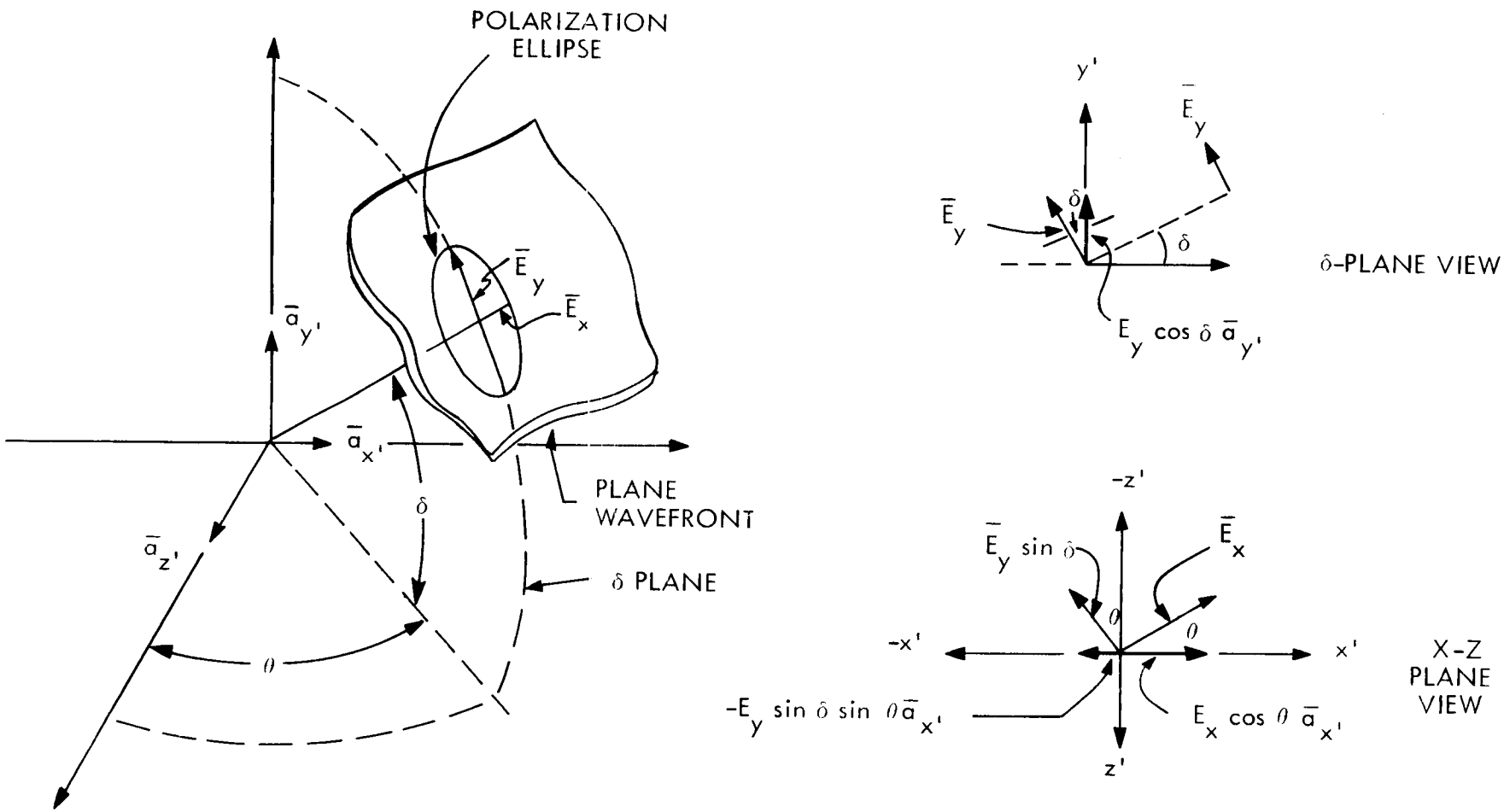

Figure 8. E-2 ELLIPTICALLY POLARIZED PLANE WAVE INCIDENT AT ANGLES θ, δ

Now assume that the incoming plane wave from a transmitter is incident at angles Θ, δ (see Fig. E-2). Resolving the component vectors E_y and $\bar{E}_x$ along the x' and y' axes

$$\bar{E}_{y'} = E_y \cos\delta \, \bar{a}_{y'} = \frac{j R \cos\delta}{1 + R^2} \bar{a}_{y'}$$

$$\bar{E}_{x'} = (E_x \cos\Theta - E_y \sin\delta \sin\Theta) \, \bar{a}_{x'}$$

$$\frac{(\cos\Theta - j R \sin\delta \sin\Theta)}{1 + R^2} \bar{a}_{x'}$$

$$\bar{E}_T = \frac{1}{1 + R_T^2} \left[(\cos\Theta - j R_T \sin\delta \sin\Theta) \bar{a}_{x'} + (j R_T \cos\delta) \bar{a}_{y'} \right]$$

$$= (E_{TX}) \bar{a}_{x'} + (E_{TY}) \bar{a}_{y'} \qquad (1)$$

Let a receiving antenna be placed at the origin (Z' = O) with its Z axis coincident with the Z' axis but with the x axis of its polarization ellipse at an angle B to the X' axis (see Fig. 8. E-3).

Then it can be shown[1] that the electric field of the receive antenna is

$$\bar{E}_R = \frac{1}{1 + R_R^2} \left[\bar{a}_{x'} (\cos B - j R_R \sin B) - \bar{a}_{y'} (\sin B + j R_R \cos B) \right]$$

$$= (E_{Rx}) \bar{a}_{x'} + (E_{Ry}) \bar{a}_{y'} \qquad (2)$$

The voltage induced in the receive antenna by the inclined plane wavefront is

$$V_R \angle \phi_R = (\bar{E}_T) \cdot (\overline{E_R}^*)$$

$$= \left[E_{Tx}\right] \left[E_{Rx}^*\right] + \left[(E_{Ty})\right] \left[E_{Ry}^*\right]$$

$$\phi_R = \text{phase of received voltage} = \frac{\mathrm{Im}\left\{\left[E_{Tx}\right]\left[E_{Rx}\right] + \left[E_{Ty}\right]\left[E_{Ry}\right]\right.}{\mathrm{Re}\left\{\left[E_{Tx}\right]\left[E_{Rx}\right] + \left[E_{Ty}\right]\left[E_{Ry}\right]\right.} \qquad (3)$$

from eq. (1)

$$E_{Tx} = \frac{1}{\sqrt{1 + R_T^2}} (\cos\Theta - j R_T \sin\delta \sin O)$$

$$E_{Ty} = \frac{1}{\sqrt{1 + R_T^2}} (j R_T \cos\delta)$$

from eq. (2)

$$E_{Rx}^* = \frac{1}{\sqrt{1 + R_R^2}} (\cos B + j R_R \sin B)$$

$$E_{Ry}^* = \frac{1}{\sqrt{1 + R_R^2}} (\sin B - j R_R \cos B)$$

$$\mathrm{Im}\left[(E_{Tx})(E_{Rx})\right] = \frac{-j R_T \cos B \sin\delta \sin\Theta + j R_R \sin B \cos\Theta}{(1 + R_R^2)(1 + R_T^2)}$$

$$\mathrm{Im}\left[(E_{Ty})(E_{Ry})\right] = \frac{+j R_T \sin \cos \delta}{(1 + R_R^2)(1 + R_T^2)}$$

$$\mathrm{Re}\left[(E_{Tx})(E_{Rx})\right] = \frac{\cos B \cos\Theta + R_T R_R \sin B \sin\delta \sin\Theta}{(1 + R_R^2)(1 + R_T^2)}$$

$$\mathrm{Re}\left[(E_{Ty})(E_{Ry})\right] = \frac{+R_T R_R \cos B \cos\delta}{1 + R_R^2)(1 + R_T^2)}$$

from eq. (3)

from eq. 3.

$$\phi_R = \frac{R_R \sin B \cos \Theta + R_T \sin B \cos \delta - R_T \cos B \sin \Theta \sin \delta}{\cos B \cos \Theta + R_R R_T \cos B \cos \delta + R_R R_T \sin B \sin \Theta \sin \delta} \quad (4)$$

Consider now a pair of elliptically polarized antennas used as an interferometer (see Fig. E-1). An elliptically polarized incoming wave is incident on the interferometer at arbitrary incidence angles Θ, δ . Then

$$V_1 \angle \phi_1 = (\overline{E_T}) \cdot (\overline{E_R}^*)$$

$$V_2 \angle \phi_2 = (E_T) \cdot (E_R^*) \cdot e^{-j \frac{2\pi D}{\lambda} \sin \Theta}$$

and

$$\phi_1 = \frac{R_1 \sin B_1 \cos \Theta + R_T \sin B_1 \cos \delta - R_T \cos B_1 \sin \Theta \sin \delta}{\cos B_1 \cos \Theta + R_1 R_T \cos B_1 \cos \delta + R_1 R_T \sin B_1 \sin \Theta \sin \delta} \quad (5)$$

$$\phi_2 = \frac{R_2 \sin B_2 \cos O + R_T \sin B_2 \cos \delta - R_T \cos B_2 \sin \Theta \sin \delta}{\cos B_2 \cos O + R_2 R_T \cos B_2 \cos \delta + R_2 R_T \sin B_2 \sin \Theta \sin \delta} \quad (6)$$

$$- \frac{2\pi D}{\lambda} \sin \Theta$$

the phase reading of the interferometer system is

$$\Delta \phi = \phi_1 - \phi_2$$

The phase error due to polarization effects

$$\Delta \phi_p = (\phi_1 - \phi_2) - 2\pi \frac{D}{\lambda} \sin \Theta \quad (7)$$

The polarization space angle error is

$$\Delta \Theta p = \frac{\Delta \phi p \cos \Theta}{2\pi \left(\frac{D}{\lambda}\right)} \cong \frac{\Delta \phi p}{2\pi \left(\frac{D}{\lambda}\right)} \tag{8}$$

APPENDIX 8F

ALTERNATIVE ANTENNA SWITCHING SYSTEMS-DIRECT PHASE READING INTERFEROMETER

1. Introduction

Various methods have been proposed to switch the second channel of the phase measuring system to the four different antenna elements (X coarse, X vernier, Y coarse, Y vernier). The purpose of this section is to indicate how the selection of an optimum switching system was made. This selection was accomplished by analyzing the performance of each system for:

a) Phase stability

b) Attenuation

c) Reliability

d) Size and weight

2. Description of Alternative Systems

The alternative switching systems are

1) Switched RF lines

2) Switched LO lines

3) Switched IF lines

4) Switched multipliers.

Each of these sytems are shown in Figs. 8.F-1 to 8.F-4.

2.1 Switched Signal Lines

The various antennas are connected alternately to a single mixer by means of an r.f. switch. This system has the advantage of using only one mixer thus avoiding the mixer phase tracking problem. It also uses short l.o. transmission lines.

Its disadvantages are a) the use of long r.f. cables which introduce phase instability and attenuation; b) the use of an r.f. switch which can introduce attenuation, phase stability and reliability problems.

2.2 Switched L.O. Lines

Mixers are placed at each antenna element, and the local oscillator power and l.f. signals are simultaneously switched in sequence.

The advantage of this system is that any losses in the l.o. lines will not adversely affect the system S/N ratio, since the r.f. signal lines are short and the mixer noise figure is approximately constant with L.O. power.

The disadvantages of this system are a) long l.o. lines are required, b) an r.f. switch is required, c) two switches are required, d) multiple mixers degrade phase stability.

2.3 Switched IF lines

The advantage of this system are a) short signal lines promote phase stability, b) only an i.f. switch is required. The disadvantages are a) long l.o. lines degrade phase stability, b) multiple mixers degrade phase stability, c) a large amount of l.o. power is required.

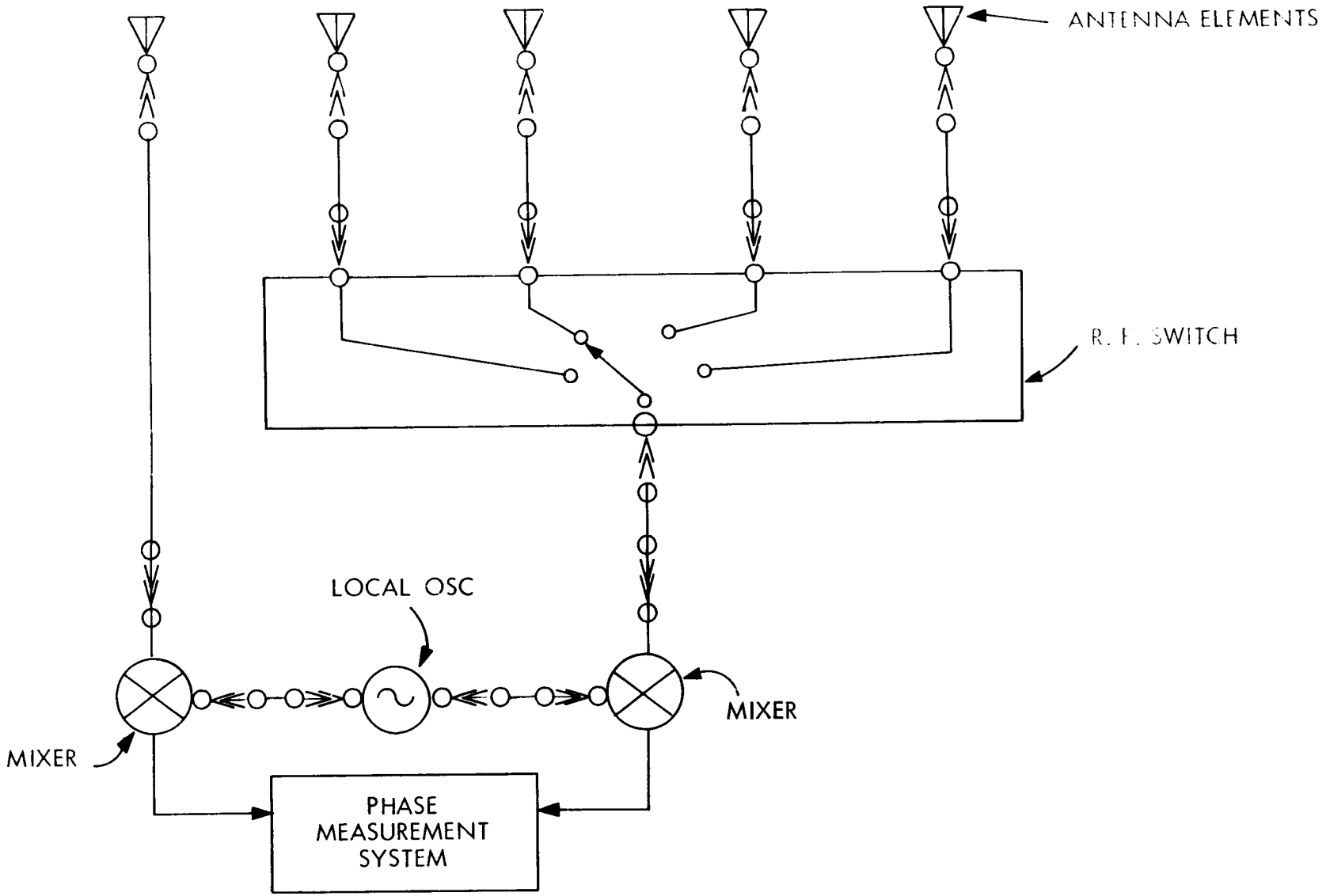

Figure 8. F-1 SWITCHED SIGNAL LINES

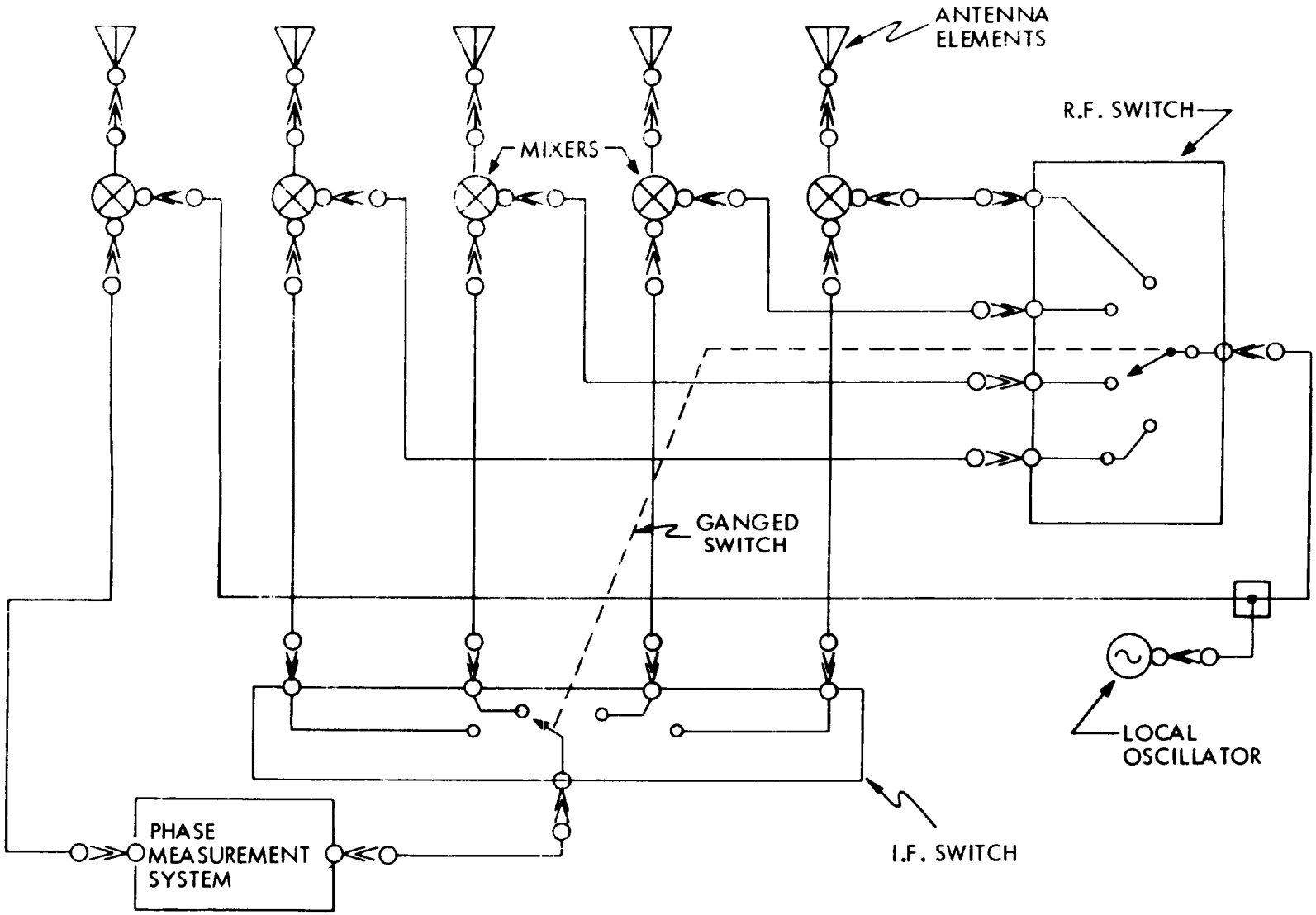

FIGURE 8.F-2 SWITCHED LOCAL OSCILLATOR LINES

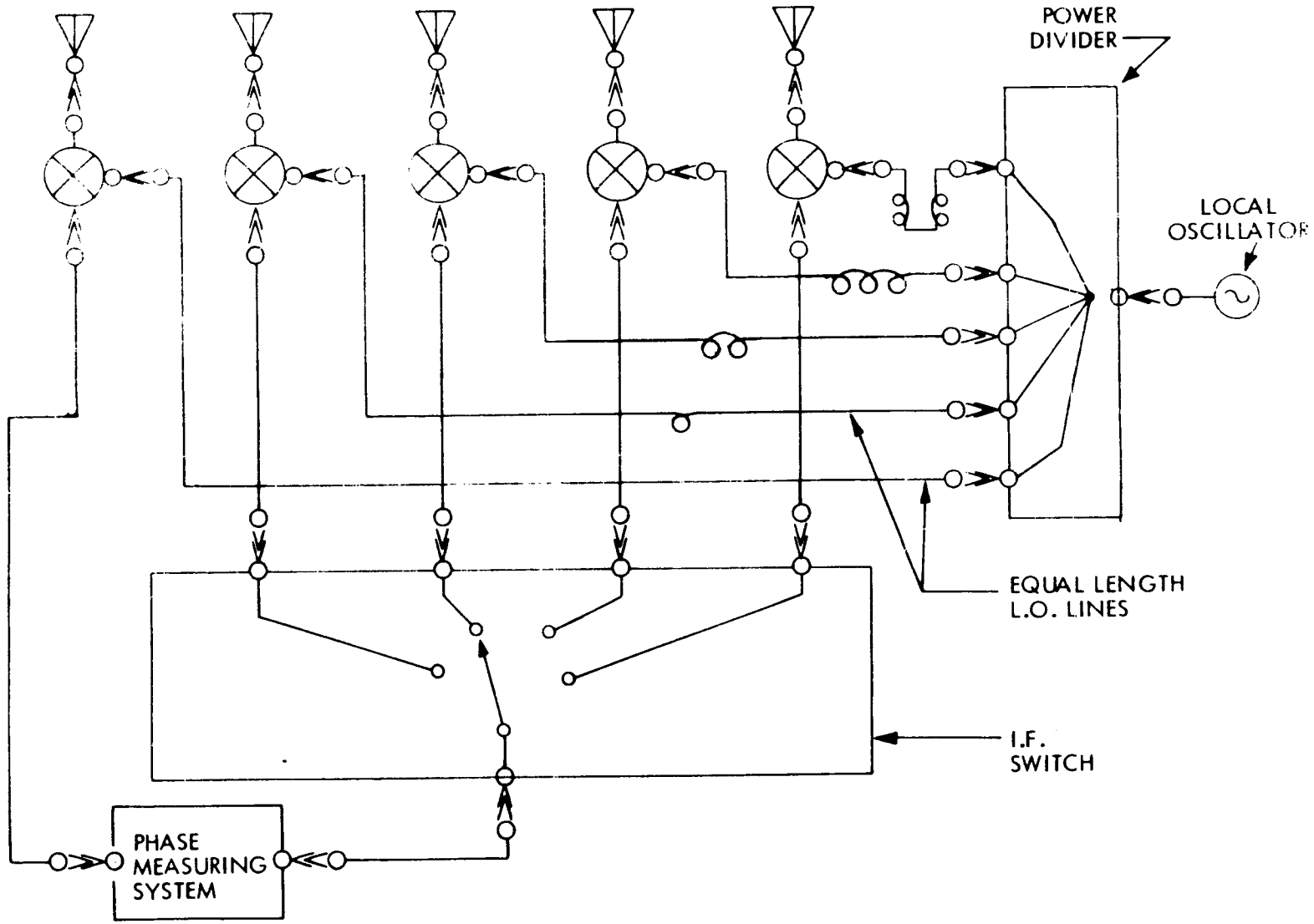

FIGURE 8.F-3 SWITCHED I.F. LINES

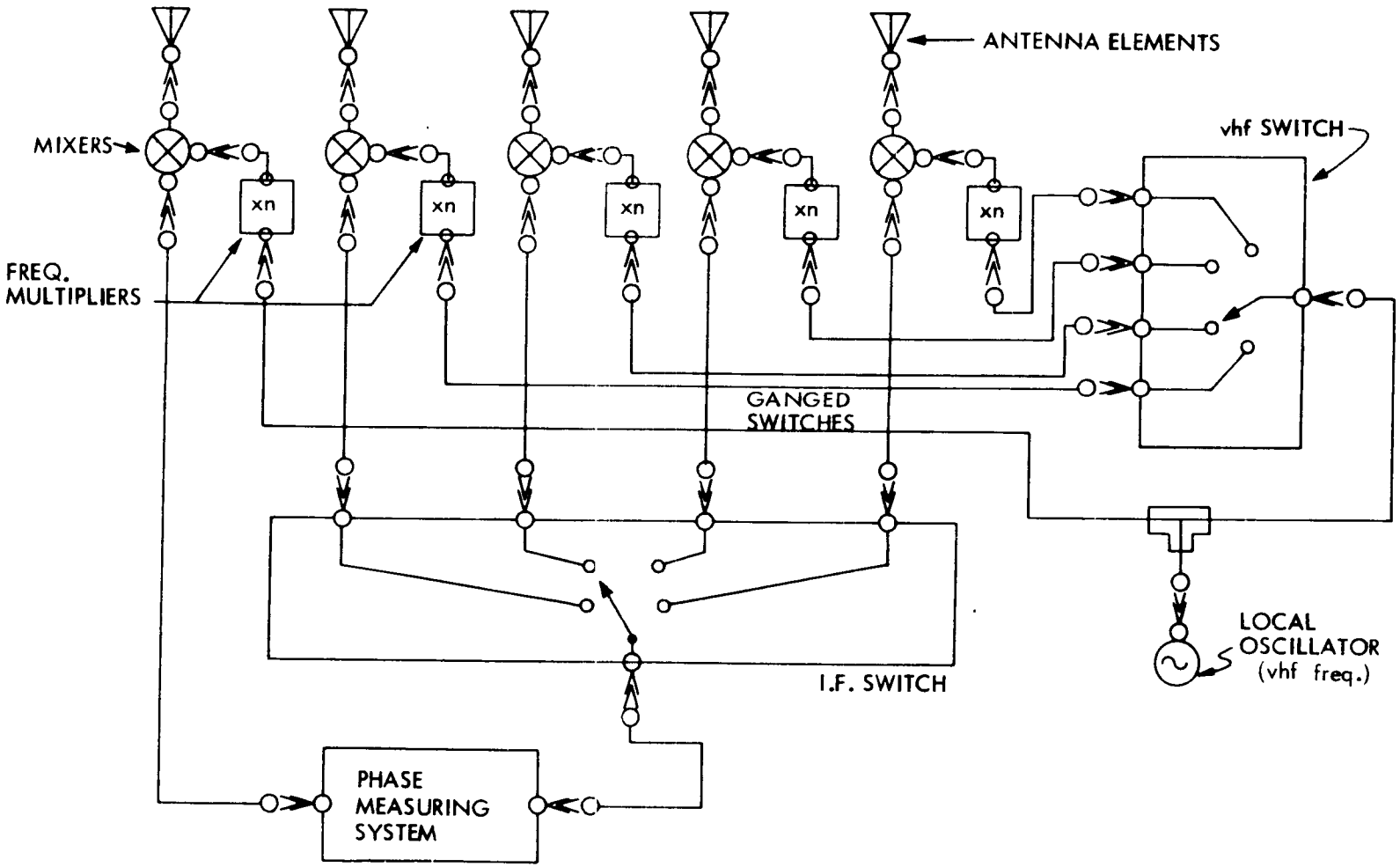

FIGURE 8. F-4 SWITCHED MULTIPLIERS

2.4 Switched Multipliers

The advantages of this system are a) short signal and l.o. lines promote phase stability, b) only i.f. and n.h.f. switches are required.

The disadvantages are a) multiple multipliers degrade phase stability, b) two switches are required, c) multiple mixers degrade phase stability.

3 Selection of Prepared System

From the material in section 4, a hierarchy of the phase stability of the various components can be established, with the most phase stable listed first

	phase stability (degrees phase shift) (temp. change)
1. transmission lines	0.2%C
2. i.f. switches, mechanical	-
3. i.f. switches, electrical	-
4. r.f. switches, mechanical	-
5. r.f. switches, electrical	-
6. mixers	0.5%C
7. frequency multipliers	1%C

Consider the switched L.O. lines system. It uses one more switch than does the switched IF system, and an r.f. switch at that. Therefore this system has no advantage over the switched i.f. system except the requirement of less L.O. power. Since only about 1mW of L.O. power is required for each mixer, this is a small disadvantage.

The switched L. O. system can therefore be eliminated from consideration.

Consider the switched multiplier system. From the hierarchy of component phase stability and from section 4.4 it can be seen that the multipliers are the least stable component. This system can therefore be eliminated.

The choice now lies between the switched signal lines system and the switched i.f. lines system. Let it be assumed that the length of the signal lines between the antennas and the r.f. switch in the switched signal line system is equal to the length of the l.o. lines between the mixers and the power divider in the switched i.f. lines system. Since the l.o. frequency and the signal frequency are nearly the same, the phase stability of the signal lines in the switched signal system and of the l.o. lines in the switched i.f. system will be nearly the same. Let it also be assumed that the phase stability of the i.f. switch and i.f. transmission lines is very good, so that they can be neglected in comparison to the phase stability of the r.f. components. Then the phase stability of the switched r.f. system will be determined by the phase stability of the r.f. switch and the single mixer, while the phase stability of the switched i.f. system will be determined by the phase tracking of the multiple mixers.

By placing the mixers close together, their thermal environment is identical. The tracking problem is minimized. A consideration of all factors shows the switched I.F. system is best.

APPENDIX 8G

DERIVATION OF COUNTER EQUATION

The purpose here is to derive an expression for what the count implies. Errors due to random noise will not be considered.

The derivation is performed in conjunction with Figure 8.7.2 of Section 8.7. From this figure, Table 8C-1 follows directly. ω_G is the ground oscillator frequency. k is the frequency multiplier constant. Actually ω_G and ω_{IF} (IF freq.) are equal.

The phase detector error signal is zero when the phases from the IF signal and the VCO are equal. This enables one to solve for the unknown frequency ω_6 and phase shift ϕ_2.

It has been assumed that the mixer is a pure multiplier such that $\cos x \cos y = 1/2 \cos (x + y) + 1/2 \cos (x - y)$. The sum term is eliminated by the bandpass characteristics of the IF section. In addition, the only significant time constant assumed is that in the IF section.

The count N is expressed in radians which avoids the problem of quantization. N is treated as a continuous variable. In practice, N will necessarily be quantized to 2π radians (2π radians equals 1 count). Therefore the exact counter expression will have a factor of 2π in the denominator.

The effects of quantization are considered in another section of these Appendices.

TABLE 8.G-1

V_0 $\cos \omega_G t$

V_1 $\cos \left[(k+1)\omega_G t\right]$

V_2 $\cos \left[(k+1)\omega_G t + \phi_G\right]$

V_{3A} $\cos \left[(k+1)\omega_G (t + R_A^*/C) + \phi_G\right]$

V_{7A} $\cos \left[k\omega_6 t + \phi_2\right]$; ω_6 & ϕ_2 unknown at this point in derivation

V_{4A} $\cos \left[k\omega_G (t + R_A^*/C) + \omega_G (t + R_A^*/C) - k\omega_6 t - \phi_2\right]$

V_{5A} $\cos \left[k\omega_G (t + R_A^*/C) + \omega_G (t + R_A^*/C) - k\omega_6 t - \phi_2 + \phi_{IFA}\right.$

V_{6A} $\cos \left[\omega_6 t + \phi_2\right]$, direct from V_{7A}

$V_{NA} = 0$ When $\omega_6 t + \phi_2 = k\omega_G (t + R_A^*/C) + \omega_G (t + R_A^*/C) - k\omega_6 t - \phi_2 + \phi_{IFA}$

$$(k+1)\omega_6 t + 2\phi_2 = (k+1)\omega_G t + (k+1)\omega_G R_A^*/C + \phi_{IFA}$$

$$A\ \omega_6 = \omega_G \text{ and } \phi_2 = (k+1)/2\, \omega_G R_A^*/C + \phi_{IFA}/2$$

V_{7A} $\cos \left[k\omega_G t + 1/2\,(k+1)\omega_G R_A^*/C + 1/2\,\phi_{IFA}\right]$

V_{4A} $\cos \left[\omega_G t + 1/2\,(k+1)\omega_G R_A^*/C - 1/2\,\phi_{IFA}\right]$

V_{4B} By Analogy $\cos\left[\omega_G t = 1/2\,(k+1)\omega_G R_B^*/C - 1/2\,\phi_{IFB}\right]$

V_{5A} $\cos\left[\omega_G t \quad 1/2\,(k+1)\omega_G R_A^*/C + 1/2\,\phi_{IFA}\right]$

V_{5B} $\cos\left[\omega_G t + 1/2\,(k+1)\,\omega_G R_B^*/C + 1/2\,\phi_{IFB}\right.$

t_{on} When $V_{5A} = 0$ or $t_{on} = n\pi/\omega_G + (k+1)/2\, R_A^*\, C + \phi_{IFA}\, 2\,\omega_G$

t_{off} When $V_{5B} = 0$ or $t_{off} = m\pi/\omega_G + (k+1)/2\, r_B^*/C + \phi_{IFB}/2\omega_G$

$$N \qquad \omega_c (t_{on} - t_{off}) = \underbrace{\frac{\pi(n-m)\,\omega_c}{\omega_G}}_{\text{Ambiguity}} = \underbrace{\frac{k+1}{2}\,\frac{R_A^* - R_B^*}{C}\,\omega_c}_{\text{desired signal}} + \underbrace{\frac{\omega_c}{2\omega_G}\,(\phi_{IFA} - \phi_{IFB})}_{\text{calibration}}$$

APPENDIX 8H
GATING TIME ERROR ANALYSIS

The problem is to determine the error in gating time due to noise superimposed on the signal.

The major assumptions are:

1. Triggering occurs when the signal is crossing zero in a positive direction.
2. The signal plus noise is passed through a high Q bandpass filter prior to the gating device.

A good approximation to the cumulation triggering time distribution will be:

$$W(t) = \left[1 - \mathrm{EXP}\left(-B^2 t^2 / 2\overline{N}_o\right)\right]^{\overline{m}_o} \qquad t < 0$$
$$= 0 \qquad t > 0 \tag{1}$$

W (t) represents the probability of triggering prior to time t

$$B = \frac{d}{dt}\left(A \sin \omega_m t\right) \approx A\,\omega_m \quad \text{at} \quad t \approx 0$$

$\overline{N}_o$ = mean noise power

$\overline{m}_o$ = total expected number of zero crossings (signal-plus-noise) in the time interval

It can be shown that

$$\overline{m}_o / 2f_o = \left[\frac{S/N + 1 + f_B^2/12f_o^2}{S/N + 1}\right] \tag{2}$$

where f_o is the center frequency of the bandpass filter

f_B is the bandwidth of this filter

S/N is the signal-to-noise ratio.

For S/N $\gg$ 10, $\overline{m}_o \approx 1$

Therefore equation 1 may be written

$$W(t) = 1 - EXP\left[-B^2 t^2 / 2\,\overline{N}_o\right] \qquad t < 0$$
$$= 0 \qquad t > 0 \tag{3}$$

The probability density function of triggering time will be

$$P(t) = \frac{d}{dt} W(t) = +\frac{B^2}{\overline{N}_o} t \; EXP\left[-\frac{B^2 t^2}{2\overline{N}_o}\right] \qquad t \leq 0 \tag{4}$$

The triggering error will be $\tau = 0 - t$

such that

$$P(\tau) = \frac{B^2}{\overline{N}_o} \tau \; EXP\left[-\frac{B^2 \tau^2}{2\overline{N}_o}\right] \qquad \tau \leq 0 \tag{5}$$
$$= 0 \qquad \tau > 0$$

The average triggering error will be

$$E(\tau) = \int_0^\infty \frac{B^2}{\overline{N}_o} \tau \, EXP\left[-\frac{B^2 \tau^2}{2\overline{N}_o}\right] \tau \, d\tau = \frac{\sqrt{\pi}}{2\omega_m} \frac{1}{\sqrt{S/N}} \tag{6}$$

The variance will be

$$\left[E(\tau)\right]^2 + \sigma^2 = E(\tau^2) - \left[E(\tau)\right]^2 = \frac{B^2}{\overline{N}_o} \int_0^\infty \tau^2 EXP\left[-\frac{B^2 \tau^2}{2\overline{N}_o}\right] \tau \, d\tau$$

$$\sigma^2 = \frac{1}{B^2/2\overline{N}_o} - \left[E(\tau)\right]^2 = \frac{1}{\omega_m^2 \, S/N} - \frac{\pi}{4\omega_m^2 \, S/N} \tag{7}$$

since $B = \omega_m A$

and $A^2/2$ = signal power = S

Therefore

$$\sigma_T^2 = \left(\frac{4-\pi}{4}\right) \frac{1}{\omega_{IF}^2 (S/N)} \approx \frac{.463}{\omega_{IF}^2 (S/N)} \qquad (8)$$

the equivalent error is

$$\sigma_\phi = \omega_{IF} \sigma_T \qquad (9)$$

Quantization Error in the Count

Assuming the counter counts only when the clock oscillator signal passes through zero in a negative (positive) direction, it is possible to produce an error in phase due to quantization at the beginning and end of the counting operation. The distribution function of the phase error produced at the beginning of the count is given by Figure 8.H-1 while the end of the count is shown in Figure 8.H-2. The quantization error is always such as to infer extra phase at the beginning of the count and deficient phase at the end of the count.

The total phase error produced by quantization is simply the sum of the two phase errors. Since it is reasonable to assume that the phase error at the beginning and the phase error at the end are statistically independent, the density function of the sum is achieved by convolution of the two density functions. The result is as shown in Figure 8.H-3. By inspection it is seen that the average phase error produced by quantication is zero. The variance of the phase error is given by

$$\sigma_{\phi_T}^2 = \int_{-2\pi}^{0} \phi^2 \rho_1(\phi)\, d\phi + \int_{0}^{2\pi} \phi^2 \rho_2(\phi)\, d\phi = 2\int_{0}^{2\pi} \phi^2 \rho(\phi)\, d\phi$$

where $\rho(\phi) = 1/_{2\pi} \left[1 - \phi/2\pi \right]$

which upon evaluation yields

$$\sigma^2_{\phi_T} = {}^2/_3\,\pi^2 \quad ; \quad \sigma_{\phi_T} = \sqrt{{}^2/_3}\,\pi \approx 2.56 \text{ radians.}$$

Now σ_{ϕ_T} is the phase error referenced to the clock frequency. It is equivalent to a timing error of

$$\sigma_T = \sigma_{\phi_T}/\omega_c = \frac{\pi\sqrt{2/3}}{2\pi \times 30 \times 10^6} = 1.36 \times 10^{-8} \text{ SEC.}$$

The phase error referenced to the 100 kc signal is then

$$\sigma_{\phi_{100KC}} = 1.36 \times 10^{-8}\,(2\pi \times 10^5) = 8.54 \text{ mr}$$

$$= 0.48 \text{ DEG.}$$

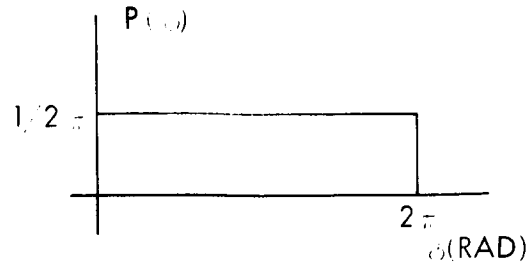

Figure 8.H-1 PHASE ERROR DISTRIBUTION

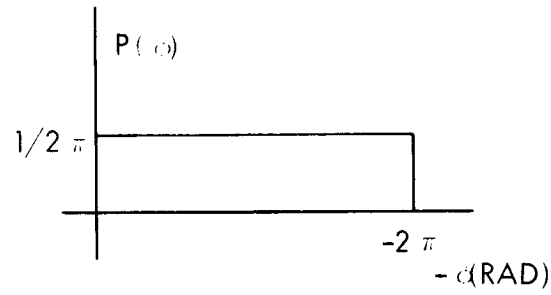

Figure 8.H-2 PHASE ERROR DISTRIBUTION

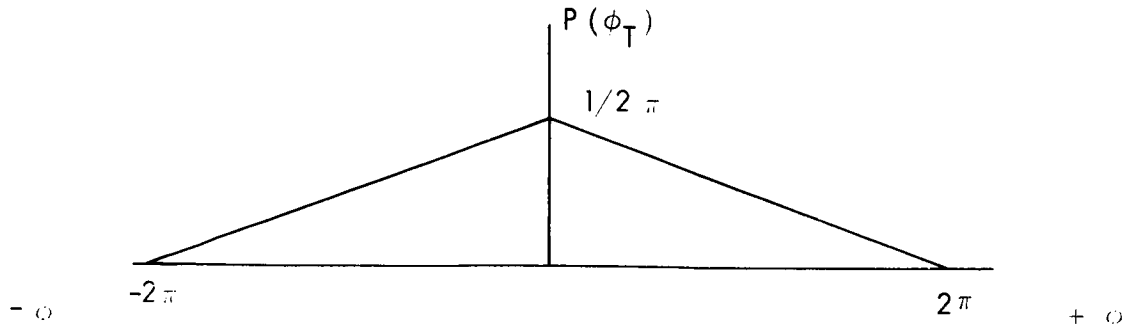

Figure 8.H-3 PHASE ERROR DENSITY FUNCTION

APPENDIX 8 I

CONVERSION OF θs INTO ATTITUDE (PART A) DEFINITIONS

Take the geocentric, equatorial, directionally fixed coordinate system X, Y, Z (unit vectors $\underline{I}$, $\underline{J}$, $\underline{K}$) as the basic reference frame. A set of axes x, y, z fixed to the vehicle are related to the inertial set as:

$$\begin{pmatrix} \underline{i} \\ \underline{j} \\ \underline{k} \end{pmatrix} = A \begin{pmatrix} \underline{I} \\ \underline{J} \\ \underline{K} \end{pmatrix} ; \quad A = \begin{pmatrix} a_{11} & a_{12} & a_{13} \\ a_{21} & a_{22} & a_{23} \\ a_{31} & a_{32} & a_{33} \end{pmatrix} \qquad (1)$$

Let $\underline{\rho}_i$ be the unit vector along the LOS (line of sight) pointing from the vehicle to the i-th STATION. And assume $\underline{\rho}_i$ in the inertial frame,

$$\underline{\rho}_i = \rho_{Xi} \underline{I} + \rho_{Yi} \underline{J} + \rho_{Zi} \underline{K} \qquad (2)$$

is known.

In the present development, for simplicity, let

$$\begin{aligned} &\text{Interferometer leg \#1 vector} = D\underline{i} \\ &\text{Interferometer leg \#2 vector} = D\underline{j} \end{aligned} \qquad (3)$$

This does not limit the generality of the development.

The phase difference measurements between the signals received at the two ends of an interferometer leg can be interpreted with reference to Figure 8 I-1.

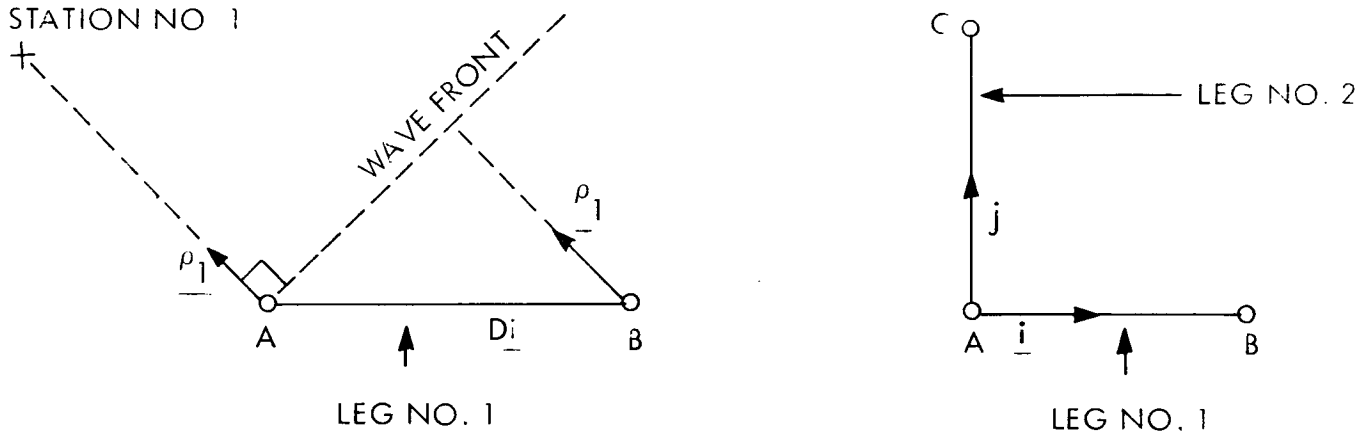

Figure 8.I-1 INTERFEROMETER ILLUMINATION

Letting

$$\Delta \phi = \phi_B - \phi_A \text{ ; or } \Delta \phi = \phi_C - \phi_A \tag{4}$$

and

$$\begin{aligned}
\Delta \phi_{1i} &= \text{measurement pertaining to Station \#1 \& Leg \#1} \\
\Delta \phi_{1j} &= \text{measurement pertaining to Station \#1 \& Leg \#2} \\
\Delta \phi_{2i} &= \text{measurement pertaining to Station \#2 \& Leg \#1} \\
\Delta \phi_{2j} &= \text{measurement pertaining to Station \#2 \& Leg \#2}
\end{aligned} \tag{5}$$

we have

$$\left.\begin{aligned}
\frac{\lambda}{2\pi D} \Delta \phi_{1i} &= \underline{\rho}_1 \cdot \underline{i} \\
\frac{\lambda}{2\pi D} \Delta \phi_{1j} &= \underline{\rho}_1 \cdot \underline{j} \\
\frac{\lambda}{2\pi D} \Delta \phi_{2i} &= \underline{\rho}_2 \cdot \underline{i} \\
\frac{\lambda}{2\pi D} \Delta \phi_{2j} &\quad \underline{\rho}_2 \cdot \underline{j}
\end{aligned}\right\} \tag{6}$$

Eq. 6 indicates that the basic interferometer measurement of $\Delta\phi$ actually gives the components of the unit LOS vectors $\underline{\rho}_1$ and $\underline{\rho}_2$ (to Stations #1 & #2) along the interferometer legs #1 & #2, which in this development are taken along the vehicle x & y axes respectively.

Let us identify as

$$\underline{\rho}_1 \cdot \underline{i} = \rho_{x1}$$
$$\underline{\rho}_1 \cdot \underline{j} = \rho_{y1}$$
$$\underline{\rho}_2 \cdot \underline{i} = \rho_{x2}$$
$$\underline{\rho}_2 \cdot \underline{j} = \rho_{y2}$$

According to Eqs. 6. These are available from measurements. Therefore, let us look upon these as having been measured. (7)

Use of the Interferometer to Sense Attitude Error

Let $\underline{\epsilon}$ be the small angle attitude error vector with components along vehicle axes x, y, z. The significance of ϵ is the following.

If, the vehicle is rotated

through the angle $\epsilon = \sqrt{\epsilon_x^2 + \epsilon_y^2 + \epsilon_z^2}$

about the axis which makes the direction cosines

$$\frac{\epsilon_x}{|\epsilon|}, \quad \frac{\epsilon_y}{|\epsilon|}, \quad \frac{\epsilon_z}{|\epsilon|}$$

with the vehicle axes; the attitude of the vehicle comes into coincidence with the desired vehicle attitude.

Note that:

(a) The components of $\underline{\epsilon}$ are not Euler angle errors

(b) The components of $\underline{\epsilon}$ can be directly used to generate torques in the correct vectorial direction to coerce the vehicle towards its desired attitude.

According to Eq. 1 the vehicle actual attitude is defined by the transformation.

$$\begin{pmatrix} \underline{i} \\ \underline{j} \\ \underline{k} \end{pmatrix} = A \begin{pmatrix} \underline{I} \\ \underline{J} \\ \underline{K} \end{pmatrix} \tag{7}$$

where A is to be determined.

Let the desired attitude be given as

$$\begin{pmatrix} \underline{i}D \\ \underline{j}D \\ \underline{k}D \end{pmatrix} = A_D \begin{pmatrix} \underline{I} \\ \underline{J} \\ \underline{K} \end{pmatrix} \tag{8}$$

where A_D is known.

From Eqs. (1) & (8)

$$\begin{pmatrix} \underline{i}D \\ \underline{j}D \\ \underline{k}D \end{pmatrix} = A_D A^{-1} \begin{pmatrix} \underline{i} \\ \underline{j} \\ \underline{k} \end{pmatrix} \tag{9}$$

$$A_D A^{-1} = E \tag{10}$$

It can be shown that, if the desired vehicle attitude can be obtained by rotating the vehicle through the small angles ϵ_x, ϵ_y, ϵ_z about the vehicle axes x, y, z respectively,

$$A_D A^{-1} = E = \begin{pmatrix} 1 & \epsilon_z & -\epsilon_y \\ -\epsilon_z & 1 & \epsilon_x \\ \epsilon_y & -\epsilon_x & 1 \end{pmatrix} \tag{11}$$

From the $\Delta\phi$ measurements (see Eqs. 6 & 7), we know the components of the unit LOS vector $\underline{\rho}_i$ along the vehicle axes x and y (i.e., we know ρ_{xi} and ρ_{yi}).

If we also know that z-axis is approximately pointing towards the earth (and not pointing the other way), as shown in Figure 8.I-2 we can write

$$\rho_{zi} = + \sqrt{1 - \left(\rho_{xi}^2 + \rho_{yi}^2\right)} \tag{12}$$

From the four ϕ measurements we have (ρ_{x1}, ρ_{y1}) and (ρ_{x2}, ρ_{y2}) and invoking (12) we can write

$$\left.\begin{aligned} \underline{\rho}_1 &= \rho_{x1}\underline{i} + \rho_{y1}\underline{j} + \rho_{z1}\underline{k} \\ \underline{\rho}_2 &= \rho_{x1}\underline{i} + \rho_{y1}\underline{j} + \rho_{z2}\underline{k} \end{aligned}\right\} \text{Measured} \tag{13}$$

and in the inertial frame

$$\left.\begin{aligned} \underline{\rho}_1 &= \rho_{x1}\underline{I} + \rho_{y2}\underline{J} + \rho_{z1}\underline{k} \\ \underline{\rho}_2 &= \rho_{x2}\underline{I} + \rho_{y2}\underline{J} + \rho_{z1}\underline{k} \end{aligned}\right\} \text{Known} \tag{14}$$

Now let us construct a right handed orthogonal set of axes out of $\underline{\rho}_1$ and $\underline{\rho}_2$ by proceeding as follows.

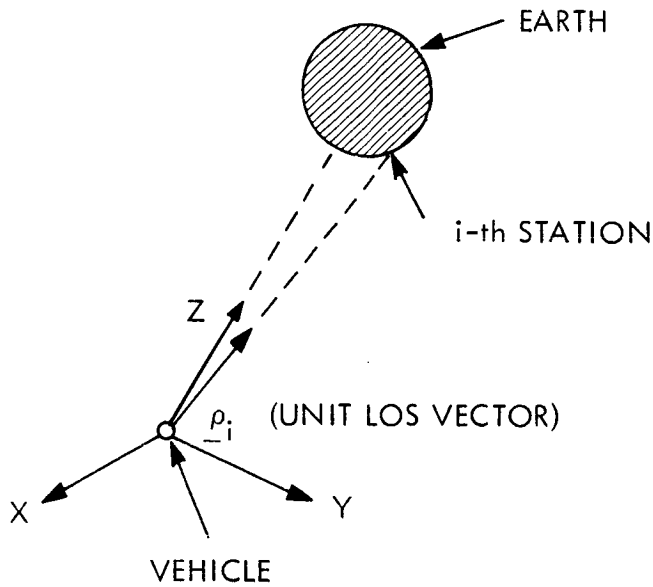

Figure 8.I-2 SPACECRAFT ORIENTATION

(a)
$$\frac{\underline{\rho}_1 \times \underline{\rho}_2}{\underline{\rho}_1 \times \underline{\rho}_2} = \underline{\rho}_{-3} \tag{15}$$

(b)
$$\underline{\rho}_3 \times \underline{\rho}_1 = \underline{\rho}_2' \tag{16}$$

The unit vectors $\underline{\rho}_1, \underline{\rho}_2', \underline{\rho}_3$ constitute a right-handed orthogonal triad.

We can express $\underline{\rho}_1, \underline{\rho}_2' \,\&\, \underline{\rho}_3$ in vehicle and inertial coordinates and write

$$\begin{pmatrix} \rho_{x1} & \rho_{y1} & \rho_{z1} \\ \rho_{x2}' & \rho_{y2}' & \rho_{z2}' \\ \rho_{x3} & \rho_{y3} & \rho_{z3} \end{pmatrix} \begin{pmatrix} \underline{i} \\ \underline{j} \\ \underline{k} \end{pmatrix} = \begin{pmatrix} \rho_{x1} & \rho_{y1} & \rho_{z1} \\ \rho_{x2}' & \rho_{y2}' & \rho_{z2}' \\ \rho_{x3} & \rho_{y3} & \rho_{z3} \end{pmatrix} \begin{pmatrix} \underline{I} \\ \underline{J} \\ \underline{K} \end{pmatrix} \tag{17}$$

where, both matrices are orthogonal.

Therefore, from Eq. 17 we have

$$\begin{pmatrix} \underline{I} \\ \underline{J} \\ \underline{K} \end{pmatrix} = \begin{pmatrix} \rho_{x1} & \rho_{x2}' & \rho_{x3} \\ \rho_{y1} & \rho_{y2}' & \rho_{y3} \\ \rho_{z1} & \rho_{z2}' & \rho_{z3} \end{pmatrix} \begin{pmatrix} \rho_{x1} & \rho_{y1} & \rho_{z1} \\ \rho_{x2}' & \rho_{y2}' & \rho_{z2}' \\ \rho_{x3} & \rho_{y3} & \rho_{z3} \end{pmatrix} \begin{pmatrix} \underline{i} \\ \underline{j} \\ \underline{k} \end{pmatrix} \tag{18}$$

where according to Eq. 1 the matrix product can be identified as A^{-1}.

Referring to Eq. 8 let in

$$\begin{pmatrix} \underline{i}_D \\ \underline{j}_D \\ \underline{k}_D \end{pmatrix} = A_D \begin{pmatrix} \underline{I} \\ \underline{J} \\ \underline{K} \end{pmatrix} \tag{19}$$

$$A_D = \begin{pmatrix} a^D_{11} & a^D_{12} & a^D_{13} \\ a^D_{21} & a^D_{22} & a^D_{23} \\ a^D_{31} & a^D_{32} & a^D_{33} \end{pmatrix} \tag{19}$$

From Eqs. (11), (18) and (19) we have

$$\begin{pmatrix} 1 & \epsilon_z & -\epsilon_y \\ -\epsilon_z & 1 & \epsilon_x \\ \epsilon_y & -\epsilon_x & 1 \end{pmatrix} = \overbrace{\underbrace{\begin{pmatrix} a^D_{11} & a^D_{12} & a^D_{13} \\ a^D_{21} & a^D_{22} & a^D_{23} \\ a^D_{31} & a^D_{32} & a^D_{33} \end{pmatrix}}_{\text{Given}}}^{A_D} \overbrace{\underbrace{\begin{pmatrix} \rho_{X1} & \rho'_{X2} & \rho_{X3} \\ \rho_{Y1} & \rho'_{Y2} & \rho_{Y3} \\ \rho_{Z1} & \rho'_{Z2} & \rho_{Z3} \end{pmatrix}}_{\text{Given}} \underbrace{\begin{pmatrix} \rho_{x1} & \rho_{y1} & \rho_{z1} \\ \rho_{x2} & \rho_{y2} & \rho_{z2} \\ \rho_{x3} & \rho_{y3} & \rho_{z3} \end{pmatrix}}_{\text{Measured}}}^{A^{-1}} \tag{20}$$

From Eq. 20 the components of

$$\underline{\epsilon} = \begin{pmatrix} \epsilon_x \\ \epsilon_y \\ \epsilon_z \end{pmatrix}$$

can be computed. For instance, for ϵ_z we have

$$\epsilon_z = \begin{pmatrix} a^D_{11} & a^D_{12} & a^D_{13} \end{pmatrix} \begin{pmatrix} \rho_{X1} & \rho'_{X2} & \rho_{X3} \\ \rho_{Y1} & \rho'_{Y2} & \rho_{Y3} \\ \rho_{Z1} & \rho'_{Z2} & \rho_{Z3} \end{pmatrix} \begin{pmatrix} \rho_{y1} \\ \rho'_{y2} \\ \rho_{y3} \end{pmatrix} \tag{21}$$

From the attitude error components ϵ_x, ϵ_y, ϵ_z, torques are computed to null the attitude errors.

Use of Interferometer as "Small Attitude Error" Sensor (Part B)

Let:

$\underline{\rho}_i$ = unit LOS vector from the vehicle to the $_i$th station.

x, y, z (unit vector $\underline{i}$, $\underline{j}$, $\underline{k}$) = axes fixed to the vehicle

x^D, y^D, z^D (unit vectors $\underline{i}^D$, $\underline{j}^D$, $\underline{k}^D$) = vehicle axes for the desired attitude.

Expressing $\underline{\rho}_i$ in actual and desired vehicle coordinates we have

$$\underline{\rho}_i = \begin{pmatrix} \rho_{ix}^D & \rho_{iy}^D & \rho_{iz}^D \end{pmatrix} \begin{pmatrix} \underline{i}^D \\ \underline{j}^D \\ \underline{k}^D \end{pmatrix} = \begin{pmatrix} \rho_{ix} & \rho_{iy} & \rho_{iz} \end{pmatrix} \begin{pmatrix} \underline{i} \\ \underline{j} \\ \underline{k} \end{pmatrix} \tag{22}$$

where for small attitude errors it can be shown that

$$\begin{pmatrix} i^D \\ j^D \\ k^D \end{pmatrix} = \begin{pmatrix} 1 & \epsilon_z & -\epsilon_y \\ -\epsilon_z & 1 & \epsilon_x \\ \epsilon_y & -\epsilon_x & 1 \end{pmatrix} \begin{pmatrix} \underline{i} \\ \underline{j} \\ \underline{k} \end{pmatrix} \tag{23}$$

Substituting 23 into 22 and letting

$$\rho_{ix} - \rho^{D}_{ix} = \Delta\rho_{ix}$$
$$\rho_{iy} - \rho^{D}_{iy} = \Delta\rho_{iy} \qquad (24)$$
$$\underbrace{\rho_{iz}}_{\text{Components of } \underline{\rho}_i \text{ actual vehicle}} - \rho^{D}_{iy} = \Delta\rho_{iz}$$

(components of ρ_{-i} along the desired vehicle axes.)

We have

$$\Delta\rho_{ix} = -\rho^{D}_{iy}\,\epsilon_z + \rho^{D}_{iz}\,\epsilon_y \qquad (25)$$
$$\Delta\rho_{iy} = \rho^{D}_{ix}\,\epsilon_z - \rho^{D}_{iz}\,\epsilon_x$$

A possible commbination of measurements from stations #1 and #2 would give

$$\begin{matrix}\Delta\rho_{ix}\\ \Delta\rho_{iy}\\ \Delta\rho_{2x}\end{matrix} = \begin{pmatrix} 0 & \rho^{D}_{iz} & -\rho^{D}_{iyD} \\ -\rho_{iz} & 0 & \rho^{D}_{ix} \\ 0 & \rho^{D}_{2z} & -\rho^{D}_{2y} \end{pmatrix} \begin{pmatrix} \epsilon_x \\ \epsilon_y \\ \epsilon_z \end{pmatrix} \qquad (26)$$

The solution of Eq. 26 gives

$$\epsilon_z = \frac{\rho^D_{iz}\,\Delta\rho_{x2} - \rho^D_{2z}\,\Delta\rho_{ix}}{\rho^D_{iy}\,\rho^D_{2z} - \rho^D_{2y}\,\rho^D_{iz}}$$

$$\epsilon_y = \left(\Delta\rho_{ix} + \rho^D_{iy}\,\epsilon_z\right) \Big/ \rho^D_{iz} \qquad (27)$$

$$\epsilon_x = \left(\rho^D_{ix}\,\epsilon_z - \Delta\rho_{iy}\right) \Big/ \rho^D_{iz}$$

These are the equations that a computing device has to solve to obtain ϵ_x, ϵ_y, ϵ_z. To do this it is necessary to transmit to the vehicle from the ground the following:

$$\rho^D_{1x}, \quad \rho^D_{1y}, \quad \rho^D_{2x}, \quad \rho^D_{2y}$$

or $\Delta\phi^D_{1j}$, $\Delta\phi^D_{1j}$, $\Delta\phi^D_{2i}$, $\Delta\phi^D_{2j}$

where subscript D on $\Delta\phi$ indicates the phase measurement that would have obtained if the attitude error had been zero.

The interferometer then measures, for instance,

$$\left(\underset{\text{actual}}{\Delta\varphi_{ij}} - \underset{\text{desired}}{\Delta\varphi_{ij}^{D}}\right)$$

from which and similar measurements it is necessary to compute

$$\begin{aligned}
\Delta\rho_{ix} &= \left(\Delta\varphi_{ij} - \Delta\varphi_{ij}^{D}\right) \frac{2\pi D}{\lambda} \\
\Delta\rho_{iy} &= \left(\Delta\varphi_{ij} - \Delta\varphi_{ij}^{D}\right) \frac{2\pi D}{\lambda} \\
\Delta\rho_{2x} &= \left(\Delta\varphi_{2i} - \Delta\varphi_{2j}^{D}\right) \frac{2\pi D}{\lambda} \\
\Delta\rho_{2y} &= \left(\Delta\varphi_{2j} - \Delta\varphi_{2j}\right) \frac{2\pi D}{\lambda}
\end{aligned} \tag{28}$$

Thus, to compute attitude errors ϵ_x, ϵ_y, ϵ_z, the interferometer performs the measurements $\Delta\varphi_{ij}$ and the computing device has to perform the operations indicated by Eqs. 28 followed by Eqs. 27.

Note.

The procedure described here works only for the small attitude error case. The method described in Part A, even though not so indicated, would work equally well for any attitude condition.

For the general case, the matrix $\begin{pmatrix} 1 & \epsilon_z & -\epsilon_y \\ -\epsilon_z & 1 & \epsilon_x \\ \epsilon_y & -\epsilon_x & 1 \end{pmatrix}$

in Eq. 20 of Part A has to be replaced by the matrix

$$\begin{matrix} \cos\psi \cos\Theta & \sin\psi \cos\Theta & -\sin\Theta \\ (-\sin\psi \cos\Theta + \cos\psi \sin\Theta \sin\bar{\phi}) & (\cos\psi \cos\Theta + \sin\psi\Theta \sin\bar{\phi}) & (\cos\Theta \sin\bar{\phi}) \\ (\sin\psi \sin\phi + \cos \sin\Theta\cos\bar{\phi} & (-\cos\psi \sin\bar{\phi} + \sin\psi \sin\Theta \cos\phi) & (\cos\Theta \cos\bar{\phi}) \end{matrix}$$

and the attitude errors $\bar{\phi}$, Θ, ψ (Euler angles) are determined.

APPENDIX 8J

LIMITATION OF RANGE AND RANGE RATE CAPABILITY

The following is an analysis of why range. range rate navigation system is not capable of meeting system pointing requirements.

Basically the problem is as shown in Figure 8J-1. The object is to determine the error $\Delta \xi$ assuming R is measured with probable error ΔR, R_e and ρ_s are known with probable errors ΔR_e and $\Delta \rho_s$ respectively.

From the law of cosines

$$R^2 = R_e^2 + \rho_s^2 - 2\rho_s R_e \cos\xi \tag{1}$$

Solving for $\cos\xi$ yields

$$\cos\xi = \frac{R_e^2 + \rho_s^2 - R^2}{2R_e\rho_s} \tag{2}$$

The effect of errors in R, ρ_s and R_e is given

by

$$\Delta\xi = \frac{\partial\xi}{\partial R}\Delta R + \frac{\partial\xi}{\partial\rho_s}\Delta\rho_s + \frac{\partial\xi}{\partial R_e}\Delta R_e \tag{3}$$

where

$$\frac{\partial\xi}{\partial R} = \frac{1}{R_e\sin\xi}\left[\frac{R}{\rho_s}\right]$$

$$\frac{\partial\xi}{\partial\rho_s} = \frac{1}{R_e\sin\xi}\left[\frac{R_e\cos\xi}{2\rho_s} - 1\right]$$

$$\frac{\partial\xi}{\partial R_e} = \frac{R_e}{\rho_s}\frac{\partial\xi}{\partial\rho_s}$$

Thus

$$\Delta\xi = \frac{1}{R_e\sin\xi}\left[\frac{R}{\rho_s}\Delta R + \left(\frac{R_e\cos\xi}{2\rho_s} - 1\right)\left(\Delta\rho_s + \frac{R_e}{\rho_s}\Delta R_e\right)\right] \tag{4}$$

The nominal values are

$R = 35.7$ km

$R_e = 6.38$ km

$\rho_s = 42.0$ km

$\xi = 39.8^\circ$

leading to

$$\Delta\xi = .245\left[.85\,\Delta R - \Delta\rho_s - .15\,\Delta R_e\right] \tag{5}$$

The variance is given by

$$\sigma_\xi^2 = (.245)^2 \left[(.85\,\sigma_R)^2 + \sigma_{\rho_s}^2 + (.15\,\sigma_{Re})^2 \right] \tag{6}$$

and it has been assumed that all three errors are uncorrelated.

The following error model has been given or was assumed.

σ_R = .015 km (15m)

σ_{Re} = .01 km (10m)

σ_{ρ_s} = .03 km (30m)

Applying these errors to equation 6 yields

σ_ξ = $.8 \times 10^{-2}$ rad

σ_ξ = .46 degrees

An investigation of the error contributions would show that the error in ρ_s is 90% of the contributor to σ_ξ. It is unlikely that σ_{ρ_s} will ever be less than 30 meters, all things considered. Therefore, the 0.46° error would seem to be a severe limitation on the RR System.

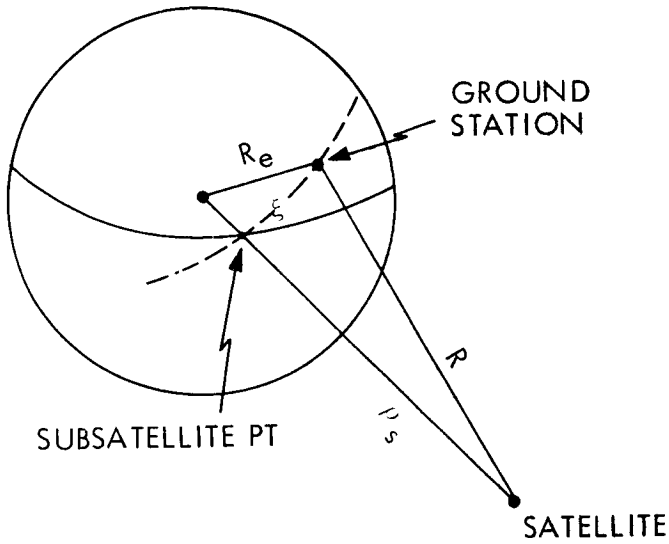

Figure 8. J-1 GEOMETRY FOR RANGE AND RANGE RATE ANALYSIS

9.0 TELEMETRY AND COMMAND SUBSYSTEMS

This section discusses the design of the onboard instrumentation system; the instrumentation is comprised of the telemetry system, the command system and the range and range rate (R&RR) transponder.

First the data transmission requirements are summarized. Based on these requirements a model of the data flow is derived. This model serves as the basis for designing the onboard instrumentation system, and the definition of interfaces.

This is followed by sections containing detailed system analyses and designs for the telemetry system, the command system and the R&RR transponder. In each of these sections, system configurations to meet the requirements are developed. Included are transmission link calculations relating the transmitter powers, antenna gains, and receiver characteristics. The design sections are concluded by estimates of the onboard equipment weight, size and power requirements, and summaries of equipment implementation.

Finally, the ground station equipment requirements are reviewed. Typical equipment to meet the interface requirements are discussed and, where possible, identified.

Command and telemetry signal catalogs and some detailed calculations are presented in Appendices 9A to 9G.

9.1 DATA FLOW

9.1.1 Definition

This section discusses the detailed data flow necessary to operate the ATS-4 Satellite System and perform the experimentation. The gross data flow was discussed in Section 2, Systems Analysis. Here the data transmission requirements between the satellite and ground stations are analyzed in detail. This enables the definition of space/ground interfaces.

Furthermore, the data flow onboard the satellite is analyzed. This permits identification of interfaces between the spacecraft subsystems. To complete an overall analysis, the flow requirements at the ground stations are also discussed.

9.1.2 Requirements

For analysis of the ATS-4 data transmission requirements, it was necessary for all team members to summarize their subsystem data requirements. To facilitate this process, a questionnaire was completed by each design group in a format suited to estimate the total requirements. A copy of this questionnaire is reproduced in Appendix 9G.

From the information received on the questionnaire, telemetry and command signal catalogs were compiled. These catalogs list the transmission signals, and describe them in sufficient detail to permit a system design. The Telemetry Signal Catalog is given in Appendix 9F; the Command Signal Catalog in Appendix 9E. These two catalogs serve as a basis for the design of the onboard telemetry and command systems.

9.1.3 Model of the Data Flow

Figure 9.1-1 depicts the data flow aboard the spacecraft and also defines the radio transmission interfaces to the ground system. Shown in the figure are the spacecraft subsystems; the instrumentation subsystem is shown as three blocks, the R & RR transponder, the telemetry system and the command system. The connecting lines between the blocks show the data flow in terms of the telemetry signal and command catalogs. A block for secondary experiments is also shown, but since they are presently not defined, no interconnections to the instrumentation subsystem are shown.

The radio transmission nominal frequency allocations and assoicated functions are as follows:

136 MHz:	Telemetry
148 MHz:	Commands
1705/2271 MHz:	R & RR Tracking
100 MHz 800 MHz 2.3 GHz 7.3 GHz	Satellite transmission, antenna experiments
1.7 GHz 2.1 GHz 8 GHz	Ground transmission, antenna experiments
8 GHz:	Interferometer experiment illumination

Figure 9.1-2 shows the essential blocks of a typical ATS-4 ground station. The top row are the receivers and transmitters required to interface the spacecraft.

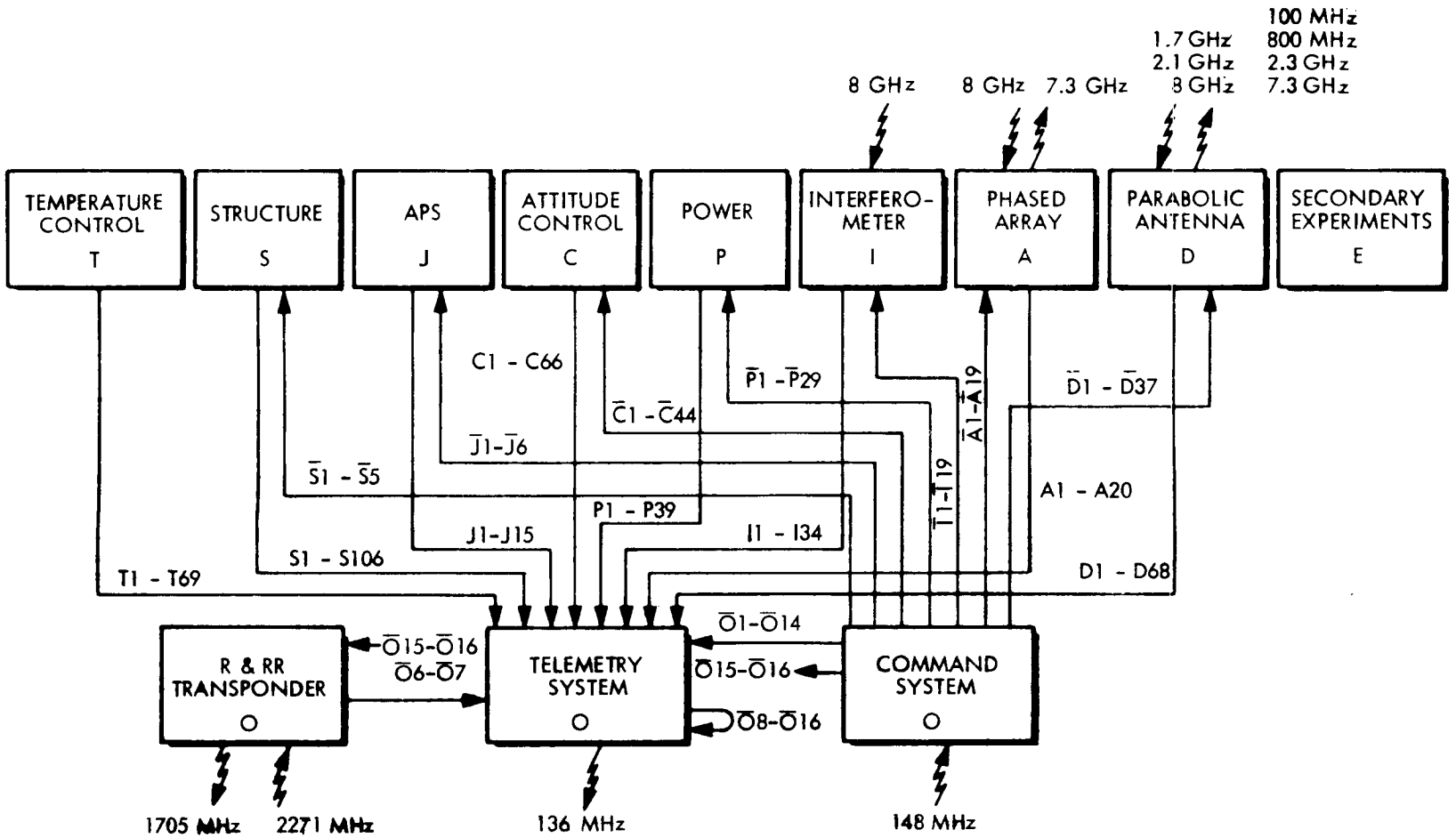

Figure 9.1-1 ONBOARD SYSTEM DATA FLOW; INTERFACES TO GROUND EQUIPMENT

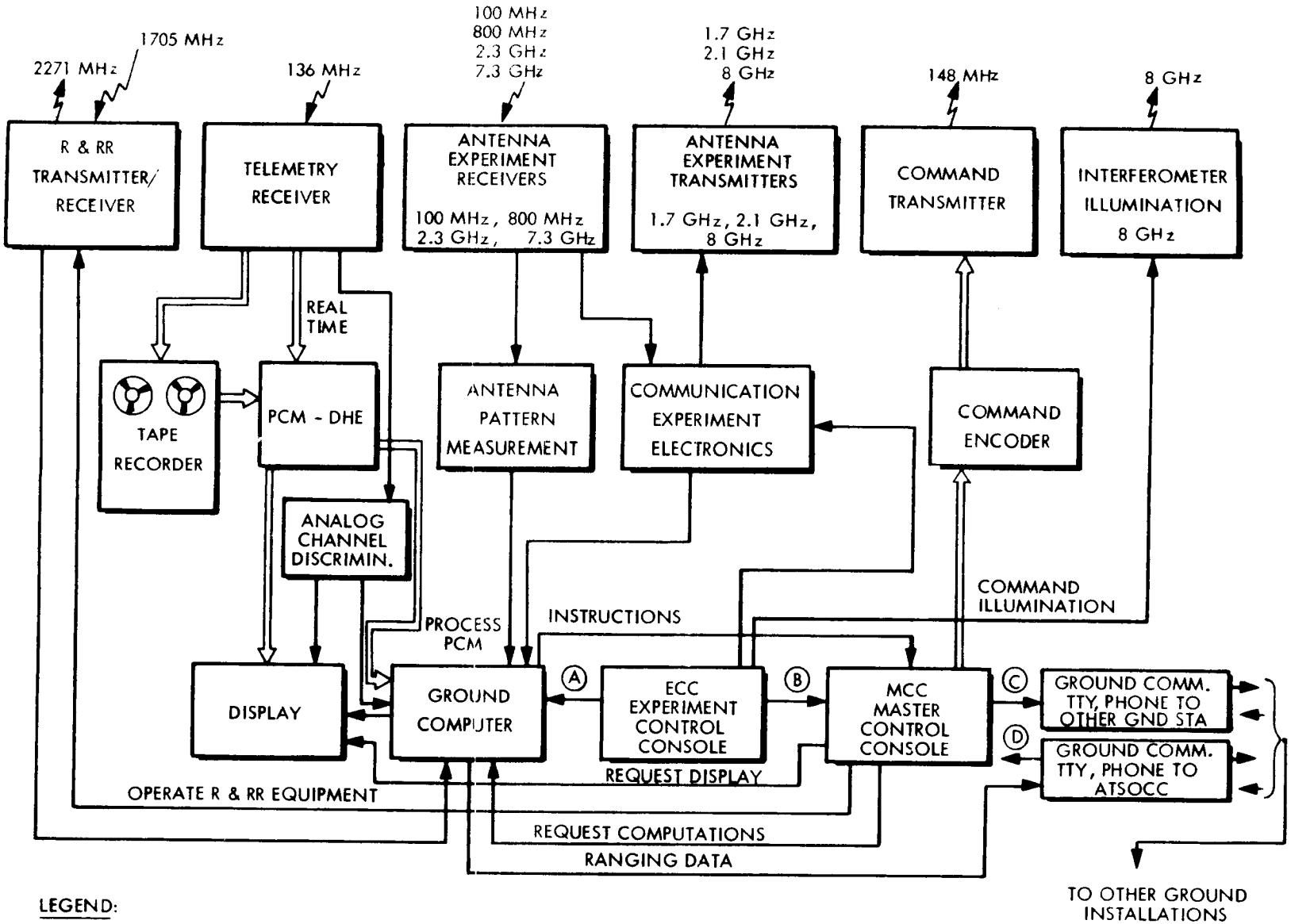

Figure 9.1-2 GROUND STATION DATA FLOW; INTERFACES TO SPACECRAFT AND OTHER GROUND STATIONS

The R & RR (Range and Range Rate) equipment interfaces the MCC (Master Control Console) from where ranging is initiated. The data output from the R & RR equipment interfaces the ground computer which reduces the data to a form suitable for transmission to ATSOCC, (ATS Operations Control Center) where the actual orbit computation takes place.

The telemetry receiver accepts the telemetry transmissions. Data handling equipment separates the PCM from the analog channels. The telemetry signals are recorded, but they can also interface the PCM-DHE (PCM Data Handling Equipment) directly. This direct interface is provided to permit real-time display of selected channels. The receiver also interfaces analog channel discriminators where the FM/PM telemetry channels are demodulated. The demodulated channels can be displayed or processed by the ground computer for further use or for transmission to ATSOCC.

The antenna experiment receivers shown in one block are actually four receivers operating at the indicated frequencies. They are connected to the communication experiment electronics where signals are suitably demodulated, or to the antenna pattern measurement equipment which is used to determine antenna patterns.

The three antenna experiment transmitters, shown in one block, operate at the indicated frequencies. The transmitters interface the communications experiment electronics.

The command transmitter operates at a nominal frequency of 148 MHz. It accepts the properly formatted commands and transmits them to the spacecraft.

The interferometer illumination operates at a nominal

frequency of 8 GHz. The transmission is controlled from the ECC (Experiment Control Console).

Another set of interfaces exists with the other ATS-4 ground stations and ATSOCC. For this purpose the ground station is equipped with teletypewriter transmission and receiving equipment. Telephones are also used; appropriate circuits are provided through NASCOM.

Also indicated in Figure 9.1-2 is the data flow between the control equipment and the ground computer. The MCC controls most of the ground operation. From the MCC the following operations can be controlled:

Display

Ground computation

Tracking through the R & RR

Ground communication

Command transmission

The MCC can also request instructions from the computer, which are transmitted to the spacecraft through the command link.

In order to simplify the operations of the MCC, the ECC (Experiment Control Console) is provided. This console controls the spacecraft experimentation. It interfaces the ground computer and can request attitude data and calculations. The commands are controlled through the MCC and consequently the ECC must interface the MCC to request commands for experimentation. The ECC directly controls the experiment electronics and the interferometer illumination transmitter.

9.2 TELEMETRY SYSTEM

9.2.1 Data Handling Requirements

The ATS-4 onboard telemetry system will be required to handle three kinds of data: spacecraft subsystem housekeeping data, experiment equipment housekeeping data, and experiment data. The handling process will include continuous monitoring and periodic sampling of sensors, data conditioning, data conversion and data formatting. Data from the following subsystems is to be accommodated.

Auxiliary Propulsion

Spacecraft Control System

Structures

Parabolic Antenna

Phased Array

Interferometer

Power

Temperature

Instrumentation

The sensor outputs from these subsystems occur in either analog, discrete or binary form. Therefore, it is necessary to design the onboard telemetry system to be flexible enough to permit the handling of all categories of data. In Appendix 9F, the Telemetry Signal Catalog identifies the parameters to be telemetered from each of the subsystems. Included for each sampled parameter is its sampling rate, duration of sampling time and accuracy requirements. It should be noted that all accuracies expressed in a percentage indicate that the sensor output is in analog form, while those

accuracies expressed in "bits" indicate that the sensor output is digital or a discrete.

9.2.2 Data Handling System Design

In order to satisfy the telemetry data requirements of Section 9.1, the onboard data handling system will have to employ both analog and digital commutation, along with continuous data monitoring. Table 9.2-1 summarizes the data sensor output requirements by breaking them down into analog, discrete and binary categories. The table also provides a further breakdown of the required sampling rates for each data category. In addition to those sensor outputs listed in tabular form, there is also a requirement to monitor several other data sources. These sources are:

- Four Structure Subsystem analog vibration outputs which must be monitored continuously from lift-off through deployment;
- One hundres discrete data sources, associated with the Structure Subsystem, which must be monitored at a rate of 1 sample/source/sec during the deployment phase (approximately 30 minutes);
- One binary output of 40 bits/sample at a sampling rate of 16 samples/sec during the deployment phase.

These "additional" data sources were not included in Table 9.2-1 because they do not have to be monitored during the entire mission. If they were included, they would greatly increase the data handling system and data transmission system design requirements. This would be undesirable considering the small portion of the mission duration in which the signals will be required.

Table 9.2-1

Summary of Sensor Outputs and Sampling Rates

Continuous Sampling Rate (Required) \ Sensor Outputs	Analog	Discrete	Binary
3/sec	1	4	1
1/sec	34	12	21
1/[illegible] sec	93	15	0
1/64 sec	104	2	0
1/4096 sec	4	37	2
TOTAL	236	70	24

Additional Data Requirements:

(1) 4 analog vibration outputs, continuous from lift-off until deployment is complete.

(2) 100 discrete outputs monitored at a 1 sample/sec rate (each) during deployment.

(3) 1 binary output of 40 bits/sample at a sampling rate of 16 samples/sec during deployment.

A review of the accuracy requirements for the analog sensor outputs indicates that 1% is the most stringent requirement. If we convert all analog data into digital form and provide 1% accuracy, we will have to use a 7 bit binary code for each sample. (7 bit accuracy provides an accuracy of approximately 0.8%). However, for the purpose of this study we will assume an 8 bit analog-to-digital conversion so that the system will have the capability to handle more stringent accuracy requirements if existing requirements are raised or if additional sensors with greater accuracy requirements are included later. (An 8 bit word will also ease digital data handling.) In order to insure that single bit errors are not added to the digital word representing each analog quantity, a parity bit will be added to each 8 data bits (each word). To ensure that a "data" word will not contain all ZEROS, odd parity will be employed. This will make it impossible to transmit a serial pulse train having a 64 bit segment occurring without a transition.

In order to efficiently utilize data words, the onboard data handling system will take discrete data outputs, convert them into a single digital bit, and then combine up to 8 discrete sensor outputs into a single data word (8bits per word). Binary data will be reformatted to also fit into an 8 bit word format. Odd parity will be employed for all data words containing discrete or binary data. Thus, the word format for all sampled data sensor outputs will be uniform (i.e., the system will employ a fixed word length.)

The sensor output requirements summarized in Table 9.2-1, were ordered into commutation groupings as shown in Table 9.2-2. A main sampling rate of 1 channel/sec was selected based on the actual data requirements. Working from this basic sampling rate, and maintaining binary factoring to derive sub-commutation and super-commutator configurations, a basic commutation scheme was derived. Table 9.2-2, shows that four commutator sampling rates were selected; 1 channel/sec (included within this rate is a super-commutated rate of 8 channels/sec), 1 channel/8sec., 1 channel/64 seconds, and 1 channel/4096 seconds. In order to conform to these sampling rates, the main commutator was allotted 128 data channels which are sampled at a frame rate of 128 channels/sec (i.e., each channel is sampled once per sec). To provide the next group of data channels sampling rate of 1 channel/ per 8 seconds, 16 sub-commutators are employed which are sampled at a frame rate of 8 channels per 8 seconds (i.e., each channel will be sampled once every 8 seconds). The next group of data sensors requires sampling at a rate of once per 64 seconds and therefore two 64 channel sub-sub-commutators are employed with each having a frame rate of 64 channels per 64 seconds. The remaining data sensors, those with a sampling rate of 1 per 4096 seconds, are assigned to a 32 channel sub-sub-sub-commutator with a frame rate of 1 channel per 128 seconds. Table 9.2-2 also presents a composite picture of the channel requirements for each of the commutators. For example, the main commutator is shown to accomodate the required 42 analog channels (34 channels at one sample/second and 8 channels, representing the output of a single sensor, at one sample per second); two channels containing discrete data from 16 sensors and 29 binary data channels (21 channels at one sample per second and 8 channels, representing the outputs of one

Commutator Sampling Rate	Analog Channels	Discrete Channels (8 per channel)	Binary Channels	Sync & Sub-Commutator Channels	Number of Channels Available	Present Channel Requirements	Spare Channels Available
Main Commutator 128 Channels @ 128 ch/sec (3 @ 8 x Supercom)	12 34+1(8)	2 (16 discretes)	29 21+1(8)	18	128	91	37
16 Sub Commutators 128 Channels (16 x 8 ch.) @ 1 ch/sec	93	2 (15 discretes)	0	18	128	113	15
2 Sub-Sub Commutators 128 Channels (2 x 64 ch.) @ 1 ch/sec	104	1 (2 discretes)	0	2	128	107	21
1 Sub-Sub-Sub Commutator 32 Channels @ 1 ch/128 sec	4	5 (37 discretes)	2	1	32	12	20
Total Channels	243	10 (70 Discretes)	31	39	416	323	93

Total Commutator Sampled Sensors = 330

Analog & Digital Commutator Channel Requirements

Table 9.2-2

digital sensor, sampled at one sample per second). In addition to the analog, digital and discrete data channels, the main commutator will have to provide two channels for frame synchronization and sixteen channels for sub-commutator inputs. Therefore, the main commutator must accomodate a minimum of 91 channels to meet the basic requirements. The system will be designed with a main commutator having 128 channels and, therefore, 37 channels will be available for future system growth.

Table 9.2-2 presents a similar type of breakdown, as described for the main commutator, for each of the remaining commutators. The entire commutation scheme can accomodate up to 416 channels, however, present requirements are for 323 channels for data, including synchronization and sub and super-commutation; this represents data from 330 sensor outputs. The system has been over-designed by almost 25% to allow for future growth.

Figure 9.2-1 presents a basic block configuration of how data commutation would be performed. Appendix 9A shows where each one of the sensor outputs has been assigned a data channel in the various commutators. In addition, synchronization channels, commutation channels, and spare channels have also been identified. Presently, two synchronization channels have been allotted to the main commutator and one synchronization channel has been allotted to each sub-commutator. If these assignments prove to be inadequate, ample space is available to permit additional assignments of channels. It will be explained in detail later that the commutation system will be capable of sampling specific commutators at a faster rate than usual while omitting the sampling of other commutators; with a basic premise

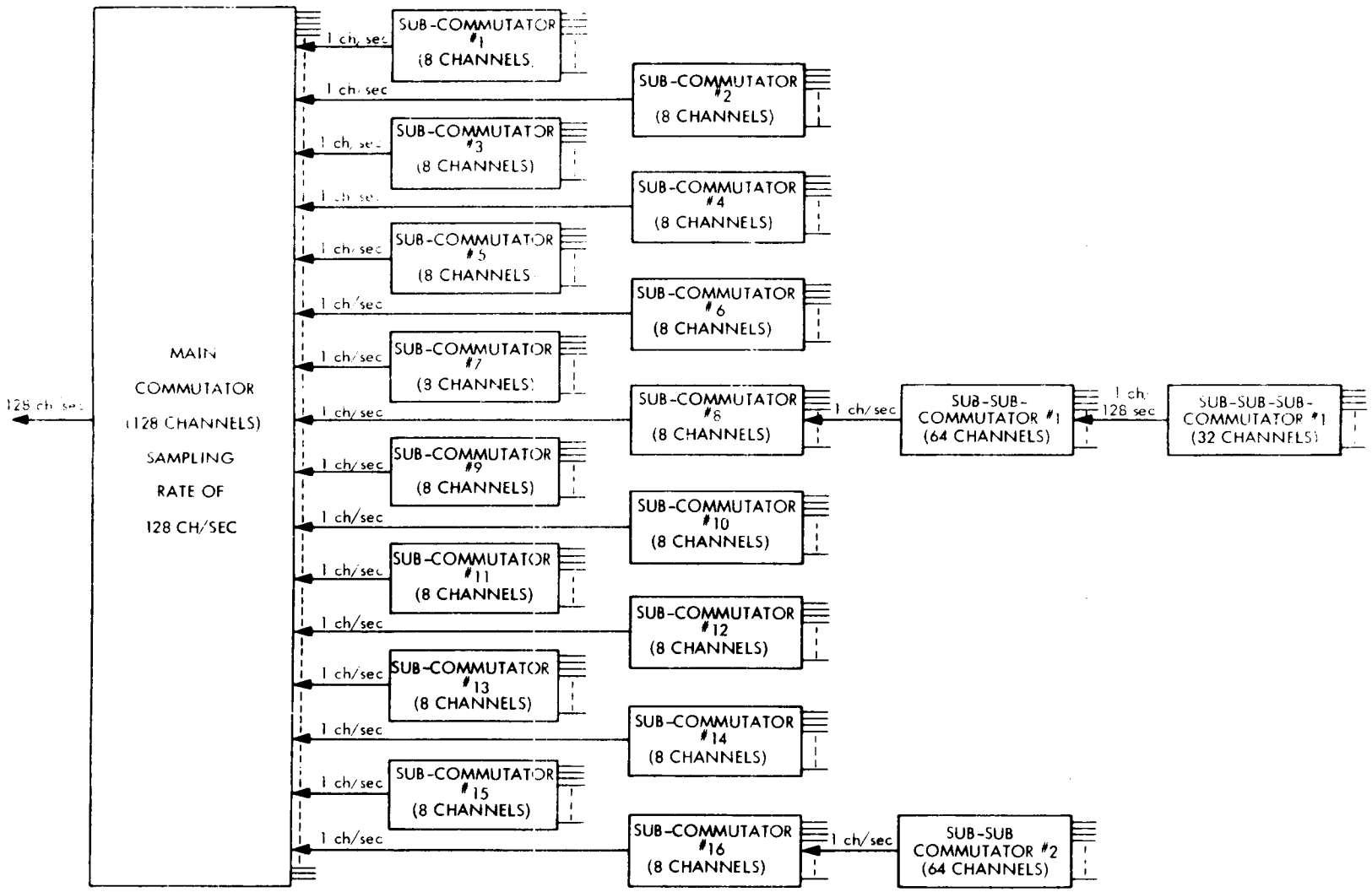

FIGURE 9.2-1 BASIC COMMUTATION CONFIGURATION

being satisfied of not exceeding the maximum data transmission rate while in a "fast sampling mode " Because of this option, there may be a requirement for a change in frame synchronization pattern and/or length. However, for the purpose of this study only the basic system synchronization is addressed and details of optional sampling modes and synchronization are omitted.

In discussing Figure 9.2-1 it should be understood that although the commutation system can accommodate 376 data channels (i.e., 416 total channels less synchronization and sub-commutation channels), in reality 376 sensor outputs are not physically connected to the commutators. Only the analog inputs (243 channels) are connected to the commutators shown in Figure 9.2-1. The discrete and digital sensor outputs are sampled by their own commutation system and data words are assembled so that the time slots (shown in Appendix 9A) for these channels are filled by these data words. Actually the assignment of data sensors to the Basic Commutation Configuration corresponds to a "time-line" for a serial data train. When a "blank" data channel is sampled, a constant voltage is present. This voltage is handled by the A/D converter in the same manner as an analog data channel, however, when the data is presented to the Word Assembler a digital or discrete word is read in over the "blank" word thus destroying the "blank" word (which is useless anyway) and inserting a real data word in its place. Thus for every digital or discrete word inserted into the PCM data train an analog word slot is lost. This loss is compensated for by assigning proper channel allocations and sampling rates to each commutator channel.

9.2.3 Data Handling System Configuration

The block diagram of the onboard data handling system is shown in Figure 9.2-2. The block for the Basic Commutator Configuration has been discussed previously in the Data Handling System Design section, however, a few additional points will be included here. The Basic Commutator Configuration is fundamentally an analog commutator. It is designed to accomodate the multiplicity of signal types set forth in the requirements list and will provide flexibility in channel capacity commensurate with a variety of mission requirements. Therefore, the design will accommodate prime channel sampling for high level or low level input gating with buffer amplifiers, low level inputs with either channel amplifiers or a wideband post amplifier, and sub-commutation circuitry containing the circuits listed above plus sub-commutation format matrix circuits for gate selection. Gate selection within the main commutator is accomplished by individual pulse lines from the programmer. The sub-commutators, cascaded onto the main commutator, receive selection pulses from the programmer and from other subcommutators. The gates are activated by selection pulses from frequency division matrix segments within the subcommutators. The output of the analog commutators is a serial PAM wavetrain. This wavetrain is fed into an A/D converter.

The conversion process to be employed by the A/D converter is the "half-split sampling method" or "successive approximation method". The A/D converter will provide for an eight bit digital representation of an analog quantity, (i.e., the quantization error will be approximately 0.4%). The encoding process begins with the receipt of a control

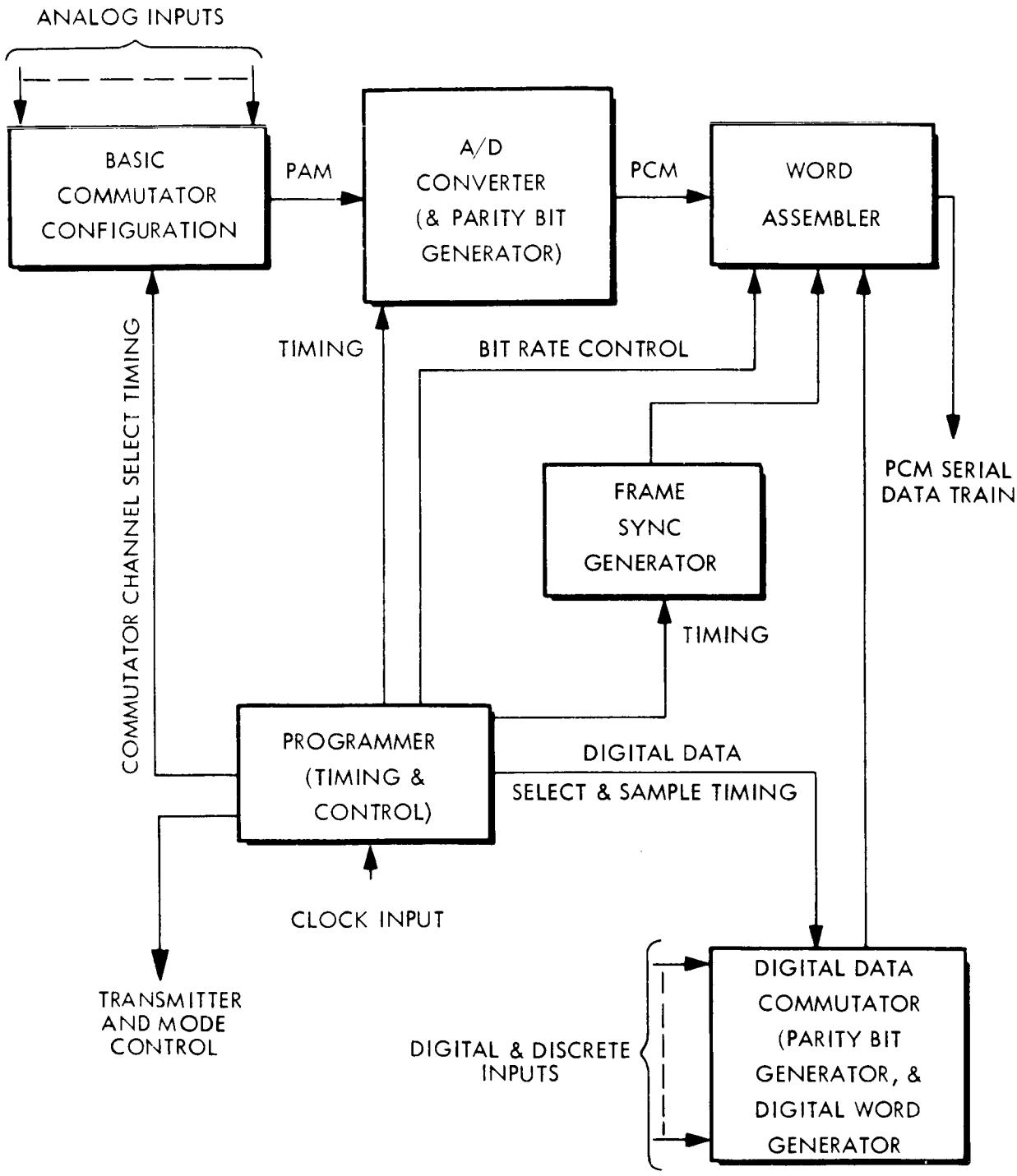

FIGURE 9.2-2 DATA HANDLING SYSTEM CONFIGURATION

pulse from the Programmer. A high speed asynchronous oscillator is enabled and at the same time the eight output register switches are reset to the zero state. The oscillator output is counted and decoded to produce eight timing pulses (2^7 through 2^0). The 2^7 pulse sets the most significant bit register switch, applies a precision voltage to one leg of a ladder network and produces an analog voltage equivalent to one-half the full scale analog input voltage. The output of the ladder network is applied to one input of a comparator for comparison with the input voltage. If the input voltage is less than the ladder network output voltage, the 2^7 register switch is reset. If the input voltage is greater than the ladder output voltage, the 2^7 register switch remains set. The next decoded pulse (2^6) sets the 2^6 register switch and produces an analog voltage equivalent to one-quarter the full-scale value of the analog input voltage. The same comparison is followed, bit-by-bit, until the decision is made to reset or not to reset the 2^0 register switch. At this time, the encoding process is completed; the ladder network output is equivalent to the analog input voltage and the status of the individual register switches are the binary equivalent of the input analog voltage. Since the timing and control logic of the programmer controls the start time of the A/D converter and also produces timing pulses to synchronize sampling of the commutators, each time slot is maintained just as it was at the output of the main commutator. However, each time slot is now comprised of eight digital bits of information which are equivalent to the analog voltage that formerly occupied the time slot. After the A/D process has been completed, the eight bit digital word is passed through a parity generator. The parity generator counts the number of ONES in each word and the "result" is fed to the

Word Assembler during the "parity bit time." If the parity generator counts an odd number of ONES in the eight bit word then the parity bit is a ZERO; if it counts an even number of ONES then the parity bit is a ONE.

The Digital Data Commutator (DDC), shown in Figure 9.2-2, handles digital and discrete data inputs in much the same manner as analog data was handled. The sampling rates available for digital and discrete data are the same as those identified previously in the Basic Commutator Configuration. The Digital Data Commutator block performs data channel multiplexing, word generation and parity bit generation for each data word. Whenever discrete signals are used as monitoring functions, the DDC groups up to eight of these inputs together to form one data word (since each bi-level set requires only one bit). Therefore, whenever a time slot is assigned for discrete data, up to eight discrete data inputs can be associated with that single time slot. Whenever digital data inputs of a given bit length are to be monitored, the DDC handles the data in eight bit bytes. If the digital data word length is less than eight bits, then the remaining bits can be left blank or, if desired, discrete data inputs could be inserted to make up a complete eight bit word. If the digital word length is greater than eight bits then more than one data word will be required to accommodate it. Therefore, an additional time slot will have to be reserved for each eight bit segment of a digital word whose length exceeds eight bits (e.g., if a digital word is 12 bits long, then one and one-half data words will be required and two time slots reserved for sampling). Each eight bit word, whether it be composed of discrete inputs, digital inputs or a mix of both types of inputs, will have a parity bit associated with it. The parity generation process will be similar to that

previously described for A/D converted data. In addition to the normal sampling rates identified for analog and digital data channels, the onboard data handling system will have an optional mode of operation whereby any commutator can be operated in a "fast sampling mode." A "fast sampling mode" is defined to mean that instead of sampling all commutators at the normal sampling rate, only one commutator (or only a specific group of commutators) is sampled but at a rate faster than its normal sampling rate. The limiting factor in determining the maximum commutator sampling rate is the "fast sampling mode" commutation rate which cannot exceed the basic main frame commutation rate. Actually it would be possible to employ the dwell mode on a single channel input if desired. So far, no operational requirement for this type of operation has been identified.

Because a serial data train comprised only of analog and digital data words would be useless upon receipt at the ground station, a synchronization pattern generator is required to provide synchronization words for insertion into the data train. Synchronization words will be used at the start of each commutation frame. The Frame Synchronization Generator will provide different synchronization words for each commutator. The patterns for these words will be selected to be optimum for the 9 bit word length of this system. No attempt will be made at this time to select the patterns for frame synchronization, however, much information is available in this area.[1][2]

The Word Assembler consists of a nine bit buffer storage register, a read-out timer, and input-output gating circuitry. The buffer storage register provides for sampling and storage of time varying digital

inputs. This register also accepts continuous parallel inputs from the A/D converter and reads synchronization and digital word inputs in broadside. The type of word selected is determined by supplying the Word Assembler with a synchronization or digital command when it is desired to insert either a synchronization or digital word into the message frame. Because the input from the A/D converter is continuous, "worthless data" (i.e., data associated with a blank time slot) is replaced by either a synchronization word or a digital word. The output serial PCM data train is formed by sequentially reading out the information stored in the buffer register with staggered parallel pulses furnished by the read-out timer. This information appears on parallel lines and is mixed in an OR gate to form the serial PCM output. In addition to reading out the contents of the buffer register, the staggered pulses also read information from the A/D converter into the buffer register.

The heart of the onboard-data handling system is the Programmer. The Programmer provides bit rate control signals to the Word Assembler, the A/D Converter, the Digital Data Word Generator and the Frame Synchronization Generator. It also coordinates the gating times for the analog commutators and the A/D converter. Timing for the Word Assembler is provided through the generation of the necessary delays between the data inputs and the read-out buffers. The Programmer provides the analog commutators with channel select timing signals and provides the digital commutators with select and sample timing pulses. Timing pulses to be used in forming data words are provided to the digital word generator. The Programmer provides the Frame Synchronization Generator with the necessary timing pulses to generate synchronization patterns and to select the

correct patterns for insertion into the Word Assembler.

In addition to providing the onboard data handling systems timing control signals, the Programmer also provides control and timing of data handling operational mode changes and telemetry system transmitter equipment configuration changes.

9.2.4 Data Transmission System Design

The telemetry data transmission system will accomodate data from the following sources:

- PCM data at data rates of up to 1.152 k bit/sec from the output of the Word Assembler;
- Analog data from the outputs of four subcarrier oscillators.

The PCM data is in a serial wavetrain and the data rate can be varied. If the data handling system is monitoring the data requirements as set forth in Table 9.2-1, the data rate will be 1.152 k bits/sec (i.e., 128 samples/sec at 9 bits per sample). However, if the system only handles the Structured Subsystem digital data during deployment, then the data rate will be 0.74 k bits/sec. All PCM data is transmitted in PCM/PM modulation form.

Data from each of the four Structures Subsystem vibration sensors (0-100 Hz) is handled by frequency modulating them onto individual subcarriers. The subcarrier oscillator frequencies selected are IRIG channels 7, 8, 9 and 10, which have center frequencies of 2.3 kHz, 3.0 kHz 3.9 kHz and 5.4 kHz respectively. These FM channels will be transmitted as FM/PM modulation.

Figure 9.2-3 is a block diagram of the major functional elements required for data transmission.

The PCM serial data train is fed into a Low-Pass Filter which has a cut-off frequency equal to one-half the digital bit rate. The output of the Low-Pass Filter is fed into a Mixing Network. The four subcarrier oscillator outputs are also fed into the Mixing Network. This network linearly combines the five data inputs into a composite signal which is used to modulate the PM transmitter. The PM transmitter will operate at a given frequency in the 136-138 MHz band and will emit 3.5 watts of RF power. The output of the transmitter can be fed either directly to the antenna diplexer or to a power amplifier and then to the antenna diplexer. The power amplifier, which provides an output power level of 15.0 watts, is included to accommodate transmission modes requiring more power than that available from the 3.5 watt transmitter.

The telemetry data transmission system will be capable of being configured into two modes of operation. Mode I will accommodate the following five data inputs:

- PCM data at a 0.74 k bit/sec data rate at baseband;
- Four analog inputs on subcarrier frequencies.

Mode II will accommodate a single PCM data input at a rate of 1.152 k bits/sec. Table 9.2-3 summarizes the data content and signal characteristics for each mode of operation. As will be shown later, Mode I requires a 15 watt telemetry transmitter in the spacecraft and a 30 MHz IF bandwidth in the ground receiver.

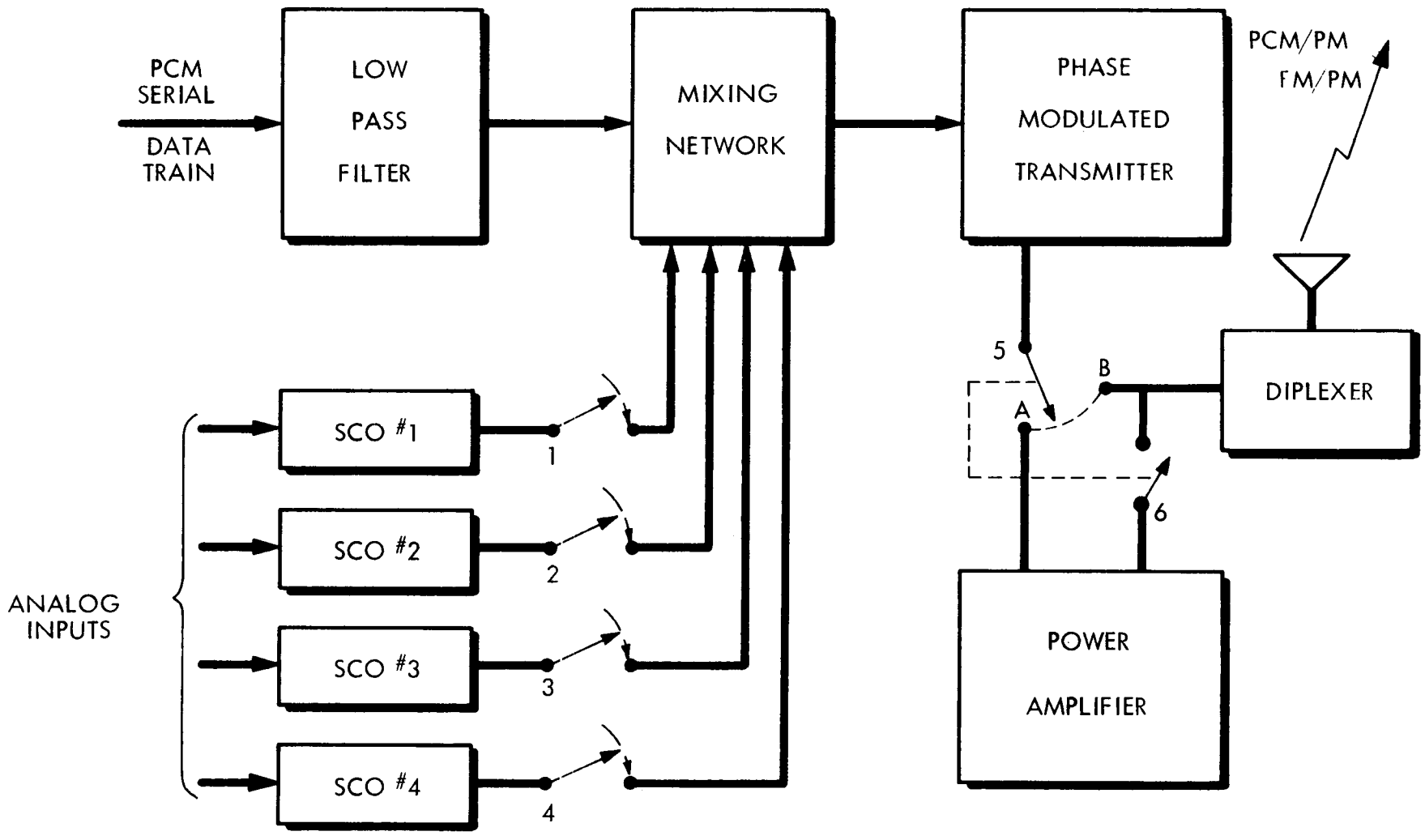

Figure 9.2-3 TELEMETRY DATA TRANSMISSION SYSTEM

Because the telemetry system is capable of operation in two different modes, there will be a requirement to switch various system functional elements into or out of the configuration. Referring to Figure 9.2-3 if the system is operating in Mode I then the switches will be set as follows:

- Switches 1, 2, 3 and 4 closed (SCO inputs);
- Switch 5 in position A (to connect transmitter to power amplifier);
- Switch 6 closed (to connect power amplifier to diplexer).

In addition to these changes, the PCM serial data train will consist of only Structures Subsystem digital data (0.74 k bits/sec), therefore, changes will be made to the encoding process taking place back in the data handling system. (Note that although Mode I calls for 0.74 k bits/sec of PCM data at baseband, the system will be designed to handle 1.152 k bits/sec of data; this will allow for future growth and allow for more efficient equipment usage onboard the spacecraft and on the ground.)

In Mode II operation the PCM data input is at a rate of 1.152 k bits/sec and the switches are set as follows:

- Switches 1, 2, 3 and 4 are open (no SCO inputs required);
- Switch 5 in position B (to connect the transmitter to the diplexer);
- Switch 6 is open (power amplifier not required).

In addition to the above-mentioned equipment switching changes, there will also be some internal system operational changes. (e.g., a change in the PCM data rate will require changes in sampling rates, synchronization codes, data formatting, and in selection of sensor outputs). When final system requirements are derived the necessary changes can be incorporated into the system design, however, no attempt will be made at this time to identify all internal system changes required.

The reliability of the telemetry system can be enhanced by employing equipment redundancy and "building block" interchangeability. Figure 9.2-4 shows that the telemetry system equipment will include two data handling systems (encoders), two telemetry transmitters, two power amplifiers, and one diplexer. These "building blocks" can be arranged so that either data handling system can be connected to either telemetry transmitter/power amplifier grouping. Also, the analog, discrete and digital data inputs can be connected to either data handling system. The outputs from both of the telemetry transmitter/power amplifier groupings are always connected to the antenna diplexer. Therefore, if any single building block fails or if any two building blocks (of unlike function) fail, the system can be rearranged to restore data transmission.

Configuration changes involving internal circuits within the "building blocks" or involving "building block" switching will be controlled by the Programmer. The Programmer will receive commands from the ground and will implement the necessary steps required to rearrange the telemetry system. Commands will be required for the following functions:

- Set up for Mode I Operation
- Set up for Mode II Operation
- Connect data inputs to Data Handling System (DHS) #1
- Connect data inputs to Data Handling System (DHS) #2
- Connect DHS #1 to Transmitter/Power Amplifier #1
- Connect DHS #1 to Transmitter/Power Amplifier #2

- Connect DHS #2 to Transmitter/Power Amplifier #1
- Connect DHS #2 to Transmitter/Power Amplifier #2
- Set up for "fast sampling mode"
- Turn Transmitter #1 on/off
- Turn Transmitter #2 on/off
- Operate Telemetry System in Standby Mode

9.2.5 Data Transmission Link Calculation

The telemetry system will employ both PCM/PM and FM/PM modulated data transmission. In order to justify the transmitter power requirements for the transmission system, calculations are presented for the various information spectra occuring in a given space-to-ground data link configuration. A review of the data channel requirements for each mode of operation (as shown in Table 9.2-3) indicates that individual space-link calculation must be made for each mode of transmission due to differences in spectrum distribution.

We specify the use of a telemetry receiving system employing a carrier-tracking phase demodulator. Therefore, the rms modulation index for each mode of operation must be selected to ensure an adequate carrier power to total power (P_c/P_{total}) ratio so that carrier tracking can be performed. In addition to this, the modulation index must be low enough to avoid phase inversion of the carrier. For Mode I operation an rms modulation index of one radian is selected to handle five multiplexed signals[3] (one baseband channel and four subcarrier channels).

The ground receiving system should employ synchronous product detection of the phase modulated wave. An extremely narrow-band

Channel	Modulation	Frequency (kHz)	Channel Filter Bandwidth (Hz/s)	Modulating Frequency (Hz/s)
1	PCM/PM	Baseband	576	576
2	FM/PM	2.3	346	100
3	FM/PM	3.0	450	100
4	FM/PM	3.9	586	100
5	FM/PM	5.4	810	100

Mode I: Channels 1, 2, 3, 4, and 5

Mode II: Channel 1

Table 9.2-3

Summary of Telemetry Channel Characteristics

phase tracking loop, of about 100 Hz, will permit the data channels to reach their thresholds prior to the level at which the carrier-tracking loop loses lock.

The PCM integrating detector will require an input SNR of 10 dB to attain a bit error probability of 1 bit in 10^4.[4] The FM detectors will require an input SNR of 10 dB in order to be above detector threshold.

The use of synchronous product detection on the incoming phase-modulated wave permits the phase-modulated output SNR to decrease linearly with input signal until the carrier tracking loop loses lock. This system is designed so that the 10 dB channel detector SNR is the significant threshold and will be reached simultaneously in all channels. The system is also designed so that the power available in the carrier at the level of channel demodulator threshold will be well above the carrier loop in lock threshold (3 dB above threshold is a nominal allowable value and it will be shown later that the signal is well above this level).

The modulation index of the main carrier due to each channel is selected in such a manner as to provide equal channel S/N ratios at the output of the subcarrier filtering networks. The deviation on the main carrier, as previously stated, is selected to be one radian (rms); a value which provides a nearly equal distribution of carrier power and channel power. In order for the channel S/N ratios to be equal at the output of the channel bandpass filters, the peak deviation of each channel must be proportional to the square root of the bandwidth of each channel. For Mode I operation, the following relationship holds:

$$\frac{\Delta\theta_o}{\sqrt{B_o}} = \frac{\Delta\theta_1}{\sqrt{B_1}} = \frac{\Delta\theta_2}{\sqrt{B_2}} = \frac{\Delta\theta_3}{\sqrt{B_3}} = \frac{\Delta\theta_4}{\sqrt{B_4}}$$

In this formulation

$\Delta\theta_i$ is the peak deviation of the carrier due to the ith channel, and B_i is the channel filter bandwidth and is equal to 15 percent of the IRIG sub-carrier center frequency (IRIG channels 7, 8, 9 and 10 were chosen) and one-half the bit rate for the baseband channel.

For an rms deviation of one radian:

$$\frac{(\Delta\theta_o)^2}{2} + \frac{(\Delta\theta_1)^2}{2} + \frac{(\Delta\theta_2)^2}{2} + \frac{(\Delta\theta_3)^2}{2} + \frac{(\Delta\theta_4)^2}{2} = (1)^2$$

Solving for the modulation index corresponding to each of the channels yields (see Appendix A):

$\Delta\theta_o$ = 0.825, the main carrier deviation due to the baseband channel

$\Delta\theta_1$ = 0.454, the main carrier deviation due to the 2.3 kHz channel

$\Delta\theta_2$ = 0.517, the main carrier deviation due to the 3.0 kHz channel

$\Delta\theta_3$ = 0.590, the main carrier deviation due to the 3.9 kHz channel

$\Delta\theta_4$ = 0.692, the main carrier deviation due to the 5.4 kHz channel

The ratio of the carrier power to the total power can be calculated as:

$$\frac{P_c}{P_{total}} = \left[J_o(\Delta\theta_o) \cdot J_o(\Delta\theta_1) \cdot J_o(\Delta\theta_2) \cdot J_o(\Delta\theta_3) \cdot J_o(\Delta\theta_4) \right]^2$$

Substituting the values from Table 9.2-4 into the above expression yields:

$$\frac{P_c}{P_{total}} = .36 \text{ (-4.4 dB) or 36\% of the total power is in the carrier.}$$

The ratio of channel power to the total power is expressed as:

$$\frac{P_{channel}}{P_{total}} = 2 \frac{P_c}{P_{total}} \left[\frac{J_1 (\Delta \theta_i)}{J_o (\Delta \theta_i)} \right]^2$$

Substituting the values from Table 9.2-4 into the preceding expression yields:

$\frac{P_{channel-0}}{P_{total}}$ = .146 (-8.4 dB) or 14.6% of the total power is in channel - 0 (baseband)

$\frac{P_{channel-1}}{P_{total}}$ = .040 (-14.0 dB) or 4.0% of the total power is in channel-1 (2.3 kHz subcarrier)

$\frac{P_{channel-2}}{P_{total}}$ = .0517 (-12.9 dB) or 5.17% of the total power is in channel-2 (3.0 kHz subcarrier).

$\frac{P_{channel-3}}{P_{total}}$ = .0684 (-11.7 dB) or 6.84% of the total power is in channel-3 (3.9 kHz subcarrier)

$\frac{P_{channel-4}}{P_{total}}$ = .0977 (-10.1 dB) or 9.77% of the total power is in channel-4 (5.4 kHz subcarrier).

Therefore, for a total rms modulation index of one radian, 36% of the power is in the carrier, 40% of the power is in the data channels and the remaining 24% is absorbed by the higher order modulation products.

We assume the ground received has a carrier tracking bandwidth ($2 B_{L0}$) of 100 Hz; therefore, the noise power in the tracking loop can be expressed as:

$$P_n = 2k T_e B_{L0}$$

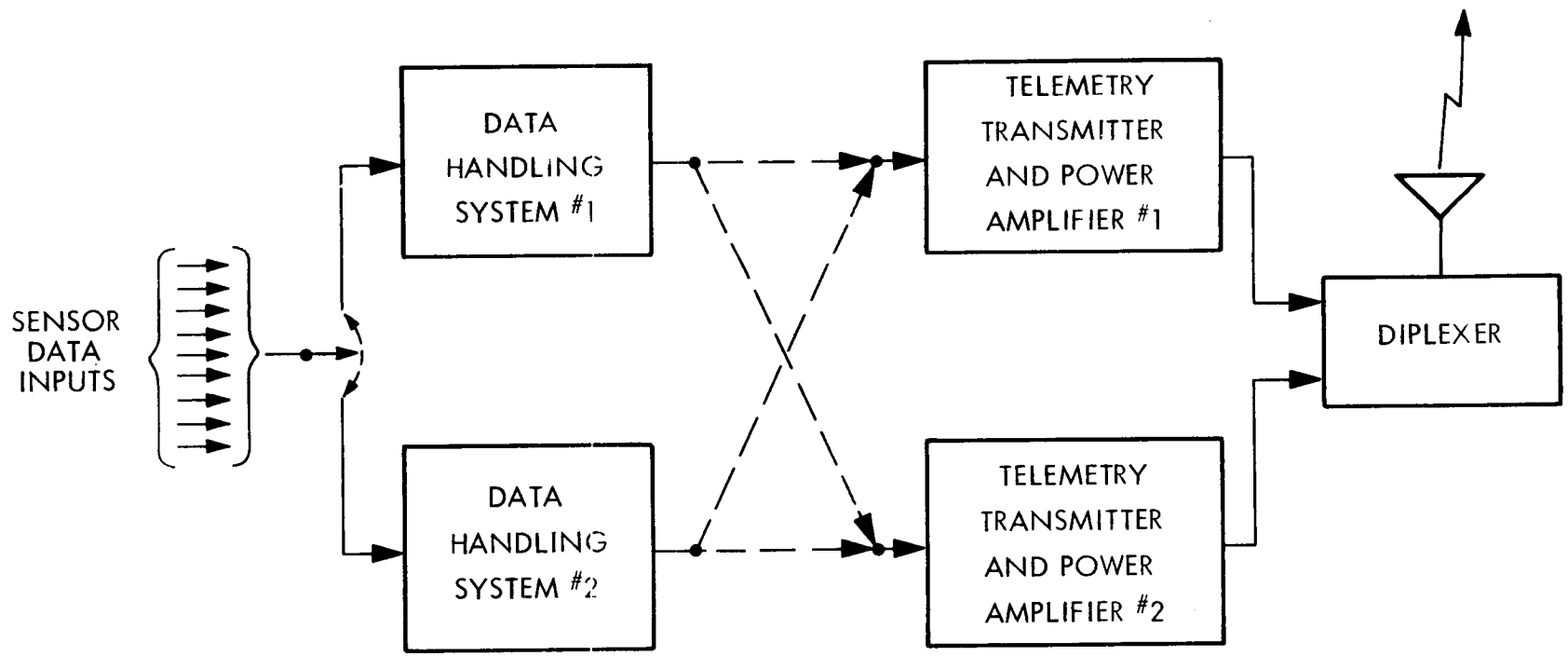

Figure 9.2-4 TELEMETRY DATA HANDLING AND TRANSMISSION CONFIGURATION

Channel	Modulation Index	J_0	J_1
Baseband	.825	.8366	.3780
1	.454	.9485	.2220
2	.517	.9310	.2498
3	.590	.9147	.2823
4	.692	.8837	.3256

Table 9.2-4

Summary of Channel Modulation Characteristics for Mode I Operation

where, k = Boltzman's constant = 1.23×10^{-23} joules/^{o}K,

$T_e = 1060^{o}$ K assuming

$T_e = T_{sky} + T_{recvr.}$, with a receiver preamplifier having a 3.5 dB NF and a radio sky of 700° K at 136 MHz.,

and $2B_{L0}$ = loop noise bandwidth = 100 Hz

$P_n = -148.3$ dBm

It has been shown in previous programs[3] that the carrier tracking loop will track to 0 dB and with adequate knowledge of the expected frequency, a 3 dB SNR will allow acquisition with moderate ease.

Therefore, the total power required at the input of the receiver to meet the tracking threshold is expressed as:

$$P_{req.\ tracking} = P_n \cdot \frac{P_c}{P_{total}} \cdot (SNR)$$

$$P_{req.\ tracking} = -140.9 \text{ dBm.}$$

As previously stated the individual channel detector thresholds have all been set at a 10 dB SNR and therefore each threshold will be calculated as:

$$P_{nc_i} = P_{nr} \frac{B_{IF}}{B_{c_i}}$$

where,

P_{nc_i} = the noise power in the ith channel at the input of the 2nd detector,

P_{nr} = the noise power in the receiver at the input to the first detector (B_{IF} = 30 kHz); see Appendix 9B,

and $\frac{B_{IF}}{B_{c_i}}$ = the ratio of IF bandwidth to channel bandwidth at the input to the second detector.

Substituting into the previous expression yields the following value of P_{nc}:

P_{nc-0} = -137.8 dBm

P_{nc-1} = -143.1 dBm

P_{nc-2} = -141.9 dBm

P_{nc-3} = -140.8 dBm

P_{nc-4} = -139.4 dBm

The total received power required at the receiver input to meet channel threshold for each channel can be expressed as:

$$P_{required\ c_i} = P_{nc_i} \quad (SNR)_{detector\ 2} \quad \frac{P_{total}}{P_{c_i}}$$

where, P_{nc_i} = the noise power required in the ith channel at the input to the 2nd detector to meet a 0 dB SNR,

$(SNR)_{2nd\ detector}$ = SNR required to be above detector, threshold (10 dB)

and $\frac{P_{c_i}}{P_{total}}$ = Percentage of total power in the ith channel.

$P_{req.\ c-0}$ = -137.8 dBm + 10 dB + 8.4 dB = -119.4 dBm

$P_{req.\ c-1}$ = -143.1 dBm + 10 dB + 14.0 dB = -119.1 dBm

$P_{req.\ c-2}$ = -141.9 dBm + 10 dB + 12.9 dB = -119.0 dBm

$P_{req.\ c-3}$ = -140.8 dBm + 10 dB + 11.7 dB = -119.1 dBm

$P_{req.\ c-4}$ = -139.4 dBm + 10 dB + 10.1 dB = -119.3 dBm

The link parameters for the ATS-4 satellite operating a transmitting frequency of 136 MHz and at synchronous altitude (22,300 statute miles) are defined as:

Spacecraft Antenna Gain (G_T) = -3 dB

Transmitter Power, P_T (15 watts) = 41.8 dBm

Spacecraft losses, L_T (diplexer, line losses) = 3 dB

Receiving Antenna Gain, G_T (9 element Yagi) = 19.2 dB

Polarization Losses, L_P (assuming diversity reception) = 3 dB

Free Space Loss, X (at a maximum slant range of 26,000 statute miles) = 168 dB

Therefore the total received power at the ground is defined as:

$$P_{received\ total} = G_T + P_T + L_T + G_R + L_P + X \quad \text{(all in dB)}$$

$$P_{received\ total} = -116 \text{ dBm}$$

Table 9.2-5 shows the various channel parameters and identifies margins. Figure 9.2-5 identifies the points in the receiving system where power requirements exist and indicates available signal levels. The letters A, B, C, E, and G in the heading of the columns in Table 9.2-5 (e.g., "A" corresponds to the power required at the input to the detector to meet a O dB SNR). The "Power Above Threshold at the Input to Detector" column is the system design margin for each of the channels. The five data channels have a 3 dB margin while the carrier channel has a margin of almost 25 dB.

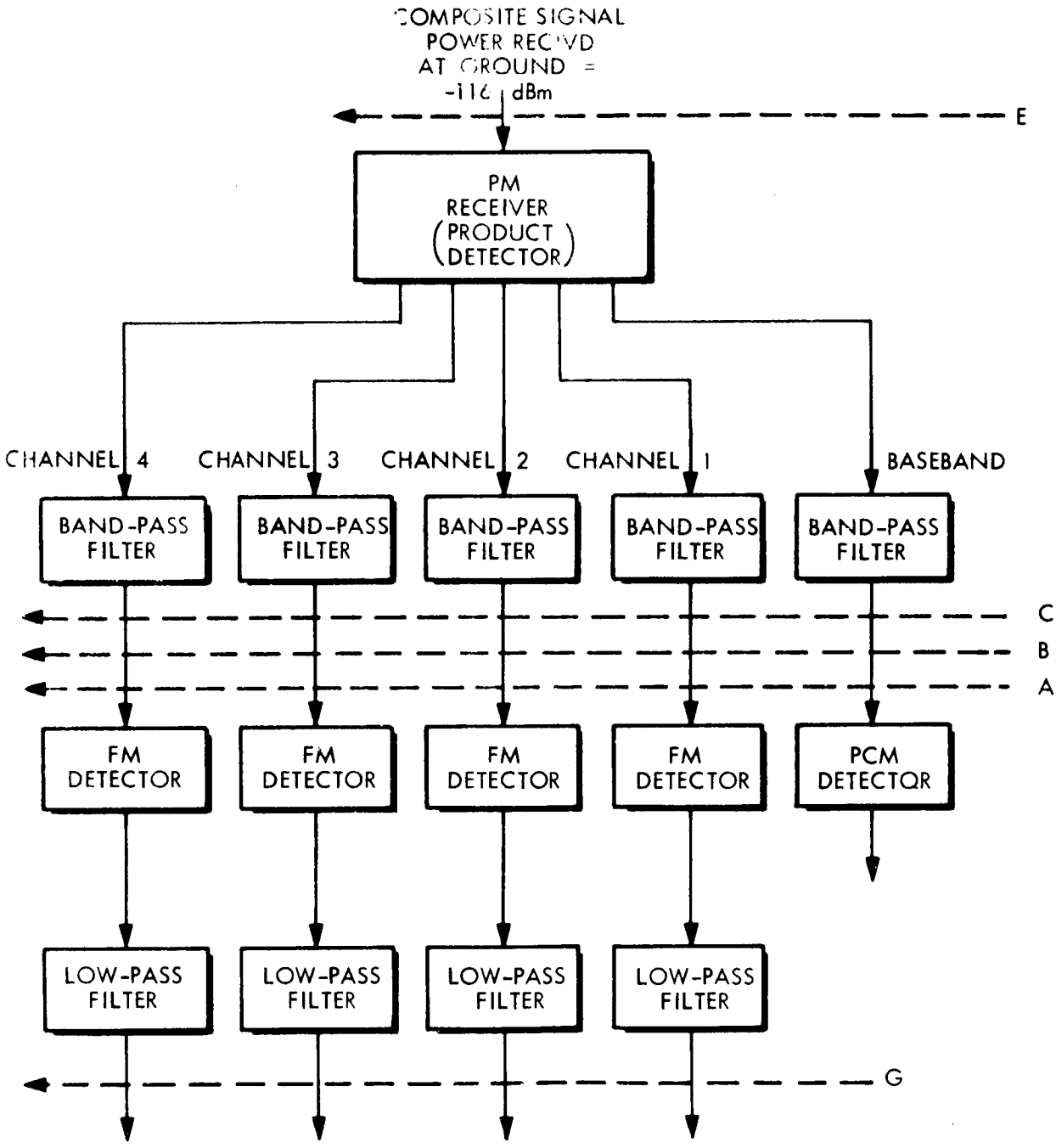

Figure 9.2-5 BLOCK DIAGRAM OF BASIC TELEMETRY RECEIVER

CHANNEL	-A- Power required at input to detector* to meet O DB SNR (P_{nc_i})	-B- SNR required to be above detector* threshold [$(SNR)_{Required}$]	-C- Power required at input to detector* to meet channel threshold requirements	-D- Ratio of channel power to total power (P_{c_i}/P_{total})	-E- Total power required at receiver input to meet channel threshold requirements ($P_{req.c_i}$)	-F- Power above threshold at input to detector* (MARGIN**)	-G- SNR at output of detector
BASEBAND	-137.8 dBm	10 dB	-127.8 dBm	-8.4 dB	-119.4 dBm	3.4 dB	-
1	-143.1 dBm	10 dB	-133.1 dBm	-14.0 dB	-119.1 dBm	3.1 dB	24.5 dB
2	-141.9 dBm	10 dB	-131.9 dBm	-12.9 dB	-119.0 dBm	3.0 dB	25.4 dB
3	-140.8 dBm	10 dB	-130.8 dBm	-11.7 dB	-119.1 dBm	3.1 dB	28.9 dB
4	-139.4 dBm	10 dB	-129.4 dBm	-10.1 dB	-119.3 dBm	3.3 dB	33.0 dB
CARRIER	-148.3 dBm	3 dB	-145.3 dBm	-4.4 dB	-140.9 dBm	24.9 dB	-

* All channels refer to 2nd detector except the carrier which refers to 1st detector.

** Power received at the ground station = 116.0 dBm

SUMMARY OF SPACE LINK POWER CALCULATIONS (MODE I)

TABLE 9.2-5

The expression for FM improvement for each of the subcarrier channels (channels 1-4) is

$$(SNR)_{out} = 3\,M^2 \frac{(B_{IF})}{2B_m} (SNR)_{in}$$

where:

$(SNR)_{out}$ = SNR at output of detector

M = Modulation index = $\frac{f_d}{f_m}$

B_{IF} = Bandwidth of the input to the detector

B_m = baseband filter bandwidth (low pass filter bandwidth equal to f_m)

$(SNR)_{in}$ = SNR at input of detector

For Channel-1:

$(SNR)_{out}$ = 260 = 24.5 dB

For Channel-2:

$(SNR)_{out}$ = 345 = 25.4 dB

For Channel-3:

$(SNR)_{out}$ = 768 = 28.9 dB

For Channel-4: $(SNR)_{out}$ = 1980 = 33.0 dB

The baseband channel will have a SNR at the input of its 2nd detector of 10dB. An input SNR of 10 dB yields a bit error probability of 1 bit in 10^4 if we assume the use of an integrating detector with an Input Bandwidth/Bit Rate ratio equal to one and a Premodulation Video Bandwidth/Bit Rate ratio equal to 0.5.

In Mode II operation the telemetry system will be required to transmit a single serial PCM data train of 1.152 k bits/sec (transmitted as PCM/PM). In Mode I, the baseband modulation index was 0.325 radians peak, however, if this modulation index is utilized in Mode II operation, an inefficient distribution of power between the baseband channel and the carrier will exist, (e.g., almost 70% of the power in the carrier and only 28.6% of the power in the baseband channel). Therefore, the modulation index for Mode II operation will be changed to 1.4 radians peak

(1.0 radians rms), which is the highest practical modulation level in this type of modulation system[4].

As previously stated, the expression for the ratio of the carrier power to the total power can be calculated as:

$$\frac{P_c}{P_{total}} \left[J_o \ (\Delta\theta_o) \right]^2 = .32 \ (-4.9 \text{ dB}),$$

or 32% of the total power is in the carrier.

The ratio of baseband channel power to the total power is expressed as:

$$\frac{P_{Baseband}}{P_{total}} = 2 \ \frac{P_c}{P_{total}} \left[\frac{J_1 \ (\Delta\theta_o)}{J_0 \ (\Delta\theta_o)} \right]^2$$

Substituting the proper values into the above expression yields

$$\frac{P_{Baseband}}{P_{total}} = .585 \ (-2.3 \text{ dB}),$$

or 58.5% of the total power is in the baseband channel.

Therefore, with an optimum modulation index of 1.0 radians rms, Mode II operation has about 58% of the power in the baseband channel, 32% of the power in the carrier, and only 10% is wasted.

As previously calculated, the ground receiver was found to have a carrier tracking threshold, P_N = -148.3 dBm and assuming a 3 dB SNR, the total power required at the input to the receiver to meet the tracking threshold is expressed as:

$$P_{Req. \ Tracking} = P_N \ \frac{P_c}{P_{total}} \ (SNR)$$

$$P_{Req. \ Tracking} = -140.4 \text{ dBm}$$

The PCM integrating detector has been assigned a 10 dB SNR above threshold and the noise power required in the baseband channel at the input to the integrating detector to meet a 0 dB SNR is expressed as:

$$P_{nc-0} = P_{nr} \frac{B_{c-0}}{B_{IF}} = 137.9 \text{ dBm, see Appendix 9C,}$$

for calculations of P_{nr} and $\frac{B_{IF}}{B_{c-0}}$

The total received power required at the input to the receiver to meet the baseband channel threshold is expressed as:

$$P_{Required\ c-0} = P_{nc-0} = (SNR)_{Detector\ 2} \frac{P_{total}}{P_{c-0}}$$

Substituting the value into the above equation yields:

$$P_{Required\ c-0} = -125.6 \text{ dBm}$$

Assuming the same space link parameters for Mode II operation as were used for Mode I operation with one exception: a 3.5 watt (35.4 dBm) transmitter. The total received power at the ground is calculated to be:

$$P_{Received\ Total} = -122.4 \text{ dBm}$$

Table 9.2-6 shows the power levels and margins for the baseband channel and the carrier channel for a 3.5 watt transmitter. As evidenced in Table 9.2-6, the baseband channel has a margin of over 3 dB and the carrier channel has a margin of 10 dB.

CHANNEL	Power Required at Input to Detector* to Meet O DB SNR (P_{nc_i})	S/N Ratio Required to be above Detector* Threshold ($(SNR)_{Required}$)	Power Required at Input to Detector* to Meet Channel Threshhold Requirements	Ratio of Channel Power to Total Power (P_{c_i}/P_{Total})	Power Required at Receiver Input to Meet Channel Threshhold Requirements ($P_{Req_{c_i}}$)	Power Above Threshold at Input to Detector* (Margin)**
BASEBAND	-137.9 dBm	10 dB	-127.9 dBm	-2.3dB	-125.6 dB	3.2 dB
CARRIER	-140.4 dB	3 dB	-137.3 dBm	-4.9 dB	-132.4 dBm	10.0 dB

* Baseband Channel Refers to 2nd Detector, Carrier Refers to 1st Detector

** $P_{Received\ Total}$ = -122.4 dBm

SUMMARY OF SPACE LINK POWER CALCULATIONS (MODE II)

TABLE 9.2-6

9.2.6 System Size, Weight, and Power Estimates

The telemetry system package is defined to include:

- Two 3.5 watt phase modulated transmitters
- Two 15 watt power amplifiers
- One antenna duplexer
- Eight subcarrier oscillators
- Two encoders (each encoder includes analog and digital communtators, an A/D converter, a programmer, a synchronization generator and a word assembler).

The equipment characteristics for each of the components in the package is summarized in Table 9.2-7. The total package will occupy a volume of approximately 210 cubic inches and will weigh approximately 15 pounds. When the system operates in the Mode I configuration the peak power requirement will be 61.8 watts and when operating in the Mode II configuration the peak power requirement will be 27.3 watts. If the system is in a non-operational standby mode, 4 watts of power will be requires.

9.2.7 Equipment Implementation

The telemetry transmission system (i.e., the phase modulated transmitter, power amplifier, diplexer, subcarrier oscillators, and low-pass filters) can be implemented through the use of "off-the-shelf" hardware. In some instances there may be requirements for minor modifications to the hardware, but in no case will major custom design be required.

The data handling requirements for the ATS-4 mission will require custom designing of some of the components. The state-of-the-art design associated with the components in the telemetry data handling system

CHARACTERISTIC / UNIT	NUMBER REQUIRED	VOLUME (Cubic Inches)	WEIGHT (Pounds)	POWER PEAK (Watts)	POWER STANDBY (Watts)
TRANSMITTER	2	18.0 (36.0)*	1.0 (2.0)	10.0	0.5 (1.0)
POWER AMPLIFIER	2	16.0 (32.0)	1.0 (2.0)	35.0	0.5 (1.0)
DIPLEXER	1	2.0 (2.0)	0.3 (0.3)	-	-
SUBCARRIER OSCILLATOR	8	0.1 (0.8)	0.06 (0.46)	0.1 (0.4)	0.1 (0.4)
ENCODER (Includes commutators, A/D converters, programmer, word assembler, and sync. generator	2	70.0 (140.0)	5.0 (10.0)	14.0	(2.0)
TOTALS		210.8 (in.^{3})	14.76 (pounds)	61.8 watts for Mode I operation 27.3 watts for Mode II operation 4.0 watts -non-operational (standby)	

* ( ) - Denotes Total

SUMMARY OF TELEMETRY SYSTEM SIZE, WEIGHT, & POWER REQUIREMENT

TABLE 9.2-7

(i.e., the A/D converter, word assemblers, programmers, frame synchronization generators, and analog/digital commutators) is advanced and sophisticated. Several components (e.g., the A/D converters, the frame synchronization generators, and the word assemblers) can be implemented by using "standard" hardware with minor modification. But other components (e.g., the programmers, the analog/digital commutators, and the system integration circuitry) will have to be custom designed.

9.3 COMMAND SYSTEM

9.3.1 Definition

The ATS-4 instruction command system is a PCM up-data link for transmission of commands to the spacecraft. Its design is compatible with the GSFC Aerospace Data Systems Standards[5].

This system shall perform the following functions:

1. Transmit discrete commands from the ground stations (Rosman and Mojave) to ATS-4 for activation of all spacecraft subsystems;
2. Transmit instructions and data to the SCS, the phased array, and the interferometer.

The onboard command system will interface directly with all other spacecraft subsystems. The interfacing is shown in Figure 9.1-1, Section 9.1

9.3.2 Requirements

The command requirements existing for the ATS-4 spacecraft subsystems were compiled and are summarized in the command catalog (see Appendix 9F). A summary of the command catalog is presented in Table 9.3-1.

From the command catalog and the summary table it can be seen that wo types of command information are required:

Table 9.3-1

Summary of Command Requirements

Subsystem	Code	Number of Signals	Remarks
Auxiliary Propulsion System	$\overline{J}$	5	Discretes only.
Structures	$\overline{S}$	5	Discretes only.
Orientation Control System (ACS & ARS)	$\overline{C}$	44	Discretes plus data sequences for programmed motion of the spacecraft.
Power System	$\overline{P}$	20	Discretes.
Parabolic Antenna Experiment Electronics	$\overline{D}$	35	Discretes.
Phased Array Experiment Electronics	$\overline{A}$	19	Discretes plus data sequence for antenna beam pointing.
Interferometer Experiment Electronics	$\overline{I}$	19	Discretes plus data for element and frequency sequencing program.
Instrumentation	$\overline{O}$	16	Discretes.

1. Discretes: These are single pulses that activate switches, or set relays and latches;
2. Data: Represents control instructions or programs needed to perform maneuvers or experiments.

Table 9.3-1 shows that presently eight subsystems require command data and that forty-four is the maximum number of commands required by any of the subsystems. Growth capability is needed because it is anticipated that ATS-4 will carry secondary experiments.

The table also shows that some of the subsystems require instruction data sequences. These instructions will be channeled to the subsystems directly. Each subsystem will have a programmer which will further identify and route the instruction words.

From the requirements the following data capabilities were derived for the command system:

1. Transmission of data words, at least twelve bits long, to the ACS and the interferometer (Mode 1);
2. Transmission of data words, 35 bits long to the phased array electronics (Mode 2);
3. Transmission of discretes to the spacecraft subsystems; up to sixty-four discretes per subsystem are provided (Mode3).

Capabilities are provided in excess of the requirements shown in Table 9.3.1. The command system is capable of addressing sixteen subsystems; the command word format permits assigning of up to 512 discretes per subsystem. This allows for growth and gives latitude for design modifications.

In order to expeditiously enter data words, particularly for array beam control, the command system should be as fast as possible. The command word length and duration are specified in the Aerospace Data System Standards; one sixty-four bit command word has a duration of 0.5 seconds. The transmission delay to a synchronous satellite is 0.12 seconds, and since command verification is required, at least 0.75 seconds are needed to transmit a command word and receive verification. This is the minimum time required for entering a command and receiving verification on the ground. Consequently the highest data rate possible is approximately forty-two bits per second (in Mode 2).

The verification scheme could increase this time significantly. For example, if the command words were to be retransmitted by the telemetry system on the ground, compared to the originally transmitted word, and then executed via an execute command, the transmission time for one command would at least double.

Therefore, a requirement is derived here to accomplish command verification and subsequent execution onboard ATS-4. This can be done either by using error control codes or by transmitting the command message and its complement in a single command system transmission word. The latter method appears sufficient for ATS-4 and hence is favored for Modes 1 and 3; it will also require less hardware than error control codes. For transmission of the 35 bit data word only a parity check is performed; hence in Mode 2 speed is traded for transmission reliability.

9.3.3 Word Format

The command system transmission word format suitable for the ATS-4 Command System is shown in Figure 9.3-1. The first twenty bit

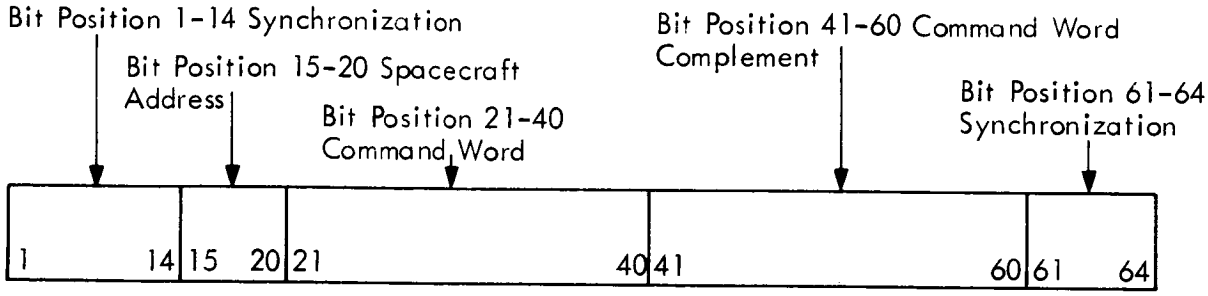

(a) Command System Transmission Word, Mode 1 and Discretes

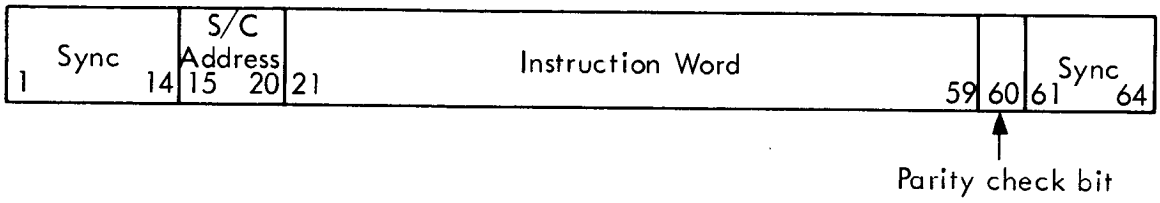

(b) Command System Transmission Word, Mode 2

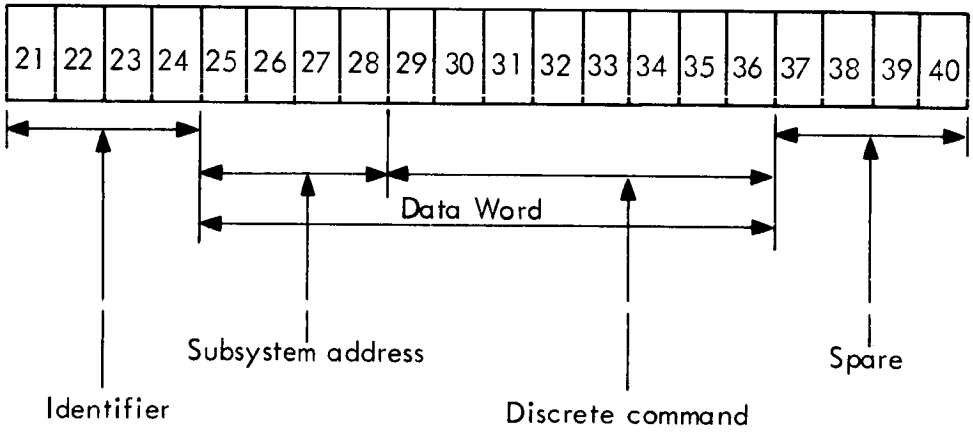

(c) Command Word, Mode 1 and Mode 3. Number indicates the bit position in the command transmission word.

Figure 9.3-1 COMMAND WORD STRUCTURE

periods are occupied by synchronization data and spacecraft address. Synchronization data must occupy at least the first fourteen bit periods (as indicated in Figure 9.3-1), the remaining bits, up to bit position 19, are reserved for the spacecraft address. Should the address assigned to ATS-4 require less than 5 bits, the synchronization data would occupy correspondingly more bit positions.

In Mode 1 the command word will occupy no more than twenty bits; the bit positions are 21 to 40. The bit positions 41 to 60 are occupied by the complement of the command word (i.e., where the command word position has a "1" the complement has a "0" and vice versa). The last four bits are synchronization data, as specified in the Aerospace System Standards.

In Mode 2 the instruction word is forty bits long and will occupy bit positions 21 to 60. The first four bits, positions 21 to 24, are identifier bits; the last bit, position 60, is a parity check bit.

The structure of the command word used in Mode 1 and Mode 3, is also shown in Figure 9.3-1(c). It consists of twenty bits. The first four bit positions (21 to 24) constitude an identifier which routes the instructions to various subsystems in the spacecraft; the identifier distinguishes between discretes and instructions.

These identifier bits are used in all Modes and determine whether the decoder operates in Modes 1, 2 or 3. The number of possible identifiers is sixteen; they may be assigned in the following way:

1... Discrete (Mode 3)
2... Interferometer data word (Mode 1)
3... Phased array (Mode 2)
4... Phased array, spare
5... ACS 12-bit pitch offset (Mode 1)
6... ACS 12-bit roll offset (Mode 1)

7... ACS 12-bit spare

8... ACS other data words (Mode 1)

9-16... Spares

The twelve bit words following the identifiers # 2-16 are either data or Mode 1 or Mode 2 instruction data; they are routed to their espective destinations.

The twelve bit words following the identifier "discrete" are the discrete commands that will be applied to the individual subsystems. The first four of these twelve bits (positions 25 to 29 in the command word) are subsystems addresses (16 possibilities); the following eight are decoded into discretes. Only six bits are used for decoding into sixty-four discretes; the remaining two bits are presently unused. The last four bits, positions 37 to 40, are not assigned and can be used as the need arises. One possibility would be to use these bits for additional coding redundancy; in the simplest form this may be a parity check.

9.3.4 Description and Operation of the Onboard System

The onboard command system consists of two command receivers and two command decoders. The dual units provide for redundancy.

Figure 9.3-2 shows the basic configuration. The two receivers are connected to a select logic that automatically samples the receiver outputs. When a signal appears at the output of the receivers, the logic selects one of the receivers and connects both decoders to the selection receiver. The selection of the proper decoder is made from the ground via the frequency of the command data tone subcarriers. In this fashion a functional command system is retained when either one receiver, one decoder or one receiver and one decoder should have failed.

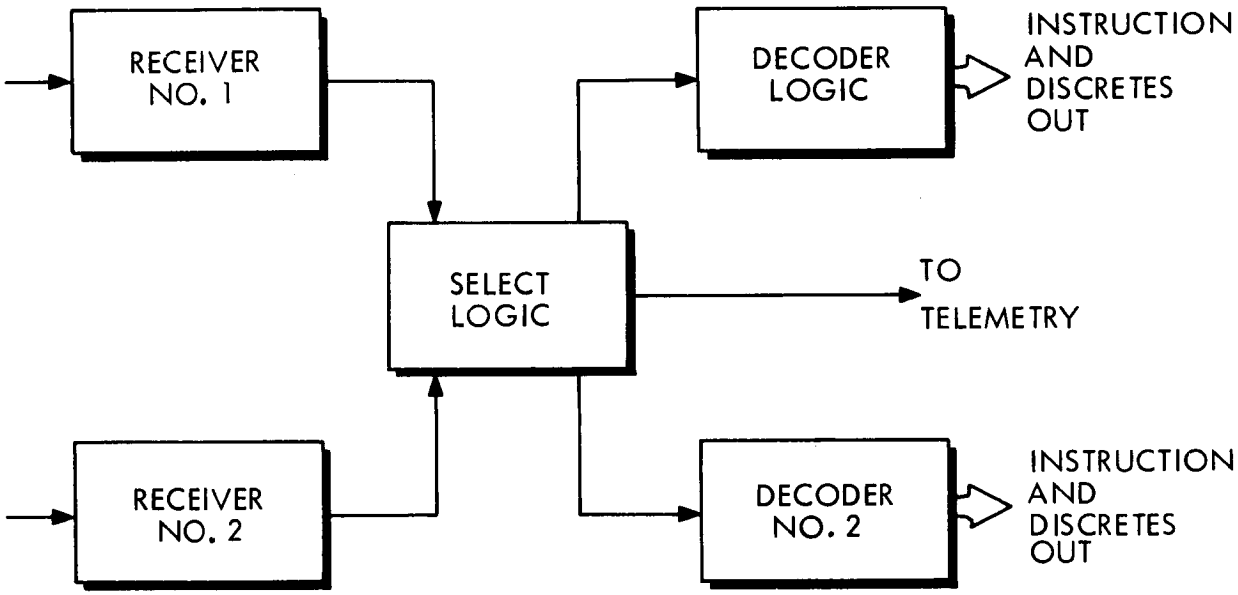

Figure 9.3-2 COMMAND SYSTEM

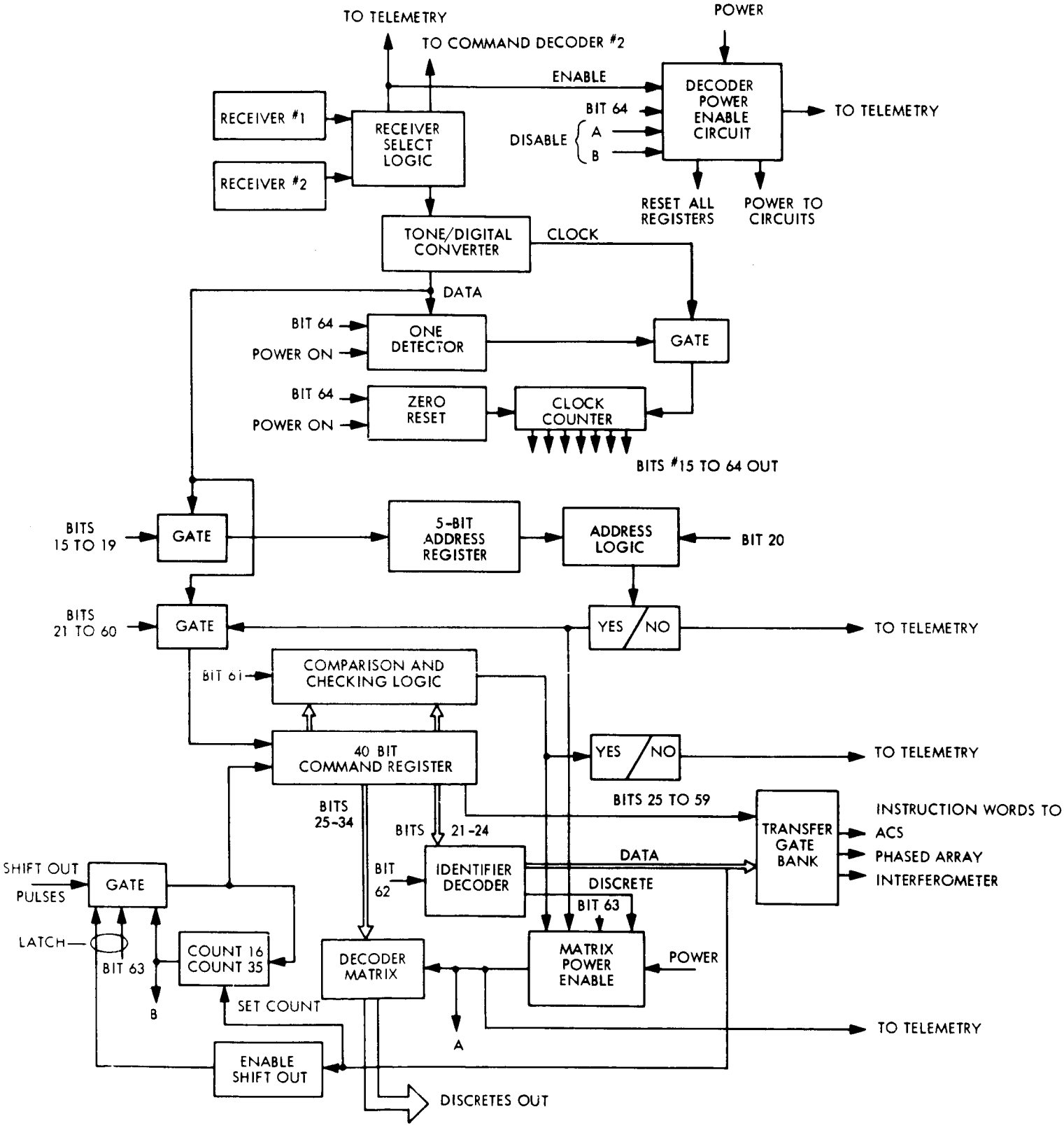

FIGURE 9.3-3 COMMAND DECODER

The command decoder is shown in Figure 9.3-3. Included in the figure are also the two receivers and the receiver select logic. The receiver select logic is sampled in such a way that during the first thirteen zero bits of the synchronization the receiver select circuit latches on to one receiver. The receiver select dircuit is then kept in the latched-on state for the furation of the command word. Indication of the state of the select circuit is transmitted via telemetry back to ground. The indication signal also activates the decoder power enable circuit, through which the decoder circuitry, except for the decoder matrix, is connected to the onboard power source. The status of the power enable circuit is checked via telemetry.

The receiver select logic is connected to the T/D converter; in this unit the PCM is demodulated from the tone subcarriers, and also the 128 Hz clock signal is extracted. The 128 Hz clock signal is conditioned to produce pulses which are fed into the clock counter. This counter counts clock pulses for bit positions 15 to 64. This is performed as follows: the first ONE, bit number 14, appearing at the conclusion of the synchronization, is detected by the "ONE detector"; the latter latches up in this position and becomes insensitive for the remainder of the command word. The output of the "ONE detector" opens the gate to the clock counter, such that the counter can start counting beginning with bit number 15 in the command word. The counter controls the activity of the decoder for the reception of one command word. At 7.8 m sec after the counter senses bit position 64, the counter is reset to zero, and the ONE detector sensitized to prepare the decoder for reception of a new command.

The command data word is routed from the T/D converter into an address register and into a word register. By proper timing the

spacecraft address (bits 15 to 19) is entered into the address register. The command register is opened only for the time corresponding to bit positions 15 to 19 and no additional bits can enter it. At the time corresponding to bit position 20 the address is sampled in the address logic. If the address is correct, a gate is enabled to permit reading the command word (bit positions 21 to 60) into the forty bit command register.

The sampling of the address register also is transmitted back to ground via telemetry. In this fashion the correctness of the spacecraft address is verified. The correct address identification also sets the decoder matrix power enable circuit into a ready state. Thus, only if a correct address is identified can the command be executed.

The command word and its complement, bit positions 21 to 60, now enter the forty bit command register through a gate that is kept open for bits 21 to 60. Once bit 60 has been entered, the gate closes and no more bits can enter the forty bit command register.

At the time corresponding to bit position 61, a comparison logic is activated. This logic senses the command word identifier (bits 21 to 24). For Modes 1 and 3 the comparison logic then ascertains that the word in bit positions 41 to 60 is the complement of the command word in bit positions 21 to 40. For Mode 2 operation the logic checks the parity bit. If the logic finds the word to be correct a verification signal is transmitted to ground via telemetry. The same verification signal also readies the matrix power enable circuit; this will ascertain that only correct commands can be executed. Connected to the forty bit command word register is identification logic and a set of transfer gates. At the time corresponding to bit position 62, the command word identification bits (21 to 24) are decoded. If the identifier indicates a

discrete, the maxtrix power enable circuit is enabled. If the identifier indicates a data word, the proper gate in the bank of transfer gates is enabled.

At the time corresponding to bit position 63 now the transfer of the command takes place. If the command is a discrete, the power is applied to the matrix. The matrix receives the data contained in bit positions 25 to 36 from the forty bit command word register, decodes it and creates the proper switching signal for the spacecraft subsystem which must be enabled. The occurence of this event creates a pulse which is monitored on the ground via telemetry. This pulse also is routed to the power enable circuit to prepare disablement at the time corresponding to bit position 64; following disablement will ready the decoder for a new command.

If the command is a data word, the identification circuit sets an enable shiftout clock circuit. The identification circuit latches the gate in an open condition at the time corresponding to bit position 63 in order to permit the application of shiftout clock pulses to the forty word command register. These shiftout clock pulses are derived from the spacecraft clock and have a frequency other than 128 Hz, the basic command decoder clock frequency. At this point the distinction between Mode 1 and Mode 2 becomes apparent. For a Mode 1 identifier a counter must be set to permit only sixteen shiftout pulses to be applied. For Mode 2 the counter is set to 35 to permit shiftout of 35 instruction bits.

If shiftout clock pulses can enter through the opened gate, they will start the counter circuit and shift the data out of the command register through the transfer gates to the respective spacecraft subsystem. The counter circuit assures that the correct number of shiftout pulses is applied. At the proper count the latching gate for shiftout clock pulses is closed and a pulse is sent to the power enable circuitry to squelch decoder power and thus

make the decoder ready for reception of a new command.

The decoder power enable circuit is squelched either at the time corresponding to bit position 64 through line A (if the command was a discrete) or at the end of the command register shiftout count through line B (if the command was an instruction). The decoder power enable circuit then produces a pulse to reset all registers.

In summary, the operation of the command system can be described as follows:

- The decoder is power-squelched until the decoder has latched onto a signal;
- The command is executed automatically if:
  - (a) A correct address is identified;
  - (b) Redundancy evaluation verifier the command;
- The decoder matrix power is turned on only to decode a discrete;
- The decoder power is turned off at the end of decoding of a discrete or shifting out of an instruction word to the respective spacecraft subsystem;
- The performance is monitored by telemetry in the following respects:
  - (a) Latching on of the decoder to a receiver signal,
  - (b) Identification of a correct spacecraft address,
  - (c) Verification of correctness of the command word,
  - (d) Decoding of the discrete in the decoder matrix,
  - (e) Status of the power enable circuit;
- The receiver select logic and the T/D converter are always on standby power.

9.3.5 Estimates of Physical Characteristics

This section summarizes estimates of the physical characteristics of the command system in terms of weight, size and input power requirements.

The receivers are assumed to be solid-state superheterodyne receivers. For an operating frequency in the VHF band (148 MHz) the following physical characteristics are estimated:

Weight	10 oz.
Size	20 cu. in.
DC power requirement	0.5W

The receiver select logic is also solid-state equipment. The following physical characteristics are estimated for this equipment:

Weight	6 oz.
Size	15 cu. in.
DC power requirement	0.2W

The decoder circuitry is also assumed to be completely solid-state equipment. Based on Figure 9.3-3, the following characteristics are estimated.

Weight	75 oz.	
Size	150 cu. in.	
DC power requirement	(a) standby	0.5W
	(b) active	5 W
	(c) decoding matrix on	11W

Table 9.3-2 summarizes the estimated physical characteristics of the command system.

Table 9.3-2

Estimated Physical Characteristics of Command System

	Weight	Size	DC Power Requirement	
	oz.	cu. in.	Standby W	In Operation W
Receiver #1	10	20	0.5	0.5
Receiver #2	10	20	0.5	0.5
Select logic	6	15	0.2	0.2
Decoder #1	75	150	0.5	11
Decoder #2	75	150	0.5	11
TOTALS	176 (11 lbs.)	355	2.2	12.7 *

* This figure includes one decoder in standby and one decoder in the active state.

9.3.6 Transmission Link Power Requirements

For solid-state receivers operating in the VHF band a sensitivity of -154 dB W is characteristic; this assumes that for a received power level of -154 dB W a 0 dB signal-to-noise ratio (SNR) is obtained. This is based on a 6 dB noise figure and a 30 kHz receiver i-f bandwidth.

The range equation in logarithmic form can be written as

$$P_R\ (\text{dBW}) = P_T\ (\text{dBW}) + G_T + G_R - L_{sp} - L_{misc}$$

where, P_R is the received power, P_T the transmitted power, G_T the transmitter antenna gain, G_R the receiver antenna gain, $L_{sp} = 20 \log \frac{4\ \pi R}{\lambda}$ is the space loss and L_{misc} are miscellaneous losses from cabling, polarization, absorption, etc.

Table 9.3-3 summarizes the values that can be expected for ATS-4.

The signal-to-noise ratio that can be expected in operation is simply the difference between the received power and the sensitivity; for this one obtains 9.5 dB. In order to estimate the receiver performance, the energy contrast $\frac{E}{N_o}$ must be calculated from the SNR. For the command system under discussion, the SNR must be multiplied by a factor of

$$T_{Bit} B_{filt} \frac{B_{IF}}{B_{filt}} = T_{Bit}\ B_{IF}$$

where, T_{Bit} is the duration of one bit (7.8 m sec), B_{filt} the bandwidth of the tone filter in the T/D converter (see Figure 9.3-3), and B_{IF} the receiver IF bandwidth (30 kHz). This factor amounts to 13.8 dB.

Table 9.3-3

Range Equation Values for Command System

P_T (transmitter 242-G-2)	23 dBW
G_T (dual Yagi)	13.5 dB
G_R (onboard antenna system)	-3 dB
L_{sp} (for 40,000 km, 148 MHz)	160 dB
L_{misc}	9 dB
P_R	-144.5 dBW

Consequently, the energy contrast for the command system is 23.3 dB. This quarantees a bit error rate of less than $1:10^{-5}$ with an operating margin of 10 dB.

If more powerful transmitters (5 kW) and higher gain antennas (SATAN) will be employed, the operating margin will increase even more.

9.3.7 Equipment Implementation

For the onboard command system three different kinds of equipment are needed. These are the command receiver, the receiver select logic and the command decoder.

For the command receiver a solid-state superheterodyne receiver is suggested. Such receivers have been used successfully in satellite programs. In particular, the command receivers used in the ATS A, B, C and D satellites have the capability required for the ATS-4 satellite.

The receiver select logic circuitry asynchronously samples the output of each receiver. The sampling rate must guarantee one sample of each receiver output during the time of the first thirteen bit positions of the command transmission word. The sampling rate must be less than 50 m sec. Equipment suitable for receiver selecting must be specifically developed for ATS-4. It is anticipated that the state-of-the-art components can be employed.

The command decoder is special equipment, that needs to be designed for ATS-4. The block diagram shown in Figure 9.3-3 can serve as basis. Transistorized circuitry is envisioned. The switching rates are in the order of milliseconds, and present state-of-the-art components can be selected for design of highly reliable equipment.

9.3.8 Ground Equipment Requirements

The ground equipment must meet the following requirements:

- Be compatible with the Aerospace PCM Command System standards;
- Allow manual entry of commands;
- Allow automatic entry of instructions and commands;
- Produce a transmitter power of at least 200 W;
- Have antenna gains of at least 13.5 dB.

Many ground stations already have equipment installed which may be suitable if modified. This equipment is the OGO command console, presently available at Quito, Gilmore Creek, Rosman, Santiago and Hartebeetshoek; in the future such equipment will be available at Carnarvon and Tananarive.

This equipment permits entering commands manually by setting switches, or automatically from a tape reader. The manual mode only allows the entering of commands into bit positions 21 to 30 and the complement of the command word into bit positions 31 to 40. Similarly the paper tape mode can automatically enter commands but only bit positions 21 to 30 can carry command words. The other bit positions are filled with addresses, complements, data or synchronization.

The verification for the paper tape mode consists of one single bit in the telemetry format. This bit, controlling the transmission of command data, is relayed from the PCM DHE to the command console.

The basic operating principle of the OGO equipment is well-suited for ATS operation. However, the following modifications are necessary in order to achieve compatibility with the command system described in Figure 9.3-3:

1. The command word must be entered into bit position 21 to 40. In a manual mode four hexadecimal switches (A to D) should be provided for the following functions:

   Switch A - bits 21 to 24 for the identifier

   Switch B - bits 25 to 28 for the spacecraft subsystem address

   Switch C - bits 29 to 32 for the first four bits of the command word

   Switch D - bits 33 to 36 for the remainder of the command word

   An optional Switch E may be provided for bit positions 37 to 40. Also, it is desirable to have the switches automatically form complements which are then entered into bit positions 41 to 60.

2. In the automatic mode of paper tape command entry a twenty bit word must be entered into bit positions 21 to 40. It may be necessary to provide for a twenty bit buffer storage between the tape reader and the command equipment. Also, in this case it is necessary to automatically form a complement word to be entered into bit positions 41 to 60. This type of operation is required for transmission of Mode 1 instructions.

3. For Mode 2 operation of the onboard command system, instructions must be entered into bit positions 21 to 60. This mode shall operate from paper tape only. It may be necessary to provide for a 40 bit buffer storage between the tape reader and the command equipment.

4. The command verification consists of several bits relayed from the PCM-DHE. These bits represent the recognition of signal, the correct address, the redundancy check, the execution of the command, and the status of the power enable circuits. A suitable combination of these telemetry bits must be received at the ground to advance the paper tape to the next command word.

5. A switch must be provided to select the proper decoder aboard the spacecraft.

The operation of the command console is suggested as follows:

1. Manual: The desired command word is entered into a register by setting switches. A transmit button facilitates transmission. Verification is obtained

from the PCM-DHE; this clears the register for entering the next command. A light indicates the status of the register. The command can be repeated up to four times. If, during this time, a correct command cannot be entered, a corrective measure must be taken.

2. Automatic: The set of commands or instructions are punched on paper tape. Upon switching the command console to the automatic mode, the paper tape is advanced to enter one command into the buffer register. This command is automatically transmitted. Upon receipt of a verification, the tape is advanced again, the next command is entered, etc. A command can be repeated four times (if the verification shown an incorrect command). After four attempts, an indicator is turned on to indicate that a dorrective measure is required. In this automatic mode the transmission of one instruction or command word requires approximately 0.75 seconds.

9.4 RANGE AND RANGE RATE TRANSPONDER

9.4.1 Accuracy Requirements

The ATS-4 satellite will require ground tracking during various mission phases (e.g., during the parking orbit, the transfer orbit, and for injection into synchronous orbit). After the satellite is injected into synchronous orbit, the transponder will be required to provide correction data for the orbital trim maneuver and for station keeping. The orbital trim maneuver will require measurement of the inclination angle to accuracies of 0.01° and, therefore, a range rate resolution of ±0.1 meters per second is required. In addition to providing the required resolution characteristics, the transponder must also be compatible with the Goddard Range and Range Rate Tracking System.

9.4.2 Transponder Operating Frequency Selection

The Goddard Range and Range Rate Tracking System is capable of operation at either VHF or UHF. The VHF system transmits ranging signals to the spacecraft at 148 MHz and receives the return signals from the spacecraft at 136 MHz. The UHF system transmits ranging signals at any one of three frequencies in the 2270 MHz range and receives the return signals from the spacecraft at about 1700 MHz. The actual choice of operating frequency is dependent on mission critical parameters.

The critical factor could be any one of or a combination of: accuracy requirements, vehicle stablization characteristic affecting antenna patterns, or size, weight and power restrictions. In the case for the ATS-4 vehicle, the range rate resolution requirement is the prime

critical factor (i.e., a resolution of ±0.1 meters per second is required). A VHF system is capable of providing range rate with ±1.0 meter per second resolution while a UHF system can provide range rate with ±0.1 meter per second resolution. The range resolution of both the VHF and UHF systems is ±15 meters. Therefore, the UHF system will be selected.

9.4.3 UHF Transponder Characteristics

The UHF Transponder will have the following characteristics:

Input Carrier Frequencies: up to 3 @ approx 2270 MHz

Input Signal Power: -40 to -100 dBm (each channel)

Transmitted Carrier Frequency: approx. 1705 MHz

Channel Information Bandwidth: 200 kHz

Transmitter Power Output: 200 mW (23 dBm)

Primary Power Requirement: 4 W (standby)
15 W (transmitting)

Weight: 8 pounds

Volume: 150 cubic inches

The ground tracking stations will employ 14 foot parabolic antennas, one for transmitting and one for receiving, with gains of 37 dB and 35 dB, respectively. The ground receivers will have an input signal power of -78 to -148 dBm. The transmitter power available will be 10 kW.

The up-link and down-link transponder system characteristics are calculated as follows:

UP-LINK (transmitting at 2270 MHz)

Transmitter Power:	70 dBm (10 kW)
Transmitter Antenna Gain:	37 dB
Space Loss:	192 dB (assuming maximum 26,000 st. mile slant range)
Spacecraft Antenna Gain:	-3 dB
Miscellaneous System Losses:	6 dB (polarization, cabling, etc.)

Therefore, the total received power at the satellite is -94 dBm. The transponder input signal power level is -100 dBm and a 6 dB margin is available.

DOWN-LINK (transmitting at 1700 MHz)

Transmitter Power:	23 dBm (200 mW)
Transmitter Antenna Gain:	-3 dB
Space Loss:	190 dB (assuming maximum 26,000 st. mile slant range)
Receiving Antenna Gain:	35 dB
Miscellaneous System Losses:	6 dB (polarization, cabling, etc.)

Therefore, the total received power received at the ground is -141 dBm. The ground receiver input signal power level is -148 dBm and a 7dB margin is available.

9.4.4 Equipment Implementation

The implementation of the on board equipment associated with the Range and Range Rate Transponder can be satisfied through the use of "off-the-shelf hardware", with minor modifications. Minor modifications may be required to accommodate specific input carrier channel center frequencies and their subcarriers. In addition, design modifications may be needed to satisfy transmitter power requirements.

9.5 GROUND STATION REQUIREMENTS

The analysis of the flight profile and mission operation (see Section 2) shows that ATS-4 requires only a small number of ground stations. Some of these stations are needed only for a short period of time, during the ascent phase, whereas others will be permanent ground stations. Table 9.5-1 presents a summary of the required ground station and shows the capacity in which the stations are needed.

The table shows that during the ascent phase, stations are needed for a relatively short period of time. The mission, as presently defined, will require only two ATS-4 ground stations, Rosman and Mojave. For support of some of the communication demonstrations, other ground stations may be used. For example, in communicating with aircraft or low flying satellites, other ground stations having a specific capability may be used.

Also, once secondary experiments are defined for ATS-4 it may be necessary to include other ground stations. For example, it may be desirable to make some measurements at a station where the ATS-4 is at a very low elevation angle. Other examples may be a small mobile ground station for demonstrations of point to point communications.

ATS-4 operation will be supported by the primary (and secondary) ground stations. The primary station will, therefore, require all equipment that is needed for ATS-4 ground support. Consequently, the discussion of the equipment will be limited here to this station.

9.5.1 Ground Station Equipment Description

A block diagram of the ground station equipment is presented in Figure 9.1-2, Section 9.1. Here the functional requirements of these blocks and, where possible, implementations will be discussed.

Table 9.5-1

Ground Station Summary

Station	Function for which required	Phase during which required	Approx. time period for which req'd.	Remarks
Kano, Nigeria	Command override for separation.	Ascent	7 min.	This station is optional; if separation is programmed, the station is not needed.
Tananarive Malagasy Rep.	R & RR Tracking	Ascent	9.5 hrs.	Most of the time the spacecraft is also visible from Carnarvon.
Carnarvon, Australia	R & RR Tracking	Ascent	10 hours	May also be used for command and telemetry in emergency situations.
Lima, Peru	Backup	Ascent	1 hour	This station provides coverage for about one hour, where ATS-4 is otherwise not covered.
Rosman, N. C	R & RR tracking, telemetry, command interferometer illumination, communcation experiments.	Total life of mission.	2 years	This is the primary ATS-4 station.
Mojave, Calif.	Telemetry, command, interferometer illumination, communication experiments.	Total life of mission.	2 years	This is the secondary ATS-4 station.

R & RR Transmitter/Receiver. This block represents the complete range and range rate system available at the ground station. It includes antenna transmitters, receivers, range tone generators and combiners, range and range rate extractors, data processor and output equipment. This equipment is described in the STADAN capabilities report.[6]

Telemetry Receiver. The block labeled telemetry receiver consists of:

- An auto track-controlled receiving antenna with 20dB gain and polarization diversity switching capability.
- A dual channel phaselock telemetry receiver with a second receiver provided as backup.
- A demodulation system with an additional system for backup.

The following functions are required of the telemetry receiver for ATS-4 operation:

- Receiving of PCM/PM and FM/PM telemetry signals of formats and bandwidth as described in Section 9.2.
- Product detector demodulation of the PM.
- Phaselock loop operation with an acquisition threshold of 3 dB.

The equipment required at the ground stations can be similar to the MOD-1 or GD-E receivers, the associated tracking filters and demodulators.

PCM-DHE. The block labeled PCM-DHE is the PCM data handling equipment. Its functions are as follows:

- Accept the PCM from the demodulator or tape recorder;
- Condition the signals;
- Extract frame synchronization;
- Extract words for quick-look display;
- Prepare signals for display and further processing.

The following capabilities are required of the PCM-DHE:

- Accept PCM telemetry of the formats described in Section 9.2.

The equipment can be similar to the Magnavox PCM Data Handling equipment described in the STADAN capabilities report.[6]

Analog Channel Discriminators. For the demodulation of the FM/PM analog channel, filters and subcarrier discriminators are required. The following functions must be performed:

- Accept the telemetry from the first demodulator.
- Filter the FM components.
- Pass the subcarrier through the discriminator and produce analog signals.

Discriminators must be available for the subcarrier frequencies as specified in Section 9.2.

Tape Recorder. A seven channel tape recorder with a backup unit is provided for recording telemetry signals. The telemetry signals can then be played back to the PCM DHE.* The recorder required

* Telemetry signals can also be connected directly from the receiver to the DHE for quick-look display.

- Transmitters: Transmitter equipment operating at 1.7, 2.1 and 8 GHz is required for ATS-4 operation. The output power requirement is moderate; it is expected to be below 1kW for all transmitters. The transmitters should have capabilities for SSBAM and FM transmission; the total transmitted signal bandwidth is estimated to be at most 10 MHz. Suitably modified existing equipment could be used for the S-band region; new equipment may be required for X-band.

- Receivers: Front end amplifiers and receivers for 100 MHz, 800 MHz, 2.3 GHz and 7.3 GHz are required. Suitable modified existing equipment may be used. The ground stations will require new X-band equipment.

- Mobile platform: A mobile transmitter platform is required for the monopulse measurement. The platform consists of an 8 GHz transmitter and a suitable antenna, mounted on a truck or van. This equipment must be self-contained and sufficiently mobile to be placed at desired locations to within a radius of about 100 miles from the site. The required transmitter power is in the order of 1kW; only short term operation is required.

  The mobile platform must be specially designed for ATS-4 operations.

- Antenna measurement electronics: The following equip- are required for antenna pattern measurements:

- A/D converter, 6 bit, 30 dB
- Tone generator
- Timing decoder, 3 bit
- Phase shift computer
- Beam position decoder
- Audio multiplexer
- Timing code generator (1 kHz)
- Delay line (1 sec)
- Synchronous receiver

Different configurations of the above-listed equipments will be used for the various measurements. Regular laboratory test equipment can be used. The receiver to be used for the the measurement is a modified Scientific Atlanta, Model 1600. The modification consists of a change in the IF bandwidth to 100 Hz and a change in the sweep rate of the local oscillator. These modifications will provide a signal-to-noise ratio sufficient to obtain the 40 dB dynamic range required for good pattern measurements.

- Communications experiments: Equipment for multichannel telephony and television transmission is required. It is expected that the Communication Test Evaluation Console, designed and used for the ATS program, can be utilized.

Command Transmitter. The block labeled command transmitter contains the following elements:

- A command antenna with a gain of at least 13.5 dB.
- A transmitter capable of delivering at least 200W output power.

The command antenna can be similar to dual Yagi antenna currently in use. The command transmitter must have at least the capability of the Collins 242 G-2 transmitter. More powerful transmitters and higher gain antennas may be employed; in this case the command link operation margin will increase.

Command Encoder. The command encoder generates the PCM command word suitable for ATS-4 operation. The functions required of the command encoder and possible equipment implementations are described in detail in Section 9.3. The command encoder will interface the MCC and some part of the controlling elements (switches for setting up commands) may be incorporated into the MCC.

For the encoder, new equipment may have to be installed; however, it may also be possible to modify the OGO command encoder to meet ATS-4 operating requirements. Requirements for new or modified equipment can only be determined when the equipment usage, degree of modification, and better definition of ATS-4 are available.

Interferometer Illumination. The interferometer illumination equipment consists of an 8 GHz transmitter and an antenna. The antenna-transmitter combination shall be capable of producing at least 64 dBW. The antenna may be a forty foot or larger parabolic reflector capable of operating at 8 GHz. The gain would be at least fifty-five dB. Consequently a transmitter power of about 10W would be sufficient. Smaller diameter antennas may be used if more power is transmitted.

The transmitted signal is an unmodulated continuous wave. The polarization of the signal shall be circular. The stability of the transmitted signal shall be $1:10^8$.

Master Control Console. The MCC is used to control the satellite operations. It interfaces the command encoder and effects the command transmission. It has the capability to request computation, support, operation of the R & RR equipment, and display of telemetry. The MCC shall control the following operations:

- Satellite attitude
- Satellite position
- Satellite subsystem status
- Telemetry data display
- Telemetry data routing to ATSOCC
- Satellite tracking
- Transmission of commands to the satellite
- Satellite experiment execution
- Ground computations to monitor satellite status.

The master control console shall have the capability to inhibit the transmission of certain commands. In some situations, the erroneous transmission of a command could lead to loss of some satellite equipment. An example would be operation during transfer orbit with the antenna petals folded, where onboard experiment transmitters must not be turned on, lest the power stages may be burned out.

Equipment for the MCC is presently not defined.

Experiment Control Console. The ECC controls the satellite experimentation and the satellite communication demonstrations. The ECC interfaces the MCC. Commands to perform experiments are requested from the ECC through the MCC. The ECC directly controls the communication experiments and the Interferometer illumination. The ECC also interfaces the ground computer and can request experiment evaluations for quick-look.

The ECC shall have the capabilities for:

- Requesting display of spacecraft telemetry
- Requesting calculations of experiment sequences
- Controlling of experiment data reduction for display and transmission to ATSOCC
- Requesting attitude changes
- Requesting command transmission
- Requesting attitude calculation
- Controlling interferometer illumination
- Controlling communication demonstration
- Requesting phased array beam pointing data calculations and transmission.

The equipment for the ECC is not presently defined. It is anticipated that new equipment must be developed for this purpose.

Ground computer. The ground computer provides for the data processing functions required at the ground atation. The ground computer interfaces the PCM-DHE, the display, the MCC, the ECC and may

for ATS-4 operation will be similar to the FR 600 recorder.

Display. The display unit presents information from the data word selectors. The data words either come from the PCM-DHE (quick-look) or from the ground computer. Display is requested through the MCC. Data is either presented on a chart recorder or on a visual numerical display.

Antenna Experiment Receivers, Antenna Experiment Transmitters, Communication Experiment Electronics and Antenna Pattern Measurement Equipment. The performance requirements of the equipment for these blocks are discussed in Section 2. Here a summary of the equipment is presented.

- Antennas: For performing the different measurements and conducting communication experiments, ground transmitter and receiver antennas are needed. At the ground stations, 40 ft. and 85 ft. diameter parabolic reflector antennas are available. Operation up to a frequency of 8 GHz is required.
- Antenna feeds: A feed group is needed for operating the parabolic reflector antennas at the nominal frequencies allocated to ATS-4. These frequencies are:

  100 MHz, 800 MHz, 2.3 GHz and 7.3 GHz for receiving of satellite transmission;

  1.7 GHz, 2.1 GHz and 8 GHz for transmission to the satellite.

  Simultaneous operation at several frequencies is planned. It is estimated that new feed groups need to be designed for ATS-4 operation.

also interface the R & RR system.* The ground computer shall have the capability to perform the following functions:

- Reduction of raw experiment data for display and transmission to ATSOCC;
- Determination of satellite attitude from tacking data in real-time;
- Computation of beam pointing data for the phased array;
- Computation of attitude control signals for communication demonstrations involving tracking;
- Computation of attitude data from interferometer readings;
- Simulation for interometer closed loop experiments;
- Computation of attitude control data for experiments requiring complex vehicle motions;
- Preparation of command and instruction sequences in format suitable for transmission to the satellite;
- Determination of experimentation operation sequences where required.

At present no recommendation for a computer can be made. After examining the requirements in more detail it can be determined whether present capabilities are sufficient or augmentation is required.

*The R & RR system has its own processor. The computer may, however, serve as an interface to the ground transmission equipment; in this interface capacity it may reformat the data.

Ground communications. Ground communication facilities to interconnect the ground stations and ATSOCC are required. These facilities are primarily teletypewriter and telephone circuits.

9.6 - REFERENCES

1. Jesse Maury and Frederick Styles, "Development of Optimum Frame Synchronization Code for GSFC PCM Telemetry Standards," presented at the National Telemetering Conference, June 1964.

2. Merwin Williard, "PCM Telemetry Synchronization," presented at the National Telemetering Conference, May 1961.

3. Benn D. Martin, "The Pioneer IV Lunar Probe; A. Minimum Power FM/PM Design," JPL Technical Report No. 32-215, 15 March 1962.

4. "Telemetry Systems Study," Final Report Aeronutronic Publication No. U-743, Volume I, December 1959.

5. Aerospace Data Systems Standards, Part II, Command Standards, Section 3, PCM Instruction Command System Standard, February 25, 1965, GSFC, NASA, Greenbelt, Md.

6. Goddard SFC, Greenbelt, Md., "Space Tracking and Data Acquisition Network Facilities," Report X-530-66-33, December 1965.

APPENDIX 9A

COMMUTATOR CHANNEL ASSIGNMENTS

The channel assignments for each of the commutators are derived from the Telemetry Signal Catalog of Section 9.1. A set of suggested commutator channel assignments follows:

Main Commutator

1	Sync
2	Sync
3	Spare
4	Spare
5	Command System Decoder Latch Status
	Command System Decoder Power Status
	Command System Address Check
	Command System Word Check
	Command System Word Execute
6	Spare
7	Vibration
8	Sub-Commutator #1
9	Coarse Sun Sensor Pitch Error
10	Coarse Sun Sensor Yaw Error
11	Fine Sun Sensor Pitch Error
12	Spare
13	Fine Sun Sensor Yaw Error
14	Roll Gyro Output
15	Pitch Gyro Output
16	Sub-Commutator #2
17	Yaw Gyro Output
18	Inverter Output
19	Spare
20	Spare
21	Command System Decoder Latch Status
	Command System Decoder Power Status
	Command System Address Check
	Command System Word Check
	Command System Word Execute
22	Spare
23	Vibration
24	Sub-Commutator #3
25	Power Supply Voltage
26	Propellant Tank and Line Pressure
27	Propellant Tank and Line Pressure
28	Spare
29	Propellant Tank and Line Pressure
30	Propellant Tank and Line Pressure
31	Propellant Tank and Line Pressure
32	Sub-Commutator #4
33	Propellant Tank and Line Pressure
34	Propellant Tank and Line Pressure
35	Spare
36	Spare

Main Commutator - continued - 2

37	Command System Decoder Latch Status
	Command System Decoder Power Status
	Command System Address Check
	Command System Word Check
	Command System Word Execute
38	Spare
39	Propellant Tank and Line Pressure
40	Sub-Commutator #5
41	Propellant Tank and Line Pressure
42	Propellant Tank and Line Pressure
43	Propellant Tank and Line Pressure
44	Spare
45	8 GHz rcvr Mono P., AGC Voltage (I.F.)
46	8 GHz rcvr Mono R., AGC Voltage (I.F.)
47	Monopulse Roll Error
48	Sub-Commutator #6
49	Monopulse Pitch Error
50	Element Temperature
51	Spare
52	Spare
53	Command System Decoder Latch Status
	Command System Decoder Power Status
	Command System Address Check
	Command System Word Check
	Command System Word Execute
54	Spare
55	Vibration
56	Sub-Commutator #7
57	Element Temperatures
58	Element Temperatures
59	Element Temperatures
60	Spare
61	Element Temperatures
62	Element Temperatures
63	Element Temperatures
64	Sub-Commutator #8
65	Element Temperatures
66	Element Temperatures
67	Spare
68	Spare
69	Command System Decoder Latch Status
	Command System Decoder Power Status
	Command System Address Check
	Command System Word Check
	Command System Word Execute
70	Spare

71	Vibration
72	Sub-Commutator #9
73	Element Temperatures
74	VCO Control Voltage
75	S. T. Error Signal
76	Roll and Pitch Error Signal (attitude)
77	Roll Error Signal (attitude)
78	Pitch Error Signal (attitude)
79	Roll (Inertia Wheel Speed)
80	Sub-Commutator #10
81	Pitch Inertia Wheel Speed
82	Yaw Inertia Wheel Speed
83	Spare
84	Spare
85	Command System Decoder Latch Status
	Command System Decoder Power Status
	Command System Address Check
	Command System Word Check
	Command System Word Execute
86	Spare
87	Valve Status
88	Sub-Commutator #11
89	Spare
90	Spacecraft Time
91	Spare
92	Spare
93	Spare
94	S/C Clock
95	S/C Clock
96	Sub-Commutator #12
97	S/C Clock
98	Roll Inertia Wheel Current
	Pitch Inertia Wheel Current
	Yaw Inertia Wheel Current
	Sun Acquisition Logic Activated
	Earth Acquisition Logic Activated
	Star Acquisition Logic Activated
	Sun Presence - CSS
	Sun Presence - FSS
99	Spare
100	Spare
101	Command System Decoder Latch Status
	Command System Decoder Power Status
	Command System Address Check
	Command System Word Check
	Command System Word Execute

Main Commutator - continued - 4

102	Spare
103	Vibration
104	Sub-Commutator #13
105	Valve Status
	Valve Status
	Valve Status
	Valve Status
	4 Discretes
106	Interferometer Smoothed - Buffered Counter Output
107	Interferometer Smoothed - Buffered Counter Output
108	Interferometer Smoothed - Buffered Counter Output
109	Interferometer Smoothed - Buffered Counter Output
110	Interferometer Smoothed - Buffered Counter Output
111	Interferometer Smoothed - Buffered Counter Output
112	Sub-Commutator #14
113	Interferometer Smoothed - Buffered Counter Output
114	Interferometer Smoothed - Buffered Counter Output
115	Interferometer Processor Output, θ
116	Interferometer Processor Output, ϕ
117	Interferometer Processor Output, ψ
118	Command System Decoder Latch Status
	Command System Decoder Power Status
	Command System Address Check
	Command System Word Check
	Command System Word Execute
119	Vibration
120	Sub-Commutator #15
121	Spare
122	Spare
123	Spare
124	Spare
125	Spare
126	Spare
127	Spare
128	Sub-Commutator #16

Sub-Commutator #1

1 Sync
2 Panel Current
3 Panel Current
4 Panel Current
5 Panel Current
6 Panel Voltage
7 Panel Voltage
8 Panel Voltage

Sub-Commutator #2

1 Sync
2 Panel Voltage
3 Load Current (DC Load)
4 Load Current (DC/DC Input)
5 Load Current (Inverter Input)
6 Load Current (DC/DC Conv.)
7 Load Current (Inverter)
8 Load Voltage (DC/DC Conv.)

Sub-Commutator #3

1 Sync
2 Load Voltage (DC Load)
3 Load Voltage (Inverter)
4 Regulator Current
5 Regulator Current
6 Regulator Voltage
7 Regulator Voltage
8 Battery Current

Sub-Commutator #4

1 Sync
2 Battery Current
3 Battery Voltage
4 Battery Voltage
5 Attitude Control Subsy. Temp.
6 Attitude Control Subsy. Temp.
7 Attitude Control Subsy. Temp.
8 Attitude Control Subsy. Temp.

Sub-Commutator #5

1	Sync
2	Attitude Control Subsy. Temp.
3	Array and Antenna Expt. Temps.
4	Array and Antenna Expt. Temps.
5	Array and Antenna Expt. Temps.
6	Array and Antenna Expt. Temps.
7	Array and Antenna Expt. Temps.
8	Array and Antenna Expt. Temps.

Sub-Commutator #6

1	Sync
2	Array and Antenna Expt. Temps.
3	Array and Antenna Expt. Temps.
4	Array and Antenna Expt. Temps.
5	Array and Antenna Expt. Temps.
6	Array and Antenna Expt. Temps.
7	Array and Antenna Expt. Temps.
8	Array and Antenna Expt. Temps.

Sub-Commutator #7

1	Sync
2	Array and Antenna Expt. Temps.
3	Interferometer Expt. Temp.
4	Interferometer Expt. Temp.
5	Interferometer Expt. Temp.
6	Interferometer Expt. Temp.
7	Telemetry Subsystem Temp.
8	Telemetry Subsystem Temp.

Sub-Commutator #8

1	Sync
2	Sub-Sub-Commutator #1
3	Telemetry Subsystem Temp.
4	Telemetry Subsystem Temp.
5	Power Subsystem Temp.
6	Power Subsystem Temp.
7	Power Subsystem Temp.
8	Power Subsystem Temp.

Sub-Commutator #9

1 Sync
2 Power Subsystem Temp.
3 Power Subsystem Temp.
4 Power Subsystem Temp.
5 Power Subsystem Temp.
6 Secondary Expts. Temp.
7 Secondary Expts. Temp.
8 Structures Subsystem Temp.

Sub-Commutator #10

1 Sync
2 Structures Subsystem Temp.
3 Structures Subsystem Temp.
4 Structures Subsystem Temp.
5 Structures Subsystem Temp.
6 Structures Subsystem Temp.
7 Structures Subsystem Temp.
8 Structures Subsystem Temp.

Sub-Commutator #11

1 Sync
2 Structures Subsystem Temp.
3 Structures Subsystem Temp.
4 Structures Subsystem Temp.
5 Structures Subsystem Temp.
6 Structures Subsystem Temp.
7 Structures Subsystem Temp.
8 Structures Subsystem Temp.

Sub-Commutator #12

1 Sync
2 Structures Subsystem Temp.
3 Structures Subsystem Temp.
4 Structures Subsystem Temp.
5 Structures Subsystem Temp.
6 Structures Subsystem Temp.
7 Structures Subsystem Temp.
8 Structures Subsystem Temp.

Sub-Commutator #13

1	Sync
2	Structures Subsystem Temp.
3	Structures Subsystem Temp.
4	Structures Subsystem Temp.
5	Structures Subsystem Temp.
6	Structures Subsystem Temp.
7	Structures Subsystem Temp.
8	Structures Subsystem Temp.

Sub-Commutator #14

1	Sync
2	Structures Subsystem Temp.
3	Structures Subsystem Temp.
4	Structures Subsystem Temp.
5	Structures Subsystem Temp.
6	Charging Select
	Charging Select
	Load Select
	Load Select
	Load Select
	Load Select
	Load Select
	Load Select
7	Load Select
	Load Select
	Load Select
	Load Current (DC/DC Conv.)
	Load Current (Inverter)
	Battery Select
	Battery Select
	1 Discrete
8	Spare

Sub-Commutator #15

1	Sync
2	Spare
3	Spare
4	Spare
5	Spare
6	Spare
7	Spare
8	Spare

Sub-Commutator #16

1	Sync
2	Sub-Sub-Commutator #2
3	Spare
4	Spare
5	Spare
6	Spare
7	Spare
8	Spare

Sub-Sub-Commutator #1

1	Sync
2	1.7 GHz rcvr, Temperature (IF)
3	1.7 GHz rcvr, Temperature (LO)
4	1.7 GHz rcvr, Power (LO)
5	1.7 GHz rcvr, Operating Voltage (LO)
6	1.7 GHz rcvr, Collector Voltage (IF)
7	1.7 GHz rcvr, AGC Voltage (IF)
8	1.7 GHz rcvr, Crystal Current (Mixer)
9	2.1 GHz rcvr, Temperature (IF)
10	2.1 GHz rcvr, Temperature (LO)
11	2.1 GHz rcvr, Power (LO)
12	2.1 GHz rcvr, Operating Voltage (LO)
13	2.1 GHz rcvr, Collector Voltage (IF)
14	2.1 GHz rcvr, AGC Voltage (IF)
15	2.1 GHz rcvr, Crystal Current (Mixer)
16	8 GHz rcvr Mono P: Crystal Current (Mixer)
17	8 GHz rcvr Mono P: Collector Voltage (IF)
18	8 GHz rcvr Mono P: Temperature (IF)
19	8 GHz rcvr Mono, Crystal Current (Mixer)
20	8 GHz rcvr Mono, Collector Voltage (IF)
21	8 GHz rcvr Mono, Temperature
22	.1 GHz xmtr, Temperature (LO)
23	.1 GHz xmtr, Operating Voltage (LO)
24	.1 GHz xmtr, Power (LO)
25	.1 GHz xmtr, Crystal Current (Mixer)
26	.1 GHz xmtr, Temperature (Ampl.)
27	.1 GHz xmtr, Operating Voltage (Ampl.)
28	.1 GHz xmtr, VSWR
29	.1 GHz xmtr, Power (RF Output)
30	.8 GHz xmtr, Temperature (LO)
31	.8 GHz xmtr, Operating Voltage (LO)
32	.8 GHz xmtr, Power (LO)
33	.8 GHz xmtr, Crystal Current (Mixer)
34	.8 GHz xmtr, Temperature (Ampl.)
35	.8 GHz xmtr, Operating Voltage (Ampl.)
36	.8 GHz xmtr, VSWR
37	.8 GHz xmtr, Power (RF Output)
38	.8 GHz rcvr, Temperature (IF)
39	.8 GHz rcvr, Temperature (LO)
40	.8 GHz rcvr, Power (LO)
41	.8 GHz rcvr, Operating Voltage (LO)
42	.8 GHz rcvr, Collector Voltage (IF)
43	.8 GHz rcvr, AGC Voltage (IF)
44	.8 GHz rcvr, Crystal Current (Mixer)
45	7.3 GHz xmtr, Temperature #1 (LO)

46	7.3 GHz xmtr, Temperature #2 (LO)
47	7.3 GHz xmtr, Power #1 (LO)
48	7.3 GHz xmtr, Power #2 (LO)
49	7.3 GHz xmtr, Crystal Current (Mixer)
50	7.3 GHz xmtr, Temperature (Amplifier)
51	7.3 GHz xmtr, Operating Voltage (Ampl.)
52	7.3 GHz xmtr, Operating Voltage #1 (LO)
53	7.3 GHz xmtr, Operating Voltage #2 (LO)
54	7.3 GHz xmtr, VSWR
55	7.3 GHz xmtr, Power (RF Output)
56	High Voltage Conv. #2 Voltage
57	High Voltage Conv. #2 Current
58	2.3 GHz xmtr Temperature (LO)
59	2.3 GHz xmtr, Operating Voltage (LO)
60	2.3 GHz xmtr, Power (LO)
61	2.3 GHz xmtr, Crystal Current (Mixer)
62	2.3 GHz xmtr, Temperature (Ampl.)
63	2.3 GHz xmtr, Operating Voltage (Ampl.)
64	Sub-Sub-Sub-Commutator #1

Sub-Sub-Commutator #2

1	Sync
2	8 GHz rcvr, Temperature (IF)
3	8 GHz rcvr, Temperature (LO)
4	8 GHz rcvr, Power (LO)
5	8 GHz rcvr, Operating Voltage (LO)
6	8 GHz rcvr, Collector Voltage (IF)
7	8 GHz rcvr, AGC Voltage (IF)
8	8 GHz rcvr, Crystal Current (Mixer)
9	7.3 GHz xmtr, Temperature #1 (LO)
10	7.3 GHz xmtr, Temperature #2 (LO)
11	7.3 GHz xmtr, Power #1 (LO)
12	7.3 GHz xmtr, Power #2 (LO)
13	7.3 GHz xmtr, Crystal Current (Mixer)
14	7.3 GHz xmtr, Temperature (amplifier)
15	7.3 GHz xmtr, Operating Voltage (Ampl.)
16	7.3 GHz xmtr, Operating Voltage #1 (LO)
17	7.3 GHz xmtr, Operating Voltage #2 (LO)
18	7.3 GHz xmtr, VSWR
19	7.3 GHz xmtr, Power (RF Output)
20	Voltage, High Voltage Conv. #1
21	Current, High Voltage Conv. #1
22	AGC Voltage
23	Crystal osc. calibration ckt voltage
24	Crystal Current #1
25	Crystal Current #2
26	Clock Crystal Current
27	Mixer Crystal Current
28	Mixer Crystal Current
29	Mixer Crystal Current
30	Mixer Crystal Current
31	Mixer Crystal Current
32	R & R Transponder Voltage
33	R & R Transponder Current
34	Spare
35	Spare
36	Identification Tone, Gnd xmtr #1
	Identification Tone, Gnd xmtr #2
	6 Discretes
37	2.3 GHz xmtr, VSWR
38	2.3 GHz xmtr, Power (RF Output)
39	Telemetry Decoder #1 Voltage
40	Telemetry Decoder #2 Voltage
41	Telemetry Decoder #1 Current
42	Telemetry Decoder #2 Current
43	Telemetry Transmitter #1 Voltage

Sub-Sub-Commutator #2 - continued - 2

44	Telemetry Transmitter #2 Voltage
45	Telemetry Transmitter #2 Current
46	Telemetry Transmitter #2 Current
47	Spare
48	Spare
49	Spare
50	Spare
51	Spare
52	Spare
53	Spare
54	Spare
55	Spare
56	Spare
57	Spare
58	Spare
59	Spare
60	Spare
61	Spare
62	Spare
63	Spare
64	Spare

Sub-Sub-Sub-Commutator #1

1	Sync
2	Gas Tank #1 Pressure
3	Gas Tank #1 Temperature
4	Gas Tank #2 Pressure
5	Gas Tank #2 Temperature
6	S. T. Yaw Gimbal Position
7	S. T. Roll Gimbal Position
8	Positive Yaw Jets On
	Negative Yaw Jets On
	Positive Pitch Jets On
	Negative Pitch Jets On
	Positive Roll Jets On
	Negative Roll Jets On
	Star Tracker #1 Sun Shutter Position
	Star Tracker #2 Sun Shutter Position
9	Earth Presence - Pitch
	Earth Presence - Roll
	Gyros Power On
	Horizon Sensor Power On
	Horizon Sensor Mode
	Gyro Mode
	Monopulse Mode
	Station Keeping Mode
10	S. T. Star Presence
	Standby Star Tracker Sec #1 On
	Standby Star Tracker Sec #2 On
	Standby Horizon Sensor On
	Standby Sun Sensor On
	Standby Roll Wheel Electronics On
	Standby Pitch Wheel Electronics On
	Standby Yaw Wheel Electronics On
11	Standby Inverter On
	Standby Roll Jet Valves On
	Standby Pitch Jet Valves On
	Standby Yaw Jet Valves On
	St andby Controller Sec #1 On
	Standby Controller Sec #2 On
	Standby Controller Sec #3 On
	Standby Controller Sec #4 On
12	Standby Controller Sec #5 On
	Standby Controller Sec #6 On
	Standby Controller Sec #7 On
	Standby Controller Sec #8 On
	Standby Controller Sec #9 On
	3 Discretes

Sub-Sub-Sub-Commutator #1 - continued - 2

13	Spare
14	Spare
15	Spare
16	Spare
17	Spare
18	Spare
19	Spare
20	Spare
21	Spare
22	Spare
23	Spare
24	Spare
25	Spare
26	Spare
27	Spare
28	Spare
29	Spare
30	Spare
31	Spare
32	Spare

APPENDIX 9B

MODULATION INDEX CALCULATIONS (MODE I)

To solve for the modulation indicies for each of the data channels so that the channel SNR's are equal at the output of the channel bandpass filters, we make the peak deviation of each channel proportional to the square root of the bandwidth of each channel.

That is:

$$\frac{\Delta\theta_o}{\sqrt{B_o}} = \frac{\Delta\theta_1}{\sqrt{B_1}} = \frac{\Delta\theta_2}{\sqrt{B_2}} = \frac{\Delta\theta_3}{\sqrt{B_3}} = \frac{\Delta\theta_4}{\sqrt{B_4}}$$

where:

$\Delta\theta_i$ is the peak deviation of the carrier due to the ith channel,

and B_i is the channel filter bandwidth and is equal to 15 percent of the IRIG subcarrier center frequency (IRIG channels 7, 8, 9, and 10 were selected) and one-half the bit rate of the baseband channel.

Substituting the filter bandwidths,

$$\frac{\Delta\theta_o}{\sqrt{1152}} = \frac{\Delta\theta_1}{\sqrt{346}} = \frac{\Delta\theta_2}{\sqrt{450}} = \frac{\Delta\theta_3}{\sqrt{586}} = \frac{\Delta\theta_4}{\sqrt{810}}$$

or

$$\frac{\Delta\theta_o}{33.9} = \frac{\Delta\theta_1}{18.6} = \frac{\Delta\theta_2}{21.2} = \frac{\Delta\theta_3}{24.2} = \frac{\Delta\theta_4}{28.4}$$

Solving for $(\Delta\theta_1)^2$, $(\Delta\theta_2)^2$, $(\Delta\theta_3)^2$, and $(\Delta\theta_4)^2$ in terms of $(\Delta\theta_0)^2$ yields

$$(\Delta\theta_1)^2 = .302\,(\Delta\theta_0)^2$$

$$(\Delta\theta_2)^2 = .391\,(\Delta\theta_0)^2$$

$$(\Delta\theta_3)^2 = .560\,(\Delta\theta_0)^2$$

$$(\Delta\theta_4)^2 = .702\,(\Delta\theta_0)^2$$

For an rms deviation of one radian:

$$\frac{(\Delta\theta_0)^2}{2} + \frac{(\Delta\theta_1)^2}{2} + \frac{(\Delta\theta_2)^2}{2} + \frac{(\Delta\theta_3)^2}{2} + \frac{(\Delta\theta_4)^2}{2} = (1)^2$$

Substituting in the above equation and rearranging yields:

$$(\Delta\theta_0)^2 \quad .5 + .151 + .196 + .280 + .351 \quad = 1$$

$$(\Delta\theta_0)^2 = .679$$

Substituting $(\Delta\theta_0)^2$ into the values of $(\Delta\theta_1)^2$, $(\Delta\theta_2)^2$, $(\Delta\theta_3)^2$, and $(\Delta\theta_4)^2$ and solving for the modulation index of each channel yields:

$$\Delta\theta_0 = .825$$

$$\Delta\theta_1 = .454$$

$$\Delta\theta_2 = .517$$

$$\Delta\theta_3 = .590$$

$$\Delta\theta_4 = .692$$

APPENDIX 9C

SOLVING FOR RECEIVER NOISE POWER AND CHANNEL BANDWIDTH RATIOS (MODE I)

Bandwidth Ratios (Mode I)

In Mode I operation, the five data channels modulating the transmitter results in an information bandwidth on the transmitter carrier:

$$B_{f_m} = 2f_m \ (\Delta\theta + 1)$$

where, f_m = **maximum modulation frequency (for a 5.4 kHz subcarrier, f_m 5.805 kHz)**

$\Delta\theta$ = composite peak deviation = 1.4 radians

Therefore:

$$B_{f_m} = (2)\ (5.805\ \text{kHz})\ (1.4 + 1)$$

$$B_{f_m} = 26.3\ \text{kHz}$$

The total RF bandwidth is equal to the summation of the information bandwidth (B_{f_m}), the doppler shift Δf, and the frequency stability of the transmitter.

Because we have a stationary satellite, doppler shift will be assumed to be negligible.

The frequency stability of the transmitter will be ± 0.005 percent of the carrier frequency. This figure includes instabilities in the transmitter and the receiver local oscillator. At 136 Mc the stability is ± 6.8 kHz or a total of 13.6 kHz.

The total RF bandwidth is equal to 39.9 kHz but since a carrier tracking receiver will be used which will have a capability of tracking over a $\pm$ 10 kc range, the transmitter instabilities will be automatically compensated for and a 30 kHz first detector IF bandwidth will be suitable.

When Mode I is being used prior to the spacecraft being in a stationary orbit, the carrier tracking receiver will also compensate for doppler shifts so the 30 kHz bandwidth will be suitable then also.

P_{nr} the noise power of the receiver is expressed as:

$$P_{nr} = kT_eB_{IF}$$

$$P_{nr} = -123.7 \text{ dBm}$$

The bandwidth ratios for each channel are:

$$\frac{B_{IF}}{B_{c-0}} = 26 = 14.1 \text{ dB}$$

$$\frac{B_{IF}}{B_{c-1}} = 87 = 19.4 \text{ dB}$$

$$\frac{B_{IF}}{B_{c-2}} = 68 = 18.2 \text{ dB}$$

$$\frac{B_{IF}}{B_{c-3}} = 51 = 17.1 \text{ dB}$$

$$\frac{B_{IF}}{B_{c-4}} = 37 = 15.7 \text{ dB}$$

APPENDIX 9D

SOLVING FOR RECEIVER NOISE POWER AND CHANNEL BANDWIDTH RATIO (MODE II)

Bandwidth Ratio (Mode II)

In Mode II operation, the baseband channel modulating the transmitter results in an information bandwidth on the transmitter carrier as:

$$B_{f_m} = 2 f_m (\Delta \theta + 1)$$

where, f_m = maximum modulating frequency or .576 kHz for the baseband channel

$\Delta \theta$ = 1.4 radians peak

Therefore:

$$B_{f_m} = 2.86 \text{ kHz}$$

However, the ground receiver will have a minimum predetection bandwidth of 10 kHz (B_{IF}) and thus 10 kHz will be used as the information bandwidth. (Note! The remarks in Appendix B relative to doppler shift and transmitter instabilities will also apply for the Mode I system).

The noise power (P_{nr}) in the receiver is expressed as:

$$P_{nr} = kT_e B_{IF} = -128.5 \text{ dBm}$$

The bandwidth ratio for the baseband channel is:

$$\frac{B_{IF}}{B_{c-0}} = 8.67 = 9.4 \text{ db}$$

APPENDIX 9E

COMMAND SIGNAL CATALOG

Note: The prefix before the signal number identifies the satellite subsystem which requires the command signal. The prefixes mean the following:

$\overline{J}$	Auxiliary Propulsion System
$\overline{C}$	Orientation Control System
$\overline{I}$	Interferometer
$\overline{O}$	Instrumentation
$\overline{D}$	Parabolic antenna experiment
$\overline{A}$	Phased array
$\overline{P}$	Power system
$\overline{E}$	Secondary experiment
$\overline{S}$	Structure
$\overline{T}$	Temperature control.

There are two command message types.

X... Discrete

M... Data

Command Number	Function	Type
$\overline{J}1$-$\overline{J}4$	Valve commands	X
$\overline{J}$-5	APS on	X
$\overline{J}$-6	APS off	X
$\overline{S}$-1	Petal squibs fire	X
$\overline{S}$-2	Locking squibs fire	X
$\overline{S}$-3	Solar panels deploy	X
$\overline{S}$-4	Turn on calibration generator	X
$\overline{S}$-5	Turn off calibration generator	X

Command Number	Function	Type
$\overline{C}$-1	Acquire sun	X
$\overline{C}$-2	Acquire earth	X
$\overline{C}$-3	Positive direction of polaris search	X
$\overline{C}$-4	Set Star Tracker roll gimbal position	X
$\overline{C}$-5	Set Star Tracker yaw gimbal position	X
$\overline{C}$-6	Negative direction of polaris search	X
$\overline{C}$-7	Set time of polaris search	X
$\overline{C}$-8	Pitch offset command	M, 12 bits
$\overline{C}$-9	Roll offset command	M, 12 bits
$\overline{C}$-10	Horizon sensor control	X
$\overline{C}$-11	Monopulse control	X
$\overline{C}$-12	Gyro control	X
$\overline{C}$-13	Jets only	X
$\overline{C}$-14	Positive roll rate command	X
$\overline{C}$-15	Negative roll rate command	X
$\overline{C}$-16	Positive pitch rate command	X
$\overline{C}$-17	Negative pitch rate command	X
$\overline{C}$-18	Gyro power off	X
$\overline{C}$-19	Gyro power on	X
$\overline{C}$-20	Horizon sensor power off	X
$\overline{C}$-21	Horizon sensor power on	X
$\overline{C}$-22	Switch standby star tracker Sect. 1	X

Command Number	Function	Type
$\overline{C}$-23	Switch standby star tracker Sect. 2	X
$\overline{C}$-24	Switch standby horizon sensor	X
$\overline{C}$-25	Switch standby sun sensor	X
$\overline{C}$-26	Switch standby roll wheel drive electronics	X
$\overline{C}$-27	Switch standby pitch wheel drive electronics	X
$\overline{C}$-28	Switch standby yaw wheel drive electronics	X
$\overline{C}$-29	Switch standby inverter	X
$\overline{C}$-30	Switch standby roll jet valves	X
$\overline{C}$-31	Switch standby pitch jet valves	X
$\overline{C}$-32	Switch standby yaw jet valves	X
$\overline{C}$-33	Switch standby controller Sec. 1	X
$\overline{C}$-34	Switch standby controller Sec. 2	X
$\overline{C}$-35	Switch standby controller Sec. 3	X
$\overline{C}$-36	Switch standby controller Sec. 4	X
$\overline{C}$-37	Switch standby controller sec. 5	X
$\overline{C}$-38	Switch standby controller Sec. 6	X
$\overline{C}$-39	Switch standby controller Sec. 8	X
$\overline{C}$-40	Switch standby controller Sec. 8	X
$\overline{C}$-41	Switch standby controller Sec. 9	X
$\overline{C}$-42	Drift time roll gyro	M, 8 bits
$\overline{C}$-43	Drift trim pitch gyro	M, 8 bits
$\overline{C}$-44	Drift time yaw gyro	M, 8 bits

Command Number	Function	Type
$\bar{P}$-1	Disconnect preorbital battery	X
$\bar{P}$-2	Select Battery A	X
$\bar{P}$-3	Select Battery B	X
$\bar{P}$-4	Select Charger A	X
$\bar{P}$-5	Select Charger B	X
$\bar{P}$-6, P-14	Turn on main load switches 1-9	X
$\bar{P}$-15, P-23	Turn off main load switches 1-9	X
$\bar{P}$-24	Turn on inverter	X
$\bar{P}$-25	Turn off inverter	X
$\bar{P}$-26	Turn on D-C/D-C converter	X
$\bar{P}$-27	Turn off D-C/D-C converter	X
$\bar{P}$-28	Select Regulator A	X
$\bar{P}$-29	Select Regulator B	X

Command Number	Function	Type
$\overline{D}$-1	8 GHz #1 rcvr on	X
$\overline{D}$-2	8 GHz #1 rcvr off	X
$\overline{D}$-3	2.1 GHz rcvr on	X
$\overline{D}$-4	2.1 GHz rcvr off	X
$\overline{D}$-5	1.7 GHz rcvr on	X
$\overline{D}$-6	1.7 GHz rcvr off	X
$\overline{D}$-7	7.3 GHz xmtr on	X
$\overline{D}$-8	7.3 GHz xmtr off	X
$\overline{D}$-9	2.3 GHz xmtr on	X
$\overline{D}$-10	2.3 GHz xmtr off	X
$\overline{D}$-11	800 MHz xmtr on	X
$\overline{D}$-12	800 MHz xmtr off	X
$\overline{D}$-13	100 MHz xmtr on	X
$\overline{D}$-14	100 MHz xmtr off	X
$\overline{D}$-15	Auxiliary LO on	X
$\overline{D}$-16	Auxiliary LO off	X
$\overline{D}$-17	Pattern modulator for LO on	X
$\overline{D}$-18	Pattern modulator for LO off	X
$\overline{D}$-19	High voltage converter #1, on	X
$\overline{D}$-20	High voltage converter #1, off	X

Command Number	Function	Type
$\bar{D}$-21	High voltage converter #2, on	X
$\bar{D}$-22	High voltage converter #2, off	X
$\bar{D}$-23	Redundant TWT to transmitter #1	X
$\bar{D}$-24	Redundant TWT to transmitter #2	X
$\bar{D}$-25	Redundant triode on	X
$\bar{D}$-26	Redundant triode off	X
$\bar{D}$-27	Redundant IF #1 on	X
$\bar{D}$-28	Redundant IF #1 off	X
$\bar{D}$-29	Redundant IF #2 on	X
$\bar{D}$-30	Redundant IF #2 off	X
$\bar{D}$-31	Redundant IF #2 off	X
$\bar{D}$-32	Redundant IF #3 off	X
$\bar{D}$-33	Monopulse to automatic mode	X
$\bar{D}$-34	Monopulse override	X
$\bar{D}$-35	Switch 8 GHz rcvr to monopulse sum channel	X
$\bar{D}$-36	Monopulse receiver pair on	X
$\bar{D}$-37	Monopulse receiver pair off	X

Command Number	Function	Type
$\bar{A}$-1	8 GHz #2 receiver on	X
$\bar{A}$-2	8 GHz #2 receiver off	X
$\bar{A}$-3	7.3 GHz #2 transmitter on	X
$\bar{A}$-4	7.3 GHz #2 transmitter off	X
$\bar{A}$-5	Auxiliary LO on	X
$\bar{A}$-6	Auxiliary LO off	X
$\bar{A}$-7	8 GHz receiver #1 to array port #1	X
$\bar{A}$-8	8 GHz receiver #1 to array port #2	X
$\bar{A}$-9	8 GHz receiver #1 to parabolic antenna	X
$\bar{A}$-10	8 GHz receiver #2 to array port #1	X
A-11	8 GHz receiver #2 to array port #2	X
$\bar{A}$-12	8 GHz receiver #2 to parabolic antenna	X
$\bar{A}$-13	7.3 GHz transmitter #1 to array port #3	X
$\bar{A}$-14	7.3 GHz transmitter #1 to array port #4	X
$\bar{A}$-15	7.3 GHz transmitter to parabolic antenna	X

Command Number	Function	Type
$\overline{A}$-16	7.3 GHz transmitter #2 to array port #3	X
$\overline{A}$-17	7.3 GHz transmitter #2 to array port #4	X
$\overline{A}$-18	7.3 GHz transmitter #2 to parabolic antenna	X
$\overline{A}$-19	Instructions for beam pointing	M-35 bits
$\overline{I}$-1	Select manual operation mode	X
$\overline{I}$-2	Tune to off band noise	X
$\overline{I}$-3	Tune to calibration	X
$\overline{I}$-4	Tune to ground station #1	X
$\overline{I}$-5	Tune to ground station #2	X
$\overline{I}$-6	Select element pair 1-2	X
$\overline{I}$-7	Select element pair 1-3	X
$\overline{I}$-8	Select element pair 1-4	X
$\overline{I}$-9	Select element pair 1-5	X
$\overline{I}$-10	Select element pair 2-3	X
$\overline{I}$-11	Select element pair 4-5	X
$\overline{I}$-12	Turn on equipment	X

Command Number	Function	Type
$\overline{I}$-13	Turn off equipment	X
$\overline{I}$-14	Select automatic mode	X
$\overline{I}$-15	Start automatic mode	X
$\overline{I}$-16	Stop automatic mode	X
$\overline{I}$-17	Connect interferometer processor to attitude control system	X
$\overline{I}$-18	Disconnect interferometer processor from attitude control system	X
$\overline{I}$-19	Interferometer data word	M-12 bits
$\overline{C}$-1 to $\overline{O}$-8	(8) Switch telemetry transmission mode	X
$\overline{O}$-9	Encoder 1 to xmtr 1 and encoder 2 to xmtr 2	X
$\overline{O}$-10	Encoder 2 to xmtr 1 and encoder 1 to xmtr 2	X
$\overline{O}$-11	Xmtr 1 on	X
$\overline{O}$-12	Xmtr 1 off	X
$\overline{O}$-13	Xmtr 2 on	X
$\overline{O}$-14	Xmtr 2 off	X
$\overline{O}$-15	Range and rate transponder on	X
$\overline{O}$-16	Range and rate transponder off	X

APPENDIX 9F

TELEMETRY SIGNAL CATALOG

Note: The prefix before the signal number identifies the satellite subsystem which generates the telemetry signal. The prefixes mean the following:

J	Auxiliary Propulsion System
C	Orientation Control System
I	Interferometer
O	Instrumentation
D	Parabolic Antenna Experiment
A	Phased Array
P	Power System
E	Secondary Experiments
S	Structure
T	Temperature Control

Attitude Control Subsystem (C) Housekeeping Telemetry

No.	Sampled Parameter	Sampling Rate	Duration	Accuracy
C-1	Positive Yaw Jets On	1/4096 sec	Continuous Intero.	Discrete
C-2	Negative Yaw Jets On			
C-3	Positive Pitch Jets On			
C-4	Negative Pitch Jets On			
C-5	Positive Roll Jets On			
C-6	Negative Roll Jets On			
C-7	Gas Tank #1 Pressure		Continuous	± 3%
C-8	Gas Tank #1 Temperature			± 3%
C-9	Gas Tank #2 Pressure			± 5%
C-10	Gas Tank #2 Temperature			± 5%
C-11	Star Tracker #1 Sun Shutter Position			Discrete
C-12	Star Tracker #2 Sun Shutter Position			Discrete
C-13	S. T. Yaw Gimbal Position			8 Bits
C-14	S. T. Roll Gimbal Position			4 Bits
C-15	S. T. Star Presence			Discrete
C-16	S. T. Error Signal	1/sec	Continuous	8 Bits
C-17	Roll Error Signal (Attitude)			12 Bits
C-18	Pitch Error Signal (Attitude)			12 Bits
C-19	Coarse Sun Sensor Pitch Error			± 5%
C-20	Coarse Sun Sensor Yaw Error			± 5%
C-21	Fine Sun Sensor Pitch Error			± 5%
C-22	Fine Sun Sensor Yaw Error			± 5%
C-23	Roll Gyro Output			± 5%
C-24	Pitch Gyro Output			± 5%
C-25	Yaw Gyro Output			± 5%
C-26	Earth Presence - Pitch	1/4096 sec	Continuous	Discrete
C-27	Earth Presence - Roll	1/4096 sec		
C-28	Sun Presence - CSS	1/sec		
C-29	Sun Presence - FSS			

Attitude Control Subsystem (C) Housekeeping Telemetry
Page 2

No.	Sampled Parameter	Sampling Rate	Duration	Accuracy
C-30	Roll Inertia Wheel Speed	1/sec	Continuous	6 Bits
C-31	Roll Inertia Wheel Current			± 5%
C-32	Pitch Inertia Wheel Speed			6 Bits
C-33	Pitch Inertia Wheel Speed			± 5%
C-34	Yaw Inertia Wheel Speed			6 Bits
C-35	Yaw Inertia Wheel Current			± 5%
C-36	Standby Star Tracker Sec #1 On	1/4096 sec		Discrete
C-37	Standby Star Tracker Sec #1 On			
C-38	Standby Horizon Sensor On			
C-39	Standby Sun Sensor On			
C-40	Standby Roll Wheel Electronics On			
C-41	Standby Pitch Wheel Electronics On			
C-42	Standby Yaw Wheel Electronics On			
C-43	Standby Inverter On			
C-44	Standby Roll Jet Valves On			
C-45	Standby Pitch Jet Valves On			
C-46	Standby Yaw Jet Valves On			
C-47	Standby Controller Sec #1 On			
C-48	Standby Controller Sec #2 On			
C-49	Standby Controller Sec #3 On			
C-50	Standby Controller Sec #4 On			
C-51	Standby Controller Sec #5 On			
C-52	Standby Controller Sec #6 On			
C-53	Standby Controller Sec #7 On			
C-54	Standby Controller Sec #8 On			
C-55	Standby Controller Sec #9 On			
C-56	Sun Acquisition Logic Activated	1/sec		
C-57	Earth Acquisition Logic Activated			
C-58	Star Acquisition Logic Activated			

Attitude Control Subsystem (C) Housekeeping Telemetry
Page 3

No.	Sampled Parameter	Sampling Rate	Duration	Accuracy
C-59	Gyros Power On	1/4096 sec	Continuous	Discrete
C-60	Horizon Sensor Power On	1/4096 sec	↓	↓
C-61	Inverter Output	1/sec	↓	± 5%
C-62	Power Supply Voltage	1/sec	↓	± 5%
C-63	Horizon Sensor Mode	1/4096 sec	↓	Discrete
C-64	Gyro Mod	↓	↓	↓
C-65	Monopulse Mod	↓	↓	↓
C-66	Station Keeping Mod	↓	↓	↓

Power Subsystem (P) Housekeeping Telemetry

No.	Sampled Parameter	Sampling Rate	Duration	Accuracy
P-1	Panel Current	1/sec	Continuous	± 2%
P-2	Panel Current			
P-3	Panel Current			
P-4	Panel Current			
P-5	Panel Voltage			
P-6	Panel Voltage			
P-7	Panel Voltage			
P-8	Panel Voltage			
P-9	Charging Select			Discrete
P-10	Charging Select			
P-11	Load Select			
P-12	Load Select			
P-13	Load Select			
P-14	Load Select			
P-15	Load Select			
P-16	Load Select			
P-17	Load Select			
P-18	Load Select			
P-19	Load Select			
P-20	Load Current (DC Load)			± 2%
P-21	Load Current (DC/DC Input)			
P-22	Load Current (Inverter Input)			
P-23	Load Current (DC/DC Conv.)			
P-24	Load Current (Inverter)			
P-25	Load Voltage (DC/DC Conv.)			
P-26	Load Voltage (DC Load)			
P-27	Load Voltage (Inverter)			

Power Subsystem (P) Housekeeping Telemetry
Page 2

No.	Sampled Parameter	Sampling Rate	Duration	Accuracy
P-28	Regulator Select	1/sec	Continuous	Discrete
P-29	Regulator Select	↓	↓	Discrete
P-30	Regulator Current	↓	↓	± 2%
P-31	Regulator Current	↓	↓	↓
P-32	Regulator Voltage	↓	↓	↓
P-33	Regulator Voltage	↓	↓	↓
P-34	Battery Select	↓	↓	Discrete
P-35	Battery Select	↓	↓	Discrete
P-36	Battery Current	↓	↓	± 2%
P-37	Battery Current	↓	↓	↓
P-38	Battery Voltage	↓	↓	↓
P-39	Battery Voltage	↓	↓	↓

Spacecraft Temperature (T) Housekeeping Telemetry

No.	Sampled Parameter	Sampling Rate	Duration	Accuracy
T-1/T-5	Attitude Control Subsy. Temp.	1/sec	Continuous	± 1%
T-6/T-18	Array and Antenna Expt. Temps.	↓	↓	↓
T-19/T-22	Interferometer Expt. Temp.	↓	↓	↓
T-23/T-26	Telemetry Subsystem Temp.	↓	↓	↓
T-27/T-34	Power Subsystem Temp.	↓	↓	↓
T-35/T-36	Secondary Expts. Temp.	↓	↓	↓
T-37/T-69	Structures Subsystem Temp.	↓	↓	↓

Auxiliary Propulsion System (J) Housekeeping Telemetry

No.	Sampled Parameter	Sampling Rate	Duration	Accuracy
-1/J-10	Propellant Tank and Line Pressure	1/sec	Continuous	1%
-11/J-14	Valve Status	1/sec	Continuous	Discrete
-15	Vibration	8/sec	Continuous	1%

Interferometer Subsystem (I) Housekeeping Telemetry

No.	Sampled Parameter	Sampling Rate	Duration	Accuracy
I-1	Identification Tone, Gnd xmtr #1	1/64 sec.	During Expt.	Discrete
I-2	Identification Tone, Gnd xmtr #2	↓	↓	Discrete
I-3	AGC Voltage	↓	↓	2%
I-4	Crystal osc. calibration ckt voltage	1/64 sec.	↓	10%
I-5	Crystal Current #1	↓	↓	↓
I-6	Crystal Current #2	↓	↓	↓
I-7/I-16	Element Temperatures	1/sec.	↓	1%
I-17	VCO Control Voltage	1/sec.	↓	1%
I-18	Clock Crystal Current	1/64 sec.	↓	10%
I-19/I-23	Mixer Crystal Current	1/64 sec.	↓	10%
I-24/I-31	Interferometer Smoothed-Buffered Counter Output	1/sec	During Expt.	9 Bits
I-32/I-34	Interferometer Processor Output θ, Φ, Ψ	1/sec	During Expt.	9 Bits

Structures Subsystems (S) Housekeeping Telemetry

No.	Sampled Parameter	Sampling Rate	Duration	Accuracy
S1-S100	Linkage Position Switches	1/Sec	30 min.	Discrete
S101	Shaft Position	1/Sec	30 min.	8 bits
S102	Surface Spacing	16/Sec	30 min.	40 bits
S103-106	Vibration	Continuous	From Lift-off through deployment	5%

Instrumentation Subsystem (O) Housekeeping Telemetry

No.	Sampled Parameter	Sampling Rate	Duration	Accuracy
O-1	Command system decoder latch status	8/sec	Continuous	Discrete
O-2	Command system decoder power status	↓	↓	↓
O-3	Command system address check	↓	↓	↓
O-4	Command system word check	↓	↓	↓
O-5	Command system word execute	↓	↓	↓
O-6	R & R transponder voltage	1/64 sec	↓	10%
O-7	R & R transponder current	1/64 sec	↓	↓
O-8	Spacecraft time	1/sec	Continuous	Digital
O-9	Telemetry decoder #1 voltage	1/64 sec	Continuous	10%
O-10	Telemetry decoder #2 voltage	↓	↓	↓
O-11	Telemetry decoder #1 current	↓	↓	↓
O-12	Telemetry decoder #2 current	↓	↓	↓
O-13	Telemetry transmitter #1 voltage	↓	↓	↓
O-14	Telemetry transmitter #2 voltage	↓	↓	↓
O-15	Telemetry transmitter #1 current	↓	↓	↓
O-16	Telemetry transmitter #2 current	↓	↓	↓

Phased Array Subsystem (A) Housekeeping Telemetry

No.	Sampled Parameter	Sampling Rate	Duration	Accuracy
A-1	8 GHz rcvr, Temperature (IF)	1/64 sec	During Expt	2%
A-2	8 GHz rcvr, Temperature (LO)	1/64 sec		2%
A-3	8 GHz rcvr, Power (LO)	1/64 sec		10%
A-4	8 GHz rcvr, Operating Voltage (LO)			10%
A-5	8 GHz rcvr, Collector Voltage (IF)			10%
A-6	8 GHz rcvr, AGC Voltage (IF)			10%
A-7	8 GHz rcvr, Crystal Current (Mixer)			10%
A-8	7.3 GHz xmtr, Temperature #1 (LO)			2%
A-9	7.3 GHz xmtr, Temperature #2 (LO)			2%
A-10	7.3 GHz xmtr, Power #1 (LO)			10%
A-11	7.3 GHz xmtr, Power #2 (LO)			10%
A-12	7.3 GHz xmtr, Crystal Current (Mixer)			10%
A-13	7.3 GHz xmtr, Temperature (Amplifier)			2%
A-14	7.3 GHz xmtr, Operating Voltage (Ampl.)			10%
A-15	7.3 GHz xmtr, Operating Voltage #1 (LO)			10%
A-16	7.3 GHz xmtr, Operating Voltage #2 (LO)			10%
A-17	7.3 GHz xmtr, VSWR			10%
A-18	7.3 GHz xmtr, Power (RF Output)			10%
A-19	Voltage, High Voltage Conv. #1			10%
A-20	Current, High Voltage Conv. #1			10%

Parabolic Antenna Subsystem (D) Housekeeping Telemetry

No.	Sampled Parameter	Sampling Rate	Duration	Accuracy
D-1	1.7 GHz rcvr, Temperature (IF)	1/64 sec	During Expt.	2%
D-2	1.7 GHz rcvr, Temperature (LO)			2%
D-3	1.7 GHz rcvr, Power (LO)			10%
D-4	1.7 GHz rcvr, Operating Voltage (LO)			
D-5	1.7 GHz rcvr, Collector Voltage (IF)			
D-6	1.7 GHz rcvr, AGC Voltage (IF)			
D-7	1.7 GHz rcvr, Crystal Current (Mixer)			
D-8	2.1 GHz rcvr, Temperature (IF)			2%
D-9	2.1 GHz rcvr, Temperature (LO)			2%
D-10	2.1 GHz rcvr, Power (LO)			10%
D-11	2.1 GHz rcvr, Operating Voltage (LO)			
D-12	2.1 GHz rcvr, Collector Voltage (IF)			
D-13	2.1 GHz rcvr, AGC Voltage (IF)			
D-14	2.1 GHz rcvr, Crystal Current (Mixer)			
D-15	8 GHz rcvr, Mono P; Crystal Current (Mixer)			
D-16	8 GHz rcvr, Mono P, Collector Voltage (IF)			
D-17	8 GHz rcvr Mono, Temperature (IF)			2%
D-18	8 GHz rcvr Mono, AGC Voltage (IF)	1/sec		10%
D-19	8 GHz rcvr Mono R; Crystal Current (Mixer)			
D-20	8 GHz rcvr Mono, Collector Voltage (IF)			
D-21	8 GHz rcvr Mono, Temperature (IF)			2%
D-22	8 GHz rcvr Mono, AGC Voltage (IF)	1/sec		10%
D-23	Monopulse Roll Error			1%
D-24	Monopulse Pitch Error			1%
D-25	.1 GHz xmtr, Temperature (LO)	1/64 sec		2%
D-26	.1 GHz xmtr, Operating Voltage (LO)			10%
D-27	.1 GHz xmtr, Power (LO)			
D-28	.1 GHz xmtr, Crystal Current (Mixer)			
D-29	.1 GHz xmtr, Temperature (Ampl.)			2%
D-30	.1 GHz xmtr, Operating Voltage (Ampl.)			10%

Parabolic Antenna Subsystem (D) Housekeeping Telemetry
Page 2

No.	Sampled Parameter	Sampling Rate	Duration	Accuracy
D-31	.1 GHz xmtr, VSWR	1/64 sec.	During Expt.	10%
D-32	.1 GHz xmtr, Power (RF Output)			10%
D-33	.8 GHz xmtr, Temperature (LO)			2%
D-34	.8 GHz xmtr, Operating Voltage (LO)			10%
D-35	.8 GHz xmtr, Power (LO)			10%
D-36	.8 GHz xmtr, Crystal Current (Mixer)			10%
D-37	.8 GHz xmtr, Temperature (Ampl.)			2%
D-38	.8 GHz xmtr, Operating Voltage (Ampl.)			10%
D-39	.8 GHz xmtr, VSWR			10%
D-40	.8 GHz xmtr, Power (RF Output)			10%
D-41	8 GHz rcvr, Temperature (IF)			2%
D-42	8 GHz rcvr, Temperature (LO)			2%
D-43	8 GHz rcvr, Power (LO)			10%
D-44	8 GHz rcvr, Collector Voltage (IF)			10%
D-45	8 GHz rcvr, Collector Voltage (IF)			
D-46	8 GHz rcvr, AGC Voltage (IF)			
D-47	8 GHz rcvr, Crystal Current (Mixer)			
D-48	7.3 GHz xmtr, Temperature #1 (LO)	1/64 sec		2%
D-49	7.3 GHz xmtr, Temperature #2 (LO)			2%
D-50	7.3 GHz xmtr, Power #1 (LO)			10%
D-51	7.3 GHz xmtr, Power #2 (LO)			
D-52	7.3 GHz xmtr, Crystal Current (Mixer)			
D-53	7.3 GHz xmtr, Temperature (Amplifier)			2%
D-54	7.3 GHz xmtr, Operating Voltage (Ampl.)			10%
D-55	7.3 GHz xmtr, Operating Voltage #1 (LO)			
D-56	7.3 GHz xmtr, Operating Voltage #2 (LO)			
D-57	7.3 GHz xmtr, VSWR			
D-58	7.3 GHz xmtr, Power (RF Output)			
D-59	High Voltage Conv. #2 Voltage			
D-60	High Voltage Conv. #2 Current			

Parabolic Antenna Subsystem (D) Housekeeping Telemetry
Page 3

No.	Sampled Parameter	Sampling Rate	Duration	Accuracy
D-61	2 3 GHz xmtr, Temperature (LO)	1/64 sec	During Expt.	2%
D-62	2. 3 GHz xmtr, Operating Voltage (LO)	↓	↓	10%
D-63	2. 3 GHz xmtr, Power (LO)	↓	↓	10%
D-64	2. 3 GHz xmtr, Crystal Current (Mixer)	↓	↓	10%
D-65	2. 3 GHz xmtr, Temperature (Ampl.)	↓	↓	2%
D-66	2. 3 GHz xmtr, Operating Voltage (Ampl.)	↓	↓	10%
D-67	2. 3 GHz xmtr, VSWR	↓	↓	10%
D-68	2. 3 GHz xmtr, Power (RF Output)	↓	↓	10%

APPENDIX 9G

DATA QUESTIONNAIRE

The attached questionnaire shows the format used to collect communication requirements. The layout was made general to permit inclusion of telemetry, command, instruction and experiment data requirements. The format includes five sections:

1. Transmission requirement. This section serves to identify why data should be transmitted, and what measurement or experiment they correspond to. This section also serves to stimulate a better formulation of the experimentation.

2. Signal characteristics. This section is used to identify the individual signals and their parameter values.

3. Sensor characteristics. This section is used to identify applicable sensors.

4. Support requirements. This section discusses support requirements and identifies how a particular measurement, requiring data transmission, impacts other spacecraft subsystems.

5. Data Handling. This section serves to identify processing and handling requirements associated with the data requirements listed in the questionnaire.

This questionnaire was composed in this form in order to identify the data requirements, aid in developing a transmission profile, identify the relationship of one measurement on other spacecraft subsystems, and to identify data handling requirements.

1.0 Transmission Requirement

1.1 Experiment or Function
(e.g., interferometer, spacecraft orientation, antenna orientation, housekeeping, etc.)

1.2 Objective and Significance of Measurements
(Describe objective, e.g., to rotate spacecraft, to slew antenna, measure an angle, etc.)

1.3 Types of Data
(Include the transmitted signals which are required to conduct the test, e.g., calibration, commands, communication signals, etc.)

1.4 Method of Measurement
(Identify the measurement procedure, e.g., video monitoring, pressure recording, etc.; also identify auxiliary equipment such as recorders, calibration requirements, etc.)

1.5 Schedules of Experiments or Data Transmission
(Estimate the total experiment duration, e.g., life of the mission, 2 months, 1 week, etc.; estimate the duration of operational periods, e.g., 5 minutes, 1 hour, etc.; and estimate the time interval between operational periods, e.g., once per day, every 8 hours, once per month, etc.)

2.0 Signal Characteristics

2.1 Measured Parameters
(Identify each parameter to be measured, e.g., source voltage, reference angle, etc.)

IN 2.2-3.7, ADDRESS EACH PARAMETER SPECIFIED ABOVE IN 2.1.

2.2 Data or Signal Types
(e.g., analog, digital, cw, etc.)

2.3 Sampling Rates and Bit Rates
(Samples/second, bits/sample for digital data - if possible, specify the expected data format and provide sufficient information to allow for the contraction of a transmission profile.)

2.4 Bandwidths (for analog signals)
(e.g., video of 50-5000 Hz, vibration of 2-25 Hz, etc.)

2.5 Total Data Bulk
(Estimate total bulk data per test, i.e., total bits per measurement, total tape volume, etc.)

2.6 Accuracy or Resolution Requirements
(e.g., give SNR in dB, amplitude accuracy in %, error rates, etc.)

2.7 Allowable Transmission Delays
(Identify real-time requirements, permissible delays, and quantize delay period if critical)

3.0 Sensor Characteristics
(Where applicable, provide information on each sensor.)

3.1 Sensor Associated with Data
(e.g., horizon, sensor, sun sensor, etc.)

3.2 Location on Spacecraft.

3.3 Physical Characteristics.
(Size, weight, power consumption.)

3.4 Interface Characteristics
(output voltage level, impedance, etc.)

4.0 Experiment Support Requirements

4.1 Spacecraft Orientation and Stabilization Requirements
(e.g., if the spacecraft antenna must be slewed in a particular manner for pattern measurements within a prescribed accuracy.)

4.2 Dependence of Other Data
(Identify requirements for support by other spacecraft data; e.g., other experiments to be conducted simultaneously, housekeeping data, etc.)

4.3 Prerequisites
(Identify data needed prior to experiment, e.g., weather data; dependence on other ATS-4 experiment results, e.g., antenna pattern measurements must precede communications tests.)

5.0 Data Handling and Processing

5.1 Onboard Requirements

5.1.1 Storage Requirements
(Identify medium, e.g., tape, buffer, etc.; amount, e.g., 1 hour of digital data, 20 minutes of analog, number of tracks required, etc.)

5.1.2 Signal Conditioning Required (if applicable)

5.1.3 Processing Requirements
(Data checks, data smoothing, command verification, etc.)

5.2 Ground Requirements

5.2.1 Data Destination
(e.g., ground station, ATSOCC, etc.)

5.2.2 Data Display Requirements
(e.g., strip chart, CRT, etc.)

5.2.3 Quick-look Requirements

5.2.4 Processing Requirements (e.g., reformatting, data stripping, etc.)

5.2.5 Priorities

5.2.6 Special Equipment Requirements
(Identify equipment dedicated to ATS-4)

6.0 Remarks

(Add any additional information deemed pertinent)